



Earth Resources
A Continuing
Bibliography
with Indexes

NASA SP-7041(33)
April 1982

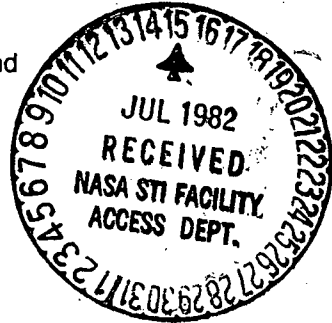
(NASA-SP-7041(33)) EARTH RESOURCES: A
CONTINUING BIBLIOGRAPHY WITH INDEXES, ISSUE
33 (National Aeronautics and Space
Administration) 100 p HC \$10.50 C SCL 05B

N 82-28695

Unclas
25482

00/43

National Aeronautics and
Space Administration



es Earth Resources
s Earth Resources
Earth Resources E
th Resources Ear
Resources Earth
Resources Earth R
resources Earth Res

ACCESSION NUMBER RANGES

Accession numbers cited in this Supplement fall within the following ranges.

STAR (N-10000 Series)	N82-10001 - N82-16039
IAA (A-10000 Series)	A82-10001 - A82-18839

This bibliography was prepared by the NASA Scientific and Technical Information Facility operated for the National Aeronautics and Space Administration by PRC Government Information Systems.

EARTH RESOURCES

A CONTINUING BIBLIOGRAPHY WITH INDEXES

Issue 33

A selection of annotated references to unclassified reports and journal articles that were introduced into the NASA scientific and technical information system and announced between January 1 and March 31, 1982 in

- *Scientific and Technical Aerospace Reports (STAR)*
- *International Aerospace Abstracts (IAA).*

This supplement is available as NTISUB/038/093 from the National Technical Information Service (NTIS), Springfield, Virginia 22161 at the price of \$10.50 domestic; \$21.50 foreign for standing orders. Please note: Standing orders are subscriptions which do not terminate at the end of a year, as do regular subscriptions, but continue indefinitely unless specifically terminated by the subscriber.

INTRODUCTION

The technical literature described in this continuing bibliography may be helpful to researchers in numerous disciplines such as agriculture and forestry, geography and cartography, geology and mining, oceanography and fishing, environmental control, and many others. Until recently it was impossible for anyone to examine more than a minute fraction of the Earth's surface continuously. Now vast areas can be observed synoptically, and changes noted in both the Earth's lands and waters, by sensing instrumentation on orbiting spacecraft or on aircraft.

This literature survey lists 436 reports, articles, and other documents announced between January 1 and March 31, 1982 in *Scientific and Technical Aerospace Reports (STAR)*, and *International Aerospace Abstracts (IAA)*.

The coverage includes documents related to the identification and evaluation by means of sensors in spacecraft and aircraft of vegetation, minerals, and other natural resources, and the techniques and potentialities of surveying and keeping up-to-date inventories of such riches. It encompasses studies of such natural phenomena as earthquakes, volcanoes, ocean currents, and magnetic fields; and such cultural phenomena as cities, transportation networks, and irrigation systems. Descriptions of the components and use of remote sensing and geophysical instrumentation, their subsystems, observational procedures, signature and analyses and interpretive techniques for gathering data are also included. All reports generated under NASA's Earth Resources Survey Program for the time period covered in this bibliography will also be included. The bibliography does not contain citations to documents dealing mainly with satellites or satellite equipment used in navigation or communication systems, nor with instrumentation not used aboard aerospace vehicles.

The selected items are grouped in nine categories. These are listed in the Table of Contents with notes regarding the scope of each category. These categories were especially chosen for this publication, and differ from those found in *STAR* and *IAA*.

Each entry consists of a standard bibliographic citation accompanied by an abstract. The citations and abstracts are reproduced exactly as they appeared originally in *STAR*, or *IAA*, including the original accession numbers from the respective announcement journals. This procedure, which saves time and money, accounts for the variation in citation-appearance.

Under each of the nine categories, the entries are presented in one of two groups that appear in the following order:

IAA entries identified by accession number series A82-10,000 in ascending accession number order;

STAR entries identified by accession number series N82-10,000 in ascending accession number order.

After the abstract section, there are five indexes:

subject, personal author, corporate source, contract number and report/accession number.

AVAILABILITY OF CITED PUBLICATIONS

IAA ENTRIES (A82-10000 Series)

All publications abstracted in this Section are available from the Technical Information Service, American Institute of Aeronautics and Astronautics, Inc. (AIAA), as follows: Paper copies of accessions are available at \$8.00 per document. Microfiche⁽¹⁾ of documents announced in *IAA* are available at the rate of \$4.00 per microfiche on demand, and at the rate of \$1.35 per microfiche for standing orders for all *IAA* microfiche.

Minimum air-mail postage to foreign countries is \$2.50 and all foreign orders are shipped on payment of pro-forma invoices.

All inquiries and requests should be addressed to AIAA Technical Information Service. Please refer to the accession number when requesting publications.

STAR ENTRIES (N82-10000 Series)

One or more sources from which a document announced in *STAR* is available to the public is ordinarily given on the last line of the citation. The most commonly indicated sources and their acronyms or abbreviations are listed below. If the publication is available from a source other than those listed, the publisher and his address will be displayed on the availability line or in combination with the corporate source line.

Avail: NTIS. Sold by the National Technical Information Service. Prices for hard copy (HC) and microfiche (MF) are indicated by a price code preceded by the letters HC or MF in the *STAR* citation. Current values for the price codes are given in the tables on page vii.

Documents on microfiche are designated by a pound sign (#) following the accession number. The pound sign is used without regard to the source or quality of the microfiche.

Initially distributed microfiche under the NTIS SRIM (Selected Research in Microfiche) is available at greatly reduced unit prices. For this service and for information concerning subscription to NASA printed reports, consult the NTIS Subscription Section, Springfield, Va. 22161.

NOTE ON ORDERING DOCUMENTS: When ordering NASA publications (those followed by the * symbol), use the N accession number. NASA patent applications (only the specifications are offered) should be ordered by the US-Patent-App-SN number. Non-NASA publications (no asterisk) should be ordered by the AD, PB, or other *report* number shown on the last line of the citation, not by the N accession number. It is also advisable to cite the title and other bibliographic identification.

Avail: SOD (or GPO). Sold by the Superintendent of Documents, U.S. Government Printing Office, in hard copy. The current price and order number are given following the availability line. (NTIS will fill microfiche requests, at the standard \$4.00 price, for those documents identified by a # symbol.)

Avail: NASA Public Document Rooms. Documents so indicated may be examined at or purchased from the National Aeronautics and Space Administration, Public Document Room (Room 126), 600 Independence Ave., S.W., Washington, D.C. 20546, or public document rooms located at each of the NASA research centers, the NASA Space Technology Laboratories, and the NASA Pasadena Office at the Jet Propulsion Laboratory.

(1) A microfiche is a transparent sheet of film, 105 by 148 mm in size containing as many as 60 to 98 pages of information reduced to micro images (not to exceed 26:1 reduction).

- Avail: DOE Depository Libraries. Organizations in U.S. cities and abroad that maintain collections of Department of Energy reports, usually in microfiche form, are listed in *Energy Research Abstracts*. Services available from the DOE and its depositories are described in a booklet, *DOE Technical Information Center - Its Functions and Services* (TID-4660), which may be obtained without charge from the DOE Technical Information Center.
- Avail: Univ. Microfilms. Documents so indicated are dissertations selected from *Dissertation Abstracts* and are sold by University Microfilms as xerographic copy (HC) and microfilm. All requests should cite the author and the Order Number as they appear in the citation.
- Avail: USGS. Originals of many reports from the U.S. Geological Survey, which may contain color illustrations, or otherwise may not have the quality of illustrations preserved in the microfiche or facsimile reproduction, may be examined by the public at the libraries of the USGS field offices whose addresses are listed in this introduction. The libraries may be queried concerning the availability of specific documents and the possible utilization of local copying services, such as color reproduction.
- Avail: HMSO. Publications of Her Majesty's Stationery Office are sold in the U.S. by Pendragon House, Inc. (PHI), Redwood City, California. The U.S. price (including a service and mailing charge) is given, or a conversion table may be obtained from PHI.
- Avail: BLL (formerly NLL): British Library Lending Division, Boston Spa, Wetherby, Yorkshire, England. Photocopies available from this organization at the price shown. (If none is given, inquiry should be addressed to the BLL.)
- Avail: Fachinformationszentrum, Karlsruhe. Sold by the Fachinformationszentrum Energie, Physik, Mathematik GMBH, Eggenstein Leopoldshafen, Federal Republic of Germany, at the price shown in deutschmarks (DM).
- Avail: Issuing Activity, or Corporate Author, or no indication of availability. Inquiries as to the availability of these documents should be addressed to the organization shown in the citation as the corporate author of the document.
- Avail: U.S. Patent and Trademark Office. Sold by Commissioner of Patents and Trademarks, U.S. Patent and Trademark Office, at the standard price of 50 cents each, postage free.
- Other availabilities: If the publication is available from a source other than the above, the publisher and his address will be displayed entirely on the availability line or in combination with the corporate author line.

ADDRESSES OF ORGANIZATIONS

American Institute of Aeronautics and
Astronautics
Technical Information Service
555 West 57th Street, 12th Floor
New York, New York 10019

British Library Lending Division,
Boston Spa, Wetherby, Yorkshire,
England

Commissioner of Patents and
Trademarks
U.S. Patent and Trademark Office
Washington, D.C. 20231

Department of Energy
Technical Information Center
P.O. Box 62
Oak Ridge, Tennessee 37830

ESA-Information Retrieval Service
ESRIN
Via Galileo Galilei
00044 Frascati (Rome) Italy

Fachinformationszentrum Energie, Physik,
Mathematik GMBH
7514 Eggenstein Leopoldshafen
Federal Republic of Germany

Her Majesty's Stationery Office
P.O. Box 569, S.E. 1
London, England

NASA Scientific and Technical Information
Facility
P.O. Box 8757
B.W.I. Airport, Maryland 21240

National Aeronautics and Space
Administration
Scientific and Technical Information
Branch (NST-41)
Washington, D.C. 20546

National Technical Information Service
5285 Port Royal Road
Springfield, Virginia 22161

Pendragon House, Inc.
899 Broadway Avenue
Redwood City, California 94063

Superintendent of Documents
U.S. Government Printing Office
Washington, D.C. 20402

University Microfilms
A Xerox Company
300 North Zeeb Road
Ann Arbor, Michigan 48106

University Microfilms, Ltd.
Tylers Green
London, England

U.S. Geological Survey
1033 General Services Administration
Building
Washington, D.C. 20242

U.S. Geological Survey
601 E. Cedar Avenue
Flagstaff, Arizona 86002

U.S. Geological Survey
345 Middlefield Road
Menlo Park, California 94025

U.S. Geological Survey
Bldg. 25, Denver Federal Center
Denver, Colorado 80225

NTIS PRICE SCHEDULES

Schedule A STANDARD PAPER COPY PRICE SCHEDULE

(Effective January 1, 1982)

Price Code	Page Range	North American Price	Foreign Price
A01	Microfiche	\$ 4.00	\$ 8.00
A02	001-025	6.00	12.00
A03	026-050	7.50	15.00
A04	051-075	9.00	18.00
A05	076-100	10.50	21.00
A06	101-125	12.00	24.00
A07	126-150	13.50	27.00
A08	151-175	15.00	30.00
A09	176-200	16.50	33.00
A10	201-225	18.00	36.00
A11	226-250	19.50	39.00
A12	251-275	21.00	42.00
A13	276-300	22.50	45.00
A14	301-325	24.00	48.00
A15	326-350	25.50	51.00
A16	351-375	27.00	54.00
A17	376-400	28.50	57.00
A18	401-425	30.00	60.00
A19	426-450	31.50	63.00
A20	451-475	33.00	66.00
A21	476-500	34.50	69.00
A22	501-525	36.00	72.00
A23	526-550	37.50	75.00
A24	551-575	39.00	78.00
A25	576-600	40.50	81.00
	601-up	-- 1/	-- 2/

A99 - Write for quote

1/ Add \$1.50 for each additional 25 page increment or portion thereof for 601 pages up.

2/ Add \$3.00 for each additional 25 page increment or portion thereof for 601 pages and more.

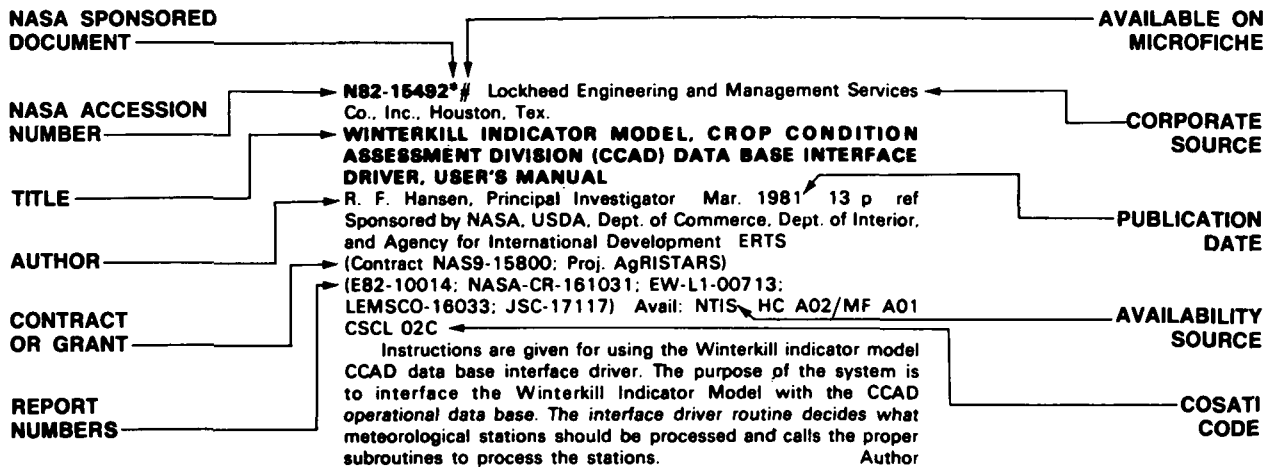
Schedule E EXCEPTION PRICE SCHEDULE Paper Copy & Microfiche

Price Code	North American Price	Foreign Price
E01	\$ 6.50	\$ 13.50
E02	7.50	15.50
E03	9.50	19.50
E04	11.50	23.50
E05	13.50	27.50
E06	15.50	31.50
E07	17.50	35.50
E08	19.50	39.50
E09	21.50	43.50
E10	23.50	47.50
E11	25.50	51.50
E12	28.50	57.50
E13	31.50	63.50
E14	34.50	69.50
E15	37.50	75.50
E16	40.50	81.50
E17	43.50	88.50
E18	46.50	93.50
E19	51.50	102.50
E20	61.50	123.50
E-99 - Write for quote		
N01	30.00 ^f	45.00

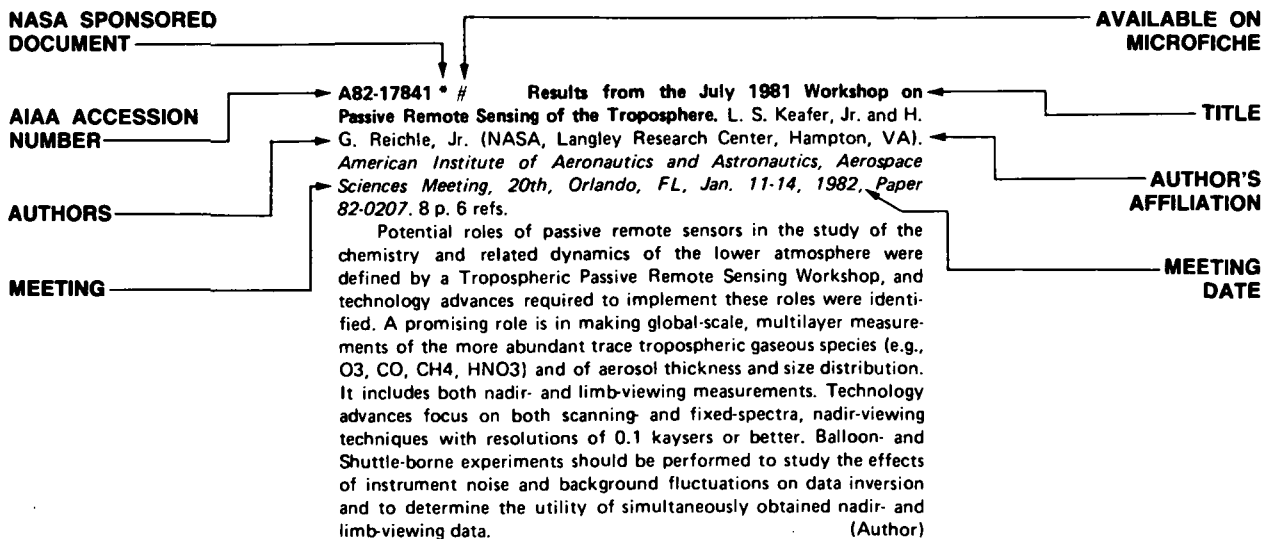
TABLE OF CONTENTS

	Page
Category 01 Agriculture and Forestry Includes crop forecasts, crop signature analysis, soil identification, disease detection, harvest estimates, range resources, timber inventory, forest fire detection, and wildlife migration patterns.	1
Category 02 Environmental Changes and Cultural Resources Includes land use analysis, urban and metropolitan studies, environmental impact, air and water pollution, geographic information systems, and geographic analysis.	7
Category 03 Geodesy and Cartography Includes mapping and topography.	15
Category 04 Geology and Mineral Resources Includes mineral deposits, petroleum deposits, spectral properties of rocks, geological exploration, and lithology.	19
Category 05 Oceanography and Marine Resources Includes sea-surface temperature, ocean bottom surveying imagery, drift rates, sea ice and icebergs, sea state, fish location	23
Category 06 Hydrology and Water Management Includes snow cover and water runoff in rivers and glaciers, saline intrusion, drainage analysis, geomorphology of river basins, land uses, and estuarine studies.	35
Category 07 Data Processing and Distribution Systems Includes film processing, computer technology, satellite and aircraft hardware, and imagery.	41
Category 08 Instrumentation and Sensors Includes data acquisition and camera systems and remote sensors.	49
Category 09 General Includes economic analysis.	55
Subject Index	A-1
Personal Author Index	B-1
Corporate Source Index	C-1
Contract Number Index	D-1
Report / Accession Number Index	E-1

TYPICAL CITATION AND ABSTRACT FROM STAR



TYPICAL CITATION AND ABSTRACT FROM IAA



EARTH RESOURCES

A Continuing Bibliography (Issue 33)

APRIL 1982

01

AGRICULTURE AND FORESTRY

Includes crop forecasts, crop signature analysis, soil identification, disease detection, harvest estimates, range resources, timber inventory, forest fire detection, and wildlife migration patterns.

A82-10039 **The effect of angular factors on popularly used indicators of vegetative vigor.** M. J. Duggin (New York, State University, Syracuse, NY). In: American Society of Photogrammetry, Annual Meeting, 46th, St. Louis, MO, March 9-14, 1980, ASP Technical Papers. Falls Church, VA, American Society of Photogrammetry, 1980, p.239-251. 19 refs.

Ground-based radiometric measurements of reflectance and radiometric data from airborne and spaceborne multispectral scanners and cameras have been used to experimentally determine biomass, vegetative cover, leaf area index, plant height, and disease severity for crops and (for some of these variables) for pastures. In studies so far reported, little or no attention has been given to the effect of sun-detector geometry on popular indices of these variables. It is shown using an experimental model that, for several different pasture targets, each angular variable (solar zenith angle, solar azimuth, and look angle) has an important effect on each of the indices. This implies that care is required in selecting angular regimes for the collection of data which can be interpreted unambiguously and for the meaningful comparison of data obtained on different occasions. B.J.

A82-10040 **Remote sensing techniques in the study of the agricultural potential of soils under the Cerrado vegetation /Brazil/.** G. J. Garcia and R. P. Harris (Universidade Estadual Paulista, Botucatu, São Paulo, Brazil). In: American Society of Photogrammetry, Annual Meeting, 46th, St. Louis, MO, March 9-14, 1980, ASP Technical Papers. Falls Church, VA, American Society of Photogrammetry, 1980, p. 252-260. 8 refs. Research supported by the Fundação de Amparo à Pesquisa do Estado de São Paulo.

A82-10041 **Mapping vegetation association boundaries with Landsat MSS data - An Oklahoma example.** J. A. Harrington, Jr. and C. W. Dunn, Jr. (Oklahoma, University, Norman, OK). In: American Society of Photogrammetry, Annual Meeting, 46th, St. Louis, MO, March 9-14, 1980, ASP Technical Papers. Falls Church, VA, American Society of Photogrammetry, 1980, p. 270-281. 15 refs.

The transition from oak forest to prairie grassland in central Oklahoma provides an excellent area to test the feasibility of using Landsat satellite remote sensing for vegetation mapping. An east-west oriented transect across the ecotone was identified as a study area for testing the mapping accuracy that is obtainable with both computer processing of the digital data and traditional aerial photographic interpretation of Landsat false color composites. Acreage statistics and locational measures of Landsat derived forest cover maps are compared with ground truth information obtained from interpretation of large scale panchromatic photography to suggest the relative accuracy of the analysis techniques. Potential applications of the use of Landsat satellite data for vegetation mapping are identified.

(Author)

A82-10042 **Phytocozonation of Sevier Lake region of Utah using digitized Landsat MSS data.** K. Lulla and P. Mausel (Indiana State University, Terre Haute, IN). In: American Society of Photogrammetry, Annual Meeting, 46th, St. Louis, MO, March 9-14, 1980, ASP Technical Papers. Falls Church, VA, American Society of Photogrammetry, 1980, p.282-292. 10 refs.

The practicality and value of Landsat MSS digital data using computer-assisted techniques were examined in a study of regional level phytocozone identification in the Sevier Lake region of the Great Basin of Utah. Four band spectral responses from Landsat scene 73500200 (May 22, 1973) were converted into principal component (PC) and biomass ratios. Unsupervised results clearly indicate that Landsat MSS data in PC and biomass ratio form can be used to delineate major phytocozone patterns at a map scale of 1:500,000 and also provide selected zonation information at 1:120,000 scale and larger. It was also found that combining PC, biomass ratio, and some original Landsat data gave the best results for delineating phytocozone regions using nonparametric supervised classification techniques. B.J.

A82-10046 **Limitations in the spectral discrimination of the Landsat MSS.** M. J. Duggin (New York, State University, Syracuse, NY) and P. J. Ellis (Department of Scientific and Industrial Research, Physics and Engineering Laboratory, Lower Hutt, New Zealand). In: American Society of Photogrammetry, Annual Meeting, 46th, St. Louis, MO, March 9-14, 1980, ASP Technical Papers. Falls Church, VA, American Society of Photogrammetry, 1980, p.329-334. 7 refs.

The variation between the mean value in output for one bandpass for the Landsat 1, 2, and 3 multispectral scanners is nearly 10% for a target that shows variations in spectral response across the bandpass (e.g., vegetation) but is less than 1% for a target that does not (e.g., soil). This paper examines the above differences for real vegetation and soil targets to show that the differences in output between the channels for a given band of a given MSS are target-dependent; that is, striping on the MSS image is target-dependent. It is also shown that in the case of multitemporal studies involving the output of scanners on two or more satellites, the differences in mean output between like channels of scanners are target-dependent, being much larger for a target which shows variations in radiance across the scanner bandpass than for one which does not. B.J.

A82-10047 * **Remote sensing for vineyard management.** W. R. Philipson, T. L. Erb, D. Fernandez, and J. N. McLeester (Cornell University, Ithaca, NY). In: American Society of Photogrammetry, Annual Meeting, 46th, St. Louis, MO, March 9-14, 1980, ASP Technical Papers. Falls Church, VA, American Society of Photogrammetry, 1980, p.371-378. Grant No. NGL-33-010-171.

Cornell's Remote Sensing Program has been involved in a continuing investigation to assess the value of remote sensing for vineyard management. Program staff members have conducted a series of site and crop analysis studies. These include: (1) panchromatic aerial photography for planning artificial drainage in a new vineyard; (2) color infrared aerial photography for assessing crop vigor/health; and (3) color infrared aerial photography and aircraft multispectral scanner data for evaluating yield related factors. These studies and their findings are reviewed. (Author)

A82-10048 **Repetitive aerial photography for assessing marsh vegetation changes.** M. G. Weaver, G. H. Cross, and R. A. Mead

01 AGRICULTURE AND FORESTRY

(Virginia Polytechnic Institute and State University, Blacksburg, VA). In: American Society of Photogrammetry, Annual Meeting, 46th, St. Louis, MO, March 9-14, 1980, ASP Technical Papers.

Falls Church, VA, American Society of Photogrammetry, 1980, p. 395-408. 21 refs. Research supported by the Virginia Commission of Game and Inland Fisheries.

The dynamic conditions of two marshes on the Rappahannock River, Virginia, were investigated using sequential aerial photography. All the historical photography was 9 inch format, black and white panchromatic, and medium scale, purchased from various government agencies. Recent photos were large-scale 35 mm color infrared and natural color positive transparencies. Vegetative classes were delineated on the recent photographs to produce a large-scale 1:2,500 map useful in current resource planning and future monitoring. The black and white historical photos were interpreted using a generalized classification system. Comparisons of changes were made by reducing or enlarging the maps made from the historical and tabularly reducing the current vegetation classes to a common scale of 1:7,000. In addition, muskrat lodges were plotted on all photographs where resolution and quality permitted. Repetitive aerial photographs provided useful information on which to formulate hypotheses that would explain changes in marsh vegetation. (Author)

A82-10862 **Stand density estimation on panoramic transparencies.** W. A. Befort, H. N. Anderson (Idaho, University, Moscow, ID), and B. L. Kessler (Idaho Department of Lands, Moscow, ID). *Photogrammetric Engineering and Remote Sensing*, vol. 47, Oct. 1981, p. 1477-1481. 9 refs.

Paired estimates of forest canopy density were made on optical bar panoramic CIR transparencies and on conventional black-and-white prints to see if different results would be obtained. Except in the portions of the photographs beyond about 36 deg of scan angle, estimates made on panoramic photos under 4x stereo magnification were not significantly different from estimates made on conventional photos with a 3x mirror stereoscope. (Author)

A82-10863 * **Spectral behavior of wheat yield variety trials.** J. L. Hatfield (California, University, Davis, CA). *Photogrammetric Engineering and Remote Sensing*, vol. 47, Oct. 1981, p. 1487-1491. 8 refs. Research supported by the U.S. Department of Agriculture; Grant No. NCA2-OR-180-607.

Little variation between varieties is seen at jointing, but the variability is found to increase during grain filling and decline again at maturity. No relationship is found between spectral response and yield, and when yields are segregated into various classes the spectral response is the same. Spring and winter nurseries are found to separate during the reproductive stage because of differences in dates of heading and maturity, but they exhibit similar spectral responses. The transformed normalized difference is at a minimum after the maximum grain weight occurs and the leaves begin to brown and fall off. These data of 100% ground cover demonstrate that it is not possible to predict grain yield from only spectral data. This, however, may not apply when reduced yields are caused by less-than-full ground cover. C.R.

A82-10864 **Satellite sensing of irrigation patterns in semi-arid areas - An Indian study.** S. Thiruvengadachari (National Remote Sensing Agency, Hyderabad, India). *Photogrammetric Engineering and Remote Sensing*, vol. 47, Oct. 1981, p. 1493-1499. 6 refs.

A82-12884 **Evaluation of digital photographic enhancement for Dutch elm disease detection.** T. M. Lillesand, D. E. Meisner, D. W. French, and W. L. Johnson (Minnesota, University, St. Paul, MN). *Photogrammetric Engineering and Remote Sensing*, vol. 47, Nov. 1981, p. 1581-1592. 11 refs. Research supported by the University of Minnesota.

A82-12886 * **Temporal spectral response of a corn canopy.** B. L. Markham, D. S. Kimes, C. J. Tucker (NASA, Goddard Space Flight Center, Earth Resources Branch, Greenbelt, MD), and J. E. McMurtrey, III (Science and Education Administration, Field Crops Laboratory, Beltsville, MD). *Photogrammetric Engineering and Remote Sensing*, vol. 47, Nov. 1981, p. 1599-1605. 14 refs.

Techniques developed for the prediction of winter wheat yields from remotely sensed data indicating crop status over the growing season are tested for their applicability to corn. Ground-based spectral measurements in the Landsat Thematic Mapper bands 3 (0.62-0.69 microns), 4 (0.76-0.90 microns) and 5 (1.55-1.75 microns) were performed at one-week intervals throughout the growing season for 24 plots of corn, and analyzed to derive spectral ratios and normalized spectral differences of the IR and shortwave IR bands with the red. The ratios of the near IR and shortwave IR bands are found to provide the highest and most consistent correlations with corn yield and dry matter accumulation, however the value of band 5 could not be tested due to the absence of water stress conditions. Integration of spectral ratios over several dates improved the correlations over those of any single date by achieving a seasonal, rather than instantaneous, estimate of crop status. Results point to the desirability of further tests under other growth conditions to determine whether satellite-derived data will be useful in providing corn yield information. S.C.S.

A82-12887 **Identification of conifer species groupings from Landsat digital classifications.** K. E. Mayer and L. Fox, III (Humboldt State University, Arcata, CA). *Photogrammetric Engineering and Remote Sensing*, vol. 47, Nov. 1981, p. 1607-1614. 12 refs.

The development of computerized classification techniques for timber species groupings in Landsat digital data is discussed in light of the problems of spectrally inhomogeneous training fields, unique patterns not covered by limited numbers of training fields and spectral class labeling encountered in such situations. The combination of guided clustering with unsupervised classification is shown to have allowed inventorying of the timber resources of the McCloud Ranger District of the Shasta-Trinity National Forest in California. To complete the classification spectral classes were assigned to resource categories by the construction of spectral curves for each class from the mean digital values in spectral bands 4, 5, 6 and 7, in association with detailed photointerpretation. An overall classification accuracy for the identification of conifer species groupings, canopy density classes, and crown diameter categories of 0.83 was thus obtained. S.C.S.

A82-15026 **The discrimination of winter wheat using a growth-state signature.** C. A. Hlavka, R. M. Haralick, S. M. Carlyle, and R. Yokoyama (Kansas, University, Lawrence, KS). *Remote Sensing of Environment*, vol. 9, June 1980, p. 277-294. 21 refs.

In this paper, a multitemporal classification procedure for crops in Landsat scenes is described. The method involves the creation of crop signatures which characterize multispectral observations as functions of phenological growth states. In this approach, crop spectral reflectance is modeled explicitly as a function of maturity rather than a function of date. This means that instead of stacking spectral vectors of one observation on another, as is usually done for multitemporal data, a correspondence of time to growth state is established for each possible crop category which minimizes the difference between the given multispectral multitemporal vector and the category mean vector indexed by growth state. The results of applying it to winter wheat show that the method is capable of discrimination with about the same degree of accuracy as more traditional multitemporal classifiers. It shows some potential to label degree of maturity of the crop without crop condition information in the training set. V.L.

A82-15038 * **Temporal relationships between spectral response and agronomic variables of a corn canopy.** D. S. Kimes, B. L. Markham, C. J. Tucker (NASA, Goddard Space Flight Center, Earth Resources Branch, Greenbelt, MD), and J. E. McMurtrey, III (U.S. Science and Education Administration, Plant Genetics and Germplasm Institute, Beltsville, MD). *Remote Sensing of Environment*, vol. 11, Nov. 1981, p. 401-411. 15 refs.

Attention is given to an experiment in which spectral radiance data collected in three spectral regions are related to corn canopy variables. The study extends the work of Tucker et al. (1979) in that more detailed measurements of corn canopy variables were made using quantitative techniques. Wet and dry green leaf biomass is considered along with the green leaf area index, chlorotic leaf biomass, chlorotic leaf area, and leaf water content. In addition,

spectral data were collected with a hand-held radiometer having Landsat-D Thematic Mapper (TM) bands TM3 (0.63-0.69 micrometers), TM4 (0.76-0.90 micrometers), and TM5 (1.55-1.75 micrometers). TM3, TM4, and TM5 seem to be well situated spectrally for making remotely sensed measurements related to chlorophyll concentration, leaf density, and leaf water content. G.R.

A82-15748 A VHF homing system with VHF radio-telephony for area-representative strip-survey flights conducted, as part of combined forest inventories, with light aircraft carrying 70 mm and 35 mm cameras (Ein VHF-Homing-System mit VHF-Sprechfunk für flächenrepräsentative Streifenbefliegungen mit 70 mm und 35 mm Kameras von leichten Flugzeugen im Rahmen kombinierter Waldinventuren). B. Rhody (Bundesforschungsanstalt für Forst- und Holzwirtschaft, Hamburg, West Germany). *Bildmessung und Luftbildwesen*, vol. 49, Nov. 1, 1981, p. 199-203. In German.

A82-15963 † Study and mapping of agricultural land use, based on space images (*Izuchenie i kartografirovaniye sel'skokhoziaistvennogo ispol'zovaniia zemel' po kosmicheskim snimkam*). L. F. Ivanova (Moskovskii Gosudarstvennyi Universitet, Moscow, USSR). *Issledovanie Zemli iz Kosmosa*, Sept.-Oct. 1981, p. 103-110. In Russian.

The possibilities of using multispectral images obtained at different times by the Fragment system to study the structure of agrarian lands and various forms of agriculture are assessed. A method is described for interpreting the agrarian areas, groups of agricultural cultures, and agrotechnical and land reclamation measures, which are based on a system of external features. The advantages of using space images as compared to ground-based methods are discussed, including the greater regional differentiation of space information. J.F.

A82-15964 † Mapping of forest vegetation on the basis of space images (*Kartografirovaniye lesnoi rastitel'nosti po kosmicheskim snimkam*). T. V. Kotova, V. I. Kravtsova, and A. K. Makarevich (Moskovskii Gosudarstvennyi Universitet, Moscow, USSR). *Issledovanie Zemli iz Kosmosa*, Sept.-Oct. 1981, p. 111-116. In Russian.

Using the upper reaches of the Northern Dvina river as an example, the possibilities of studying and mapping forests by images obtained by the Fragment system were analyzed. The images were used to separate forest and non-forest areas, and to distinguish the forest areas as either coniferous, mixed, or deciduous. The outlines of forest and nonforest regions with areas greater than 0.5 sq km are established in detail, and the characteristics of the various species are discussed in general terms. J.F.

A82-16162 Rural development in the humid tropics. F. C. d'Audretsch and H. F. Gelens (International Institute for Aerial Survey and Earth Sciences, Enschede, Netherlands). *ITC Journal*, no. 3, 1981, p. 266-277.

The status of on-going rural development projects in Southeast Asia was the subject of a seven-week research tour of Thailand, Indonesia and the Philippines. The tour was jointly sponsored by the International Institute for Aerial Survey and Earth Sciences and the United Nations University. The study focused on the development of resources management in agro-forestry, forest conservation, reforestation and settlement in the humid tropics. Problems in the use of aerial photographs and coordination of resource management were identified. S.C.S.

A82-16622 † Analysis of the information content of the polarimetric method of remote sensing (*Analiz informativnosti polarimetriceskogo metoda distantsionnogo zondirovaniia*). V. V. Egorov and B. S. Zhukov. In: Airborne and spaceborne multispectral photography of the earth. Moscow, Izdatel'stvo Nauka, 1981, p. 203-210. 8 refs. In Russian.

The comparative information content of polarization characteristics in remote sensing studies is analyzed. The optimal combination of spectral-polarization measurements is calculated for actual sets of soil-vegetation objects. Intensity and the degree of optical polariza-

tion were found to be the most informative polarization characteristics. B.J.

A82-17564 * Aircraft radar response to soil moisture. G. A. Bradley and F. T. Ulaby (University of Kansas Center for Research, Inc., Lawrence, KS). *Remote Sensing of Environment*, vol. 11, Dec. 1981, p. 419-438. 12 refs. Contracts No. NAS9-14052; Grant No. NAG5-30.

An analysis is presented of aircraft response to soil moisture in the upper surface layer of agricultural fields. Measurements (taken at 1.6 GHz and 4.75 GHz using HH and HV polarizations, and at 13.3 GHz using VV polarization from an experiment conducted in 1978 at Colby, Kansas) are used to derive the radar soil moisture sensitivities and correlations. It is shown that the aircraft response to soil moisture is optimum at C-band frequencies and incidence angles of 10-20 deg, confirming previous truck-radar results. Like-polarization radar response is unaffected by vegetation but is dependent on row-tillage patterns; cross-polarization response also is unaffected by vegetation but is approximately independent of tillage patterns. These results show that remote sensing radars can be used effectively for the detection and estimation of near-surface soil moisture in agricultural fields. (Author)

A82-17997 Remote sensing of crop moisture status. B. L. Blad, B. R. Gardner, D. G. Watts, and N. J. Rosenberg (Nebraska University, Lincoln, NE). *Remote Sensing Quarterly*, vol. 3, Apr. 1981, p. 4-20. 11 refs. Research sponsored by the University of Nebraska.

Relations between crop temperatures and levels of water stress are determined to serve as a basis for the remote sensing of the extent and severity of water stress according to thermal imagery. Experiments were performed on stands of sorghum and corn grown near Mead and North Platte, Nebraska, respectively, under either full irrigation, a water gradient during the vegetative, pollination and grain-fill periods, or dryland conditions. Thermal imagery acquired at altitudes of 610 and 1220 m reveals the irrigated and nonirrigated sorghum plots to display the same temperatures in the morning, while the nonirrigated plot was a few degrees warmer in the afternoon and exhibited considerable temperature variability. Mid-afternoon temperature differences of up to 12.8 C are found in the corn plots accompanied by a great amount of interplot variability. Significant changes in crop temperature, particularly on nonirrigated lands, are observed under variably cloudy skies, making it difficult to quantify the degree of stress under these conditions from temperature data. The data reveal the optimum time of day for detecting maximum plant temperatures to be between 1300 and 1500 h. Crop temperatures measured by attached leaf thermocouples are found to be within 1.2 and 2.6 C of IR thermometer temperatures for the unstressed and stressed plants, respectively. Finally, differences in seasonal evapotranspiration are found to be correlated with seasonally accumulated temperature differences. A.L.W.

A82-17998 The use of digitally processed Landsat imagery for vegetation mapping in Sulawesi, Indonesia. R. M. Warwick-Smith (London, University, London, England). *Remote Sensing Quarterly*, vol. 3, Apr. 1981, p. 21-26. 13 refs. Research supported by the Royal Aircraft Establishment.

N82-10489# Intermountain Forest and Range Experiment Station, Ogden, Utah.

LARGE-SCALE COLOR AERIAL PHOTOGRAPHY AS A TOOL IN SAMPLING FOR MORTALITY RATES

David A. Hamilton, Jr. Jan. 1981 14 p refs Sponsored by USDA Forest Service

(PB81-214777; FSRP/INT-269) Avail: NTIS HC A02/MF A01 CSCL 02F

Mortality rates specify the proportion of trees with a given set of characteristics that are expected to die in a fixed time interval. Results indicate that 1 year mortality trees can be dated and species can be assigned to green trees and to 1 year mortality trees with acceptable accuracy on 70 mm color photography at scales of 1:1600 and 1:2400. GRA

N82-11910# Army Engineer Waterways Experiment Station, Vicksburg, Miss. Environmental Lab.

01 AGRICULTURE AND FORESTRY

INCLUSION OF A SIMPLE VEGETATION LAYER IN TERRAIN TEMPERATURE MODELS FOR THERMAL INFRARED (IR) SIGNATURE PREDICTION Final Report, 1 Oct. 1979 - 1 Oct. 1980

Lee K. Ballick, Randy K. Scoggins, and Lewis E. Link, Jr. Aug. 1981 44 p refs
(DA Proj. 4A7-62730-AT-42; DA Proj. 4A7-62719-AT-40)
(AD-A104469; WES/MP/EL-81-4) Avail: NTIS HC A03/MF A01 CSCL 17/5

Thermal infrared signatures of natural and cultural features are dynamic, varying with time and weather conditions. Prediction of thermal signatures for specific conditions requires first that the actual temperature of the features be determined; for vegetation canopies this involves the average temperatures of canopy components and for planar (nonvegetated) surfaces the temperature of the surface. Models have been developed to handle layered vegetation canopies and layered ground surfaces; however, efforts have only begun to formulate a comparable capability for intermediate conditions such as grass covered surfaces where both the terrain surface and vegetation influence the average surface temperature. This report presents a procedure, named VEGIE, that predicts the temperature of terrain surfaces which contain a simple layer of vegetation. VEGIE is designed as an interim procedure for immediate application in lieu of more sophisticated and theoretical treatments of this problem. Operational flexibility and simplicity are preserved by using VEGIE as a submodel to the Terrain Surface Temperature Model (TSTM) developed previously at the U.S. Army Engineer Waterways Experiment Station. The TSTM predicts the surface temperature of nonvegetated layer and planar features using material thermophysical properties and meteorological conditions. These models are applied to a deciduous and a coniferous canopy where the CSU model is valid but VEGIE is not. VEGIE is applied to the problem of estimating thermal signatures for terrain surfaces with less than total foliage cover, the consequences of changes in foliage cover, differing emissivities for the soil and vegetation, and reflected sky radiation. GRA

N82-12500*# California Univ., Berkeley.

VEGETATION PATTERNS

David M. Carneggie and Brain T. Fine (California Univ. at Davis) In NASA. Johnson Space Flight Center Skylab Explores the Earth 1977 p 243-262 refs

Avail: NTIS MF A01; SOD HC \$16.50 CSCL 08F

In an effort to make meaningful observations of vegetation resources, the following sites and features were examined: (1) wheat in Argentina, Australia, and the U.S.; (2) rangelands in Australia, Africa, and the U.S.; (3) land use in Malaysia; (4) vegetation in New Zealand; (5) agriculture in California; (6) drought in northern Australia; (7) insect and disease damage in any of the sites; and (8) forest and range fires wherever found. The important factors that governed the ability of the crew to observe these features were angle of view from the spacecraft; atmospheric conditions; Sun angle; speed of the spacecraft; characteristics of natural and cultivated vegetation; and familiarity with the phenomena to be observed. User reaction to the imagery is discussed and photograph quality is evaluated. A.R.H.

N82-15480*# Environmental Research Inst. of Michigan, Ann Arbor. Infrared and Optics Div.

DEVELOPMENT AND EVALUATION OF AN AUTOMATIC LABELING TECHNIQUE FOR SPRING SMALL GRAINS Technical Report, 15 Nov. 1979 - 31 Dec. 1980

Eric P. Crist and William A. Malila, Principal Investigators Aug. 1981 67 p refs Sponsored by NASA, USDA, Dept. of Commerce, Dept. of Interior, and Agency for International Development ERTS

(Contract NAS9-15476; Proj. AgRISTARS)

(E82-10001; NASA-CR-161080; SR-EL-04065;

ERIM-152400-3-T) Avail: NTIS HC A04/MF A01 CSCL 05A

A labeling technique is described which seeks to associate a sampling entity with a particular crop or crop group based on similarity of growing season and temporal-spectral patterns of development. Human analyst provide contextual information, after which labeling decisions are made automatically. Results of a test of the technique on a large, multi-year data set are reported. Grain labeling accuracies are similar to those achieved

by human analysis techniques, while non-grain accuracies are lower. Recommendations for improvements and implications of the test results are discussed. Author

N82-15481*# South Dakota State Univ., Brookings. Remote Sensing Inst.

REMOTE SENSING APPLICATIONS TO RESOURCE PROBLEMS IN SOUTH DAKOTA Annual Progress Report, 1 Jul. 1980 - 30 Jun. 1981

Victor I. Myers, Principal Investigator 30 Jun. 1981 154 p refs Original contains color imagery. Original photography may be purchased from the EROS Data Center, Sioux Falls, S.D. 57198 ERTS

(Grant NGL-42-003-007)

(E82-10002; NASA-CR-164892; SDSU-RSI-81-11) Avail: NTIS HC A08/MF A01 CSCL 05A

The procedures used as well as the results obtained and conclusions derived are described for the following applications of remote sensing in South Dakota: (1) sage grouse management; (2) censusing Canada geese; (3) monitoring grasshopper infestation in rangeland; (4) detecting Dutch elm disease in an urban environment; (5) determining water usage from the Belle Fourche River; (6) resource management of the Lower James River; and (7) the National Model Implantation Program: Lake Herman watershed. A.R.H.

N82-15482*# California Univ., Berkeley. Space Sciences Lab.

APPLICATION OF REMOTE SENSING TO SELECTED PROBLEMS WITHIN THE STATE OF CALIFORNIA Annual Report

Robert N. Colwell, Principal Investigator, Andrew S. Benson, John E. Estes, and Claude Johnson 1 May 1981 258 p refs Original contains color imagery. Original photography may be purchased from the EROS Data Center, Sioux Falls, S.D. 57198. ERTS (Grant NsG-7220)

(E82-10004; NASA-CR-164893; SSL-Ser-22-Issue-18) Avail: NTIS HC A12/MF A01 CSCL 05A

Specific case studies undertaken to demonstrate the usefulness of remote sensing technology to resource managers in California are highlighted. Applications discussed include the mapping and quantization of wildland fire fuels in Mendocino and Shasta Counties as well as in the Central Valley; the development of a digital spectral/terrain data set for Colusa County; the Forsythe Planning Experiment to maximize the usefulness of inputs from LANDSAT and geographic information systems to county planning in Mendocino County; the development of a digital data bank for Big Basin State Park in Santa Cruz County; the detection of salinity related cotton canopy reflectance differences in the Central Valley; and the surveying of avocado acreage and that of other fruits and nut crops in Southern California. Special studies include the interpretability of high altitude, large format photography of forested areas for coordinated resource planning using U-2 photographs of the NASA Bucks Lake Forestry test site in the Plumas National Forest in the Sierra Nevada Mountains. A.R.H.

N82-15485*# Instituto de Pesquisas Espaciais, Sao Jose dos Campos (Brazil).

WHEAT CULTIVATION: IDENTIFICATION AND ESTIMATION OF AREAS USING LANDSAT DATA [CULTURA DO TRIGO IDENTIFICACAO E AVALIACAO DE AREAS ATRAVES DE DADOS DO LANDSAT]

Nelson deJesusParada, Principal Investigator, Francisco Jose Mendonca, Dall Arthur Cottrell, Antonio Tebaldi Tardin, David Chung Liang Lee, Yosio Edemir Shimabukuro, Mauricio Alves Moreira, and Angela Maria deLimaFernandoCelsoSoaresMaia May 1981 5 p refs In PORTUGUESE Sponsored by NASA ERTS

(E82-10007; NASA-CR-164905; INPE-2054-RPE/300) Avail: NTIS HC A02/MF A01 CSCL 02C

The feasibility of using automatically processed multispectral data obtained from LANDSAT to identify wheat and estimate the areas planted with this grain was investigated. Three 20 km by 40 km segments in a wheat growing region of Rio Grande do Sul were aerially photographed using type 2443 Aerochrome film. Three maps corresponding to each segment were obtained from the analysis of the photographs which identified wheat, barley, fallow land, prepared soil, forests, and reforested land. Using basic information about the fields and maps made from the photographed areas, an automatic classification of wheat

was made using MSS data from two different periods: July to September and July to October 1979. Results show that orbital data is not only useful in characterizing the growth of wheat, but also provides information of the intensity and extent of adverse climate which affects cultivation. The temporal and spatial characteristics of LANDSAT data are also demonstrated.

Transl. by A.R.H.

N82-15490*# Instituto de Pesquisas Espaciais, Sao Jose dos Campos (Brazil).

REMOTE SENSING IN FORESTRY: APPLICATION TO THE AMAZON REGION

Nelson deJesusParada, Principal Investigator, Antonio T. Tardin, Armando dosSantos, Pedro Hernandez Filho, and Yosio E. Shimabukuro Apr. 1981 72 p refs Sponsored by NASA ERTS

(E82-10012; NASA-CR-164755; INPE-2035-RPE/292) Avail: NTIS HC A04/MF A01 CSCL 02F

The utilization of satellite remote sensing in forestry is reviewed with emphasis on studies performed for the Brazilian Amazon Region. Timber identification, deforestation, and pasture degradation after deforestation are discussed. A.R.H.

N82-15491*# Lockheed Engineering and Management Services Co., Inc., Houston, Tex.

FISCAL YEAR 1980-81 IMPLEMENTATION PLAN IN SUPPORT OF TECHNICAL DEVELOPMENT AND INTEGRATION OF SAMPLING AND AGGREGATION PROCEDURES

Mar. 1981 88 p refs Sponsored by NASA, USDA, Dept. of Commerce, Dept. of Interior, and Agency for International Development ERTS

(Contract NAS9-15800; Proj. AgRISTARS)

(E82-10013; NASA-CR-161030; FC-LO-00612; LEMSCO-15168; JSC-16819) Avail: NTIS HC A05/MF A01 CSCL 02C

The specific objectives of the FY 1980-81 tasks are: (1) further refinements to the weighted aggregation procedure; (2) improved approaches for estimating within-stratum variance; (3) more intensive investigation of alternative sampling strategies such as full-frame sampling strategy, and (4) further developments in regard to a simulated approach for assessing the performance of the overall designed sampling and aggregation system. Author

N82-15492*# Lockheed Engineering and Management Services Co., Inc., Houston, Tex.

WINTERKILL INDICATOR MODEL, CROP CONDITION ASSESSMENT DIVISION (CCAD) DATA BASE INTERFACE DRIVER, USER'S MANUAL

R. F. Hansen, Principal Investigator Mar. 1981 13 p ref Sponsored by NASA, USDA, Dept. of Commerce, Dept. of Interior, and Agency for International Development ERTS

(Contract NAS9-15800; Proj. AgRISTARS)

(E82-10014; NASA-CR-161031; EW-L1-00713; LEMSCO-16033; JSC-17117) Avail: NTIS HC A02/MF A01 CSCL 02C

Instructions are given for using the Winterkill indicator model CCAD data base interface driver. The purpose of the system is to interface the Winterkill Indicator Model with the CCAD operational data base. The interface driver routine decides what meteorological stations should be processed and calls the proper subroutines to process the stations. Author

N82-15494*# National Aeronautics and Space Administration, Lyndon B. Johnson Space Center, Houston, Tex.

US/CANADA WHEAT AND BARLEY CROP CALENDER EXPLORATORY EXPERIMENT IMPLEMENTATION PLAN

Sep. 1980 23 p refs Sponsored by NASA, USDA, Dept. of Commerce, Dept. of Interior, and Agency for International Development ERTS

(Proj. AgRISTARS)

(E82-10016; NASA-TM-84034; FC-JO-00611; JSC-16812) Avail: NTIS HC A02/MF A01 CSCL 02C

A plan is detailed for a supplemental experiment to evaluate several crop growth stage models and crop starter models. The objective of this experiment is to provide timely information to aid in understanding crop calendars and to provide data that will allow a selection between current crop calendar models. Author

ENVIRONMENTAL CHANGES AND CULTURAL RESOURCES

Includes land use analysis, urban and metropolitan studies, environmental impact, air and water pollution, geographic information systems, and geographic analysis.

A82-10034 * **Introducing remote sensing to county-level agencies in Michigan through the Cooperative Extension Service.** W. R. Enslin and R. Hill-Rowley (Michigan State University, East Lansing, MI). In: American Society of Photogrammetry, Annual Meeting, 46th, St. Louis, MO, March 9-14, 1980, ASP Technical Papers. Falls Church, VA, American Society of Photogrammetry, 1980, p. 157-164. 11 refs. Research supported by the Michigan State University; Grant No. NGL-23-004-083.

State and regional planning agencies in Michigan are aware of remote sensing technology, however, many agencies at the county and township level have not been introduced to its potential. This paper describes an educational effort undertaken by the MSU Remote Sensing Project and the Michigan Cooperative Extension Service aimed at reaching local decision makers. Remote sensing materials and a questionnaire were used to elicit interest and aid in planning the program. A series of seven workshops were held throughout Michigan for governmental officials and the staff of public agencies from 38 counties. Emphasis was placed on the characteristics, availability and usefulness of remotely-sensed data through a series of successful applications conducted in the state. The workshops were highly successful and many local decision makers are not aware of a new tool to call upon in their responses to land use and natural resource concerns. (Author)

A82-10043 * **An improvement in land cover classification achieved by merging microwave data with Landsat multispectral scanner data.** S. T. Wu (NASA, National Space Technology Laboratories, Earth Resources Laboratory, Bay St. Louis, MS). In: American Society of Photogrammetry, Annual Meeting, 46th, St. Louis, MO, March 9-14, 1980, ASP Technical Papers. Falls Church, VA, American Society of Photogrammetry, 1980, p. 293-309. 5 refs.

The improvement in land cover classification achieved by merging microwave data with Landsat MSS data is examined. To produce a merged data set for analysis and comparison, a registration procedure by which a set of Seasat SAR digital data was merged with the MSS data is described. The Landsat MSS data and the merged Landsat/Seasat data sets were processed using conventional multi-channel spectral pattern recognition techniques. An analysis of the classified data sets indicates that while Landsat data delineate different forest types (i.e., deciduous/coniferous) and allow some species separation, SAR data provide additional information related to plant canopy configuration and vegetation density as associated with varying water regimes, and therefore allow for further subdivision in the classification of forested wetlands of the coastal region of the southern United States. B.J.

A82-10044 * **Preliminary results of mapping urban land cover with Seasat SAR imagery.** F. M. Henderson (New York, State University, Albany, NY), S. W. Wharton, and D. L. Toll (NASA, Goddard Space Flight Center, Greenbelt, MD). In: American Society of Photogrammetry, Annual Meeting, 46th, St. Louis, MO, March 9-14, 1980, ASP Technical Papers. Falls Church, VA, American Society of Photogrammetry, 1980, p. 310-317.

The detectability of urban land cover types is explored using digitally processed Seasat SAR imagery of the Denver, Colorado area. Test sites within the metropolitan area were selected to include a cross section of Anderson, et. al. Level II land cover classes and cover types representative of the urban area growth stages. Using the Image 100 interactive processing system each test site was level sliced in an attempt to define specific reflectance boundaries for each cover type and to determine the spectral and spatial characteristics of homogeneous response regions. The rural-urban fringe boundary was readily definable, but a precise Level I and Level II land cover classification was not possible. High density housing could be separated from low

density housing and from parks, but reflectance values were often look angle dependent. Confusion between some water and vegetation responses also posed problems. (Author)

A82-10616 **An investigation of a polar low with a spiral cloud structure.** E. Rasmussen (Copenhagen, University, Copenhagen, Denmark). *Journal of the Atmospheric Sciences*, vol. 38, Aug. 1981, p. 1785-1792. 9 refs.

A synoptic case study where a small-scale low, a so-called polar low, can be followed as a closed circulation on the surface maps around 2000 km from Iceland to the North Sea is presented. Satellite images show that the polar low develops a cloud pattern of convective clouds very much like that of a tropical cyclone. The 1000-500 mb thickness field shows that the polar low has a warm core during the time when it is best developed. It is concluded that the polar low discussed in this work probably is a phenomenon different from a comma cloud and also different from small-scale vortices associated with strong mid-tropospheric positive vorticity advection. (Author)

A82-10700 **Trace pollutant concentrations in a multiday smog episode in the California South Coast Air Basin by long path length Fourier transform infrared spectroscopy.** E. C. Tuazon, A. M. Winer, and J. N. Pitts, Jr. (California, University, Riverside, CA). *Environmental Science and Technology*, vol. 15, Oct. 1981, p. 1232-1237. 48 refs. U.S. Environmental Protection Agency Grant No. R-804546.

A82-11949 * **Automated analyzer for aircraft measurements of atmospheric methane and total hydrocarbons.** W. R. Cofer, III and G. C. Purgold (NASA, Langley Research Center, Hampton, VA). *Review of Scientific Instruments*, vol. 52, Oct. 1981, p. 1560-1564. 10 refs.

An automated methane/total hydrocarbon analyzer is presented, which can produce alternate methane/total hydrocarbon measurements every 7 seconds to provide the spatial resolution required for regional hydrocarbon measurements at aircraft speeds. The construction and sampling techniques developed for the aircraft mounted system are discussed. A technique to periodically measure atmosphere oxygen is incorporated into the analyzer to ensure accurate hydrocarbon measurements, and a data collection methodology is developed to minimize errors resulting from changes in flame ionization detector sensitivity at different altitudes. Aircraft data acquired at the 1979 Southeastern Virginia Urban Plume Study are also presented, which illustrate the application of the instrument to a troposphere pollution plume. D.L.G.

A82-12517 # **Spacelab-research of European regions with strong negative environmental influences, based on AVHRR-data of the satellites Tiros-N and NOAA.** H. Kaminski. In: International Scientific Conference on Space, 21st, Rome, Italy, March 25, 26, 1981, Proceedings. Rome, Rassegna Internazionale Elettronica Nucleare ed Aerospaziale, 1981, p. 197-206. 10 refs.

Remote sensing data from the Tiros-N-AVHRR satellites are considered as a base for further appraisals of air and water pollution in Europe by multispectral scanning from Spacelab. A short program is envisioned to verify the 10% anthropogenous induced clouding increase due to air traffic, as an aid to land use planning. Zones of meadows and woods between large towns are noted to be areas with no significant atmospheric heat build-up. Pollution from the Rhine and Po rivers has been sensed in the infrared and found to remain in coastal areas, mixing too slowly with sea water to disperse. A recommendation is offered to change the declination of Spacelab's orbit from 50 to 55 deg to allow more accurate sensing of pollutant problems in Belgium, the Netherlands, West Germany, and Italian industrialized regions. M.S.K.

A82-12591 **Areawide soil loss predictions using CIR air-photos.** K. M. Morgan (Texas Christian University, Fort Worth, TX) and R. Nalepa. In: Civil engineering applications of remote sensing; Proceedings of the Specialty Conference, Madison, WI, August 13, 14, 1980. New York, American Society of Civil

02 ENVIRONMENTAL CHANGES AND CULTURAL RESOURCES

Engineers, 1980, p. 24-32. 10 refs. Research supported by the Texas Christian University Research Foundation.

It is pointed out that the Universal Soil Loss Equation (USLE) is a widely accepted tool for erosion prediction and conservation planning. In this study, manual interpretation of color infrared photography is used, along with the USLE and a computer-land information system, to identify critical areas of soil loss in Quil Miller Creek watershed in Johnson County, Texas. The low altitude color infrared photos used to record land use activities are at a scale of 1:48,000. C.R.

A82-12594 Remote sensing that motivated community action. R. H. Brownlee, J. P. Scherz (Wisconsin, University, Madison, WI), and J. M. Dennis (Chetek High School, Chetek, WI). In: Civil engineering applications of remote sensing; Proceedings of the Specialty Conference, Madison, WI, August 13, 14, 1980. New York, American Society of Civil Engineers, 1980, p. 60-77.

An account is given of the way in which the algal problem afflicting Prairie Lake, near Chetek, Wisconsin, was solved. Lake classification schemes developed at the University of Wisconsin with Multispectral Landsat Analysis indicated the source of pollution to be at the mouth of Rice Creek, which emptied into the lake. High-level and low-level aerial photos of the creek showed a cattle feedlot located near springs which fed into the creek. When residents of the area were shown the remote sensing data, they took steps to ensure that fewer cows used the spring. This solved the problem. C.R.

A82-12816 Study of stack emissions by combination of lidar and correlation spectrometer. P. Camagni, E. De Blust, C. Koehler, R. Michelon, A. Pedrini, M. De Groot, and S. Sandroni (Commission of the European Communities, Joint Research Centre, Ispra, Italy). *Nuovo Cimento C, Serie 1*, vol. 4C, May-June 1981, p. 359-371. 6 refs.

Examples are presented of the application of the combined techniques of lidar and correlation spectrometry to the monitoring of stack plume pollutants. Following a brief review of the principles of lidar observation of scattering particle spatial distribution and mask correlation spectrometer determination of gas integral-path thickness, attention is given to the results of combined measurements of particle and SO₂ distributions above the three tallest stacks of the ENEL power plant at Turbigo, Italy. It is found that the plume aerosols behave differently from the gas component, which result demonstrates the potential of the combination technique in mass balance and mass flow evaluation. A.L.W.

A82-13268 * Nitric oxide delta band emission in the earth's atmosphere - Comparison of a measurement and a theory. D. W. Rusch (Colorado, University, Boulder, CO) and W. E. Sharp (Michigan, University, Ann Arbor, MI). *Journal of Geophysical Research*, vol. 86, Nov. 1, 1981, p. 10111-10114. 21 refs. Grants No. NSG-5372; No. NGR-23-005-360.

Attention is given to the altitude dependent emission rate in the delta-bands of nitric oxide as measured in the earth's atmosphere at night by a scanning ultraviolet spectrometer. It is noted that the reaction responsible is the two-body association of nitrogen and oxygen atoms. The measurements show a vertical intensity beneath the layer for the delta-band system of 19 R. The horizontal emission rate is found to increase from 70 R at 117 km to 140 R at 150 km. The data are analyzed with a one-dimensional, time-dependent, vertical-transport model of odd nitrogen photochemistry. The calculated and measured intensities agree so long as the quenching of N(2D) by atomic oxygen is near 5×10 to the -13 cu cm/sec. C.R.

A82-14320 Radiative heating rates and some optical properties of the St. Louis aerosol, as inferred from aircraft measurements. T. J. Method and T. N. Carlson (Pennsylvania State University, University Park, PA). *Atmospheric Environment*, vol. 16, no. 1, 1982, p. 53-66. 25 refs. U.S. Environmental Protection Agency Grants No. R-805500-01; No. R-806048-01-2.

Analyses of airborne measurements of solar and terrestrial radiation and aerosol profile measurements of the St. Louis

boundary layer collected during two summers are summarized. Spectral pyranometers, radiometers, a pyrgeometer, an automatic particle counter, and an integrating nephelometer were used to collect data samples on 20 profile flights. Estimates of the vertical flux divergence and aerosol heating rates for solar, longwave, and total spectrum fluxes, in addition to total bulk estimates of aerosol parameters are provided. Results include a maximum aerosol heating in the visible exceeding three C/day near the bottom of the mixing layer, solar heating near one C/day near the ground, and zero heating near the top of the mixing layer. The total short and longwave radiative heating rates were slightly negative; with large particle aerosol concentration, the greatest extinction was near the surface. It is concluded that although St. Louis has a slightly greater aerosol loading than surrounding rural areas, the findings do not differ greatly from weakly absorbing natural soil particles commonly observed over nonurban and semiarid regions. M.S.K.

A82-15027 Thermal inertia, thermal admittance, and the effect of layers. G. F. Byrne and J. R. Davis (Commonwealth Scientific and Industrial Research Organization, Div. of Land Use Research, Canberra, Australia). *Remote Sensing of Environment*, vol. 9, June 1980, p. 295-300. 12 refs.

The effect of a diurnally varying flux on a solid surface is analysed in terms of thermal admittance, the reciprocal of complex thermal conductance. The presence of a surface layer of differing thermal characteristics from the bulk material, which can significantly affect the phase and amplitude of the temperature wave of the exposed surface, is discussed in terms of the admittance concept. It is suggested that the latter concept provides a better approach to the characterization of solid surfaces, particularly in the remote sensing context where varying water contents or organic materials are involved. (Author)

A82-15749 Aerial-photography flights over Upper Franconia in 1980 - Operation and first application-related experience (Die Luftbildbefliegung Oberfranken 1980 - Ablauf und erste Anwendungserfahrungen). B. Arnal (Höhere Landesplanungsbehörde, Bayreuth, West Germany). *Bildmessung und Luftbildwesen*, vol. 49, Nov. 1, 1981, p. 205-208. In German.

A82-15965 † Study of the anthropogenic influence on the environment, based on multispectral scanning images (Izuchenie antropogennogo vozdeistviia na prirodnuu sredu po materialam mnogoazonal'noi skanernoi s'emki). V. I. Kravtsova and I. S. Nizkaia (Moskovskii Gosudarstvennyi Universitet, Moscow, USSR). *Issledovanie Zemli iz Kosmosa*, Sept.-Oct. 1981, p. 117-123. In Russian.

The possibilities of using images obtained by the Fragment multispectral scanning system to study the anthropogenic influence on the environment are analyzed. The analysis uses the taiga regions of the north European part of the USSR and the desert regions of Central Asia as examples. Maps are compiled of the anthropogenic influence on forest vegetation in the Kotlas region and on the desert landscapes of the central Ustiurt plateau. It is shown that the data obtained by the Fragment system are useful for establishing the occurrence, character, and degree of landscape changes; it can be used to compile thematic maps, to make recommendations on the use of resources, and to predict unfavorable effects of intense anthropogenic influences. J.F.

A82-15966 † Investigation and mapping of the erosion relief of the Kalachkaia upland on the basis of multispectral scanner images (Izuchenie i kartografirovaniye erozionnogo rel'efa Kalachskoi vozvshennosti po mnogoazonal'nym skanernym snimkam). N. I. Lapteva and N. N. Tal'skaia (Moskovskii Gosudarstvennyi Universitet, Moscow, USSR). *Issledovanie Zemli iz Kosmosa*, Sept.-Oct. 1981, p. 124-129. 5 refs. In Russian.

Geomorphological, lithological, and erosion maps were compiled for the Kalachkaia upland on the basis of the interpretation of multispectral scanner images obtained in different seasons with the Meteor-satellite Fragment system. The resolution and reliability of the images make it possible to convey the morphological structural plan of the region, the natural pattern, and the density of valleys and ravines. It is shown that the Fragment images can be effectively used to study the erosion relief of plains and to compile medium-scale geomorphological maps. B.J.

02 ENVIRONMENTAL CHANGES AND CULTURAL RESOURCES

A82-15967 † Space photographs obtained with the Fragment system as a base for landscape mapping and physical-geographical classification of arid territories (Kosmicheskie snimki, poluchennyye sistemoi 'Fragment' kak osnova landshaftnogo kartografirovaniia i fiziko-geograficheskogo raionirovaniia aridnykh territorii). L. I. Ivashutina and V. A. Nikolaev (Moskovskii Gosudarstvennyi Universitet, Moscow, USSR). *Issledovanie Zemli iz Kosmosa*, Sept.-Oct. 1981, p. 130-138. 9 refs. In Russian.

Space images obtained with the Meteor-satellite Fragment system have high landscape resolution and make it possible to investigate landscape structures of arid territories on several geosystem levels, from natural landscapes to physical-geographical regions. Detailed medium-scale landscape schemes of the southern Mugodzhazhar desert regions and of the northern Ustiurt were composed along with a consolidated scheme of physical-geographical division. Various interpretation criteria were used, the most important of which were optical density and image pattern. B.J.

A82-15968 Analysis of variance of thematic mapping experiment data. G. H. Rosenfield (U.S. Geological Survey, Reston, VA). *Photogrammetric Engineering and Remote Sensing*, vol. 47, Dec. 1981, p. 1685-1692. 23 refs.

The considered study has the objective to determine and document for the remote sensing researcher the minimum statistical methodology needed to perform and interpret an analysis of variance experiment. To illustrate the procedures, a set of data from the National Land Use and Land Cover Mapping Program of the U.S. Geological Survey was used. The set of proportions of correctly interpreted test data was subjected to three treatments of transformation as suggested by Snedecor and Cochran (1967). The transformed data were tested for the three assumptions of analysis of variance, taking into account normality, homogeneity of variance, and additivity. A weighted analysis of variance was performed, and multiple range tests were applied to those computed means deemed significant. From this research, a data analysis method and an operational computer program were developed to assist the analyst in considering the theoretical statistical concepts that are important for solving this type of problem. G.R.

A82-16325 Upper tropospheric cyclonic vortices in the tropical South Atlantic. V. E. Kousky and M. A. Gan (Conselho Nacional de Desenvolvimento Científico e Tecnológico, Instituto de Pesquisas Especiais, São José dos Campos, São Paulo, Brazil). *Tellus*, vol. 33, Dec. 1981, p. 538-551. 15 refs. Financiadora de Estudos e Projetos Contract No. B/28-79-002-00-00; Conselho Nacional de Pesquisas Contract No. 37/78.

An analysis of subtropical 200 mb cyclones is made for the South Atlantic. The cyclones are observed to occur primarily during the summer months and generally form near the axes of the mid-oceanic troughs. The relationship between cyclone formation and the presence of 200 mb anticyclones over the continental areas is discussed. Proposed mechanisms for cyclone formation are considered. The cyclones are characterized by a cold core and a direct thermal circulation - the cold air sinking and warm air on the periphery rising. The cloud pattern associated with the cyclones is found to depend on the direct thermal circulation, the vortex location and its direction of movement. The effects of South Atlantic 200 mb cyclonic vortices on Brazilian weather are discussed. (Author)

A82-16619 † Polarimetric surveys of oil slicks (Poliariatsionnaia s'emka neftiannykh zagriaznenii vodnoi poverkhnosti). B. S. Zhukov. In: Airborne and spaceborne multispectral photography of the earth. Moscow, Izdatel'stvo Nauka, 1981, p. 175-188. 16 refs. In Russian.

A theoretical study is presented of polarimetric remote-sensing surveys of oil slicks. The oil-water contrast is calculated as a function of the polarimetric analyzer, the spectral range, the thickness of the slick, and the transparency of the water. The influence of the atmosphere on the remote measurements of oil slicks is analyzed, and polarimetric measurement data on oil slicks are presented. B.J.

A82-16837 * A new method for inferring carbon monoxide concentrations from gas filter radiometer data. H. A. Wallio, H. G.

Reichle, Jr. (NASA, Langley Research Center, Hampton, VA), J. C. Casas (Old Dominion University, Norfolk, VA), and B. B. Gormsen (Systems and Applied Sciences Corp., Hampton, VA). In: Conference on Atmospheric Radiation, 4th, Toronto, Canada, June 16-18, 1981, Preprints. Conference sponsored by the American Meteorological Society, Boston, MA, American Meteorological Society, 1981, p. 248-254. 14 refs.

A method for inferring carbon monoxide concentrations from gas filter radiometer data is presented. The technique can closely approximate the results of more costly line-by-line radiative transfer calculations over a wide range of altitudes, ground temperatures, and carbon monoxide concentrations. The technique can also be used over a larger range of conditions than those used for the regression analysis. Because the influence of the carbon monoxide mixing ratio requires only addition, multiplication and a minimum of logic, the method can be implemented on very small computers or microprocessors. D.L.G.

A82-17841 * # Results from the July 1981 Workshop on Passive Remote Sensing of the Troposphere. L. S. Keafer, Jr. and H. G. Reichle, Jr. (NASA, Langley Research Center, Hampton, VA). *American Institute of Aeronautics and Astronautics, Aerospace Sciences Meeting, 20th, Orlando, FL, Jan. 11-14, 1982, Paper 82-0207*. 8 p. 6 refs.

Potential roles of passive remote sensors in the study of the chemistry and related dynamics of the lower atmosphere were defined by a Tropospheric Passive Remote Sensing Workshop, and technology advances required to implement these roles were identified. A promising role is in making global-scale, multiflayer measurements of the more abundant trace tropospheric gaseous species (e.g., O₃, CO, CH₄, HNO₃) and of aerosol thickness and size distribution. It includes both nadir- and limb-viewing measurements. Technology advances focus on both scanning- and fixed-spectra, nadir-viewing techniques with resolutions of 0.1 kaysers or better. Balloon- and Shuttle-borne experiments should be performed to study the effects of instrument noise and background fluctuations on data inversion and to determine the utility of simultaneously obtained nadir- and limb-viewing data. (Author)

A82-18052 # The radiowave propagation environment - Science and technology objectives for the 80's. J. M. Goodman (U.S. Navy, E. O. Hulburt Center for Space Research, Washington, DC) and J. Aarons (USAF, Geophysics Laboratory, Bedford, MA). In: Symposium on the Effect of the Ionosphere on Radiowave Systems, Washington, DC, April 14-16, 1981, Preprints. Washington, DC, U.S. Naval Research Laboratory, 1981. 10 p.

The ionosphere has a strong influence on the personality of radiowaves which propagate beneath, within, or through it; and this influence derives from the spatial and temporal nonuniformity in the refractivity of the magneto-ionic medium. Basic research objectives in environmental monitoring are examined, taking into account ionospheric research, magnetospheric research, interplanetary field and solar wind research, solar radiation and magnetic field research, and propagation studies. Operational systems which basic research will support are related to communications systems, navigation systems, and surveillance. Environmental effects/system deficiencies by frequency band are discussed, giving attention to the ELF frequency band (30-300 Hz), the VLF band (3-30 kHz), the MF/HF band (300 kHz - 30 MHz), and the UHF/SHF (300 MHz - 30 GHz). It is concluded that there is already a need to study the ionosphere and its coupling to the magnetosphere above and the troposphere below in order to more fully develop the insight required to specify the radiowave propagation effects introduced by the various media. G.R.

N82-11513*# Environmental Research and Technology, Inc., Concord, Mass.

AN EVALUATION OF THE SPATIAL RESOLUTION OF SOIL MOISTURE INFORMATION Final Report

Kenneth R. Hardy, Stephen H. Cohen, Linda Koshio Rogers, Hsiao-hua K. Burke, Robert C. Leupold, and Michael D. Smallwood Mar. 1981 83 p refs

(Contract NAS5-25527)

(NASA-CR-166724; ERT-P-7505-F)

Avail: NTIS

HC A05/MF A01 CSCL 08M

Rainfall-amount patterns in the central regions of the U.S.

02 ENVIRONMENTAL CHANGES AND CULTURAL RESOURCES

were assessed. The spatial scales of surface features and their corresponding microwave responses in the mid western U.S. were investigated. The usefulness for U.S. government agencies of soil moisture information at scales of 10 km and 1 km. was ascertained. From an investigation of 494 storms, it was found that the rainfall resulting from the passage of most types of storms produces patterns which can be resolved on a 10 km scale. The land features causing the greatest problem in the sensing of soil moisture over large agricultural areas with a radiometer are bodies of water. Over the mid-western portions of the U.S., water occupies less than 2% of the total area, the consequently, the water bodies will not have a significant impact on the mapping of soil moisture. Over most of the areas, measurements at a 10-km resolution would adequately define the distribution of soil moisture. Crop yield models and hydrological models would give improved results if soil moisture information at scales of 10 km was available. A.R.H.

N82-11514*# Jet Propulsion Lab., California Inst. of Tech., Pasadena.

RADAR MAPPING, ARCHAEOLOGY, AND ANCIENT LAND USE IN THE MAYA LOWLANDS

R. E. W. Adams (Cambridge Univ.), W. E. Brown, Jr., and T. Patrick Culbert (Arizona Univ.) 31 Mar. 1981 27 p refs (Contract NAS7-100)

(NASA-CR-164931) Avail: NTIS HC A03/MF A01 CSCL 08B

Data from the use of synthetic aperture radar in aerial survey of the southern Maya lowlands suggest the presence of very large areas drained by ancient canals for the purpose of intensive cultivation. Preliminary ground checks in several very limited areas confirm the existence of canals and raised fields. Excavations and ground surveys by several scholars provide valuable comparative information. Taken together, the new data suggest that Late Classic period Maya civilization was firmly grounded in large-scale and intensive cultivation of swampy zones. A.R.H.

N82-11536# Hawaii Univ., Honolulu. Dept. of Planning and Economic Development.

A METHOD FOR USING AERIAL PHOTOS IN DELINEATING HISTORIC PATTERNS OF BEACH ACCRETION AND RETREAT

Dennis Hwang Dec. 1980 50 p refs (Contract NA79AA-D-00085)

(PB81-223836; UNIH-SG-CR-81-04; NOAA-81042706) Avail: NTIS HC A03/MF A01 CSCL 08C

A method is presented with a maximum estimated error of about 12 feet for measuring beach changes. This is believed to be an accurate estimate, as indicated by a comparison of field and photographic measurements and by the consistent distances obtained for nearby sections of the beach in the Kailua pilot study. The methods described in this report were applied for a pilot study of Kailua Beach. GRA

N82-11635*# Mitre Corp., McLean, Va. Metrek Div. **SHUTTLE APPLICATIONS IN TROPOSPHERIC AIR QUALITY OBSERVATIONS Final Report**

E. Friedman, J. Gupta, and J. Carmichael Aug. 1978 122 p refs Sponsored by NASA

(Contract F19628-78-C-001) (NASA-CR-145374) Avail: NTIS HC A06/MF A01 CSCL 13B

The role which might be played by the space shuttle in obtaining data which describes the air quality of the north-eastern United States was investigated. The data requirements of users, a model for statistical interpretation of the observations, the influence of orbit parameters on the spatial and temporal sampling and an example of application of the the model were considered. R.J.F.

N82-11639# Atmospheric Radiation Consultants, Acton, Mass. **PROOF OF CONCEPT STUDY**

A. S. Zachor, F. P. DelGreco, and M. Ahmadjian (AFGL) Hanscom AFB, Mass. AFGL 23 Mar. 1981 42 p refs Prepared for Utah State Univ., Logan

(Contract F19628-77-C-0203; AF Proj. 2310) (AD-A104338; AFGL-TR-81-0134; SR-6) Avail: NTIS HC A03/MF A01 CSCL 17/5

Field test data were analyzed and computer simulations

performed to validate the predictions of an earlier study, which calculated the minimum detectable quantities (MDQ's) of trace gases that can be detected remotely using high-resolution spectroscopy. The study demonstrates convincingly that reliable detection can be achieved near the MDQ level in a benign real-world environment. Author (GRA)

N82-11649# Sandia Labs., Albuquerque, N. Mex.

ENVIRONMENTAL MONITORING REPORT, SANDIA NATIONAL LABS., ALBUQUERQUE, NEW MEXICO, 180

Gloria Chavez Millard, Theodore N. Simmons, Charles E. Gray, and Bill L. O'Neal Apr. 1981 27 p refs (Contract DE-AC04-76DP-00789)

(DE81-027839; SAND-81-0566) Avail: NTIS HC A03/MF A01

Radionuclides are potentially released from five technical areas from the laboratories research activities. The program searches for cesium-137, tritium, uranium, alpha emitters, and beta emitters in water, soil, air, and vegetation. No activity was found in public areas in excess of that found in local background in 1980. The Albuquerque population receives only 0.11 person-rem (estimated) from airborne radioactive releases. While national security research is the laboratories major responsibility, energy research is a major area of activity. Both these research areas cause radioactive releases. T.M.

N82-11718 Washington Univ., Seattle. **ADAPTATION OF LAND USE TO SURFICIAL GEOLOGY IN METROPOLITAN WASHINGTON, D.C. Ph.D. Thesis**

Robert Houston Alexander 1981 236 p- Avail: Univ. Microfilms Order No. 8121177

Implicit in the investigation is a process of communicating geologic information, and incorporating such information into land-use decisions. Land-use data were derived from high-altitude color infrared aerial photography, and the information on geologic suitability was obtained from a U.S. Geological Survey map of landforms and surface materials compiled to aid non-geologists in land use planning decisions. The new map was further interpreted and subdivided into those areas geologically suitable and unsuitable for residential and agricultural uses, respectively. The study found significant relationships among land uses and geologic map units, and significant differences in land-use and geologic suitability regimes in subregions based on distance from city center. More recently-developed areas near the urban core have higher proportional associations of residential and agricultural land use with appropriate surficial geologic characteristics than do the outlying areas on the metropolitan fringe. Dissert. Abstr.

N82-12499*# Texas Univ. at Austin. **CULTURAL FEATURES IMAGED AND OBSERVED FROM SKYLAB 4**

Robert K. Holz *In* NASA. Johnson Space Flight Center Skylab Explores the Earth 1977 p 225-242 refs

Avail: NTIS MF A01; SOD HC \$16.50 CSCL 08B

Data from Skylab 4 observations of metropolitan complexes are limited to city outline, major transportation arteries, suburban built-up areas, overall textural patterns of the city as compared to those of adjacent areas, and the color or albedo. Typical agricultural patterns, forest regions, and transportation networks on rural landscapes can be discerned, as well as the disturbances of soil during construction and mining which expose surface materials of a different albedo. Photographs of Denver, Colorado; San Antonio, Texas, Chicago, Illinois, and San Diego, California are analyzed. A.R.H.

N82-12505*# Air Resources Lab., Las Vegas, Nev. **QUANTITATIVE ANALYSIS OF ATMOSPHERIC POLLUTION PHENOMENA**

Darryl Randerson *In* NASA. Johnson Space Flight Center Skylab Explores the Earth 1977 p 381-406 refs

Avail: NTIS MF A01; SOD HC \$16.50 CSCL 13B

Approximately 75 photographs of air pollution events were taken during the 84-day Skylab 4 mission. This imagery may be separated into two categories according to the sources of the pollution: natural pollution, which consists of dust generated by wind, naturally induced forest fires, and smoke generated by volcanic activity, and manmade pollution, which includes brush fires, smoke plumes from stacks or open burning, contrails, and

02 ENVIRONMENTAL CHANGES AND CULTURAL RESOURCES

ship trails. Results of the analysis of some of the most interesting photographs are discussed in this section. Photographs of the following are analyzed: the Sakura-zime volcanic activity; dust clouds, the Los Angeles pollution pall; long smoke plumes; an African brush fire, an Argentine forest fire, cirrus cloud plumes, and a snow streak. A.R.H.

N82-12506*# National Aeronautics and Space Administration. Goddard Space Flight Center, Greenbelt, Md.

METEOROLOGICAL LAB APPLICATIONS OF SKYLAB HANDHELD-CAMERA PHOTOGRAPHS

W. C. Skillman and William E. Shenk *In* NASA, Johnson Space Flight Center *Skylab Explores the Earth* 1977 p 407-416

Avail: NTIS MF A01; SOD HC \$16.50 CSCL 04B

The high resolution and image contrast of Skylab 4 photographs reveal details of the cloud structure associated with extratropical storms that normally cannot be seen in routinely available meteorological satellite images. A stereopair take over southern Arizona and northwestern Mexico east of the Gulf of California provides a good example of the cirrus clouds associated with a subtropical jet stream and demonstrates the height differences of multilayered clouds. The effects of cold air flowing over the warmer waters of the eastern Great Lakes, New York, southern New England, and the Atlantic Ocean are detailed as well as the cloud structure of an occluded cyclone. A.R.H.

N82-12507*# National Hurricane and Experimental Meteorology Lab., Coral Gables, Fla.

SOME ASPECTS OF TROPICAL STORM STRUCTURE REVEALED BY HANDHELD-CAMERA PHOTOGRAPHS FROM SPACE

Peter G. Black *In* NASA, Johnson Space Flight Center *Skylab Explores the Earth* 1977 p 417-462 refs

Avail: NTIS MF A01; SOD HC \$16.50 CSCL 04B

The most important contribution to the fields of tropical storm research was the stereophotography of tropical storm Ellen during the Skylab 4 mission. Features of mature tropical storms revealed by Skylab 4 photographs are discussed and compared with data obtained by NOAA-2, Nimbus-5, and a DMSP satellite. A.R.H.

N82-12508*# Chicago Univ., Ill.
MESOSCALE WAKE CLOUDS IN SKYLAB PHOTOGRAPHS

T. Theodore Fujita and Jaime J. Tecson *In* NASA, Johnson Space Flight Center *Skylab Explores the Earth* 1977 p 463-478 refs

Avail: NTIS MF A01; SOD HC \$16.50 CSCL 04B

Examination of mesoscale cloud patterns within the wakes of obstacles seen in Skylab photographs reveals the existence of specific types of wake clouds. Cumulus streets occur when the lapse rate above the surface is adiabatic with a medium to slow flow rate. Karman vortex streets occur when the lapse rate above the surface is small, zero, or negative, with a slow to medium flow impinging against a relatively large obstacle. Wake waves occur when the lapse rate above the surface is small with a medium to fast flow rate impinging against a relatively small obstacle. When the flow rate exceeds a critical value, the transverse waves tend to disappear, leaving only the diverging waves. These phenomena are illustrated in Skylab photographs of the Aleutian Islands, the Kuril Islands, the Antipodes, South Pacific Islands, and the Bouvet Island in the South Atlantic. A.R.H.

N82-12509*# National Aeronautics and Space Administration. Lyndon B. Johnson Space Center, Houston, Tex.

MESOSCALE CLOUD FEATURES OBSERVED FROM SKYLAB

David E. Pitts, J. T. Lee (National Severe Storms Lab.), J. Fein (Oklahoma Univ., Norman), Y. Sasaki (Oklahoma Univ., Norman), Kit Wagner, and R. Johnson (Lockheed Electronics Co., Houston, Tex.) *In* *its* *Skylab Explores the Earth* 1977 p 479-501 refs

Avail: NTIS MF A01; SOD HC \$16.50 CSCL 04B

The Skylab 4 mission study of severe storm development was designed to photograph cloud-street patterns, to estimate the physical dimensions of cloud streets, and to describe their relationship to other cloud features and to land features. The moisture convergence of cloud streets and whether cloud-street

curvature was an indicator of the source of angular momentum that results in the generation of rotating storms as precursors to tornadoes was analyzed from photographs taken over the Great Lakes and South America. A.R.H.

N82-12511# Utah State Univ., Logan. Electro-Dynamics Lab.

LIMIT ON REMOTE FTIR DETECTION OF TRACE GASES

A. S. Zachor (Atmospheric Radiation Consultants, Inc.), B. Bartschi, and M. Ahmadjian (AFGL) Sep. 1981 7 p refs

(Contract F19628-77-C-0203; AF Proj. 7670)

(AD-A104842; AFGL-TR-81-0272)

Avail: NTIS

HC A02/MF A01 CSCL 20/6

We studied the capability of a Fourier spectrometer system to remotely detect trace gases in localized clouds, e.g., stationary source effluents. Detection is based on the degree to which the observed IR spectral radiance contrast between the cloud and adjacent background is correlated with a computed reference spectrum. It is shown that trace gases can be reliably detected when spectral features are well below the noise level. The minimum detectable quantities (MDQ's) for various trace gases at one atmosphere total pressure are given. The MDQ's determine the combinations of gas column thickness and gas-background temperature difference that correspond to 95 percent detection probability and one percent false detection probability when an FTS system with modest-size foreoptics views the target through a path equivalent to approximately one air mass. Author (GRA)

N82-12685* National Aeronautics and Space Administration. Pasadena Office, Calif.

MICROWAVE LIMB SOUNDER Patent

Jacob J. Gustincic, inventor (to NASA) (JPL, California Inst. of Tech., Pasadena) Issued 4 Aug. 1981 9 p Filed 24 Sep. 1979 Supersedes N79-34014 (17 - 24, p 3285) Sponsored by NASA

(NASA-Case-NPO-14544-1; US-Patent-4,282,525;

US-Patent-Appl-SN-078612; US-Patent-Class-343-100ME;

US-Patent-Class-343-100PE; US-Patent-Class-343-781P) Avail:

US Patent and Trademark Office CSCL 04A

Trace gases in the upper atmosphere can be measured by comparing spectral noise content of limb soundings with the spectral noise content of cold space. An offset Cassegrain antenna system and tiltable input mirror alternately look out at the limb and up at cold space at an elevation angle of about 22. The mirror can also be tilted to look at a black body calibration target. Reflection from the mirror is directed into a radiometer whose head functions as a diplexer to combine the input radiation and a local oscillator (klystron) beam. The radiometer head is comprised of a Fabry-Perot resonator consisting of two Fabry-Perot cavities spaced a number of half wavelengths apart. Incoming radiation received on one side is reflected and rotated 90 deg in polarization by the resonator so that it will be reflected by an input grid into a mixer, while the klystron beam received on the other side is also reflected and rotated 90 deg, but not without passing some energy to be reflected by the input grid into the mixer.

Official Gazette of the U.S. Patent and Trademark Office

N82-12707# Automation Industries, Inc., Silver Spring, Md. Vitro Labs. Div.

ENVIRONMENTAL DATA FOR SITES IN THE NATIONAL SOLAR DATA NETWORK

Aug. 1981 176 p Prepared for Argonne National Lab.

(Contract DE-AC01-79CS-30027)

(DE82-000071; SOLAR/0010-81/08)

Avail: NTIS

HC A09/MF A01

Environmental information collected at the sites of the National Solar Data Network is tabulated for each solar site. The sites are grouped into 12 zones, each of which consists of several adjacent states. The insolation table presents the total, diffuse, direct, maximum, and extraterrestrial radiation for the site. It also shows the ratio of total to extraterrestrial radiation. The temperature table gives the average, daytime, nighttime, maximum, minimum, and inlet-water temperature for the site. All of the passive and some active solar sites are equipped with wind sensors which provide information on wind speed and direction. For some sites, a humidity table provides relative humidity values for day and night. It also gives values for the maximum and minimum humidity for each day. A technical

02 ENVIRONMENTAL CHANGES AND CULTURAL RESOURCES

discussion of the instruments and measurements used to obtain the data is included. DOE

N82-12714 Meteorologisches Observatorium, Hohenpeissenberg (West Germany).

SPECIAL OBSERVATIONS BY THE HOHENPEISSENBERG METEOROLOGICAL OBSERVATORY. NUMBER 42: RESULTS OF AEROLOGICAL AND SURFACE OZONE MEASUREMENTS DURING THE FIRST SEMESTER OF 1980 [SONDERBEOBACHTUNGEN DES METEOROLOGISCHEN OBSERVATORIUMS HOHENPEISSENBERG. NR 42: ERGEBNISSE DER AEROLOGISCHEN UND BODENNAHEN OZONMESSUNGEN IM 1. HALBJAHR 1980]

1980 194 p refs In GERMAN and ENGLISH

(Sonderbeob-42; ISSN-0581-1287) Avail: Issuing Activity

Tabular and graphical ozonometry results are presented. Surface ozone measurement data cover day of measurement, daily mean of ozone near the ground (nbar), daily maximum of ozone near the ground (nbar), hour of maximum (GMT), duration of extreme values in excess of 100 nbar in tens of minutes, daily minimum (nbar), and monthly mean (without extreme values). Total ozone measurement data, determined by Dobson-spectrophotometer, include day of measurement, time of observation, type of measurement, i.e., direct Sun blue zenith, number of measurements for daily mean, and total ozone amount for AD and C wavelengths (daily mean values). The pairs of wavelengths used are: 305.5 nm, 325.4 nm; 311.45 nm, 332.4 nm; and 317.6 nm, 339.8 nm. Author (ESA)

N82-13669# Meteorology Research, Inc., Santa Rosa, Calif. **AIRCRAFT DATA SUMMARIES OF THE SURE INTENSIVES, VOLUME 4 Final Report**

W. S. Keifer, D. L. Blumenthal, J. B. Tommerdahl, J. A. Anderson, J. A. McDonald, R. B. Strong, and J. H. White Sep. 1981 190 p Sponsored by Electric Power Research Inst. Prepared in cooperation with Research Triangle Inst., Research Triangle Park, N.C.

(EPRI Proj. RP-862)

(DE82-900311; EPRI-EA-1019-Vol-4) Avail: NTIS HC A09/MF A01

As part of the sulfate regional experiment (SURE), six air quality sampling programs were conducted in the eastern United States using instrumented aircraft. The air quality and meteorological samples were taken near the Duncan Falls, Ohio sulfate regional experiment (SURE) Station and near the Research Triangle Park, North Carolina, SURE Station. Sampling data are presented for all measured parameters. DOE

N82-13631# National Oceanic and Atmospheric Administration, Boulder, Colo.

GEOPHYSICAL MONITORING FOR CLIMATIC CHANGE, NUMBER 8: SUMMARY REPORT, 1979

Gary A. Herbert Dec. 1980 129 p refs

(PB81-233355; NOAA-81062615) Avail: NTIS HC A07/MF A01 CSCL 04B

Continuous measurement of CO₂ and aerosol scattering at four wavelengths, using a nephelometer, began at the South Pole station. A filter collection system was installed at the Barrow station to make possible the determination of the mass of the carbonaceous aerosols. It is shown that graphic carbon makes up a significant part of the arctic haze, and because of its optical absorptivity, it may cause a significant contribution to the radiative energy budget. At the Mauna Loa Observatory a cooperative measurement program to obscure the chemical composition of aerosols was initiated. GRA

N82-14572# Ecole Nationale Supérieure des Mines, Sophia-Antipolis (France). Centre de Teledetection et d'Analyse des Milieux Naturels.

OIL SPILLS: LARGE SCALE MONITORING BY LANDSAT M. Albuisson, J. M. Monget, and L. Wald In ESA Appl. of Remote Sensing Data on the Continental Shelf Jul. 1981 p 171-172 refs Sponsored by Joint Research Center of the European Communities

Avail: NTIS HC A13/MF A01; ESA, Paris FF 125

Oil pollution at sea using the LANDSAT multispectral scanner channel was detected. The variations of the reflection

coefficient between rough sea and the oil spill was measured. The oil spill flattens the sea and reflects in only one direction while the capillary waves of rough sea scatter the light; a fraction of the incident light only reaches the satellite. An underestimate of pollution is expected during winter because of low solar elevation angles. This method is used to inventory pollution by hydrocarbons in the Mediterranean Sea. An estimation from 800 images shows the cumulative area covered by hydrocarbons, spread over the Mediterranean Sea each year, as 175,000 sq km. Author (ESA)

N82-14573# Ministère de l'Environnement et du Cadre de Vie, Neuilly (France). Direction de la Prevention des Pollutions.

THE OPERATIONAL OIL POLLUTION SURVEILLANCE SYSTEM BEING USED IN FRANCE: FORECASTED FUTURE DEVELOPMENTS IN CONSIDERATION OF THE NATO/CCMS REMOTE SENSING PILOT STUDY CONCLUSIONS J. M. Massin In ESA Appl. of Remote Sensing Data on the Continental Shelf Jul. 1981 p 173-180 ref

Avail: NTIS HC A13/MF A01; ESA, Paris FF 125

The requirements of an ideal system for detecting, identifying, classifying, mapping, and tracking oil spills are defined. A core package consisting of a human observer, photographic cameras, side-looking airborne radar, infrared/ultraviolet line scanner, and passive television is proposed. The French airborne remote sensing system is shown to satisfy these requirements. Problems with a remote sensing system able to operate under all weather conditions, transmitting specific information in real time which permits the identification of hydrocarbons without having to check in situ, are discussed. Satellite possibilities are estimated. Author (ESA)

N82-14588# Norwegian Air Survey Co., Oslo.

USE OF SIDE LOOKING AIRBORNE RADAR (SLAR) FOR OIL POLLUTION MONITORING IN NORWAY

Svein Erik Hoest In ESA Appl. of Remote Sensing Data on the Continental Shelf Jul. 1981 p 281-282 ref

Avail: NTIS HC A13/MF A01; ESA, Paris FF 125

Integration of the system with a data annotation unit and a navigation system is outlined. Position data, date, time, and mission parameters are annotated on film. Data are also displayed on a TV monitor while the radar image and data can be recorded on an onboard video cassette recorder. The installation of the system and its operation are covered and its potential use in oil spill monitoring (particularly at night and in low visibility) is explained. Other possible uses are summarized (search and rescue missions, geology, oceanography) together with possible future extensions of the sensor package and survey aircraft. Author (ESA)

N82-14590# Atmospheric Sciences Lab., White Sands Missile Range, N. Mex.

SENSITIVITY ANALYSIS OF A MESOSCALE MOISTURE MODEL Final Report

James L. Cogan Mar. 1981 53 p refs

(DA Proj. 1L1-61102-B-53A)

(AD-A101528; ERADCOM/ASL-TR-0079) Avail: NTIS HC A04/MF A01 CSCL 04/1

Results from the model were computed for a variety of atmospheres and terrain types. A limited sensitivity analysis showed the effect of different model input parameters on meteorological variables for one vertical column through the atmosphere at a central horizontal grid point. A detailed analysis of selected cases for the entire domain of the model indicated the effect of input parameters on vertical velocity, precipitation amount, and precipitation rate. For one set of input parameters, analyses were performed of the variation of vertical velocity and precipitation every 2 hours for a 12-hour period. An example of a potential application to electro-optical algorithms is discussed and suggestions are made for future work. T.M.

N82-14591# Aerospace Corp., El Segundo, Calif. Space Sciences Lab.

SATELLITE OBSERVATIONS OF THE MT. ST. HELENS' ERUPTION OF 18 MAY 1980

Carl J. Rice 21 Aug. 1981 32 p refs (Contract F04701-80-C-0081)

02 ENVIRONMENTAL CHANGES AND CULTURAL RESOURCES

(AD-A105784; TR-0081(6640)-3; SD-TR-81-70) Avail: NTIS HC A03/MF A01 CSCL 08/7

The explosive eruption of Mt. St. Helens on 18 May 1980 was monitored by infrared sensors aboard two U.S. Air Force satellites. Essentially continuous data are available following the initial sighting of the eruption cloud less than one minute after the earthquake which triggered the eruption. Dual monitoring permits triangulation so that both the horizontal and vertical development of the eruption can be determined with good temporal resolution. The sequence of events occurring early in the eruption can therefore be established. Author (GRA)

N82-15488*# Lockheed Engineering and Management Services Co., Inc., Houston, Tex.

INVESTIGATION OF THE APPLICATION OF REMOTE SENSING TECHNOLOGY TO ENVIRONMENTAL MONITORING

M. L. Rader, Principal Investigator Aug. 1980 76 p ERTS (Contract NAS9-15800)

(E82-10010; NASA-CR-161071; JSC-16759; LEMSCO-15175)

Avail: NTIS HC A05/MF A01 CSCL 13B

Activities and results are reported of a project to investigate the application of remote sensing technology developed for the LACIE, AgRISTARS, Forestry and other NASA remote sensing projects for the environmental monitoring of strip mining, industrial pollution, and acid rain. Following a remote sensing workshop for EPA personnel, the EOD clustering algorithm CLASSY was selected for evaluation by EPA as a possible candidate technology. LANDSAT data acquired for a North Dakota test sight was clustered in order to compare CLASSY with other algorithms.

A.R.H.

N82-15697# National Oceanic and Atmospheric Administration, Washington, D. C. Office of Federal Coordinator for Meteorological Services and Supporting Research.

NATIONAL HURRICANE OPERATIONS PLAN

May 1981 81 p

(PB81-247231; NOAA-FCM-P12-1981; NOAA-81071411)

Avail: NTIS HC A05/MF A01 CSCL 04B

The hurricane warning service is an interdepartmental effort to provide the nation and designated international recipients with environmental data, forecasts, and assessments concerning tropical and subtropical weather systems. GRA

Page intentionally left blank

Page intentionally left blank

GEODESY AND CARTOGRAPHY

Includes mapping and topography.

A82-10028 **Digital image technology - MC&G impact.** M. Faintich (U.S. Defense Mapping Agency, Aerospace Center, St. Louis Air Force Station, MO). In: American Society of Photogrammetry, Annual Meeting, 46th, St. Louis, MO, March 9-14, 1980, ASP Technical Papers. Falls Church, VA, American Society of Photogrammetry, 1980, p. 32-43. 9 refs.

The Defense Mapping Agency Aerospace Center has developed a program to exploit digital image technology for the advancement of mapping, charting, and geodesy. Primary studies include image processing, analysis, and display techniques, and computer image generation. State-of-the-art digital image technology concepts have had a dramatic influence on the ability to analyze various digital data bases produced by the Defense Mapping Agency. In addition, emerging technologies in image processing and digital image analysis for automated feature extraction are demonstrating the potential for significant improvement in the utilization of imagery and significant reduction of production costs. Analyses of Landsat images and Viking Mars images are considered as examples. B.J.

A82-10029 **Factorial analysis of terrain feature positioning parameters used in combining radar and digital terrain model data.** R. Brock (New York, State University, Syracuse, NY) and D. I. Zulch (USAF, Rome Air Development Center, Griffiss AFB, NY). In: American Society of Photogrammetry, Annual Meeting, 46th, St. Louis, MO, March 9-14, 1980, ASP Technical Papers. Falls Church, VA, American Society of Photogrammetry, 1980, p. 44-51.

The significance of selected data collection parameters in the combination of radar data and digital terrain model data is evaluated in three phases: (1) the development of deterministic radar models from given digital terrain models and varying radar parameters; (2) the perturbation of the terrain feature coordinates which result from errors in radar position, radar orientation, range, and resolution; and (3) a factorial analysis of the terrain feature errors to establish the significance of the main fixed factors and their interactions; the main factors are azimuth from radar to terrain feature, range, resolution, terrain height, and coordinate. It is found that order of greatest to least importance of the factors is coordinate, range, resolution, terrain height, and azimuth. B.J.

A82-10056 **Application of satellite Doppler techniques to the national mapping program.** F. E. White, Jr. (U.S. Geological Survey, Topographic Div., Denver, CO). In: American Congress on Surveying and Mapping, Annual Meeting, 40th, St. Louis, MO, March 9-14, 1980, ACSM Technical Papers. Falls Church, VA, American Congress on Surveying and Mapping, 1981, p. 406-410.

Operational experience related to an employment of a Doppler system in Alaska during 1978 is discussed. There were certain problems in connection with equipment failure, poor weather conditions, and the destruction of one of the antennas by a grizzly bear. For a continuation of the operations, two MX 1502 Satellite Surveyor Systems were acquired in January 1979. Advantages of these systems over other systems currently in use are briefly examined. A description is presented of a research experiment which had been proposed in order to test and evaluate the acquired type of system at 29 deg, 40 deg, and 48 deg latitude. During the 1979 field season in Alaska, two teams established 45 Doppler stations and 65 electronic traverse stations from north of the Brooks Range area in the Arctic. Attention is given to a new instrument which would transcribe the cassette data of the Doppler Survey System to 9-track magnetic tape. G.R.

A82-10057 **Bureau of Land Management satellite Doppler positioning techniques.** W. E. Ball, Jr. (U.S. Bureau of Land Management, Denver, CO). In: American Congress on Surveying and Mapping, Annual Meeting, 40th, St. Louis, MO, March 9-14, 1980, ACSM Technical Papers. Falls Church, VA, American Congress on Surveying and Mapping, 1981, p. 411-421. 6 refs.

The U.S. Department of the Interior Bureau of Land Management has been using satellite Doppler positioning techniques to supplement existing survey control in Alaska since 1973. Multi-station simultaneous positioning techniques are employed to obtain accurate relative positions among stations observed. Computed relative position coordinates are subsequently adjusted to conform to the known coordinates of the primary station, and to assure compatibility between all other satellite observation stations and existing local geodetic control stations. (Author)

A82-10645 * **GPS application to mapping, charting and geodesy.** W. J. Senus (U.S. Defense Mapping Agency, Advanced Technology Div., Washington, DC) and R. W. Hill (U.S. Navy, Naval Surface Weapons Center, Dahlgren, VA). (*Institute of Navigation, National Aerospace Meeting, Warminster, Pa., Apr. 8-10, 1981.*) *Navigation*, vol. 28, Summer 1981, p. 85-92. 6 refs. Research sponsored by the U.S. Defense Mapping Agency, U.S. Geological Survey, NASA, and NOAA.

GPSPAC, a receiver being developed for space applications by the Defense Mapping Agency and NASA, will use signals from GPS constellations to generate real-time values of host vehicle position and velocity. The GPSPAC has an L-band antenna and preamp capable of receiving the 1575 MHz and 1227 MHz spread spectrum signals; its stable oscillator at 5.115 MHz provides the basic frequency reference, resulting in a long term drift of less than one part in 10 to the -10th day. The GPSPAC performs many functions on board the spacecraft which were previously relegated to large-scale ground-based computer/receiver systems. A positional accuracy of better than 8 can be achieved for those periods when four or more NAVSTAR satellites are visible to the host satellite. The GPS geodetic receiver development, which will provide prototype receivers for utilization in terrestrial surveying operations, has the potential to significantly enhance the accuracy of point geodetic surveys over the current user hardware capability. J.F.

A82-10859 **Digitizing and automated output mapping errors.** L. G. S. Thompson (U.S. Military Academy, West Point, NY). *Photogrammetric Engineering and Remote Sensing*, vol. 47, Oct. 1981, p. 1455-1457.

Computer assisted cartography and mapping have become a reality. However, the errors concerned with these operations are still somewhat uncertain. Under the conditions found at the Army Survey Regiment, Bendigo, Australia, the errors associated with the digitizing of discrete points and the automated output of these points onto contact film were found to be 3.3 m and 1.9 m at ground scale (+ or - 0.082 mm and + or - 0.037 mm at table scale). The frequency of capturing digits and the expected errors when digitizing nondiscrete points (i.e., when the cursor is continuously in motion) are also discussed. (Author)

A82-12186 * **Magnetic field-aligned electron distributions in the dayside cusp.** L. J. Zanetti, T. A. Potemra (Johns Hopkins University, Laurel, MD), J. P. Doering, J. S. Lee (Johns Hopkins University, Baltimore, MD), and R. A. Hoffman (NASA, Goddard Space Flight Center, Greenbelt, MD). *Journal of Geophysical Research*, vol. 86, Oct. 1, 1981, p. 8957-8970. 35 refs. Contract No. NAS5-11415.

Observations of low-energy electron fluxes made over a 6 year period with the photoelectron spectrometer on the AE-C and AE-D satellite are used to investigate electron pitch angles in the low altitude cusp. A 16 point energy spectrum from 2 to 500 eV was obtained at every .25 s, and the location of the cusp was verified by the presence of protons detected by the low-energy electron instrument. Isotropic fluxes of precipitating electrons with Maxwellian energy spectra were observed in the low-altitude cusp, and the presence of low-energy electrons with pitch angles less than 15 deg was determined streaming into the cusp ionosphere. The energies of the streaming electrons sometimes appeared as a peak superimposed on the normal cusp Maxwellian background of isotropic electrons, and it is concluded that the energies and pitch angle distributions of the precipitating electrons may explain the enhancements of auroral emissions and discrete arcs. D.L.G.

A82-12215 **Distant magnetic field effects associated with Birkeland currents /made possible by the evaluation of TRIAD's**

03 GEODESY AND CARTOGRAPHY

attitude oscillations/ G. Gustafsson (Kiruna Geophysical Institute, Kiruna, Sweden), T. A. Potemra, S. Favin (Johns Hopkins University, Laurel, MD), and N. A. Saflekos (Boston College, Chestnut Hill, MA). *Journal of Geophysical Research*, vol. 86, Oct. 1, 1981, p. 9219-9223. 13 refs. NSF-Navy-supported research.

Principal oscillations of the TRIAD satellite are studied in 150 passes and are identified as the librations of a gravity-stabilized satellite. The libration periods are $T(O)/2$ and $T(O)/(3) \exp 1/2$, where $T(O)$ is the orbit period of about 100 min. The amplitude and phase change over periods of a few days, sometimes vanishing altogether, and these attitude changes are numerically evaluated and removed. Data from three consecutive passes spanning over three hours show a magnetic profile which extends as far as 10 deg in latitude from a single region 1 Birkeland current sheet, confirming the permanent and global nature of large-scale Birkeland currents.

D.L.G.

A82-12912 † Phototriangulation with map referencing of photographs in linear surveys (Fototriangulirovanie s priviazkoi snimkov k karte pri lineinykh izyskaniakh). A. I. Kaigorodov. *Geodeziia i Kartografiia*, Sept. 1981, p. 30, 31. In Russian.

A82-12914 † A new method for computing distortion (O novom sposobe vychisleniia distorsii). A. Sh. Shakhverdov and E. Z. Shliam. *Geodeziia i Kartografiia*, Sept. 1981, p. 34-36. In Russian.

An improved method is proposed for computing distortion arising in the calibration of aerial topographic cameras. The new method is especially suitable for implementation on a large computer, and was found to lead to a fivefold-to-sixfold improvement in the computation of distortion as compared with traditional methods.

B.J.

A82-12915 † Aerial and space methods in cartography (Aerokosmicheskie metody v kartografii). L. I. Zlobin and Iu. G. Kel'ner. *Geodeziia i Kartografiia*, Sept. 1981, p. 39-42. 9 refs. In Russian.

A82-15032 * The surface albedo of the earth in the near ultraviolet /330-340 nm/. J. E. Frederick (NASA, Goddard Space Flight Center, Laboratory for Planetary Atmospheres, Greenbelt, MD) and R. B. Abrams (Computer Sciences Corp., Silver Spring, MD). *Remote Sensing of Environment*, vol. 11, Nov. 1981, p. 337-347. 13 refs.

Satellite-borne measurements of solar radiation backscattered by the earth and atmosphere allow a determination of the surface albedo in the near ultraviolet. The data yielded albedos at tropical latitudes during a 15-month period in 1979-1980. The wavelengths studied are 331.2 and 339.8 nm. Sixty-nine percent of the measurements imply albedos less than 0.3. Higher values include a contribution due to reflection from clouds and are consistent with previous estimates of the fractional cloudcover in the tropics. An albedo histogram based on a bin width of 0.1 shows results in the range 0.1-0.2 to be the most frequent, appearing in 29% of the cases, although values which span the entire range 0.0-1.0 are present. The derived albedos show no correlation with solar zenith angle. This result is consistent with the fact that, at the wavelengths considered, the diffuse integrated intensity is larger than the attenuated direct solar beam near the ground. (Author)

A82-16161 Some problem areas in the field of quality control for aerotriangulation. M. Molenaar (International Institute for Aerial Survey and Earth Sciences, Enschede, Netherlands). *ITC Journal*, no. 3, 1981, p. 253-265. 20 refs.

Attention is given to problem areas in quality control for aerotriangulation. These include: (1) the possible occurrence of gross errors; (2) the presence of systematic deformations; (3) unified testing procedures; (4) the analysis of the stochastic model; (5) aerotriangular block accuracy as a function of ground control distribution; (6) variance component estimation; and (7) accuracy methods in practice. S.C.S.

A82-16868 Use of hydromagnetic waves to map geomagnetic field lines. R. A. Greenwald, A. D. M. Walker (Johns

Hopkins University, Laurel, MD), and M. Candidi (CNR, Laboratorio per il Plasma nello Spazio, Frascati, Italy). *Journal of Geophysical Research*, vol. 86, Dec. 1, 1981, p. 11251-11257. 12 refs. NSF Grant No. ATM-80-03300.

It is pointed out that if ionospheric and magnetospheric regions showing highly correlated temporal variations could be identified, it would be possible to determine the region in the ionosphere conjugate to a given location in the magnetosphere. A cross-correlation analysis is presented of Pc 5 magnetic field oscillations observed by GEOS 2 with drift velocity oscillations (electric field) observed with the STARE radars in the ionosphere. It is noted that GEOS 2 is in geostationary orbit with its conjugate point nominally located in the STARE field of view. Several comparisons are made over a 1-hour period in the early afternoon sector, and correlation coefficients reaching 0.84 over a limited area in the ionosphere are obtained. It is found that between the beginning and end of the hour, the measured footpoint is displaced by approximately 1 deg in latitude and approximately 2.5 deg in longitude. C.R.

A82-18797 # Space techniques to monitor movements in the earth's crust. S. Hieber (ESA, Directorate of Application Programmes, Paris, France). *ESA Bulletin*, no. 28, Nov. 1981, p. 62-67.

Space techniques to monitor movements in the earth's crust such as very slow drift of tectonic plates or regional fault motions are discussed. Major research objectives in geodynamics are given. Space techniques include a number of satellite remote sensing missions, very-long-baseline interferometry and laser tracking methods, and satellite gradiometry. It is concluded that satellite imagery can be used in many more ways to enhance interdisciplinary research in geophysics and geology. D.L.G.

N82-11696*# Smithsonian Astrophysical Observatory, Cambridge, Mass.

STUDY OF THE TIME EVOLUTION OF THE LITHOSPHERE Semiannual Progress Report, 1 Mar. - 31 Aug. 1981

Micheline C. Roufousse Nov. 1981 7 p

(Grant NAG5-150)

(NASA-CR-164968; SAPR-1) Avail: NTIS HC A02/MF A01 CSCL 08G

A three dimensional geoid of all oceanic regions was obtained using a data set derived from the GEOS-3 radar altimeter. The editing and organization of the complete SEASAT geophysical data set are described. The geographical area located between 25 and 35 degrees south, and between 320 and 335 degrees east, around the Rio Grande Rise in the south Atlantic, was selected for continued study. T.M.

N82-13606# National Geodetic Survey, Rockville, Md. REPORT OF SURVEY FOR MCDONALD OBSERVATORY, HARVARD RADIO ASTRONOMY STATION, AND VICINITY

William E. Carter and James E. Pettey May 1981 91 p refs (PB81-234338; NOAA-TM-NOS-NGS-32; NOAA-81062603) Avail: NTIS HC A05/MF A01 CSCL 08E

A special purpose three dimensional geodetic survey was conducted near Ft. Davis, Texas. The observing program included astronomic positions and azimuths, zenith distances, electromagnetic distance measurements, leveling, gravity measurements, Doppler satellite positioning, and a variety of ancillary measurements. Information on the methods employed in the collection, reduction, and analysis of the survey data, tabulations of the observational data, and numerical and interpretive results is reported. GRA

N82-14041*# National Aeronautics and Space Administration, Washington, D. C.

REPORTS OF PLANETARY GEOLOGY PROGRAM, 1981

Henry E. Holt, comp. Dec. 1981 580 p refs

(NASA-TM-84211) Avail: NTIS HC A25/MF A01 CSCL 03B

Abstracts of 205 reports from Principal investigators of NASA's Planetary Geology Program succinctly summarize work conducted and reflect the significant accomplishments. The entries are arranged under the following topics: (1) Saturnian satellites; (2) asteroids, comets and Galilean satellites; (3) cratering processes and landform development; (4) volcanic processes and

landforms; (5) Aerolian processes and landforms; (6) fluvial, preglacial, and other processes of landform development; (7) Mars polar deposits, volatiles, and climate; (8) structure, tectonics, and stratigraphy; (9) remote sensing and regolith chemistry; (10) cartography and geologic mapping; and (11) special programs. A.R.H.

N82-15520# National Ocean Survey, Rockville, Md.
A HISTORY OF FLYING AND PHOTOGRAPHY: IN THE PHOTOGRAMMETRY DIVISION OF THE NATIONAL OCEAN SURVEY 1919 - 1979

John T. Smith, Jr. 1980 493 p refs
 (PB81-246738; NOAA-81071405) Avail: NTIS
 HC A21/MF A01 CSCL 14E

A history of aerial photography and its impact on photogrammetric geodesy is presented. The work of pilots, navigators, and photographers as teams is narrated. Early mapping activities are reported. Development of the nine lens camera is described. Other topics include pilot training, testing of color and infrared photography, the B-17 photographic aircraft, beginning the Liberian survey, adaptation to new equipment, Saudi Arabia mapping, the Buffalo aircraft, and the RC-10 camera. GRA

N82-15812 Deutsches Geodaetisches Forschungsinstitut, Munich (West Germany).

DESCRIPTION AND COMPARISON OF ALGORITHMS FOR SOLVING LARGE SETS OF SPARSE MATRIX NORMAL EQUATIONS IN GEODESY AND PHOTOGRAMMETRY
 Ph.D. Thesis - Technischen Univ., Munich [DARSTELLUNG UND VERGLEICHE VON LOESUNGSSTRATEGIEN FUER GROSSE SCHWACH BESETZTE NORMALGLEICHUNGSSYSTEME IN DER GEODAESIE UND IN DER PHOTOGRAMMETRIE]

Franz Steidler Verlag der Bayerischen Akademie der Wissenschaften 1980 117 p refs In GERMAN
 (Ser-C-261; ISSN-0065-5325; ISBN-3-7696-9313-2) Avail: Issuing Activity

Algorithms were investigated in relation to calculation time and data storage capability. For geodetic networks, direct techniques for sparse matrices are very well suited. For photogrammetric bundle-block adjustments with self calibration the conventional use of band algorithms is the best choice. For generating a digital terrain model following the finite element method, the band algorithm solves the normal equations in the fastest way. Author (ESA)

Page intentionally left blank

Page intentionally left blank

04
**GEOLOGY AND MINERAL
RESOURCES**

Includes mineral deposits, petroleum deposits, spectral properties
of rocks, geological exploration, and lithology.

A82-11039 * A closer examination of the reduction of satellite magnetometer data for geological studies. R. D. Regan (Barringer Resources, Golden, CO), D. W. Handschumacher (U.S. Navy, Naval Ocean Research and Development Activity, Bay St. Louis, MS), and M. Sugiura (NASA, Goddard Space Flight Center, Greenbelt, MD). *Journal of Geophysical Research*, vol. 86, Oct. 10, 1981, p. 9567-9573. 19 refs. Contracts No. N00014-79-C-0653; No. NAS5-25882.

Results of a detailed examination of magnetic field residuals obtained from POGO satellite magnetometer data are presented which illustrate some problems which may be encountered in the reduction and analysis of Magsat data. Comparisons of field residuals determined from OGO 2, 4 and 6 data for the region between 270 and 290 deg E reveals significant differences between the satellite data sets which are related to differences in the residual field level on individual satellites, external field contamination and effects from ring current correction in the data reduction process. When a new map is prepared from OGO 2 and 4 satellite data by compensating for these factors, dramatic differences with the original map are noted, including the disappearance of a major positive anomaly and the better definition of various magnetic highs and lows. The new map is also noted to be more consistent with conventional airborne and marine magnetic measurements. The results thus demonstrate the necessity for the inspection of satellite data and the adequate removal of the external field signal prior to geological analysis.

A.L.W.

A82-12366 * # Coordinates of features on the Galilean satellites. M. E. Davies and F. Y. Katayama (Rand Corp., Santa Monica, CA). *Journal of Geophysical Research*, vol. 86, Sept. 30, 1981, p. 8635-8657. 13 refs. Contracts No. JPL-953613; No. NASw-3321.

Control nets of the four Galilean satellites have been established photogrammetrically from pictures taken by the two Voyager spacecraft during their flybys of Jupiter in 1979. Coordinates of 504 points on Io, 112 points on Europa, 1547 points on Ganymede, and 439 points on Callisto are listed. Selected points are identified on U.S. Geological Survey maps of the satellites. Measurements of these points were made on 234 pictures of Io, 115 pictures of Europa, 282 pictures of Ganymede, and 200 pictures of Callisto. The systems of longitude were defined by craters on Europa, Ganymede, and Callisto. Preliminary solutions have been found for the directions of the axes of rotation of the Galilean satellites. New mean radii have been determined as 1815 + or - 5 km for Io, 1569 + or - 10 km for Europa, 2631 + or - 10 km for Ganymede, and 2400 + or - 10 km for Callisto. (Author)

A82-12590 Remote sensing study of sinkhole occurrence. J. W. Casper, B. E. Ruth, M. Asce, and J. D. Degner (Florida University, Gainesville, FL). In: Civil engineering applications of remote sensing; Proceedings of the Specialty Conference, Madison, WI, August 13, 14, 1980. New York, American Society of Civil Engineers, 1980, p. 1-14. 10 refs.

N82-10485 Utah Univ., Salt Lake City.
**MORPHOSTRUCTURAL ANALYSES OF SPACE IMAGERY
IN THE CENTRAL COLORADO PLATEAU** Ph.D. Thesis
Abdelrahman Mohammad Shafik Maarouf 1981 130 p.
Avail: Univ. Microfilms Order No. 8118146

Coincidences of increase or decrease in frequency of most of the lineament trends common to both Skylab and Landsat photos and images of the Colorado Plateau suggest that the peaks or troughs are not artificially introduced by sampling bias, and there are actual preferred orientations represented by peak or trough coincidences. Interpretation of lineaments from Skylab and Landsat data, along with study of magnetic and gravity

maps, suggest strong correlation between lineaments and faults in the Precambrian basement. It is shown that the basement faults influenced the present surface drainage and structures through a sedimentary cover of more than 6 km. The faults were formed during the middle Precambrian, and were rejuvenated later in varying degrees and at various times. Dissert. Abstr.

N82-10476# Bendix Field Engineering Corp., Grand Junction, Colo.
STATISTICAL TECHNIQUES APPLIED TO AERIAL RADIO-METRIC SURVEYS (STAARS): SERIES INTRODUCTION AND THE PRINCIPAL-COMPONENTS-ANALYSIS METHOD
Fredric L. Pirkle Apr. 1981 62 p refs
(Contract DE-AC13-76GJ-01664)
(DE81-029177; GJ8X-114(81)) Avail: NTIS
HC A05/MF A01

A series of open-file reports established to provide the latest interpretation techniques to those using aerial radiometric data is announced. Geological applications of the technique are emphasized in case histories. A bibliography is provided which defines the detailed theory and statistics of the technique to assist researchers in ascertaining the statistical validity and merit of the technique. The use of multivariate statistical analysis in delineating regions favorable to uranium deposition in the Lubbock and Plainview quadrangles of Texas, and along the Texas Gulf coast is demonstrated in this issue. GRA

N82-10618 Idaho Univ., Moscow.
GEOLOGY AND LINEARS OF LIBYA Ph.D. Thesis
Milud Abdulkrim Mansur 1981 276 p
Avail: Univ. Microfilms Order No. 8119882

The geology of Libya is described in detail with some reference to economic resources. An analysis of LANDSAT space photographs revealed about 2,000 linears, unequally distributed in the different parts of the country, and characterized by considerable variations in their length, strike, and density. Some of them coincide with known structural features including fault scarps, topographic features, dikes, alignments of igneous bodies, and straight drainage systems. Dissert. Abstr.

N82-12491 Cornell Univ., Ithaca, N. Y.
**REMOTE SENSING STUDIES OF SOME IRONSTONE
GRAVELS AND PLINTHITE IN THAILAND** Ph.D. Thesis
Pichit Jamnongpipatkul 1980 336 p
Avail: Univ. Microfilms Order No. 8177113

Ironstone gravels and plinthite in eastern Thailand were found to be associated with alluvial terraces as well as shale and basalt formation. Selected stereopairs of airphotos of known areas of ironstone gravels and plinthite were studied. The keys for airphoto interpretation were developed on the basis of the relation with types of landform, vegetation and appearance on the airphotos. Visual analysis of LANDSAT data provided information on the types of LANDSAT and vegetation which could lead to more detailed investigation of probable areas of ironstone gravels and plinthite. Digital analysis of LANDSAT data indicated that the difference of spectral reflectances from areas of ironstone gravels and those from the surrounding areas is considerable. Field study was conducted to verify the results of airphotos interpretation and LANDSAT data analysis and to obtain information in regard to genesis and morphology of soils with ironstone gravels and plinthite. Soil profile descriptions for typical soils with ironstone gravels and plinthite are included. Dissert. Abstr.

N82-12492*# National Aeronautics and Space Administration.
Lyndon B. Johnson Space Center, Houston, Tex.
SKYLAB EXPLORES THE EARTH
Washington 1977 512 p refs Original contains color illustrations
(NASA-SP-380; LC-77-829) Avail: NTIS MF A01; SOD
HC \$16.50 CSCL 08B

Data from visual observations are integrated with results of analyses of approximately 600 of the nearly 2000 photographs taken of Earth during the 84-day Skylab 4 mission to provide additional information on (1) Earth features and processes; (2) operational procedures and constraints in observing and photographing the planet; and (3) the use of man in real-time analysis of oceanic and atmospheric phenomena.

04 GEOLOGY AND MINERAL RESOURCES

N82-12493* Geological Survey, Denver, Colo.

DESERT SAND SEAS

Edwin D. McKee, Carol S. Breed (Geological Survey, Flagstaff, Ariz.), and Steven G. Fryberger (Geological Survey, Flagstaff, Ariz.) /n NASA. Johnson Space Flight Center Skylab Explores the Earth 1977 p 5-48 refs

Avail: NTIS MF A01; SOD HC \$16.50 CSCL 08B

The usefulness of manned observations and handheld-camera photographs from space is confirmed by the immediate application of Skylab 4 data to the study of sand seas. The Skylab 4 crew provided information that: (1) confirms a tentative global classification of eolian sand deposits based on observed similarities in most of the major deserts of the world; (2) allows the preparation of maps that show the relationships of sand deposits to each other, to sand source areas, to natural sand distribution barriers, and to human land use; and (3) allows the regional patterns of large-scale dune morphology to be studied in relation to rainfall distribution and surface winds. Four sites in the Sahara and sub-Sahara of northern Africa, four in the Namib and Kalahari Deserts of southern Africa, two in the Empty Quarter of Saudi Arabia, five in the Takla Makan and Gobi Deserts of China, and three in the trans-Caspian deserts of the U.S.S.R. were selected as well as additional areas in northern Africa, India, Mexico, and Australia. A.R.H.

N82-12494* Texas Univ. at Austin.

GLOBAL TECTONICS: SOME GEOLOGIC ANALYSES OF OBSERVATIONS AND PHOTOGRAPHS FROM SKYLAB

W. R. Muehlberger, P. R. Gucwa, A. W. Ritchie, and E. R. Swanson /n NASA. Johnson Space Flight Center Skylab Explores the Earth 1977 p 49-88 refs

Avail: NTIS MF A01; SOD HC \$16.50 CSCL 08G

Spreading zones, transform faults, and subduction zones were observed visually and by hand-held camera on Skylab 4. Geological studies of these observations are discussed for the Near and Middle East, the Atacama fault in Chile, the Alpine Fault zone in New Zealand, the Sierra Madre Occidental, in Mexico, and the Caribbean/Americas plate boundary in Guatemala and Southern Mexico. A.R.H.

N82-12495* California Inst. of Tech., Pasadena.

GEOLOGICAL FEATURES OF SOUTHWESTERN NORTH AMERICA

L. T. Silter, T. H. Anderson, C. M. Conway, J. D. Murray, and R. E. Powell /n NASA. Johnson Space Flight Center Skylab Explores the Earth 1977 p 89-136 refs

Avail: NTIS MF A01; SOD HC \$16.50 CSCL 08G

Photographic and visual observation of geological target areas were integrated with other aspects of the ground investigations to: (1) identify and evaluate zones of major faulting in south eastern California, Baja California, and northwestern Sonora; (2) develop a new key to the regional stratigraphy of the prebatholithic rocks of northern Baja California; (3) discover the most southwesterly known occurrence of Precambrian crystalline rocks in North America; (4) discover a previously unmapped section of Mesozoic volcanic rocks in southeastern California; and (5) contribute important overview perspectives to many regional geologic problems. Skylab 4 data are discussed for the San Andreas fault system and architecture of Southern California; Northern Baja, California; Sierra Mazatan and Sierra del Alamo in Sonora, Mexico; the northwest Sonora coast fault zones; and Arizona, including that portion of the Colorado Plateau in the vicinity of the Grand Canyon. A.R.H.

N82-12496* Geological Survey, Denver, Colo.

SKYLAB 4 OBSERVATIONS OF VOLCANOES. PART A: VOLCANOES AND VOLCANIC LANDFORMS. PART B: SUMMIT ERUPTION OF FERNANDIAN CALDERA, GALAPAGOS ISLANDS, ECUADOR

Jules D. Friedman, Grant Heiken (Low Alamos Scientific Labs., New Mexico), Tom Simkin (Smithsonian Inst., Washington, D.C.), and Arthur F. Krueger (NOAA, Washington, D.C.) /n NASA. Johnson Space Flight Center Skylab Explores the Earth 1977 p 137-173 refs

Avail: NTIS MF A01; SOD HC \$16.50 CSCL 08K

Terrestrial volcanic features were observed and photographed from Skylab 4 under a variety of viewing conditions and Sun angles. Eruptions of Sakura-zima in southern Kyushu, Japan and

the remote Fernandina volcano in the Galapagos Islands provided rare documentation of eruption clouds. Remote volcanic regions were also surveyed including the Tibesti volcanic massif and the Erni Koussi Caldera in Chad; the Altiplano volcanic field of Bolivia, Argentina, and Chile; the Kanchatcha Peninsula, U.S.S.R.; and the southeastern central plateau of Mexico. The landforms of volcanic provinces of Hawaii, southern Italy, the Aleutian Islands, Oregon, and Washington State were also investigated. Previously unobserved relationships between geomorphology and structure and previously unmapped tectonic ligaments were revealed as well as stratigraphic or relative age distinctions between partly overlapping basaltic flows. A.R.H.

N82-12497* Energy, Mines and Resources Canada, Ottawa (Ontario).

THE MANICOUAGAN IMPACT STRUCTURE OBSERVED FROM SKYLAB

M. R. Dence /n NASA. Johnson Space Flight Center Skylab Explores the Earth 1977 p 175-190 refs

(Contrib-544) Avail: NTIS MF A01; SOD HC \$16.50 CSCL 08B

From comprehensive views of eastern Canada provided by Skylab oblique photographs, the main elements of the multi-ring Manicouagan structure can be defined. By gravitational scaling, the structure is an analog for 200 km diameter structures on Mars and Mercury and 400 km to 500 km basins on the Moon. Because much larger structures on the other planets have rings spaced at intervals of 2 to the 1/2 power spacing, it is of interest to know if rings with intermediate spacing can be identified. A.R.H.

N82-12713* University Coll., Cardiff (Wales). Dept. of Applied Mathematics and Astronomy.

INFRARED SPECTROSCOPY OF MICROORGANISMS NEAR 3.4 MICRONS IN RELATION TO GEOLOGY AND ASTRONOMY

F. Hoyle, N. C. Wickramasinghe, S. Al-Mufti, and A. H. Olavesen Jun. 1981 11 p refs Submitted for publication

(Preprint-69) Avail: NTIS HC A02/MF A01

Cracking of microorganisms at high temperature and pressure were examined for the existence of microfossils in sedimentary rocks of the Isna series. Microorganism specimens were examined for degradation by infrared spectroscopy over the wavelength range from 2.5 microns to 15 microns. Stability up to 380 C after which there is degradation towards graphite is shown. It is concluded that the preservation of microfossils is feasible in rocks metamorphosed at temperatures of 400 C. Author (ESA)

N82-14600* Carson Helicopters, Inc., Perkasie, Pa.
NURE AERIAL GAMMA-RAY AND MAGNETIC RECONNAISSANCE SURVEY OF MAINE AND PORTIONS OF NEW YORK, VOLUME 2 Final Report

Jul. 1981 124 p refs

(Contract DE-AC13-76GJ-01664)

(DE82-000781; GJBX-327-81-Vol-2-SHERBROOKE) Avail: NTIS HC A06/MF A01

Contents includes: the flight line base map, anomaly maps (uranium, thorium, potassium, uranium/thorium, uranium/potassium, thorium/potassium), total count map, magnetic field map, uranium map, thorium map, potassium map, ratio maps for uranium/thorium, uranium/potassium, thorium/potassium, radiometric multiple-parameter stacked profiles, magnetic and ancillary stacked profile data, and histograms. DOE

N82-14601* Carson Helicopters, Inc., Perkasie, Pa.
NURE AERIAL GAMMA-RAY AND MAGNETIC RECONNAISSANCE SURVEY OF MAINE AND PORTIONS OF NEW YORK, VOLUME 2 Final Report

Jul. 1981 140 p refs

(Contract DE-AC13-76GJ-01664)

(DE82-000401; GJBX-327-81-Vol-2-OGDENSBURG) Avail: NTIS HC A07/MF A01

Content includes: the flight line base map anomaly maps (uranium, thorium, potassium, uranium/thorium, uranium/potassium, thorium/potassium), total count map, magnetic field map, uranium map, thorium map, potassium map, ratio maps for uranium/thorium, uranium/potassium, thorium/potassium, radiometric multiple-parameter stacked profiles, magnetic and ancillary stacked profile data, and histograms. DOE

N82-14602# Carson Helicopters, Inc., Perkasie, Pa.
**NURE AERIAL GAMMA-RAY AND MAGNETIC RECON-
 NAISSANCE SURVEY OF MAINE AND PORTIONS OF NEW
 YORK, VOLUME 2 Final Report**
 Jun. 1981 168 p refs
 (Contract DE-AC13-76GJ-01664)
 (DE82-000780: GJBX-327-81-Vol-2-MILLINOCKET) Avail:
 NTIS HC A08/MF A01

Content contains: the flight line base map, anomaly maps (uranium, thorium, potassium, uranium/thorium, uranium/potassium, thorium/potassium), total count map, potassium map, ratio maps for uranium/thorium, uranium/potassium, thorium/potassium, radiometric multiple-parameter stacked profiles, magnetic and ancillary stacked profile data, and histograms.DOE

N82-14603# Carson Helicopters, Inc., Perkasie, Pa.
**NURE AERIAL GAMMA-RAY AND MAGNETIC RECON-
 NAISSANCE SURVEY OF MAINE AND PORTIONS OF NEW
 YORK, VOLUME 2 Final Report**
 Jul. 1981 80 p refs
 (Contract DE-AC13-76GJ-01664)
 (DE82-000872: GJBX-327-81-Vol-2-LEWISTON) Avail: NTIS
 HC A05/MF A01

Content contains: the flight line base map, anomaly maps (uranium, thorium, potassium, uranium/thorium, uranium/potassium, thorium/potassium), total count map, magnetic field map, uranium map, thorium map, potassium map, ratio maps for U/T, U/K, T/K, radiometric multiple-parameter stacked profiles, magnetic and ancillary stacked profile data, and histograms.DOE

N82-14604# Carson Helicopters, Inc., Perkasie, Pa.
**NURE AERIAL GAMMA-RAY AND MAGNETIC RECON-
 NAISSANCE SURVEY OF MAINE AND PORTIONS OF NEW
 YORK, VOLUME 2 Final Report**
 Jun. 1981 306 p refs
 (Contract DE-AC13-76GJ-01664)
 (DE82-000772: GJBX-327-81-Vol-2-FREDERICTON) Avail:
 NTIS HC A14/MF A01

Content contains: the flight path maps, anomaly maps (uranium, thorium, potassium, uranium/thorium, uranium/potassium, thorium/potassium), radiometric multiple parameter stacked profiles, magnetic and ancillary stacked profile data, histograms, total count maps, magnetic field maps, uranium maps, thorium maps, potassium maps, ratio maps for U/T, U/K, and T/K. DOE

N82-14605# Carson Helicopters, Inc., Perkasie, Pa.
**NURE AERIAL GAMMA-RAY AND MAGNETIC RECON-
 NAISSANCE SURVEY OF MAINE AND PORTIONS OF NEW
 YORK, VOLUME 2 Final Report**
 Jun. 1981 242 p refs
 (Contract DE-AC13-76GJ-01664)
 (DE82-000785: GJBX-327-81-Vol-2-EDMUNDSTON) Avail:
 NTIS HC A11/MF A01

Content contains: the flight line base maps, nomaly maps (uranium, thorium, potassium, uranium/thorium, uranium/potassium, thorium/potassium), radiometric multiple parameter stacked profiles, magnetic and ancillary stacked profile data, histograms, total count maps, magnetic field maps, uranium maps, thorium maps, potassium maps, ratio maps for U/T, U/K, and T/K. DOE

N82-14606# Carson Helicopters, Inc., Perkasie, Pa.
**NURE AERIAL GAMMA-RAY AND MAGNETIC RECON-
 NAISSANCE SURVEY OF MAINE AND PORTIONS OF NEW
 YORK, VOLUME 2 Final Report**
 Jul. 1981 150 p refs
 (Contract DE-AC13-76GT-01664)
 (DE82-000869: GJBX-327-81-Vol-2-BINGHAMTON) Avail:
 NTIS HC A07/MF A01

Content contains: the flight line base map, anomaly maps (uranium, thorium, potassium, uranium/thorium, uranium/potassium, thorium/potassium), total count map, magnetic field map, uranium map, thorium map, potassium map, ratio maps for U/T, U/K, T/K, radiometric multiple parameter stacked profiles, magnetic and ancillary stacked profile data, and histograms.DOE

N82-14607# Carson Helicopters, Inc., Perkasie, Pa.
**NURE AERIAL GAMMA-RAY AND MAGNETIC RECON-
 NAISSANCE SURVEY OF MAINE AND PORTIONS OF NEW
 YORK, VOLUME 2 Final Report**
 Jul. 1981 260 p refs

(Contract DE-AC13-76GJ-01664)
 (DE82-000794: GJBX-327-81-Vol-2-BANGOR) Avail: NTIS
 HC A12/MF A01

Content contains: the flight line base maps, anomaly maps (uranium, thorium, potassium, uranium/thorium, uranium/potassium, thorium/potassium), total count maps, magnetic field maps, uranium maps, thorium maps, potassium maps, ratio maps for U/T, U/K, T/K, radiometric multiple parameter stacked profiles, magnetic and ancillary stacked profile data, and histograms.DOE

N82-14608# Carson Helicopters, Inc., Perkasie, Pa.
**NURE AERIAL GAMMA-RAY AND MAGNETIC RECON-
 NAISSANCE SURVEY OF MAINE AND PORTIONS OF NEW
 YORK, VOLUME 2 Final Report**
 Jul. 1981 166 p refs
 (Contract DE-AC13-76GJ-01664)
 (DE82-000784: GJBX-327-81-Vol-2-UTICA) Avail: NTIS
 HC A08/MF A01

Content contains: the flight line base map, anomaly maps (uranium, thorium, potassium, uranium/thorium, uranium/potassium, thorium/potassium), radiometric multiple parameter stacked profiles, magnetic and ancillary stacked profile data, histograms, total count map, magnetic field map, uranium map, thorium map, potassium map, ratio maps for U/T, U/K, and T/K. DOE

N82-15487# Massachusetts Univ., Amherst. Dept. of
 Geology.
THE MINERALOGY OF GLOBAL MAGNETIC ANOMALIES
Progress Report, Jan. - Sep. 1981
 Stephen E. Haggerty, Principal Investigator 19 Sep. 1981
 27 p ERTS
 (Contract NAS5-26414)
 (E82-10009: NASA-CR-164907) Avail: NTIS
 HC A03/MF A01 CSCL 08G

Progress is reported in developing predictive abilities to evaluate the potential stabilities of magnetic minerals in the Earth crust and mantle by: (1) computing oxidation state profiling as a function of temperature and pressure; (2) compiling data on basalts to establish validity of the oxidation state profiles; (3) determining Fe-Ni alloys in association with magnetite as a function of temperature and oxidation state; and (4) acquiring large chemical data banks on the mineral ilmenite which decomposes to mineral spinel in the presence of high sulfur or carbonate environments in the lower crust upper mantle. In addition to acquiring these data which are related to constraining Curie isotherm depths, an excellent correlation was found between MAGSAT anomaly data and the geology of West Africa. A.R.H.

N82-15489# Geological Survey, Denver, Colo.
**GEOLOGIC APPLICATIONS OF THERMAL-INERTIA
 MAPPING FROM SATELLITE Final Report**
 Terry W. Offield, Principal Investigator, Kenneth Watson, and
 Susanne Hummer-Miller Jul. 1981 109 p refs Original contains
 imagery. Original imagery may be purchased from NASA Goddard
 Space Flight Center, (Code 601), Greenbelt, Md. 20771.
 Domestic users send orders to 'Attn: National Space Science
 Data Center'; non-domestic users send orders to 'Attn: World
 Data Center A for Rockets and Satellites'. HCMM
 (NASA Order S-40256-B)
 (E82-10011: NASA-CR-164818) Avail: NTIS
 HC A06/MF A01 CSCL 08B

In the Powder River Basin, Wyo., narrow geologic units having thermal inertias which contrast with their surroundings can be discriminated in optimal images. A few subtle thermal inertia anomalies coincide with areas of helium leakage believed to be associated with deep oil and gas concentrations. The most important results involved delineation of tectonic framework elements some of which were not previously recognized. Thermal and thermal inertia images also permit mapping of geomorphic textural domains. A thermal lineament appears to reveal a basement discontinuity which involves the Homestake Mine in the Black Hill, a zone of Tertiary igneous activity and facies control in oil producing horizons. Applications of these data to the Cabeza Prieta, Ariz., area illustrate their potential for igneous rock type discrimination. Extension to Yellowstone National Park resulted in the detection of additional structural information but surface hydrothermal features could not be distinguished with any confidence. A thermal inertia mapping algorithm, a fast and accurate image registration technique, and an efficient topographic slope and elevation correction method were developed. Author

04 GEOLOGY AND MINERAL RESOURCES

**N82-15506# Geological Survey, Denver, Colo.
PRELIMINARY ANALYSIS OF GRAVITY AND AEROMAGNETIC SURVEYS OF THE TIMBER MOUNTAIN AREA, SOUTHERN NEVADA**

M. F. Kane, M. W. Webring, and B. K. Bhattacharyya 1981
143 p refs

(Contract DE-AI08-78ET-44802)
(DE81-029462; DOE/ET-44802/T2; USGS-Open-File-81-189)
Avail: NTIS HC A07/MF A01

Gravity and aeromagnetic surveys revealed details of subsurface structure and lithology. Information caused by volcanic events, accommodated along straight line faults combining to give a curvilinear appearance to regional structure is suggested. The magnetic data suggest that rock units may have been altered, perhaps thermally, from their original state. The gravity data indicate that the south part of Timber Mountain is underlain by relatively dense and possibly intrusive rock, like that which crops out along its southeast side. The gravity data also suggest that the Silent Canyon caldera may extend considerably south of its presently indicated southern limit and may underlie much of the area of Timber Mountain. The most areas appear to be more rectangular or triangular than annular in shape. The southern part of Timber Mountain caldera is separated from the Yucca Mountain area to the south by a triangular horst. The structural relations of the rock units making up the horst are complex. Several linear terrain features in the southern part of the caldera area are closely aligned with geophysical features, implying that the terrain features are fault controlled. DOE

**N82-15925# Preussag A.G. Metall, Goslar (West Germany).
Arbeitsgebiet Rohstoffe.**

**AN INVESTIGATION INTO THE APPLICABILITY OF THERMAL INFRARED SCANNING FOR EXPLORATION
Final Report, Feb. 1981**

Heribert Broicher Bonn Bundesministerium fuer Forschung und Technologie Jun. 1981 18 p refs In GERMAN; ENGLISH summary Sponsored by Bundesministerium fuer Forschung und Technologie

(BMFT-FB-T-81-087; ISSN-0340-7608) Avail: NTIS HC A02/MF A01; Fachinformationszentrum, Karlsruhe, West Germany DM 3,80

Pratt's theory of thermal inertia stripping lead to thermal inertia calculations for subsurface zones subjected to diurnal and annual temperature variations, as well as to temperatures at the zone limits. Thermal inertia mapping after separating these zones gains in importance for exploration since forebodies might cause detectable subsurface temperature anomalies. T.M.

OCEANOGRAPHY AND MARINE

Includes sea-surface temperature, ocean bottom surveying imagery, drift rates, sea ice and icebergs, sea state, fish location.

A82-10671 Analysis of SEASAT wind observations over the Indian Ocean. J. J. Fernandez-Partagas and M. A. Estoque (Miami, University, Miami, FL). *Tellus*, vol. 33, Oct. 1981, p. 463-475. Contract No. NOAA-NA-79SAC00737.

Surface winds as observed by the Seasat-A satellite over the Indian Ocean for the period July 15-17, 1978 are analyzed. The purposes of the analysis are: (1) to evaluate the accuracy of the Seasat wind measurements by comparing these measurements with ship observations and (2) to determine the improvement introduced to the description of the synoptic-scale wind field at the surface by adding Seasat data to ship and island wind observations. The results of the study indicate that: (1) on the synoptic scale, the accuracy of Seasat-derived winds is comparable to that of conventional surface observations and (2) a significant improvement in the surface wind analysis is achieved by incorporating Seasat wind information, especially in data sparse areas. (Author)

A82-11201 The observation of tidal patterns, currents, and bathymetry with SLAR imagery of the sea. G. P. De Loor (Centrale Organisatie voor Toegepast-Natuurwetenschappelijk Onderzoek, Fysisch Laboratorium TNO, The Hague, Netherlands). *IEEE Journal of Oceanic Engineering*, vol. OE-6, Oct. 1981, p. 124-129. 9 refs.

Work done until 1978 on the visualization of currents, bathymetry, internal waves, etc., in SLAR imagery of the sea is reported. It did not receive much attention until the SEASAT SAR imagery showed these effects on a global scale. Although we know, qualitatively, how these images come about we are yet far from knowing how to extract more quantitative data from them on depth, current speed, etc. Much research effort is still needed here and for this work a simple real-aperture SLAR can be a very useful tool. (Author)

A82-11202 * SAR imaging of ocean waves - Theory. A. Jain (California Institute of Technology, Jet Propulsion Laboratory, Pasadena, CA). *IEEE Journal of Oceanic Engineering*, vol. OE-6, Oct. 1981, p. 130-139. 26 refs. Contract No. NAS7-100.

A SAR imaging integral for a rough surface is derived. Aspects of distributed target imaging and questions of ocean-wave imaging are considered. A description is presented of the results of analyses which are performed on aircraft and a spacecraft data in order to gain an understanding of the SAR imaging of ocean waves. The analyzed data illustrate the effect of radar resolution on the images of azimuthally traveling waves, the dependence of image distortion on the angle which the waves make with the radar flight path, and the dependence of the focusing parameter of the radar matched filter on the ocean wave period for azimuthally traveling waves. A dependence of ocean-wave modulation on significant wave height is also observed. The observed dependence of the modulations of azimuth waves on radar resolution is in contradiction to the hypothesis that these modulations are caused mainly by velocity bunching. G.R.

A82-11203 Wave orbital velocity, fade, and SAR response to azimuth waves. R. K. Raney (Canada Centre for Remote Sensing, Ottawa, Canada). *IEEE Journal of Oceanic Engineering*, vol. OE-6, Oct. 1981, p. 140-146. 18 refs.

Orbital motion of azimuth waves imposes differential Doppler shifts on wave imagery as seen by a SAR. This paper shows that these Doppler shifts are a function only of the wave and sensor geometry, and are not a function of SAR parameters. The azimuth wave reflectivity so modulated is equivalent to a redistributed scatterer density which can be used as an input with the SAR modulation transfer function for general distributed scenes to derive the azimuth wave image. The static scatterer density is calculated for a variety of sea states. Wave accelerations are not of first-order importance.

Scatterer fade (decorrelation) is of central importance, as it impacts the SAR transfer function that is effective in wave imaging. (Author)

A82-12885 * Synoptic thermal and oceanographic parameter distributions in the New York Bight Apex. R. W. Johnson (NASA, Langley Research Center, Hampton, VA), G. S. Bahn (Kentron International, Inc., Hampton, VA), and J. P. Thomas (NOAA, Northeast Fisheries Center, Highlands, NJ). *Photogrammetric Engineering and Remote Sensing*, vol. 47, Nov. 1981, p. 1593-1598. 11 refs.

Concurrent surface water measurements made from a moving oceanographic research vessel were used to calibrate and interpret remotely sensed data collected over a plume in the New York Bight Apex on 23 June 1977. Multiple regression techniques were used to develop equations to map synoptic distributions of chlorophyll a and total suspended matter in the remotely sensed scene. Thermal (which did not have surface calibration values) and water quality parameter distributions indicated a cold mass of water in the Bight Apex with an overflowing nutrient-rich warm water plume that originated in the Sandy Hook Bay and flowed south near the New Jersey shoreline. Data analysis indicates that remotely sensed data may be particularly useful for studying physical and biological processes in the top several metres of surface water at plume boundaries. (Author)

A82-13214 Oceanic wind and balanced pressure-height fields derived from satellite measurements. R. M. Endlich, D. E. Wolf, C. T. Carlson, and J. W. Maresca, Jr. (SRI International, Menlo Park, CA). *Monthly Weather Review*, vol. 109, Sept. 1981, p. 2009-2016. 14 refs. Contract No. NOAA-NA-79SAC0073.

The surface wind field over part of the northern Pacific on July 17 and October 3, 1978, was analyzed in light of (1) Seasat-A scatterometer system (SASS) measurements of wind speed and direction, and (2) GOES-2 satellite measurements of cloud motion directions. Agreement was found upon comparison of the surface pressure fields computed from the nondivergent, SASS-derived wind velocity fields using the balance equation with National Meteorological Center surface pressure fields. The linear correlation coefficient between the two fields was 0.91 for July 17 and 0.84 for October 3, indicating that the surface wind and pressure fields of the global oceans, excluding a narrow equatorial zone where the balance equation is invalid, can be determined with good accuracy by the exclusive use of satellite measurements. O.C.

A82-14586 # Water vapour absorption in the 3.5-4.2 micron atmospheric window. I. J. Barton (Oxford University, Oxford, England; Commonwealth Scientific and Industrial Research Organization, Div. of Atmospheric Physics, Aspendale, Victoria, Australia). *Royal Meteorological Society, Quarterly Journal*, vol. 107, Oct. 1981, p. 967-972. 16 refs. Research supported by the Natural Environment Research Council.

An analysis of the results of Nimbus 5 Chopper Radiometer data of sea surface water vapor temperature in the 3.5-4.2 micron interval are reported. The interval was chosen because the temperature dependence of the Planck radiance gives better temperature discrimination than at longer wavelengths and the water absorption is smaller, although e-type absorption was observed. Derivation of the absorption coefficients is described, along with measurement techniques used with the Nimbus-5 instruments. A transmittance model was developed to account for absorptances by atmospheric gases, resulting in a value of 4/g² cm/atm for a self-broadened coefficient at 3.55 microns, implying the possibility of remotely sensing tropical sea surface temperatures to an accuracy of 1 K. M.S.K.

A82-14730 Radar backscattering from ocean waves at low grazing angles. H. C. Glaser and T. F. Havig (Boeing Aerospace Co., Seattle, WA). In: NAECON 1981; Proceedings of the National Aerospace and Electronics Conference, Dayton, OH, May 19-21, 1981. Volume 1. New York, Institute of Electrical and Electronics Engineers, Inc., 1981, p. 406-411. 6 refs.

Measurement of backscattering from sea clutter at grazing angles of zero to eight degrees is presented. During the qualification testing of the E-3A maritime radar (S-band, horizontally polarized, short pulse length), sea clutter data were recorded. Almost two billion range gate amplitudes were recorded over the period between

05 OCEANOGRAPHY AND MARINE RESOURCES

November 1979 and May 1980. Data judged outside the dynamic range of the system and that contaminated by land clutter were deleted. Conditions from flat calm to sea state five with forty knot winds have been recorded. Surface truth was reported by NOAA weather buoys every hour by satellite link. Wind speed was reported by the buoys and by the operator of the target vessel used in the testing. Absolute backscattering levels were determined by comparing the clutter returns with those from a dihedral reflector of measured cross section. Flight-to-flight variation in system gain is less than 2 dB, allowing reliable comparison between all of the data.

(Author)

A82-15030 **Comparison of polar and geostationary satellite infrared observations of sea surface temperatures in the Gulf of Maine.** R. Legeckis, E. Legg (NOAA, National Environmental Satellite Service, Washington, DC), and R. Limeburner (Woods Hole Oceanographic Institution, Woods Hole, MA). *Remote Sensing of Environment*, vol. 9, June 1980, p. 339-350. 10 refs. Grants No. NOAA-04-7-158-44104; No. NOAA-04-8-M01-149.

A82-15031 * **Remote sensing of benthic microalgal biomass with a tower-mounted multispectral scanner.** D. J. Jobson, S. J. Katzberg (NASA, Langley Research Center, Flight Electronics Div., Hampton, VA), and R. G. Zingmark (South Carolina University, Columbia, SC). *Remote Sensing of Environment*, vol. 9, June 1980, p. 351-362. 18 refs. Grant No. NSG-1334.

A remote sensing instrument was mounted on a 50-ft tower overlooking North Inlet Estuary, South Carolina in order to conduct a remote sensing study of benthic microalgae. The instrument was programmed to take multispectral imagery data along a 90 deg horizontal frame in six spectral bands ranging from 400-1050 nm and had a ground resolution of about 3 cm. Imagery measurements were encoded in digital form on magnetic tape and were stored, decoded, and manipulated by computer. Correlation coefficients were calculated on imagery data and chlorophyll a concentrations derived from ground truth data. The most significant correlation occurred in the blue spectral band with numerical values ranging from -0.81 to -0.88 for three separate sampling periods. Mean values of chlorophyll a for a larger section of mudflat were estimated using regression equations. The scanner has provided encouraging results and promises to be a useful tool in sampling the biomass of intertidal benthic microalgae.

(Author)

A82-15076 **Ocean surface height-slope probability density function from SEASAT altimeter echo.** B. J. Lipa (SRI International, Menlo Park, CA) and D. E. Barrick (NOAA, Wave Propagation Laboratory, Boulder, CO). *Journal of Geophysical Research*, vol. 86, Nov. 20, 1981, p. 10921-10930. 25 refs. Grant No. NOAA-MO-A01-78-00-4319.

A82-15213 † **Determination of the length of sea waves by an airborne radar technique (Opredelenie dliny morskikh voln radiolokatsionnym metodom s letatel'nogo apparata).** A. A. Garnaker'ian, V. L. Karakush'ian, and V. D. Bukharin. *Radiotekhnika i Elektronika*, vol. 26, Nov. 1981, p. 2447-2450. 6 refs. In Russian.

A82-15318 * # **An analysis of short pulse and dual frequency radar techniques for measuring ocean wave spectra from satellites.** F. C. Jackson (NASA, Goddard Space Flight Center, Greenbelt, MD). *Radio Science*, vol. 16, Nov.-Dec. 1981, p. 1385-1400. 17 refs.

A four frequency moment characterization of backscatter from the near-vertical is applied to an analysis of the short pulse and dual frequency microwave techniques. The range reflectivity modulation spectrum closely approximates the directional wave slope spectrum, while harmonic distortion is small and is a minimum near 10 deg incidence. The short pulse measurement signal-to-noise ratio (SNR) is typically greater than the narrowband dual frequency SNR, with the difference being the ratio of the range beam extent to pulse length, minus the ratio of beam-limited to pulse-limited Doppler spreads. It is concluded that dual frequency measurements are basically impractical, although short pulse measurements are useful and can employ existing space-qualified microwave hardware.

D.L.G.

A82-15960 † **Investigation of survey conditions for the ocean surface in the 0.4-1.1 micron spectral range (Issledovanie**

uslovii s'emki poverkhnosti okeana v spektral'nom diapazone 0.4-1.1 mkm). A. S. Selivanov, Iu. M. Gektin, A. S. Panfilov, and A. B. Fokin. *Issledovanie Zemli iz Kosmosa*, Sept.-Oct. 1981, p. 82-89. 18 refs. In Russian.

The optimal survey conditions were determined for frontal zones, meanders, eddies, and internal waves in the ocean, based on Meteor-satellite observations of the ocean surface in the visible and near-infrared spectral band. A theoretical model is presented, which takes into account these surface phenomena. It is shown that surveys should be performed in the sunny areas, where contrasts reach their maximum values; the maximum values of contrast were observed at solar zenith distances and at angles of sight of about 40 deg. The width of the spectral survey band does not have great significance in the study, since the observed phenomena do not have a marked spectral selectivity. Contrasts on the surfaces were found to disappear when the speed of the ocean surface wind exceeded 5-7 m/sec.

J.F.

A82-15962 † **Development of a coastal relief of the Gulf of Riga, based on results of an analysis of space images (Razvitie rel'efa poberezhii Rihzskogo zaliva po rezul'tatam analiza kosmicheskikh snimkov).** G. A. Saf'ianov and V. I. Kravtsova (Moskovskii Gosudarstvennyi Universitet, Moscow, USSR). *Issledovanie Zemli iz Kosmosa*, Sept.-Oct. 1981, p. 97-102. In Russian.

Based on an interpretation of relief forms of the coast of the Gulf of Riga, a geomorphological scheme of the coast was compiled, and an analysis of the dynamics of its development was performed. The direction of the alluvial drift in the past was established, and the main tendency of the dynamic processes of the coastal zone during the past thousand years were determined, namely, the separation of the single flow of deposits due to a change in the external conditions of their displacement.

J.F.

A82-16341 **U.S. Navy planning for satellite oceanographic data exploitation.** V. E. Noble (U.S. Navy, Naval Research Laboratory, Washington, DC) and R. Y. Felt (U.S. Navy, Naval Oceanography Div., Washington, DC). In: *International space technical applications; Proceedings of the Nineteenth Goddard Memorial Symposium*, Arlington, VA, March 26, 27, 1981. San Diego, CA, Univelt, Inc., 1981, p. 117-130. (AAS 81-072)

The authors present an unofficial view of the basis for planning within the Navy Environmental Remote Sensing Program (NERSP). The NERSP includes all phases of research, development, and operational applications related to exploitation of oceanographic data from satellites. The existing 'end-to-end' system will be expanded to provide for: direct and central-site readout, assimilation of satellite data into analysis and prediction programs, dissemination and display of products, and generation of system-specific Tactical Decision Aids. NERSP priorities are driven by requirements, opportunities, and difficulty of R&D problems.

(Author)

A82-16620 † **Images of sea waves obtained in polarimetric surveys (Ob izobrazhenii volneniia pri poliarizatsionnoi s'emke).** V. V. Egorov and B. S. Zhukov. In: *Airborne and spaceborne multispectral photography of the earth.* Moscow, Izdatel'stvo Nauka, 1981, p. 188-196. 13 refs. In Russian.

An analysis is presented of the influence of the orientation of the analyzer on the structure and contrast of sea-wave images in polarimetric remote-sensing surveys. The imaging process is accompanied by a distinctive wave-filtering which depends on the survey conditions. Experimental results on such polarimetric surveys are presented.

B.J.

A82-17168 **Detection of monsoon inversion by TIROS-N satellite.** M. S. Narayanan and B. M. Rao (Space Applications Centre, Ahmedabad, India). *Nature*, vol. 294, Dec. 10, 1981, p. 546-548. 6 refs.

A link is established between the extent of inversion regions and the convective processes with the Indian monsoon at its different phases. TIROS N satellite data provided sea surface temperature (SST), a 15-layer atmospheric temperature profile from 1000 to 0.4 mbar, and three levels of water vapor content. A horizontal map of the SST and the 1000-850 mb layer-mean temperature with time and spatial averaging, confirmed by comparison with aircraft dropsonde data, revealed the inversion over the Arabian Sea. A 5 x 5 deg grid

was devised to account for underlap of the maps, and showed a temperature increase west to east with the growth of a monsoon. A 10 min water vapor curve for the 700-500 mbar level, drawn from the TIROS data, revealed higher values to the east, with the curve oscillating in weak, active, and revival periods of the monsoon. The middle level moisture changes were consistent with the shifts of low level inversions, and were linked to the monsoon circulation. D.H.K.

A82-17292 * # Clear water radiances for atmospheric correction of coastal zone color scanner imagery. H. R. Gordon (Miami University, Coral Gables, FL) and D. K. Clark (NOAA, National Earth Satellite Service, Washington, DC). *Applied Optics*, vol. 20, Dec. 15, 1981, p. 4175-4180. 18 refs. Contract No. NAS5-22963; Grant No. NOAA-NA-79SA00741.

The possibility of computing the inherent sea surface radiance for regions of clear water from coastal zone color scanner (CZCS) imagery given only a knowledge of the local solar zenith angle is examined. The inherent sea surface radiance is related to the upwelling and downwelling irradiances just beneath the sea surface, and an expression is obtained for a normalized inherent sea surface radiance which is nearly independent of solar zenith angle for low phytoplankton pigment concentrations. An analysis of a data base consisting of vertical profiles of upwelled spectral radiance and pigment concentration, which was used in the development of the CZCS program, confirms the virtual constancy of the normalized inherent sea surface radiance at wavelengths of 520 and 550 nm for cases when the pigment concentration is less than 0.25 mg/cu m. A strategy is then developed for using the normalized inherent sea surface radiance in the atmospheric correction of CZCS imagery.

A.L.W.

A82-17492 The near-infrared radiation received by satellites from clouds. G. J. Bell and M. C. Wong (Royal Observatory, Hong Kong). *Monthly Weather Review*, vol. 109, Oct. 1981, p. 2158-2163. 12 refs.

An analysis of certain Tiros N IR data of cloud tops and the sea at 3.7 microns which show that the sea is cooler than the clouds is presented. Noting that data taken at 10 microns showed the sea surface to be warmer than the clouds, the total radiation within the satellite's passband reaching the radiometer is defined by the net flux radiated by the element, the flux radiated by the atmospheric molecules and aerosols, and the solar flux reflected by the element. Calculations of the albedo of the clouds and sea show that under certain circumstances the reflected radiance from the sea will yield satellite IR scans which show that the sea is cooler than the clouds, because the sensor is receiving more radiation from the clouds. A steady decrease of albedo occurs with increasing wavelength and angle incidence.

M.S.K.

A82-17494 Annual and nonseasonal variability of monthly low-level wind fields over the Southeastern Tropical Pacific. B. Enfield (Oregon State University, Corvallis, OR). *Monthly Weather Review*, vol. 109, Oct. 1981, p. 2177-2190. 20 refs. NSF Grants No. ATM-78-20419; No. OCE-80-24116; Contract No. NOAA-NA-80RAC00003.

A82-17565 The use of satellite infrared imagery for describing ocean processes in relation to spawning of the northern anchovy (*Engraulis mordax*). R. Lasker, R. M. Laurs (NOAA, Southwest Fisheries Center, La Jolla, CA), and J. Pelaez (California University, San Diego, CA). *Remote Sensing of Environment*, vol. 11, Dec. 1981, p. 439-453. 10 refs.

Using satellite infrared thermal imagery in conjunction with extensive sampling for anchovy eggs and adults during March and April 1980, it is confirmed that large areas of the coastal ocean off California were avoided by anchovies during the peak of spawning due to entrainment into the California Current of water at a temperature of less than or equal to 14 C that upwelled north of Point Conception. Upwelling began coincident with the onset of winds from the north and proceeded in pulses separated by a few days. Plumes of upwelled water appeared to be advected southward in ladder-like rows by the California Current. A saline warm water pool more than 50 m deep 40 km off Ensenada, Baja California, Mexico also was avoided by anchovies. The appearance of an inshore

16 C refuge and an extensive 220-km warm-water 'wake' associated with Santa Catalina Island also were observed. Each of these oceanographic features was confirmed by ship observations. (Author)

A82-17567 Variations in upper ocean heat storage determined from satellite data. J. R. Miller (Rutgers University, New Brunswick, NJ). *Remote Sensing of Environment*, vol. 11, Dec. 1981, p. 473-482. 12 refs.

The development of new microwave sensors to measure oceanic surface parameters from satellites will provide information applicable to studies of variations in upper ocean heat storage. An algorithm was developed to use satellite-derived values of sea-surface temperature and surface wind speeds to predict changes in subsurface heat storage. The algorithm, which is based on a one-dimensional model of the upper ocean, is used to determine the effect of inherent limitations of satellite data, such as discontinuous coverage and errors in the derived fields. Errors in the temperature field become more important as the surface mixed-layer deepens, and accurate specification of the temperature field appears to be more important than accurate specification of the wind field. However, it is important to obtain information about high wind speed events when they occur. The technique, which also provides information on the total heat flux into the ocean between successive satellite passes, could be improved by obtaining information from more than one satellite and from multiple sensors. (Author)

A82-17915 # The development of the Tiros Global Environmental Satellite System. A. Schnapf. *American Institute of Aeronautics and Astronautics, Aerospace Sciences Meeting, 20th, Orlando, FL, Jan. 11-14, 1982, Paper 82-0383*. 11 p.

A table giving the orbital performance of the Tiros satellites is included. It is noted that the infrared data from the Tiros-N/NOAA satellites can be used to produce charts showing the sea-surface temperature over a larger area and with greater frequency than is possible from any other source. Satellite pictures display the extent and character of ice fields in the Arctic and Antarctic seas and on the Great Lakes with a frequency and geographic coverage never before attained. Tiros also collects and locates data from fixed or moving platforms and monitors electron and proton particles emanating from the sun.

C.R.

A82-18074 # Measurement of sea and ice backscatter reflectivity using an OTH radar system. W. F. Ring and G. S. Sales (USAF, Rome Air Development Center, Bedford, MA). In: *Symposium on the Effect of the Ionosphere on Radiowave Systems*, Washington, DC, April 14-16, 1981, Preprints. Washington, DC, U.S. Naval Research Laboratory, 1981. (3B-2). 9 p. 8 refs.

Backscattered radio wave characteristics may permit the recognition of coastal regions or islands through differences in scattering by land and water. This technique is developed for the quantification of sea water, sea ice and Greenland ice cap surface reflectivities so that they may serve as references for the calibration of HF, Over-the-Horizon (OTH) radar sensitivity. Such references are necessary when no aircraft targets-of-opportunity are available to serve as calibration sources. Attention is drawn to the azimuthal or latitudinal variation in radar scattering cross section found. Previous measurements and models do not show the consistent increase in absorption from 65 to 72 deg geomagnetic latitude exhibited by the data presented. An ionospheric absorption or scattering loss mechanism is postulated as an explanation of this phenomenon. O.C.

A82-18716 * Evaluation of the Seasat wind scatterometer. W. L. Jones, E. M. Bracalente, L. C. Schroeder (NASA, Langley Research Center, Hampton, VA), D. H. Boggs, D. Shelton (California Institute of Technology, Jet Propulsion Laboratory, Pasadena, CA), R. A. Brown (Washington University, Seattle, WA), and T. H. Guymr (Institute of Oceanographic Sciences, Wormley, Surrey, England). *Nature*, vol. 294, Dec. 24-31, 1981, p. 704-707. 16 refs.

Surface wind velocities have been derived from backscatter measurements of the ocean surface made by a satellite-borne, microwave sensor. Comparisons with high-quality surface-based measurements obtained during the Joint Air-Sea Interaction experiment are described. The accuracy of the scatterometer winds at this mid-latitude site, + or - 1.6 m/s in speed and + or - 18 deg in

05 OCEANOGRAPHY AND MARINE RESOURCES

direction, for winds between 3 and 16 m/s is within the design specification. (Author)

A82-18724 * Anomalous wind estimates from the Seasat scatterometer. T. H. Guymer (Institute of Oceanographic Sciences, Wormley, Surrey, England), J. A. Businger (Washington, University, Seattle, WA), W. L. Jones (NASA, Langley Research Center, Hampton, VA), and R. H. Stewart (California Institute of Technology, Jet Propulsion Laboratory, Pasadena, CA). *Nature*, vol. 294, Dec. 24-31, 1981, p. 735-737. 10 refs.

The Seasat-A Satellite Scatterometer (SASS) measured the radar backscatter intensity from the sea surface using a four-beam microwave antenna. Estimates of wind speed and direction derived from these data agree well with surface measurements made during the Joint Air-Sea Interaction experiment, but there are occasions (3 out of 23 satellite passes) when the results are anomalous. One such occasion when the satellite measurements differed substantially from those at the surface of the sea has been studied, and it has been concluded that the interpretation of the SASS measurements may have been vitiated by a mid-level convective system deep enough to produce thunderstorms and lightning. (Author)

N82-10461# National Oceanic and Atmospheric Administration, Seattle, Wash.

CTD/02 MEASUREMENTS DURING THE EQUATORIAL PACIFIC OCEAN CLIMATE STUDY (EPOCS) IN 1979

L. J. Mangum, N. N. Soreide, B. D. Davies, B. D. Spell, and S. P. Hayes Oct. 1980 641 p refs (PB81-211203; NOAA-DR-ERL-PMEL-1; NOAA-81041501) Avail: NTIS HC A99/MF A01 CSCL 081

Neil Brown instrument System (NBIS) CTD/02 measurements recorded on five cruises are summarized. A description of the acquisition and processing systems and calibration techniques are presented. These data were collected along longitudes of 105 W and 110 W between 15 N and 5 S. Additional casts in the vicinity of 0 degrees, 153 W also presented. Station locations, meteorological conditions, and profiles of temperature, salinity, sigma T, and oxygen are shown for each cast. GRA

N82-10467 Danish Meteorological Inst., Copenhagen.
THE ICE-CONDITIONS IN THE GREENLAND WATERS, 1965. COASTAL MAPS

1980 66 p refs (ISBN-87-7478-183-9) Avail: NTIS HC A04/MF A01

Maps indicating the size, distribution, and character of Greenland's coastal ice formations are presented. Data is derived from visual flight observations and supplemented by aerial radar reconnaissance and ship observations. Narrative evaluations of ice conditions for several coastal locations are presented. R.J.F.

N82-10473# Nova Univ., Dania, Fla.
SEASAT ALTIMETRY ADJUSTMENT MODEL INCLUDING TIDAL AND OTHER SEA SURFACE EFFECTS

Georges Blaha Hanscom AFB, Mass. AFGL Mar. 1981 113 p refs (Contract F19628-78-C-0013; AF Proj. 2309) (AD-A104188; SR-3; AFGL-TR-81-0152) Avail: NTIS HC A06/MF A01 CSCL 22/2

This study is a part of the on-going effort aimed at improved determinations of the Earth's gravity field through the adjustment of satellite altimeter data in the short-arc mode. Until recently the key role in such adjustments has been played by GEOS-3 altimeter data. However, Seasat altimetry is envisioned as providing a more accurate means for addressing this task. In view of the improved quality of altimeter data and of the corresponding more stringent requirements for the data reduction, several improvements in the existing altimetry model have been designed and are described herein. For example, the criteria have been established specifying the maximum and the minimum allowable lengths of Seasat arcs. An important improvement in the economy has been achieved through a reduction in the number of spherical-harmonic potential coefficients entering the orbital integrator, without a noticeable compromise in the excellent quality of the Seasat observational system. GRA

N82-10486# Science Research Council, Slough (England).
STUDY ON SATELLITE RADAR ALTIMETRY IN CLIMATO-

LOGICAL AND OCEANOGRAPHIC RESEARCH, VOLUME 1 Final Report

Paris ESA Dec. 1980 450 p refs Prepared in cooperation with Natural Environment Research Council, Godalming, England 2 Vol.

(Contract ESA-4355/80/F-FC(SC)) (SP/153/06/01/FR(80)-Vol-1; ESA-CR(P)-1437-Vol-1) Avail: NTIS HC A19/MF A01

The contribution of satellite radar altimetry to climate, oceanographic and glaciological research is analyzed. The current position, the need for improved data and the relevance of existing altimeter data to climate, oceanographic and glaciological studies are discussed. Experience gained from previous missions is reviewed and the corrections which need to be made to the basic altimeter data are considered, along with the requirements for supporting measurements needed to aid in interpretation of this data. Sampling requirements in relation to particular aspects of oceanography and glaciology are treated. The role of circulation models in satellite altimetry, and those features of instrument design relating to scientific requirements, are examined. Supporting and complementary instruments are reviewed. The value of multi-satellite missions and possible future developments are discussed. Author (ESA)

N82-10487# Science Research Council, Slough (England).
STUDY ON SATELLITE RADAR ALTIMETRY IN CLIMATOLOGICAL AND OCEANOGRAPHIC RESEARCH, VOLUME 2 Final Report

Paris ESA Dec. 1980 47 p Prepared in cooperation with Natural Environment Research Council, Godalming, England 2 Vol.

(Contract ESA-4355/80/F-FC(SC)) (SP/153/06/01/FR(80)-Vol-2; ESA-CR(P)-1437-Vol-2) Avail: NTIS HC A03/MF A01

The potential contribution of satellite radar altimetry to climatology, oceanography, and glaciology is discussed. The altimetry requirements for future programs are considered. Tradeoffs between spatial and temporal coverage, sampling rate and error budget, involved in defining an optimum mission are examined. Accuracy of + or - 10 cm, pulse lengths of 1.5 nsec and integration times of 3 sec are recommended. Orbital inclination should be between 60 and 65 deg. Author (ESA)

N82-10660 Texas Univ. at Arlington.
A GLOBAL ATLAS OF GEOS-3 SIGNIFICANT WAVEHEIGHT AND COMPARISON OF THE DATA WITH NATIONAL BUOY DATA Ph.D. Thesis

James Douglas McMillan 1981 147 p Avail: Univ. Microfilms Order No. 8119337

The GEOS-3 significant waveheight estimation algorithm is derived by analyzing the return waveform characteristics of the altimeter. It is shown that the difference between the waveform expected from a flat surface and the actual waveform observed returning from a nonflat sea surface can be analyzed to determine the magnitude of the significant waveheight. This technique employs a curve fitting procedure utilizing least squares estimation. The rationale for a smoothing technique is presented and the convergence characteristics of the smoothed estimate are discussed. Then, a statistically representative sampling of GEOS-3 data is selected for comparison with buoy measurements and the accuracy of the GEOS-3 significant waveheight estimates is deduced, through statistical analysis, to be 50 cm. The GEOS-3 significant waveheight estimates gathered during the entire mission of the spacecraft are assembled in the form of a global atlas of contour maps. Both high and low sea state contour maps are presented, and the data are displayed both by seasons and for the entire duration of the GEOS-3 mission. The contour maps are then compared with contour maps compiled by the U.S. Navy and significant differences are found. Dissert. Abstr.

N82-10661*# National Aeronautics and Space Administration, Langley Research Center, Hampton, Va.

CHESAPEAKE BAY PLUME STUDY: SUPERFLUX 1980

Janet W. Campbell, ed. and James P. Thomas, ed. (National Marine Fisheries Service, Highland, N.J.) Oct. 1981 504 p refs Symp. held at Williamsburg, Va., 21-23 Jan. 1981; sponsored in part by National Marine Fisheries Service, NOAA, and Dept. of Commerce

(NASA-CP-2188; L-14680; NOAA/NEMP-111-81-ABCD-0042) Avail: NTIS HC A22/MF A01 CSCL 08C

The results of the Chesapeake Bay plume study are reported. The role of remote sensing in monitoring and assessing the effects of pollution of marine resources is delineated.

N82-10663*# National Marine Fisheries Service, Highlands, N.J. Div. of Environmental Assessment.
A MARINE ENVIRONMENTAL MONITORING AND ASSESSMENT PROGRAM

John B. Pearce *In* NASA. Langley Research Center Chesapeake Bay Plume Study Oct. 1981 p 15-28 refs

Avail: NTIS HC A22/MF A01 CSCL 08C

The need for the use of modern, extremely sensitive techniques to aid in rapidly and synoptically assessing the relative health and production of coastal waters and estuaries is reported. Major emphasis is placed on establishing a solid foundation for the use of remote sensing in basic oceanographic studies and the management of human wastes. R.C.T.

N82-10664*# National Aeronautics and Space Administration. Langley Research Center, Hampton, Va.

SUPERFLUX I, II, AND III EXPERIMENT DESIGN: REMOTE SENSING ASPECTS

Janet W. Campbell, Wayne E. Esaias, and Warren D. Hypes *In* its Chesapeake Bay Plume Study Oct. 1981 p 29-42 refs

Avail: NTIS HC A22/MF A01 CSCL 08C

The Chesapeake Bay plume study called Superflux is described. The study was initiated to incorporate the disciplines of both resources management and remote sensing in accomplishing the following objectives: (1) process oriented research to understand the impact of estuarine outflows on continental shelf ecosystems; (2) monitoring and assessment to delineate the role of remote sensing in future monitoring and assessment programs; and (3) remote sensing research: to advance the state of the art in remote sensing systems as applied to sensing of the marine environment, thereby hastening the day when remote sensing can be used operationally for monitoring and assessment and for process oriented research. R.C.T.

N82-10665*# National Marine Fisheries Service, Highlands, N.J. Northeast Fisheries Center.

SUPERFLUX I, II, AND III EXPERIMENT DESIGNS: WATER SAMPLING AND ANALYSES

James P. Thomas *In* NASA. Langley Research Center Chesapeake Bay Plume Study Oct. 1981 p 43-60

Avail: NTIS HC A22/MF A01 CSCL 08C

Both airborne remote sensors and seagoing research vessels were used to study the effects of man's continual use of the Chesapeake Bay offshore environments. The major focus of the study was to: (1) advance the development and transfer of improved remote sensing systems and techniques for monitoring environmental quality and effects on living marine resources; (2) increase understanding of the influence of estuarine outwelling (plumes) on contiguous shelf ecosystems; and (3) provide a synoptic, integrated and timely data base for application to problems of marine resources and environmental quality. R.C.T.

N82-10668*# Research Triangle Inst., Research Triangle Park, N. C.

MONITORING THE CHESAPEAKE BAY USING SATELLITE DATA FOR SUPERFLUX III

Fred M. Vukovich and Bobby W. Crissman *In* NASA. Langley Research Center Chesapeake Bay Plume Study Oct. 1981 p 93-110

(Grant NA81FA-C-00002)

Avail: NTIS HC A22/MF A01 CSCL 08C

The TIROS-N and NOAA-6, and GOES visible infrared satellite data were used to identify and locate surface oceanographic thermal fronts for the purpose of issuing daily and premission advisory briefings in support of the Superflux 3 in situ and remote sensing experiment in the Chesapeake Bay region. Satellite data were collected for the period 1 - 22 October 1980. A summary of that data is presented. R.C.T.

N82-10670*# National Aeronautics and Space Administration. Langley Research Center, Hampton, Va.

REMOTE SENSING OF THE CHESAPEAKE BAY PLUME SALINITY VIA MICROWAVE RADIOMETRY

Bruche M. Kendall *In* its Chesapeake Bay Plume Study Oct. 1981 p 131-140 refs

Avail: NTIS HC A22/MF A01 CSCL 08C

The NASA-Langley-developed L-Band microwave radiometer was used to remotely measure sea surface salinity during the Chesapeake Bay plume studies. Obtained measurements of microwave brightness temperatures of the sea surface were combined with measurements of sea surface temperature obtained with an infrared radiometer and inverted to produce corresponding values of sea surface salinity. Results from the plume measurements, which indicate the southward extent of the plume along the Virginia-North Carolina coast, are presented and discussed. Additional measurements obtained for the Delaware Bay Mouth flight, and the James River-Shelf flight, are also discussed. R.C.T.

N82-10672*# National Aeronautics and Space Administration. Langley Research Center, Hampton, Va.

PRELIMINARY ANALYSIS OF OCEAN COLOR SCANNER DATA FROM SUPERFLUX III

Craig W. Ohlhorst *In* its Chesapeake Bay Plume Study Oct. 1981 p 159-174

Avail: NTIS HC A22/MF A01 CSCL 08C

The ocean color scanner collected data Superflux III Experiment Single channel gray scale data products generated 5 minutes after the scanner data were collected showed details of the Chesapeake Plume structure, suggesting that this quick-look capability could have potential use to experimenters in real time. The Chesapeake Bay Plume extended offshore between 5 and 7 nautical miles on two occasions. The scanner data also show many other water features within the lower bay itself. R.C.T.

N82-10682*# National Aeronautics and Space Administration. Langley Research Center, Hampton, Va.

ANALYSIS OF TESTBED AIRBORNE MULTISPECTRAL SCANNER DATA FROM SUPERFLUX II

David E. Bowker, Charles A. Hardesty, Daniel J. Jobson, and Gilbert S. Bahn (Kenton International, Inc.) *In* its Chesapeake Bay Plume Study Oct. 1981 p 323-338

Avail: NTIS HC A22/MF A01 CSCL 08C

A test bed aircraft multispectral scanner (TBAMS) was flown during the James Shelf, Plume Scan, and Chesapeake Bay missions as part of the Superflux 2 experiment. Excellent correlations were obtained between water sample measurements of chlorophyll and sediment and TBAMS radiance data. The three-band algorithms used were insensitive to aircraft altitude and varying atmospheric conditions. This was particularly fortunate due to the hazy conditions during most of the experiments. A contour map of sediment, and also chlorophyll, was derived for the Chesapeake Bay plume along the southern Virginia-Carolina coastline. A sediment maximum occurs about 5 nautical miles off the Virginia Beach coast with a chlorophyll maximum slightly shoreward of this. During the James Shelf mission, a thermal anomaly (or front) was encountered about 50 miles from the coast. There was a minor variation in chlorophyll and sediment across the boundary. During the Chesapeake Bay mission, the Sun elevation increased from 50 degrees to over 70 degrees, interfering with the generation of data products. M.G.

N82-10684*# National Aeronautics and Space Administration. Wallops Flight Center, Wallops Island, Va.

APPLICATION OF THE NASA AIRBORNE OCEANOGRAPHIC LIDAR TO THE MAPPING OF CHLOROPHYLL AND OTHER ORGANIC PIGMENTS

F. E. Hoge and R. N. Swift (EG&G Washington Analytical Services Center, Inc.) *In* NASA. Langley Research Center Chesapeake Bay Plume Study Oct. 1981 p 349-374 refs

Avail: NTIS HC A22/MF A01 CSCL 08C

Laser fluorosensing techniques used for the airborne measurement of chlorophyll a and other naturally occurring waterborne pigments are reviewed. Previous experiments demonstrating the utility of the airborne oceanographic lidar (AOL) for assessment of various marine parameters are briefly discussed. The configuration of the AOL during the NOAA/NASA Superflux experiments is described. The participation of the AOL in these experiments is presented and the preliminary results are discussed. The

05 OCEANOGRAPHY AND MARINE RESOURCES

importance of multispectral receiving capability in a laser fluorosensing system for providing reproducible measurements over wide areas having spatial variations in water column transmittance properties is addressed. This capability minimizes the number of truthing points required and is usable even in shallow estuarine areas where resuspension of bottom sediment is common. Finally, problems encountered on the Superflux missions and the resulting limitations on the AOL data sets are addressed and feasible solutions to these problems are provided. M.G.

N82-10694*# National Aeronautics and Space Administration, Langley Research Center, Hampton, Va.
ASSESSMENT OF SUPERFLUX RELATIVE TO REMOTE SENSING

Janet W. Campbell *In its Chesapeake Bay Plume Study* Oct. 1981 p 501-502

Avail: NTIS HC A22/MF A01 CSCL 08C

The state-of-the-art advancements in remote sensor technology due to the Superflux program are examined. Three major individual sensor technologies benefitted from the program: laser fluorosensors, optical-range scanners, and passive microwave sensors. Under Superflux, convincing evidence was obtained that the airborne oceanographic lidar fluorosensor can map chlorophyll, i.e., is linear, over a wide range from less than 0.5 to 5.0 mg/cu m. The lidar oceanographic probe dual-excitation concept for addressing phytoplankton color group composition was also demonstrated convincingly. Algorithm development, real time capabilities, and multisensor integration are also addressed. M.G.

N82-11511*# Ball Aerospace Systems Div., Boulder, Colo.
DEVELOPMENT OF THE COASTAL ZONE COLOR SCANNER FOR NIMBUS 7. VOLUME 1: MISSION OBJECTIVES AND INSTRUMENT DESCRIPTION Final Report

May 1979 76 p refs

(Contract NAS5-20900)

(NASA-CR-166720-Vol-1; F78-11-Rev-A) Avail: NTIS HC A05/MF A01 CSCL 14B

An Earth scanning six channel (detector) radiometer using a classical Cassegrain telescope and a Wadsworth type grating spectrometer was launched aboard Nimbus 7 in order to determine the abundance or density of chlorophyll at or near the sea surface in coastal waters. The instrument also measures the sediment or gelbstoffe (yellow stuff) in coastal waters, detects surface vegetation, and measures sea surface temperature. Block diagrams and schematics are presented, design features are discussed and each subsystem of the instrument is described. A mission overview is included. A.R.H.

N82-11515*# OAO Corp., Hampton, Va.
TECHNOLOGY TRANSFER OF NASA MICROWAVE REMOTE SENSING SYSTEM Final Report

N. D. Akey Oct. 1981 38 p refs

(Contract NAS1-16380)

(NASA-CR-165791) Avail: NTIS HC A03/MF A01 CSCL 14B

Viable techniques for effecting the transfer from NASA to a user agency of state-of-the-art airborne microwave remote sensing technology for oceanographic applications were studied. A detailed analysis of potential users, their needs and priorities; platform options; airborne microwave instrument candidates; ancillary instrumentation; and other, less obvious factors that must be considered were studied. Conclusions and recommendations for the development of an orderly and effective technology transfer of an airborne microwave system that could meet the specific needs of the selected user agencies are reported. R.J.F.

N82-11537# National Oceanic and Atmospheric Administration, Seattle, Wash. Pacific Marine Environmental Lab.
ICE CONDITIONS IN THE EASTERN BERING SEA FROM NOAA AND LANDSAT IMAGERY: WINTER CONDITIONS 1974, 1976, 1977, 1979

Lyn McNutt Feb. 1981 186 p refs Prepared in cooperation with Science Applications, Inc., Bellevue, Wash.

(PB81-220188; NOAA-TM-ERL-PMEL-24; CONTRIB-500;

NOAA-81043005) Avail: NTIS HC A09/MF A01 CSCL 08L

The LANDSAT and NOAA satellite images from the University of Alaska LANDSAT library were used to make maps of ice conditions in the eastern Bering Sea. The analyses included daily

charts of the ice, polynya locations, floe trajectories, and comparisons between data taken from the two sources. A zoom transfer scope (ZTS) was used to transfer the data from an image to a map base for later winter condition in 1974, 1976, 1977, and 1979. GRA

N82-11743# National Oceanic and Atmospheric Administration, Miami, Fla.

THE DETERMINATION OF NAVIGATIONAL AND METEOROLOGICAL VARIABLES MEASURED BY NOAA/RFC WP3D AIRCRAFT

Francis J. Merceret and Harlan W. Davis Apr. 1981 28 p refs

(PB81-225468; NOAA-TM-ERL-RFC-7; NOAA-81051503)

Avail: NTIS HC A03/MF A01 CSCL 04B

For each variable, the sensor inputs and equations used are described and an estimate of the error in the result is provided. The report is divided into two sections: quantities displayed on-board in real-time and additional quantities computed and available to the user on request in the final data set. The aircraft and much of the instrumentation are described. T.M.

N82-12502# Office of Naval Research, Pasadena, Calif.

VISUAL OBSERVATIONS OF THE OCEAN

Robert E. Stevenson, L. David Carter (Geological Survey, Menlo Park, Calif.), Stephen P. VonderHaar (Univ. of Southern California, Los Angeles), and Richard O. Stone *In NASA. Johnson Space Flight Center Skylab Explores the Earth 1977* p 287-338 refs

Avail: NTIS MF A01; SOD HC \$16.50 CSCL 08J

The Skylab 4 mission allowed large scale, dynamic features such as ocean currents and associated eddies to be observed, described, and photographed repeatedly. Examples of regional and topical studies are included which discuss ocean currents, plankton, internal waves, coastal-sediment plumes, subtropical convergence, windborne sediment entering the ocean, and the interaction of ocean waves and currents. The importance of the observation of mesoscale phenomena is discussed as well as the amendment of charts of ocean currents. A.R.H.

N82-12503*# National Oceanic and Atmospheric Administration, Miami, Fla. Atlantic Oceanographic and Meteorological Labs.

AN ASSESSMENT OF THE POTENTIAL CONTRIBUTIONS TO OCEANOGRAPHY FROM SKYLAB VISUAL OBSERVATIONS AND HANDHELD-CAMERA PHOTOGRAPHS

George A. Maul and Michael McCaslin *In NASA. Johnson Space Flight Center Skylab Explores the Earth 1977* p 339-352

Avail: NTIS MF A01; SOD HC \$16.50 CSCL 08J

The possible roles that space observes may play in oceanographic experimentation are considered in a discussion of several ocean photographs and visual observations made during the Skylab 4 mission. While hand-held camera photography has a distinct role in reconnaissance, it cannot surpass the quantitative-ness of a multispectral observation from a known altitude. Significantly, many of the most interesting scenes were taken by the S190B camera, which produced very high resolution photographs taken from a vertical position. From the standpoint of long term oceanographic observation, quantitative observations are needed with accurate geographical positioning. Concurrent ocean surface observations are also needed to correlate the data. A.R.H.

N82-12533# Danish Meteorological Inst., Copenhagen.

THE ICE CONDITIONS IN THE GREENLAND WATERS

1980 69 p

(ISBN-87-7478-183-9) Avail: NTIS HC A04/MF A01

Charts showing weekly ice conditions for 1965 are presented. Thickness of fast ice measured at coastal stations is given and the number of icebergs sighted is reported. Polar ice progress is followed. Information on the size, boundary, age, water features, and topography is provided. For ice of land origin, the relative frequencies of bergy bits and growlers are indicated. Author (ESA)

N82-12734*# EG and G Washington Analytical Services Center, Inc., Pocomoke City, Md.

BOUNDARY DETECTION CRITERIA FOR SATELLITE ALTIMETERS

C. F. Martin and R. L. Taylor Nov. 1981 61 p refs
(Contract NAS6-3075)
(NASA-CR-156880) Avail: NTIS HC A04/MF A01 CSCL
148B

A procedure for using satellite altimeter data to determine the time of crossing of a surface boundary, such as ocean land or ocean ice, with the primary objective to flag altimeter data that do not properly represent oceanographic measurements were studied. Water to land crossing and water to sea ice crossing were investigated. For ocean ice crossings, a large increase in AGC occurred. Waveform tests for increasing the probability of detecting an ocean land crossing were investigated. It is recommended that the boundary test be based on a fit of the full waveform to a limited parameter set at a rate of 5 to 10 second. E.A.K.

N82-13484# National Oceanic and Atmospheric Administration, Rockville, Md. Office of Marine Pollution Assessment.
DEEP OCEAN MINING ENVIRONMENTAL STUDY. ENVIRONMENTAL EFFECTS OF COMMERCIAL-SCALE MINING
Nov. 1980 319 p refs
(PB81-227753; NOAA-81052103) Avail: NTIS
HC A14/MF A01 CSCL 081

Papers on deep ocean mining environmental study are presented. The titles are: estimated discharge characteristics of a commercial nodule mining operation; dissolved components of the discharge; increased oxygen demand and microbial biomass; trace metal exchange between ferromanganese nodules and artificial seawater; dispersion of deep sea mining particulates and their effect on light in ocean surface layer; environmental investigation of the effect of deep sea mining on marine phytoplankton and primary productivity in the tropical eastern north Pacific ocean; potential effects on deep sea minerals mining on macrozooplankton in the north equatorial Pacific; dispersal and resedimentation of the benthic plume from deep sea mining operations; and limits in prediction and detecting benthic community response to manganese nodule mining. GRA

N82-13639# SACLANT ASW Research Center, La Spezia (Italy).
THE SACLANTCEN OCEANOGRAPHIC DATA BASE. VOLUME 1: DESIGN CRITERIA AND DATA STRUCTURE AND CONTENT
Richard F. J. Winterburn 15 Jun. 1981 30 p refs
(AD-A103277; SACLANTCEN-SM-150-Vol-1) Avail: NTIS
HC A03/MF A01 CSCL 08/10

An oceanographic data base established at SACLANTCEN on a UNIVAC 1106 computer system is described. The design criteria used in setting up the data base, its structure and content, how data were acquired either from outside institutions or from SACLANTCEN experiments are reformatted and entered are discussed. Data are accessed, interrogated, and display, including the plotting of charts with coastlines and of contoured data are described. Author

N82-13641# Naval Oceanographic Office, Bay St. Louis, Miss.
Environmental Systems Div.
ICAPS OCEANOGRAPHIC DATA FOR THE INDIAN OCEAN Final Report
Dec. 1980 93 p refs
(AD-A103173; NOO-RP-32C) Avail: NTIS HC A05/MF A01
CSCL 08/10

The integrated command ASW prediction system (ICAPS) oceanographic data files for the Indian Ocean are presented. Graphic displays provide an illustration of the historical data stored within the ICAPS data base. Depth, temperature and salinity values are shown on a split-depth scale providing a depiction of the near surface structure and a less detailed picture of the slowly varying deeper structure. The corresponding oceanographic data for the Atlantic Ocean and Mediterranean Sea and Pacific Ocean are presented in companion publications. Author

N82-13642# Massachusetts Inst. of Tech., Cambridge. Dept. of Meteorology.
SURFACE SIGNS OF INTERNAL OCEAN DYNAMICS
Erik Mollo-Christensen 1980 8 p refs
(Contract N00014-80-C-0273)
(AD-A101380) Avail: NTIS HC A02/MF A01 CSCL 08/3

There are various processes internal to the ocean that can interact with the surface. The resulting interaction causes changes in the surface wave structure that may well be recognizable by

remote sensing systems. Vertical motion occurs when a wind driven surface Ekman layer is set up. Such 'pumping' can also take place in deeper Ekman layers especially over sloping bottom surfaces. Internal waves, topographic waves, and current shear can also cause changes in the surface wave field. A combination of ship, buoy, and remote sensors like those aboard LANDSAT and Seasat, coupled with the output of modeling analyses, can immeasurably improve our knowledge of ocean dynamics. Author

N82-14550*# National Aeronautics and Space Administration, Langley Research Center, Hampton, Va.
SPECTRAL ATMOSPHERIC OBSERVATIONS AT NANTUCKET ISLAND, MAY 7-14, 1981
T. A. Talay and L. R. Poole Nov. 1981 56 p refs
(NASA-TM-83196) Avail: NTIS HC A04/MF A01 CSCL
04A

An experiment was conducted by the National Langley Research Center to measure atmospheric optical conditions using a 10-channel solar spectral photometer system. This experiment was part of a larger series of multidisciplinary experiments performed in the area of Nantucket Shoals aimed at studying the dynamics of phytoplankton production processes. Analysis of the collected atmospheric data yield total and aerosol optical depths, transmittances, normalized sky radiance distributions, and total and sky irradiances. Results of this analysis may aid in atmospheric corrections of remote sensor data obtained by several sensors overflying the Nantucket Shoals area. Recommendations are presented concerning future experiments using the described solar photometer system and calibration and operational deficiencies uncovered during the experiment. A.R.H.

N82-14553# European Space Agency, Paris (France).
APPLICATION OF REMOTE SENSING DATA ON THE CONTINENTAL SHELF: PROCEEDINGS OF AN EARoL-ESA SYMPOSIUM
N. Longdon, comp. and G. Levy, comp. Jul. 1981 298 p refs
Symp. held in Voss, Norway, 19-20 May 1981 Prepared in cooperation with Royal Norwegian Council for Scientific and Industrial Research, Kjeller
(ESA-SP-167; ISSN-0379-6566) Avail: NTIS
HC A13/MF A01; ESA, Paris FF 125

A symposium which studied the application of remote sensing techniques to oceanography, fishing, pollution monitoring, and coastal zone management is reported. National programs, operational requirements, and state of the art are reviewed. The use of satellites, including LANDSAT, Seasat and ERS is highlighted.

N82-14554# European Space Agency, Paris (France). Directorate of Application Programmes.
ERS-1: MISSION OBJECTIVES AND SYSTEM CONCEPT
G. Duchossois and D. Lennertz *In its Appl. of Remote Sensing Data on the Continental Shelf* Jul. 1981 p 5-16

Avail: NTIS HC A13/MF A01; ESA, Paris FF 125

The objectives of the first ESA remote sensing (ERS-1) satellite program are the development and promotion of commercial applications related to a better knowledge of ocean parameters; monitoring of sea ice and icebergs for industrial oceanic activities at high latitudes; and to increase understanding of coastal zones and global ocean processes which, together with the monitoring of the polar regions, can provide a major contribution to the World Climate Research Program. The ERS-1 system (space segment and ground segment) is described including the instruments which are part of the Earth applications payload, active microwave instrumentation, an ocean color monitor, and a radar altimeter. The procedures used in selecting the Earth sciences payload complement, the parameters which can be obtained from the applications payload, and a development plan for the ERS-1 system are outlined. Author (ESA)

N82-14556# Naval Oceanographic Office, Washington, D. C.
THE POTENTIAL AND REQUIREMENTS FOR SPACE OCEANOGRAPHY
Ross N. Williams *In ESA Appl. of Remote Sensing Data on the Continental Shelf* Jul. 1981 p 23-27 refs

Avail: NTIS HC A13/MF A01; ESA, Paris FF 125

05 OCEANOGRAPHY AND MARINE RESOURCES

The use of satellite systems for communications, navigation, weather, oceanographic, and military purposes is reviewed. The trend is towards automated measurement, analysis, forecast and display of environmental effects. Both Marisat and Fleetsatcom, the shore based naval environmental data network and the commercial satellite data distribution system solve display and dissemination problems; and large dedicated computer capacity and atmospheric prediction models solve analysis and prediction software problems. Meteorological satellite programs together with more traditional atmospheric and oceanographic data inputs is used to demonstrate that globally sensed oceanographic data to initialize the models is not yet fully available, but could be determined with improved accuracy and resolution by employing an ocean satellite system, such as NOSS. Author (ESA)

N82-14557# Conoco Norway, Inc., Oslo.
OFFSHORE PETROLEUM INDUSTRY ENVIRONMENTAL DATA REQUIREMENTS: EMPHASIS ON REMOTE SENSING

Ronald L. Gratz /In ESA Appl. of Remote Sensing Data on the Continental Shelf Jul. 1981 p 31-43 refs

Avail: NTIS HC A13/MF A01; ESA, Paris FF 125

Data quality and coverage requirements for the remote sensing of oceanographic and meteorological factors affecting the development of offshore hydrocarbon resources are considered, using a combination of fine-grid hindcasting and surface truth measurements. The establishment of data banks able to accumulate 20-30 years of climatological data for use in future designs is recommended. Special measurement programs are planned for data collection during storms. Remote sensing was used to measure several factors important to the petroleum industry, i.e., waves, winds, currents, and sea ice. Application to weather forecasting is shown. The use of surface truth data in the calibration and verification of measurements for remote sensing is suggested. Possible communications channels for the exchange of remote sensing data are assessed. Author (ESA)

N82-14558# Nice Univ. (France). Lab. d'Océanographie Biologique.
REQUIREMENTS IN POLLUTION MONITORING AND COASTAL MANAGEMENT

J. Constans (Fondation Cousteau, Monaco) and G. Leger /In ESA Appl. of Remote Sensing Data on the Continental Shelf Jul. 1981 p 45-46

Avail: NTIS HC A13/MF A01; ESA, Paris FF 125

Results of tests during a survey of Mediterranean coasts by the research vessel Calypso show general chemical pollution to be too low to justify the rapid decrease in fish, seaweed, and phanerogam populations. However, mechanical and/or physical attacks on the environment, such as land filling and associated constructions, or massive discharges of warm effluents have a devastating impact on coastal ecosystems. Development decision are based on individual/local perspectives. An approach, based on clear, overall, long-term strategies is called for before irreversible damage is done. Optimum use should be made of existing data acquisition techniques, such as ESA and Telespazio satellite imagery. Author (ESA)

N82-14559# Institute of Marine Research, Bergen (Norway).
FISHERIES INVESTIGATIONS AND MANAGEMENT BENEFITS FROM REMOTE SENSING

R. Ljoen /In ESA Appl. of Remote Sensing Data on the Continental Shelf Jul. 1981 p 47-54 refs

Avail: NTIS HC A13/MF A01; ESA, Paris FF 125

Physical and biological research in areas of particular interest to Norwegian fisheries is described and present problems connected with the management of cod, haddock and mackerel are indicated. Echo sounding techniques are used and salinity and water temperature at different depths are noted. The significance of ice edge dynamics, ocean fronts, and vertical stratification to biological conditions and fish distribution is surveyed. The application of remote sensing is primarily valued as a tool for providing real time physical data in order to optimize biological sampling programs and for indicating drift and variable distributions of eggs and young fish. The utility of IR and visible images from polar orbiting satellites for monitoring purposes is briefly considered. Author (ESA)

N82-14561# Jet Propulsion Lab., California Inst. of Tech., Pasadena.

THE SEASAT COMMERCIAL DEMONSTRATION PROGRAM

S. W. McCandless (User Systems Engineering, Annandale, Va.), B. P. Miller (Econ, Inc., Princeton, N.J.), and D. R. Montgomery /In ESA Appl. of Remote Sensing Data on the Continental Shelf Jul. 1981 p 59-72 refs

Avail: NTIS HC A13/MF A01; ESA, Paris FF 125

The background and development of the Seasat commercial demonstration program are reviewed and the Seasat spacecraft and its sensors (altimeter, wind field scatterometer, synthetic aperture radar, and scanning multichannel microwave radiometer) are described. The satellite data distribution system allows for selected sets of data, reformatted or tailored to specific needs and geographical regions, to be available to commercial users. Products include sea level and upper atmospheric pressure, sea surface temperature, marine winds, significant wave heights, primary wave direction and period, and spectral wave data. The results of a set of retrospective case studies performed for the commercial demonstration program are described. These are in areas of application such as marine weather and ocean condition forecasting, offshore resource exploration and development, commercial fishing, and marine transportation. Author (ESA)

N82-14562# Copenhagen Univ. (Denmark). Inst. of Physical Oceanography.

THE COLOR OF THE SEA AND ITS RELATION TO SURFACE CHLOROPHYLL AND DEPTH OF THE EUPHOTIC ZONE

N. K. Højerslev /In ESA Appl. of Remote Sensing Data on the Continental Shelf Jul. 1981 p 73-76 refs

Avail: NTIS HC A13/MF A01; ESA, Paris FF 125

Algorithms based on signal ratios from the available channels in Nimbus 7, for the estimation of chlorophyll and phaeophytin are found to be inadequate. This is shown for coastal waters where the concentration of yellow substance (dissolved organic matter) which masks the chlorophyll signal can be variable by orders of more than 10. However, a single globally valid algorithm, based on two wavelengths in the blue and green parts of the spectrum, gives a good estimation of the depth of the euphotic zone as well as for intermediate quanta percentage levels. It is suggested that a relationship be sought involving the depth of the euphotic zone and plankton pigments, standing stock, and primary productivity. Author (ESA)

N82-14564# Oceanroutes, Inc., Palo Alto, Calif.

AN EVALUATION OF SEASAT-A DATA IN RELATION TO OPTIMUM TRACK SHIP WEATHER ROUTING AND SITE SPECIFIC FORECASTING FOR THE OFFSHORE OIL INDUSTRY

C. Daley, R. G. Johnson, and J. C. Thomson /In ESA Appl. of Remote Sensing Data on the Continental Shelf Jul. 1981 p 93-102 refs

Avail: NTIS HC A13/MF A01; ESA, Paris FF 125

The usefulness of Seasat-A SASS and altimeter measurements is reviewed. Five oceanic areas were selected: the Gulf of Alaska, central and western north Atlantic, eastern north Pacific, southern Indian Ocean, and the North Sea. Both Seasat-aided and conventional analyses were used in offshore hindcast and optimum ship routing situations. Where conventional observations are relatively dense, Seasat wind and wave data have greater impact in determining the shape of major map features than in positioning the features. In data sparse areas, Seasat data permit greater definition of surface features as well as their precise location. The use of Seasat data in optimum ship routing is quantified by means of comparative studies in the Gulf of Alaska. Author (ESA)

N82-14565# University Coll., Galway (Ireland).

DETERMINATION OF SURFACE WIND SPEED FROM REMOTELY MEASURED WHITECAP COVERAGE, A FEASIBILITY ASSESSMENT

E. C. Monahan, I. G. Muirheartaigh, and M. P. Fitzgerald /In ESA Appl. of Remote Sensing Data on the Continental Shelf Jul. 1981 p 103-109 refs

(Grant N00014-78-G-0052)

Avail: NTIS HC A13/MF A01; ESA, Paris FF 125

The relationship between wind speed and oceanic whitecap coverage was determined to facilitate the development of an algorithm for the remote determination of low elevation wind speed from the teledetected enhancement of sea surface microwave brightness temperature due to the presence of whitecaps. A basis is provided for estimating (and correcting for) the contribution to radiance, coming from whitecaps, in the various visible bands measured by satellite instruments. Combining results of the JASIN experiment with earlier observations, the effect of variations in air and sea surface temperature on this relationship is investigated. The wind speed at which whitecaps appear, and thus the lowest wind speed susceptible to teledetection via whitecap signature, is reassessed. Author (ESA)

N82-14566# National Aeronautics and Space Administration, Langley Research Center, Hampton, Va.

THE NORWEGIAN REMOTE SENSING EXPERIMENT (NORSEX) IN A MARGINAL ICE ZONE

B. Farrelly (Bergen Univ.), J. Johannessen (Bergen Univ.), O. M. Johannessen (Bergen Univ.), E. Svendsen (Bergen Univ.), K. Kloster (C. Michelson Inst.), I. Horjen (Norwegian Hydrodynamic Labs.), W. J. Campbell (Geological Survey, Tacoma, Wash.), J. Crawford, R. Harrington, L. Jones et al. *In* ESA Appl. of Remote Sensing Data on the Continental Shelf Jul. 1981 p 113-118 refs Sponsored in cooperation with NASA Bergen Univ., and Royal Norwegian Council for Scientific and Industrial Research

(Grants N00014-80-G-0003; NATO-9-4-02-SRG.19)

Avail: NTIS HC A13/MF A01; ESA, Paris FF 125 CSCL 171

Passive and active microwave measurements from surface based, airborne, and satellite instruments were obtained together with surface observations northwest of Svalbard. Emissivities of different ice patches in the ice edge region over the spectral range from 4.9 to 94 GHz are presented. The combination of a 6.6 GHz microwave radiometer with a 14.6 GHz scatterometer demonstrates the usefulness of an active/passive system in ice classification. A variety of mesoscale features under different meteorological conditions is revealed by a 1.36 GHz synthetic aperture radar. Ice edge location by Nimbus 7 scanning multifrequency microwave radiometer is shown accurate to 10 km when the 37 GHz horizontal polarized channel is used. Author (ESA)

Author (ESA)

N82-14567# Institute of Oceanographic Sciences, Wormley (England).

A PRELIMINARY EVALUATION OF SEASAT PERFORMANCE OVER THE AREA OF JASIN AND ITS RELEVANCE TO ERS-1

T. D. Allan and T. H. Guymer *In* ESA Appl. of Remote Sensing Data on the Continental Shelf Jul. 1981 p 119-127 refs

Avail: NTIS HC A13/MF A01; ESA, Paris FF 125

The microwave sensor data of Seasat was checked using Joint Air-Sea Interaction Experiment surface observations. The results of passes under light, and moderate to strong winds, show that sea surface conditions are revealed more accurately by Seasat than by weather charts based on ship reports. Wind observations are similar for satellite and surface observers. Author (ESA)

Author (ESA)

N82-14569# National Inst. of Oceanography, Goa (India).

STUDIES OF THE INDIAN CONTINENTAL SHELF: APPLICATION OF REMOTE SENSING DATA

L. V. GangadharaRao and V. R. Rao (Indian Space Research Organization, Bangalore) *In* ESA Appl. of Remote Sensing Data on the Continental Shelf Jul. 1981 p 131-141 refs

Avail: NTIS HC A13/MF A01; ESA, Paris FF 125

Early studies of coastal areas of India are reviewed and the state of the art of current studies is presented, including the identification of possible applications of remote sensing data in the context of ongoing programs and future study needs. Multidisciplinary studies with the Indian oceanographic research vessel RV Gaveshani are considered. Ocean engineering and coastal zone management (with application to offshore drilling and harbor development, fisheries, and pollution monitoring are discussed. Remote sensing data from satellites can contribute significantly to this program. Author (ESA)

Author (ESA)

N82-14570# Centre d'Etudes de Meteorologie Spatiale, Lannion (France). Antenne ORSTOM.

A SHORT REVIEW OF AN OCEANOGRAPHIC USE OF METEOSAT DATA BY THE ORSTOM REMOTE SENSING SERVICE

J. Citeau and F. Domain (Centre Oceanologique de Bretagne, France) *In* ESA Appl. of Remote Sensing Data on the Continental Shelf Jul. 1981 p 145-156 refs

Avail: NTIS HC A13/MF A01; ESA, Paris FF 125

Using the thermal infrared band, migration of schools of fish along coasts of Mauritania and Senegal was determined according to the latitudinal position of a thermal front and equatorial upwelling in the Gulf of Guinea was detected. For the latter study, an oceanographic program was instigated to furnish sea truth data. Despite a high degree of cloud cover, the Meteosat data shows good agreement on sea surface temperature. The beginning and development of the equatorial upwelling are adequately followed. The zonal extension of a large warm water band confirms that this upwelling is a phenomenon related to the equatorial process and that no advection from southern latitudes appears on the surface. Author (ESA)

Author (ESA)

N82-14571# Dundee Univ. (Scotland). Carnegie Lab. of Physics.

COASTAL ZONE RESEARCH USING REMOTE SENSING TECHNIQUES

A. P. Cracknell and S. M. Singh *In* ESA Appl. of Remote Sensing Data on the Continental Shelf Jul. 1981 p 157-168 refs

Avail: NTIS HC A13/MF A01; ESA, Paris FF 125

For the prelaunch exercise in connection with the EURASEP project, sea truth data was analyzed with data collected simultaneously from LANDSAT. Maps of chlorophyll and suspended sediment distributions over a substantial area of the North Sea off the Belgian and Dutch coastlines were generated. Analysis results of simultaneous airborne ocean color scanner data are compared. The NIMBUS 7 coastal zone color scanner (CZCS) in flight calibration data are compared with preflight calibration constants. Atmospheric corrections are applied. A satisfactory set of procedures for calibrating CZCS data, correlating that data with sea truth measurements, were established. Author (ESA)

Author (ESA)

N82-14574# Centre d'Etudes Techniques de l'Equipement, Aix-en-Provence (France).

OPERATIONAL USE OF REMOTE SENSING FOR COASTAL ZONE MANAGEMENT AND POSSIBLE CONTRIBUTION OF SPECIALIZED SATELLITES

C. Valerio *In* ESA Appl. of Remote Sensing Data on the Continental Shelf Jul. 1981 p 183-188

Avail: NTIS HC A13/MF A01; ESA, Paris FF 125

A multispectral remote sensing system, based on aerial photography, was developed in order to satisfy the requirements of coastal zone management. Data requirements (hydrodynamics, nature of the sea bottom, shore and land use) are interpreted in remote sensing terms. Technoeconomic results for study of the sewage treatment in Antibes on the Mediterranean coast are taken as a remote sensing example. Surface currents were investigated under different wind and climatic conditions. Vertical temperature and salinity profiles show vertical thermal stratification of the sea in that area. Author (ESA)

Author (ESA)

N82-14576# Swedish Meteorological and Hydrological Inst., Norrköping.

MARINE ACTIVITIES IN SWEDEN FOR WHICH REMOTE SENSING DATA MAY BE OF INTEREST

Thomas Thompson *In* ESA Appl. of Remote Sensing Data on the Continental Shelf Jul. 1981 p 195-196

Avail: NTIS HC A13/MF A01; ESA, Paris FF 125

Coastal and offshore activities (physical oceanography, marine meteorology, fishing, marine transportation, environmental protection, and climatology) for which satellite data, particularly microwave measurements available on an operational basis is useful, were reviewed. These involve weather analyses and forecasting, ship routing, ice accretion measurement, sea ice surveillance, sea surface temperature measurement, wave analyses and forecasts, pollution surveillance, sea water level measurement, and surface currents monitoring. Present data has many deficiencies which can be remedied by remote sensing techniques, but a fully operational system is required. Author (ESA)

Author (ESA)

05 OCEANOGRAPHY AND MARINE RESOURCES

N82-14581# University Coll., Galway (Ireland).
THE FEASIBILITY OF USING REMOTELY SENSED COLOR AS AN INDEX OF IRISH COASTAL WATER PROPERTIES
E. C. Monahan, I. G. O'Muircheartaigh, and M. P. Fitzgerald *In* ESA Appl. of Remote Sensing Data on the Continental Shelf Jul. 1981 p 233-237 refs

Avail: NTIS HC A13/MF A01; ESA, Paris FF 125

Sea truth data collected at 250 oceanographic stations in coastal waters south and west of Ireland are used with statistical methodologies (including least squares fitting and the approach of Box and Cox) to obtain, where feasible, expressions for the relationships between water color and other surface water properties. Close correlation is found between surface salinity, Gelbstoff concentration and water color as expressed by Munsell hue. For the same waters, poor correlation is found between surface chlorophyll-a and water color. Such satellite instruments as the coastal zone color scanner are applicable to the delineation of coastal and offshore water boundaries near Ireland, but are not appropriate for estimating the standing crop of phytoplankton. Author (ESA)

N82-14582# Instituto de Investigaciones Pesqueras, Barcelona (Spain).
NECESSITY OF REMOTE SENSING FOR OCEAN STUDIES. PART 1: NORTHWEST AFRICAN MISSIONS, SAHARA-1 AND ATLOR-1

A. Ballester Nolla and C. Romeu Nedwed *In* ESA Appl. of Remote Sensing Data on the Continental Shelf Jul. 1981 p 239-241 refs

Avail: NTIS HC A13/MF A01; ESA, Paris FF 125

Results of two oceanographic missions studying the general conditions of the northwest African offshore upwelling are summarized. Strong correlation between temperature, nutrients (nitrate, phosphate, and silicate) and chlorophyll is found. The upwelling area, 60 to 100 miles offshore, does not correspond to normally accepted mechanisms. Preliminary results suggest a collision between intermediate subequatorial water masses and the southward surface Canary current. The hypothesis is supported by tests comparing sea truth data with remotely sensed temperature data (NOAA 2 VHR). The employment of remotely sensed data as a formal method of study, and not simply as a complementary aid, is discussed. Author (ESA)

N82-14585# Deutsche Forschungs- und Versuchsanstalt fuer Luft- und Raumfahrt, Oberpfaffenhofen (West Germany). Inst. fuer Optoelektronik.

MARITIME APPLICATIONS OF IMAGE PROCESSING AT DFVLR, OBERPFAFFENHOFEN, WEST GERMANY

Klaus A. Ulbricht *In* ESA Appl. of Remote Sensing Data on the Continental Shelf Jul. 1981 p 255-261 refs

Avail: NTIS HC A13/MF A01; ESA, Paris FF 125

A digital interactive image analysis system is described and plans for a larger system are summarized. Examples of digital image processing of LANDSAT multispectral scanner images, showing contents otherwise easily missed, are given. Zones of different reflectivity, representing currents or drifts, are pointed out. The LANDSAT pictures of the Baltic Sea from four multispectral channels, processed to display the mass appearance of blue green algae, are included. Phytoplankton development in nearshore and inshore waters of the southwest Baltic, and its drift to deeper areas, are followed. Complexes of banks and channels revealed by LANDSAT in the Tay river and its delta in northeast Scotland are compared with current charts and maps of sediments. Author (ESA)

N82-14586# Atomic Energy Research Establishment, Harwell (England). Marine Technology Support Unit.

A LOOK AT NONSATELLITE REMOTE SENSING SYSTEMS FOR MARINE USE

R. J. Moulton *In* ESA Appl. of Remote Sensing Data of the Continental Shelf Jul. 1981 p 263-271 refs Sponsored by UK Dept. of Industry

Avail: NTIS HC A13/MF A01; ESA, Paris FF 125

Cost/benefit figures are given (but in some cases the costs are distorted by military investment). The main applications of remote sensing are fish location, pollution monitoring, shallow water bathymetry, and sea state measurement (with its implications for optimum ship routing). User needs for a system are classified by choice of function, operational choices, technical

decisions, relevant sensors, and sensing techniques (H.F.: radar; u.v.: fluorimetry; pulsed laser bathymetry; low light television; cameras; passive multifrequency microwave imaging. The U.S. oil surveillance system as well as Swedish and French systems are described. Nonsatellite systems can be best used to verify satellite data. Author (ESA)

N82-14587# Indian Space Research Organization, Bangalore.
SCIENTIFIC STUDIES USING BHASKARA SATELLITE MICROWAVE RADIOMETER (SAMIR) DATA: A SHORT OVERVIEW

V. R. Rao *In* ESA Appl. of Remote Sensing Data on the Continental Shelf Jul. 1981 p 273-278 refs

Avail: NTIS HC A13/MF A01; ESA, Paris FF 125

The three-channel microwave radiometric system SAMIR (two frequencies at 19 GHz and one at 22 GHz) which is one of the two payloads on board the Bhaskara satellite, is described; along with the satellite itself and its complete payload. Data quality and methods of analysis are reviewed and the use of the data for investigation of sea states, water vapor and liquid water content in the atmosphere and over oceans adjoining India is examined. The derivation of these and further ocean related parameters (sea surface winds; rainfall rates) for monitoring sea state conditions in India was demonstrated. Author (ESA)

N82-14592# Kansas Univ. Center for Research, Inc., Lawrence. Remote Sensing Lab.

MEASUREMENTS OF RADAR BACKSCATTER FROM ARCTIC SEA ICE IN THE SUMMER

R. G. Onstott, S. Gogineni, C. V. Delker, and R. K. Moore Jul. 1981 16 p

(Contract N00014-76-C-1105)

(AD-A105586; CRINC/RSL-TR-331-20)

Avail: NTIS

HC A02/MF A01 CSCL 17/9

Measurements of radar backscatter from sea ice located near Svalbard and Greenland were made during the summer of 1980 as part of Project YMER. These data were acquired using the University of Kansas helicopter-borne microwave active spectrometer (HELOSCAT II) which operated over a frequency range of 8 to 18 GHz and an angle of incidence range of 0 degrees to 50 degrees. The presence of meltponds, the transformation of the snowpack into an ice layer, and the warmer temperatures have contributed to radar signatures that may be significantly different than those observed during the winter and spring. A wide variety of ice conditions were investigated. These included multiyear, thick first-year, thin first-year, young, new, and pressure-ridged ice. The measurement program is described herein. Author (GRA)

N82-14593# Kansas Univ. Center for Research, Inc., Lawrence. Remote Sensing Lab.

MEASUREMENTS OF RADAR BACKSCATTER FROM ARCTIC SEA ICE IN THE SUMMER, APPENDICES A AND B

R. G. Onstott, S. Gogineni, R. K. Moore, and C. V. Delker Jul. 1981 96 p

(Contract N00014-76-C-1105)

(AD-A105736; CRINC/RSL-TR-331-22)

Avail: NTIS

HC A05/MF A01 CSCL 17/9

Computer output measurements of radar backscatter from arctic sea ice in the summer are presented, including raw radar backscatter data and sea ice salinity profiles N.W.

N82-14617# Physics Lab. RVO-TNO, The Hague (Netherlands). Research Group: Physics.

PROJECT NOORDWIJK. PART 1: MEASUREMENTS OF THE RADAR BACKSCATTER COEFFICIENT GAMMA (SIGMA DEG) IN 1977 AND 1978

G. P. deLoor Nov. 1979 42 p refs 2 Vol.

(PHL-1979-49-Pt-1; TDCK-73426)

Avail: NTIS

HC A03/MF A01

Radar backscatter measurements obtained from a sea platform are compared with airborne and spaceborne observations. A short range FM radar was mounted beside a television camera and directed into the prevailing winds. Upwind and crosswind data were collected, but downwind data are scarce, and more windspeed data are required. A systematic difference is observed between airborne and ground based data. The value of gamma is dependent on windspeed; dependency differs for the specular

region (low incidence angles) and the diffuse (incidence angles > 45 deg). Author (ESA)

N82-14618# Physics Lab. RVO-TNO. The Hague (Netherlands). Research Group 4: Microwaves.

PROJECT NOORDWIJK. PART 2: RESULTS OF NORTH SEA CLUTTER MEASUREMENTS IN THE I-BAND PERFORMED FROM THE PLATFORM NOORDWIJK IN SEPTEMBER/OCTOBER 1977

H. Sittrop and H. Gravesteijn Aug. 1980 79 p refs 2 Vol. (PHL-1980-28-Pt-2; TDCK-74302) Avail: NTIS HC A05/MF A01

Radar backscatter off the sea at low incidence angles was measured. A low frequency spectral analysis method is used to show that an appreciable periodic content exists in the sea return. This component in the scintillation spectra is 0.14 Hz and is related to the sea wave period. Wind-wave interaction effects are observed for up, down and crosswind directions. The clutter patch size and the incidence angle are used as a parameter. An optimum spectral response exists for upwind observations at an incidence angle of 1 deg and pulselength 0.08 microsec. The radar cross section per unit area measured is compared with an experimental sea clutter model. For wind directions resulting in an adequate fetch over open sea, reasonable agreement is found. No significant conclusions can be drawn with respect to megaripple observations. Author (ESA)

N82-14789*# Illinois Univ., Urbana. Radio Research Lab. **REMOTE SENSING OF SEA STATE BY LASER ALTIMETERS**

B. Tsai and C. S. Gardner Dec. 1981 51 p refs (Grant NsG-5049) (NASA-CR-165049; RRL-Publ-514) Avail: NTIS HC A04/MF A01 CSCL 08C

The reflection of short laser pulses from the ocean surface was analyzed based on the specular point theory of scattering. The expressions for the averaged received signal, shot noise and speckle induced noise were derived for a direct detection system. It is found that the reflected laser pulses have an average shape closely related to the probability density function associated with the surface profile. This result is applied to estimate the mean sea level and significant wave height from the receiver output of the laser altimeter. T.M.

N82-15498*# EG and G Washington Analytical Services Center, Inc., Pocomoke City, Md.

A GLOBAL ATLAS OF GEOS-3 SIGNIFICANT WAVEHEIGHT DATA AND COMPARISON OF THE DATA WITH NATIONAL BUOY DATA

J. D. McMillan Wallops Island, Va. NASA. Wallops Flight Center Nov. 1981 163 p refs (Contract NAS6-2639) (NASA-CR-156882) Avail: NTIS HC A08/MF A01 CSCL 08C

The accuracy of the GEOS-3 significant waveheight estimates compared with buoy measurements of significant waveheight were determined. A global atlas of the GEOS-3 significant waveheight estimates gathered is presented. The GEOS-3 significant waveheight estimation algorithm is derived by analyzing the return waveform characteristics of the altimeter. Convergence considerations are examined, the rationale for a smoothing technique is presented and the convergence characteristics of the smoothed estimate are discussed. The GEOS-3 data are selected for comparison with buoy measurements. The GEOS-3 significant waveheight estimates are assembled in the form of a global atlas of contour maps. Both high and low sea state contour maps are presented, and the data are displayed both by seasons and for the entire duration of the GEOS-3 mission. E.A.K.

N82-15684# Royal Netherlands Meteorological Inst., De Bilt. Oceanographic Research Div.

METEOROLOGICAL AND OCEANOGRAPHIC OBSERVATIONS ON BOARD NETHERLANDS LIGHTVESSELS AND THE LIGHTPLATFORM 'GOEREE' IN THE NORTH SEA Annual Report, 1976

1981 143 p In ENGLISH and DUTCH (KNMI-141-28) Avail: NTIS HC A02/MF A01; KNMI, De Bilt, Netherlands FL 17.50

Three-hourly meteorological and wave observations as well as hourly current and salinity measurements were compiled. Tables

show: (1) meteorological results; (2) oceanographic results; (3) general air circulation, air pressure, precipitation, and fog; (4) visibility and cloud amount; (5) air temperature; (6) sea surface temperature; (7) air-sea temperature differences; and (8) wind and wave frequencies. A.R.H.

Page intentionally left blank

Page intentionally left blank

06
**HYDROLOGY AND WATER
MANAGEMENT**

Includes snow cover and water runoff in rivers and glaciers, saline intrusion, drainage analysis, geomorphology of river basins, land uses, and estuarine studies.

A82-10031 **Comparison of conventional and remotely sensed estimates of runoff curve numbers in southeastern Pennsylvania.** T. R. Bondelid, R. H. McCuen (Maryland, University, College Park, MD), and T. J. Jackson (Science and Education Administration, Plant Physiology Institute, Beltsville, MD). In: American Society of Photogrammetry, Annual Meeting, 46th, St. Louis, MO, March 9-14, 1980, ASP Technical Papers. Falls Church, VA, American Society of Photogrammetry, 1980, p. 81-96.

The present study compares estimates of runoff curve numbers obtained using three different methods of identifying land cover: conventional surveys, land cover maps developed by the U.S. Geological Survey, and Landsat data. Data were tested on three watersheds in southeastern Pennsylvania. Accuracy was evaluated for various levels of drainage basin size, land use, and inhomogeneity of land cover distribution. It is found that the estimates of the runoff curve number were not highly sensitive to the source of the land cover data for typical watershed sizes and characteristics in this study area. Thus, accurate estimates can be obtained using less expensive remote sensing techniques. B.J.

A82-10032 **Satellite rainfall estimation for hydrologic forecasting.** R. K. Farnsworth (NOAA, Hydrologic Research Laboratory, Silver Spring, MD) and R. P. Canterford. In: American Society of Photogrammetry, Annual Meeting, 46th, St. Louis, MO, March 9-14, 1980, ASP Technical Papers. Falls Church, VA, American Society of Photogrammetry, 1980, p. 97-105. 14 refs.

The paper presents a method for evaluating current rainfall estimation techniques in terms of the requirements for flood and stage forecasting of rivers. An evaluation scheme has been developed based on equivalent rain gage density (ERGD). This scheme involves assigning ERGDs to the satellite techniques for specified time and space scales down to the order of three hours and 1/4 deg x 1/4 deg latitude/longitude grids. The scheme makes it possible to make intercomparisons among satellite techniques and to measure their improvement, if any, over information from existing operational rain gage networks. B.J.

A82-10033 **Mapping of the 1978 Kentucky River Flood from NOAA-5 satellite thermal infrared data.** C. P. Berg, D. F. McGinnis, Jr., and D. G. Forsyth (NOAA, National Environmental Satellite Service, Washington, DC). In: American Society of Photogrammetry, Annual Meeting, 46th, St. Louis, MO, March 9-14, 1980, ASP Technical Papers. Falls Church, VA, American Society of Photogrammetry, 1980, p. 106-111.

The December 1978 Kentucky River Flood was analyzed using remotely sensed thermal infrared (IR) data from the Very High Resolution Radiometer (VHRR) onboard the NOAA-5 satellite. Computer-enhanced imagery and computer printouts permitted delineation of the flood boundaries; ground-based measurements indicate that this flood was a 200-year flood. Both manual photo-interpretive and automated computer analyses of the data indicate that NOAA-5 VHRR-IR data is a useful tool for flood delineation. (Author)

A82-10054 **Data sources for analyses of Great Lakes wetlands.** J. G. Lyon (Michigan, University, Ann Arbor, MI). In: American Society of Photogrammetry, Annual Meeting, 46th, St. Louis, MO, March 9-14, 1980, ASP Technical Papers.

Falls Church, VA, American Society of Photogrammetry, 1980, p. 516-528. 14 refs. Grant No. NOAA-04-8-M01-134.

This paper presents a comparison of data sources for assessing quantity and variety of coastal zone wetlands. The information supplying capabilities of aerial photography, Landsat imagery and SEASAT radar data were evaluated. This was accomplished by mapping wetlands, and by a change-detection analysis of wetlands in

relation to Great Lake water levels. The value of each source is examined in a framework of data gathering and analysis for purposes of coastal zone management. (Author)

A82-10208 **Analysis of bright bands from 3-D radar data.** C. G. Collier (Meteorological Office, Malvern, Worcs., England), S. Lovejoy, and G. L. Austin (McGill Radar Weather Observatory, Montreal, Canada). In: Conference on Radar Meteorology, 19th, Miami Beach, FL, April 15-18, 1980, Preprints. Boston, MA, American Meteorological Society, 1980, p. 44-47.

A practical scheme has been developed to automatically classify observed echo data into either stratiform rain, showers, or ground clutter using high resolution three-dimensional scanning radar. The technique involves the statistical determination of boundaries in n-dimensional space into m classes by the minimization of a general loss function, f. The reflectivity values are divided evenly into 30 classes, and a two-dimensional histogram of frequency-of-occurrence of the different 2-km, 3-km dBZ combinations is produced. The concentration of points is examined in relation to the line defined by reflectivity level at 3 km equals reflectivity level at 2 km. Points below the line indicate a positive vertical Z gradient, while points above indicate a negative one. Lines drawn to indicate the 50% contours represent the optimum boundaries for the technique when no more than two classes overlay at any one location with the two-dimensional 3 to 2 km reflectivity level plane. Errors in classification were found to be small (about 10%), and were usually a result of an error in only one category. J.F.

A82-10694 * # **A comparison of radiative transfer models for predicting the microwave emission from soils.** T. J. Schmugge (NASA, Goddard Space Flight Center, Hydrological Sciences Branch, Greenbelt, MD) and B. J. Choudhury (NASA, Goddard Space Flight Center, Hydrological Sciences Branch, Greenbelt; Computer Sciences Corp., Silver Spring, MD). *Radio Science*, vol. 16, Sept.-Oct. 1981, p. 927-938. 19 refs.

Noncoherent and coherent numerical models for predicting emission from soils are compared. Coherent models use the boundary conditions on the electric fields across the layer boundaries to calculate the radiation intensity, and noncoherent models consider radiation intensities directly. Interference may cause different results in the two approaches when coupling between soil layers in coherent models causes greater soil moisture sampling depths. Calculations performed at frequencies of 1.4 and 19.4 GHz show little difference between the models at 19.4 GHz, although differences are apparent at the lower frequency. A definition for an effective emissivity is also given for when a nonuniform temperature profile is present, and measurements made from a tower show good agreement with calculations from the coherent model. D.L.G.

A82-12553 **Effect of grain size and snowpack water equivalence on visible and near-infrared satellite observations of snow.** J. Dozier (California, University, Santa Barbara, CA), S. R. Schneider, and D. F. McGinnis, Jr. (NOAA, National Earth Satellite Service, Washington, DC). *Water Resources Research*, vol. 17, Aug. 1981, p. 1213-1221. 24 refs.

Satellite observations of snow in the near-infrared wavelengths can be used to roughly estimate snow grain size. When the grain size is large, it is possible to use measurements in the visible wavelengths to estimate snow water equivalence below some threshold value of around 100 mm. While sufficient data to fully evaluate these possibilities are not available, model calculations, selected satellite observations, and limited ground truth are in qualitative agreement. Complications arise because the effect of contamination by atmospheric aerosols is similar to that of finite depth, and because the near-infrared channel on the NOAA TIROS-N series satellites is not in the wavelength region where snow reflectance is most sensitive to grain size. (Author)

A82-12589 **Civil engineering applications of remote sensing; Proceedings of the Specialty Conference, University of Wisconsin, Madison, WI, August 13, 14, 1980.** Conference sponsored by ASCE, ASP, and University of Wisconsin. Edited by R. W. Kiefer (Wisconsin, University, Madison, WI). New York, American Society of Civil Engineers, 1980. 199 p. \$19.50.

Topics discussed include land applications, water applications,

06 HYDROLOGY AND WATER MANAGEMENT

thermography applications, and general applications of remote sensing. Papers are presented on Landsat imagery for hydrologic modeling, satellite imagery and shoreline erosion prediction, water temperature mappings by infrared scanner, and aerial photography in fire risk assessment. Attention is also given to a data base system for real-time hydrologic modeling, the application of Landsat to the inventory of dams, and the operational use of Landsat for lake quality assessment. C.R.

A82-12592 * **Landsat imagery for hydrologic modeling.** R. S. Taylor, R. P. Shubinski, and T. S. George (Camp, Dresser and McKee, Inc., Springfield, VA). In: Civil engineering applications of remote sensing; Proceedings of the Specialty Conference, Madison, WI, August 13, 14, 1980. New York, American Society of Civil Engineers, 1980, p. 44-52. NASA-supported research.

The cost and effectiveness of developing land cover information derived from Landsat imagery for hydrologic studies are compared with the cost and effectiveness of conventional sources. The analysis shows that the conventional and Landsat methods are nearly equally effective in providing adequate land cover data for hydrologic studies. The total cost effectiveness analysis demonstrates that the conventional method is cost effective for a study area of less than 26 sq km and that the Landsat method is to be preferred for areas of more than 26 sq km. C.R.

A82-12593 **Application of Landsat to the inventory of DAMS.** A. R. Blystra (Federal Energy Regulatory Commission, Washington, DC) and R. R. Dumás (Chicago District, Corps of Engineers, Chicago, IL). In: Civil engineering applications of remote sensing; Proceedings of the Specialty Conference, Madison, WI, August 13, 14, 1980. New York, American Society of Civil Engineers, 1980, p. 54-59.

A82-12595 **Satellite imagery and shoreline erosion prediction.** C. W. Welby (North Carolina State University, Raleigh, NC). In: Civil engineering applications of remote sensing; Proceedings of the Specialty Conference, Madison, WI, August 13, 14, 1980. New York, American Society of Civil Engineers, 1980, p. 78-87. 11 refs.

A82-12596 * **The operational use of Landsat for lake quality assessment.** F. L. Scarpace (Wisconsin, University, Madison, WI) and L. T. Fisher (Maine, University, Orono, ME). In: Civil engineering applications of remote sensing; Proceedings of the Specialty Conference, Madison, WI, August 13, 14, 1980. New York, American Society of Civil Engineers, 1980, p. 88-100. 10 refs. Research supported by the Wisconsin Department of Natural Resources, U.S. Environmental Protection Agency, and NASA.

A cooperative program between the Wisconsin Department of Natural Resources and the University of Wisconsin for the assessment, with Landsat data, of the trophic status of all the significant inland lakes in Wisconsin is described. The analysis technique is a semiautomatic data acquisition and handling system which, in conjunction with an analytical categorization scheme, can be used for classifying inland lakes into one of seven categories of eutrophication and one of four problem types. C.R.

A82-12597 **Field study for Landsat water quality verification.** D. S. Graham and J. M. Hill (Louisiana State University, Baton Rouge, LA). In: Civil engineering applications of remote sensing; Proceedings of the Specialty Conference, Madison, WI, August 13, 14, 1980. New York, American Society of Civil Engineers, 1980, p. 101-117. 8 refs.

It is found that MSS data can be used to separate many water types in Apalachicola Bay, in Florida. Here, the images can be used to deduce circulation patterns. Circulation patterns for Landsat images are found to correspond clearly with both field data and numerical model results. The color intensity in the bay results from both dispersive mixing and a chemical reaction dependent on pH. C.R.

A82-12598 **Water temperature mapping by infrared scanner.** J. B. Evans (Texas Instruments, Inc., Dallas, TX). In: Civil engineering applications of remote sensing; Proceedings of the

Specialty Conference, Madison, WI, August 13, 14, 1980.

New York, American Society of Civil Engineers, 1980, p. 118-122.

The state-of-the-art method of mapping water temperature using an airborne calibrated infrared scanner combined with computer corrections is described. The radiation measurements are digitized and coded onto computer tape during airborne survey operations. It is noted that the computer corrects for atmospheric effects that also change with scan angle, physics of temperature to radiation, water surface cooling or heating, system parameters, and map linearities. Scale maps of temperature are printed or plotted in any form that is available to the computer. The accuracy thus obtained allows computer maps to be combined to cover a large area with one-half degree accuracy. C.R.

A82-15037 **Use of visible and thermal satellite data to monitor an intermittently flooding marshland.** G. F. Byrne, G. N. Goodrick (Commonwealth Scientific and Industrial Research Organization, Div. of Land Use Research, Canberra, Australia), and K. Dabrowska-Zielinska (Instytut Geodezji i Kartografii, Warsaw, Poland). *Remote Sensing of Environment*, vol. 11, Nov. 1981, p. 393-399. 5 refs.

Selected thermal and visible data from the Heat Capacity Mapping Mission satellite for the Macquarie Marshes of Eastern Central Australia are examined in the light of a substantial volume of data from other sources, including Landsat, with a view to evaluating meteorological satellite data as ecological monitors for this landform. The results indicate that at least four important components of marshland can be mapped using HCMM data. The ecological status of marshland is intimately connected to their water status and visible and thermal imagery appears to be an economical and effective method of monitoring such systems. (Author)

A82-15961 † **Study of the dynamics of the Danube delta using space images (Izuchenie dinamiki del'ty Dunaia s ispol'zovaniem kosmicheskikh snimkov).** O. N. Efremova and V. I. Kravtsova (Moskovskii Gosudarstvennyi Universitet, Moscow, USSR). *Issledovanie Zemli iz Kosmosa*, Sept.-Oct. 1981, p. 90-96. In Russian.

Multispectral scanning images of the Danube delta, obtained by the Fragment system in September 1980, were compared with analogous images obtained by the Landsat satellite in September 1972. A study of these images revealed the dynamics of the delta over an eight year period. A map was constructed, reflecting the seaward extension of the Kiliiskaia part of the delta; it revealed an increase in water supply in some parts of the inner delta, and a decrease in water supply in other parts; it also showed a significant growth in agricultural land, featuring the appearance of rice fields in drained marshes, as well as other crop fields on terraces. J.F.

A82-15969 * **In situ spectral reflectance studies of tidal wetland grasses.** D. S. Bartlett (NASA, Langley Research Center, Marine and Applications Technology Div., Hampton, VA) and V. Klemas (Delaware, University, Newark, DE). *Photogrammetric Engineering and Remote Sensing*, vol. 47, Dec. 1981, p. 1695-1703. 16 refs. Research supported by the University of Delaware; Contract No. NAS5-20983.

Field measurements of wetland spectral canopy reflectance in the Landsat-MSS wavebands were correlated with biotic factors. The highest single band correlations were observed between visible (MSS Band 4: 0.5 to 0.6 micron and Band 5: 0.6 to 0.7 micron) canopy reflectance and the percentage, by weight, of live (green) vegetation in the canopies of *Spartina alterniflora* (salt marsh cordgrass), *Spartina patens* (salt meadow grass), and *Distichlis spicata* (spike grass). Infrared canopy reflectance displayed significant but weaker dependence on canopy parameters such as live and total biomass and canopy height. The Band 7 (0.8 to 1.1 microns)/Band 5 (0.6 to 0.7 micron) reflectance ratio was found to be highly correlated with green biomass for *S. alterniflora*. Highest spectral separability between the 'low marsh' *S. alterniflora* and the 'high marsh' Salt Hay (*S. patens* and *D. spicata*) communities in Delaware occurs during December. (Author)

A82-17892 # **Role of remote sensing in the study of acid rain impact on aquatic systems.** J. R. Schott (Rochester Institute of Technology, Rochester, NY) and M. A. Wilkinson (New York, State

University, Buffalo, NY). *American Institute of Aeronautics and Astronautics, Aerospace Sciences Meeting, 20th, Orlando, FL, Jan. 11-14, 1982, Paper 82-0336*. 10 p. 12 refs. Research supported by the New York State Energy Research and Development Authority.

Results are presented of a study of the capabilities of image analysis of remotely sensed data in the evaluation of the present state and past history of lakes subject to acidification by acid precipitation. Analysis of surface sampling data from nine Adirondack lakes reveals lake pH and alkalinity to be reflected in parameters related to optical properties, exhibiting a positive correlation with chlorophyll and total solids and a negative correlation with Secchi depth. Aerial photographic measurements of lake volume spectral reflectance, when compared with a simple laboratory model of the dependence of chlorophyll, lignin and humic acid contents of water on its optical properties, are also found to correlate with the differences between the in situ lake properties. Finally, analysis of Landsat band 4, 5 and 7 data obtained in September 1972 and 1979 for 18 lakes demonstrates the potential of the data for the isolation of lakes with low alkalinity, and for monitoring the rate of acidification over time providing data is properly calibrated for atmospheric, illumination and sensor response effects. Results thus demonstrate considerable potential for remote sensing in monitoring the impact of acidification on lakes, and point up the need for further studies of multi-temporal Landsat data and the techniques of aerial analysis.

A.L.W.

A82-17999 An application of Landsat derived data to a regional hydrologic model. D. P. Killpack and R. M. McCoy (Utah, University, Salt Lake City, UT). *Remote Sensing Quarterly*, vol. 3, Apr. 1981, p. 27-33. 8 refs.

An empirical, regional hydrologic model for predicting stream flow is developed based on the use of planimetric terrain variables obtainable from satellite imagery without stereo coverage. Measurements of basin area, basin perimeter, network length and main channel length were obtained from topographic maps and from Landsat imagery for 12 undiverted gaged streams essentially free of reservoirs and lakes in the Wasatch Mountains, and compared with stream flow variables in order to derive a regression equation for estimating stream discharge. Use of the equation expressing runoff as a function of basin area to predict runoffs in eight additional basins results in a correlation coefficient between predicted and observed values of 0.92, thus demonstrating the validity of the approach.

A.L.W.

A82-18000 The potential for use of Landsat data in water resources planning for the Missouri River Basin. T. W. Lowe (Missouri River Basin Commission, Omaha, NE). *Remote Sensing Quarterly*, vol. 3, Apr. 1981, p. 34-41. 10 refs.

A82-18166 An inertially-aided aircraft track recovery system for coastal mapping. D. B. Reid, W. S. Gesing, B. N. McWilliam (Philip A. Lapp, Ltd., Toronto, Canada), and J. R. Gibson (Canada Centre for Remote Sensing, Ottawa, Canada). In: *PLANS '80 - Position Location and Navigation Symposium*, Atlantic City, NJ, December 8-11, 1980, Record. New York, Institute of Electrical and Electronics Engineers, Inc., 1980, p. 422-429. 10 refs.

A description is given of a new airborne system developed for charting shallow coastal and inland waters. The main components of this system are an aerial survey camera, a profiling laser radar, an analytical stereo plotter, and a multisensor track recovery system (TRS). The TRS comprises a gimbaled inertial navigation system and several auxiliary sensors which require redundant position and attitude information. The sensor data are combined postmission with the aid of a U-D factorized Kalman filter and modified Bryson-Frazier smoother to compute precise estimates of the orientation parameters of the survey camera at the times of film exposure. These parameters are used in order to position each overlapping pair of photographs on the analytical plotter to form a stereo image and a corresponding analytical stereomodel from which water depth measurements are made. Flight trial results demonstrate that the TRS is able to achieve radial position and attitude accuracies which exceed 1 meter and 2 arcmin (RMS), respectively, and that this level of performance is sufficient to enable water depth measurements to be made to an accuracy of better than 0.65 m (RMS).

C.R.

N82-11530# National Oceanic and Atmospheric Administration, Boulder, Colo. Office of Weather Research and Modification. **A SYSTEMS APPROACH TO THE REAL-TIME RUNOFF ANALYSIS WITH A DETERMINISTIC RAINFALL-RUNOFF MODEL**

Robert J. C. Burnash and R. Larry Ferral Apr. 1981 24 p refs

(PB81-224495; NOAA-TM-NWS-WR-162; NOAA-81050703) Avail: NTIS HC A02/MF A01 CSCL 08H

The responsibility for providing the U.S. with warnings of river conditions was assigned to the National Weather Service in 1890. This requirement led to the development of a systems approach to hydrologic data collection, runoff computation, and forecast production. This system is focused on producing information on the future distribution of water in time and space which affects the safety, welfare, and economic well being of the nation and its inhabitants. A principal element of any hydrologic warning system is an effective rainfall-runoff model. GRA

N82-12498*# Environmental Research and Technology, Inc., Concord, Mass.

SNOW-MAPPING EXPERIMENT

James C. Barnes, Clinton J. Bowley, J. Thomas Parr, and Michael D. Smallwood In NASA. Johnson Space Flight Center Skylab Explores the Earth 1977 p 191-224 refs

Avail: NTIS MF A01; SOD HC \$16.50 CSCL 08L

More than 300 hand-held camera photographs were taken of most part of the United States in which snow existed during the mission. The sites include the Sierra Nevada in California; the Salt-Verde Watershed in central Arizona; the Rocky Mountains in Colorado; the Great Salt Lake and Yellowstone Park in Utah and Wyoming; the Cascade Range in Washington and Oregon; the Black Hills in South Dakota; the Central Plains; and the Great Lakes. Snow in the European Alps; the Caucasus and Himalaya Mountains; the Pacific coastal areas of the U.S.S.R.; and New Zealand was also mapped. The experiment shows that: (1) a space observer can identify snow that photointerpreters cannot distinguish on a photograph of the same area, (2) can integrate, through partial cloud cover, to view the terrain, and (3) can select the optimum viewing angle and Sun angle and the appropriate film and filter combination to acquire the best data. A.R.H.

N82-12501*# American Univ., Washington, D. C. Drought Analysis Lab.

REPORT ON SKYLAB 4 AFRICAN DROUGHT AND ARID LAND EXPERIMENT

N. H. MacLeod, J. S. Schubert, and P. Anaejonu In NASA. Johnson Space Flight Center Skylab Explores the Earth 1977 p 263-286 refs

Avail: NTIS MF A01; SOD HC \$16.50 CSCL 08B

Vegetation patterns, flooding, soil erosion, interdunal water accumulation, natural drainage systems, and drainage patterns in the Black Volta and White Volta River basins were observed and photographed in an effort to determine the causes of desertification in the Sahel. The Niger Island delta in Mali was selected to examine the distribution and changing patterns of vegetation and flooding of the major freshwater resources in that drought-prone area. Observations Nimbus-3, Apollo-9, and Skylab of dust and cloud movements, vegetation patterns, land surface features, the color and distribution of surface water, and color changes of lakes within the drought zone show that widespread destructive land practices contribute to the arid conditions. A.R.H.

N82-12504*# Geological Survey, Tacoma, Wash.

VISUAL OBSERVATIONS OF FLOATING ICE FROM SKYLAB

W. J. Campbell, R. O. Ramseier (Dept. of Environment, Ottawa, Ontario), W. F. Weeks (Cold Regions Research and Engineering Lab.), and J. A. Wayenberg In NASA. Johnson Space Flight Center Skylab Explores the Earth 1977 p 353-380 refs

Avail: NTIS MF A01; SOD HC \$16.50 CSCL 08L

The lake and sea ice visual observation experiment performed during the Skylab 4 mission was very successful. In the initial experiment design, the Gulf of St. Lawrence and Lake Ontario were chosen as prime sites at which ground-truth measurements and aircraft remote-sensing data were to be obtained. In addition, the Skylab 4 astronauts obtained excellent photographs of sea ice in the Sea of Okhotsk and in the James

06 HYDROLOGY AND WATER MANAGEMENT

Bay portion of Hudson Bay and of icebergs in the Southern Ocean. Some of the sequential photographs contain very useful broad-scale information on the distribution of ice and ice types, the overall deformation patterns, and the amount of relative ice motion.
A.R.H.

N82-12510*# Kansas Univ. Center for Research, Inc., Lawrence. Remote Sensing Lab.

PROGRESS IN RADAR SNOW RESEARCH

W. Stiles, F. T. Ulaby, A. K. Fung, and A. Aslam Feb. 1981 167 p refs

(Grant NsG-5335)

(NASA-CR-166709; RSL-TR-410-1)

Avail: NTIS

HC A08/MF A01 CSCL 08L

Multifrequency measurements of the radar backscatter from snow-covered terrain were made at several sites in Brookings, South Dakota, during the month of March of 1979. The data are used to examine the response of the scattering coefficient to the following parameters: (1) snow surface roughness, (2) snow liquid water content, and (3) snow water equivalent. The results indicate that the scattering coefficient is insensitive to snow surface roughness if the snow is dry. For wet snow, however, surface roughness can have a strong influence on the magnitude of the scattering coefficient. These observations confirm the results predicted by a theoretical model that describes the snow as a volume of Rayleigh scatterers, bounded by a Gaussian random surface. In addition, empirical models were developed to relate the scattering coefficient to snow liquid water content and the dependence of the scattering coefficient on water equivalent was evaluated for both wet and dry snow conditions. Author

N82-14549*# National Aeronautics and Space Administration. Goddard Space Flight Center, Greenbelt, Md.

A SIMULATION STUDY OF THE RECESSION COEFFICIENT FOR ANTECEDENT PRECIPITATION INDEX

Bhaskar J. Choudhury and Bruce J. Blanchard Nov. 1981 25 p refs Submitted for publication

(NASA-TM-83860) Avail: NTIS HC A02/MF A01 CSCL 08M

The antecedent precipitation index (API) is a useful indicator of soil moisture conditions for watershed runoff calculations and recent attempts to correlate this index with spaceborne microwave observations have been fairly successful. It is shown that the prognostic equation for soil moisture used in some of the atmospheric general circulation models together with Thornthwaite-Mather parameterization of actual evapotranspiration leads to API equations. The recession coefficient for API is found to depend on climatic factors through potential evapotranspiration and on soil texture through the field capacity and the permanent wilting point. Climatological data for Wisconsin together with a recently developed model for global isolation are used to simulate the annual trend of the recession coefficient. Good quantitative agreement is shown with the observed trend at Fennimore and Colby watersheds in Wisconsin. It is suggested that API could be a unifying vocabulary for watershed and atmospheric general circulation modelers. Author

N82-14575# Canada Centre for Remote Sensing, Ottawa (Ontario).

RECENT WORK IN PASSIVE OPTICAL IMAGING OF WATER

H. H. Zwick and S. C. Jain (Monitek Ltd.) In ESA Appl. of Remote Sensing Data on the Continental Shelf Jul. 1981 p 189-194 refs

Avail: NTIS HC A13/MF A01; ESA, Paris FF 125

The estimation of water quality and bathymetry with passive optical multispectral data imagery are described. A water quality algorithm was developed from a coordinated set of airborne, multispectral scanner, in situ water, and ground based atmospheric measurements made during coastal zone color scanner NIMBUS 7 passes over Lake Ontario. Modeling of atmosphere, the air water interface, and macroscopic as well as microscopic water optical characteristics gives fresh water estimates of the independently varying chlorophyll-a and total suspended mineral concentrations. Remotely measured radiances are corrected for atmosphere, specular sky reflection, and water refractivity in effects. The required parameters are estimated using a computer optimization routine. Author (ESA)

N82-14579# Roskilde Univ. (Denmark). Institute of Geography, Socio-Economic Analysis and Computer Science.

MAPPING OF SURFACE CURRENTS IN GREENLAND

FIORDS BY MEANS OF LANDSAT IMAGES

Sten Folving In ESA Appl. of Remote Sensing Data on the Continental Shelf Jul. 1981 p 211-219 refs

Avail: NTIS HC A13/MF A01; ESA, Paris FF 125

Data from LANDSAT were used to study the propagation of meltwater into Soendre Stroemfjord. Water masses are classified on the basis of intensity profiles. These data trace meltwater sediment plumes and the character of the fronts between meltwater and pure fiord water. The main currents are mapped. River discharge from the south side is always up fiord due to pronounced Coriolis influence. A permanent down fiord current is found on the north side, with very complex patterns of current arising when the direction of the fiord channel shifts significantly. Author (ESA)

N82-14580# Southampton Univ. (England).

THE USE OF LANDSAT MSS TO OBSERVE SEDIMENT DISTRIBUTION AND MOVEMENT IN THE SOLENT COASTAL AREA

I. S. Robinson and D. Srisaengthong In ESA Appl. of Remote Sensing Data on the Continental Shelf Jul. 1981 p 221-232 refs Sponsored by UK Dept. of Industry

Avail: NTIS HC A13/MF A01; ESA, Paris FF 125

The LANDSAT multispectral data from the Solent area was used to explore the potential value to marine scientists of archived data on estuaries and coastal regions. Ten images from the archives were digitally enhanced by color slicing, yielding useful qualitative information when interpreted as suspended sediment. Two further clear weather images were obtained. An approximate calibration algorithm based on six archives band-5 images and non coincident field observations show good agreement with a synoptic calibration of the last two images. The calibrated archived images show similar seasonal variations to those observed. The possibility, for certain estuaries, of obtaining quantitative information from archived data, using only recent field observations, is suggested. Author (ESA)

N82-14589# Virginia Univ., Charlottesville. Dept. of Environmental Sciences.

THE EFFECT OF SPATIAL VARIABILITY IN PRECIPITATION ON STREAMFLOW

Keith J. Beven and George M. Hornberger Sep. 1981 40 p refs Submitted for publication Prepared in cooperation with Illinois State Water Survey, Urbana

(Contract DAAG29-80-K-0053; Grant NSF ATM-78-08865)

(AD-A105955; TR-6; ARO-16816.3-GS)

Avail: NTIS

HC A03/MF A01 CSCL 04/2

In most approaches to modelling the rainfall/runoff process, a spatially lumped description of precipitation has been assumed adequate for modelling the important aspects of catchment response. However, theories of catchment hydrology as well as some recent modelling studies suggest that spatial variability in precipitation may be important in determining the characteristics of streamflow hydrographs. Data from two intensive rainfall recording experiments in Illinois have been used to examine the effects of rainfall pattern on stream hydrographs for summer convective storms. A threshold analysis was used to distinguish storms of markedly different pattern. A mixed deterministic/stochastic modelling procedure was used to determine the length of record required to differentiate the hydrograph characteristics resulting from storms of different patterns. It was found that differences in peak timing were highly significant but that differences in the distributions of peak flow and stormflow volumes were generally insignificant even given a long period of record. Author (GRA)

N82-14724# National Oceanic and Atmospheric Administration, Washington, D. C. Nationale Earth Satellite Service.

ANALYSIS OF RAINFALL FROM FLASH FLOOD PRODUCING THUNDERSTORMS, USING GOES DATA

Roderick A. Scofield In ESA Nowcasting: Mesoscale Observations and Short-Range Prediction Jun. 1981 p 51-58 refs

Avail: NTIS HC A19/MF A01; ESA, Paris FF 160 Member States, AU, CN and NO (+20% others)

The use of the Scofield-Oliver GOES technique for estimating convective precipitation from flash flood producing thunderstorms is discussed. The technique is applied using imagery displayed with a digital enhancement curve. Estimates of convective rainfall are done by comparing the changes in two

consecutive pictures, both infrared and high resolution visible. The method is applied to two flash flood events. The estimates as compared to the observed rainfall are good. However, a warm top modification is needed for thunderstorms whose expected anvil temperatures are warmer than -62C. Author (ESA)

N82-15486*# Instituto de Pesquisas Espaciais, Sao Jose dos Campos (Brazil).

QUANTITATIVE ANALYSIS OF DRAINAGE OBTAINED FROM AERIAL PHOTOGRAPHS AND RBV/LANDSAT IMAGES [ANALISE QUANTITATIVA DA DRENAGEM OBTIDA ATRAVES DE FOTOGRAFIAS AEREAS E IMAGENS DO RBV/LANDSAT]

Nelson deJesusParada, Principal Investigator, Antonio Roberto Formaggio, Jose Carlos Neves Epiphanio, and Mario Valerio Filho May 1981 29 p refs In PORTUGUESE; ENGLISH summary Presented at the 33rd Reuniao Anual de SBPC Sponsored by NASA ERTS

(E82-10008; NASA-CR-164906) Avail: NTIS HC A03/MF A01 CSCL 08H

Data obtained from aerial photographs (1:60,000) and LANDSAT return beam vidicon imagery (1:100,000) concerning drainage density, drainage texture, hydrography density, and the average length of channels were compared. Statistical analysis shows that significant differences exist in data from the two sources. The highly drained area lost more information than the less drained area. In addition, it was observed that the loss of information about the number of rivers was higher than that about the length of the channels. Author

N82-15673# California Univ., Santa Barbara. Computer Systems Lab.

USE OF ENVIRONMENTAL SATELLITE DATA FOR INPUT TO ENERGY BALANCE SNOWMELT MODELS Final Report

Jeff Dozier Dec. 1980 125 p refs

(Grant NOAA-04-8-MO)

(PB81-227795; TR-CSL-8001; NOAA-81050501) Avail: NTIS HC A06/MF A01 CSCL 04A

The development of solar and longwave radiation models for alpine snow covered terrain, techniques for atmospheric correction of satellite radiometric data and for snow albedo determination from satellite, a very fast solution to the terrain horizon problem, investigations of the use of NOAA satellite data for snow surface temperature, mapping, and work on canopy cover measurements from satellite for use in solar and longwave radiation models are described. GRA

Page intentionally left blank

Page intentionally left blank

DATA PROCESSING AND DISTRIBUTION SYSTEMS

Includes film processing, computer technology, satellite and aircraft hardware, and imagery.

A82-10027 American Society of Photogrammetry, Annual Meeting, 46th, St. Louis, MO, March 9-14, 1980, ASP Technical Papers. Falls Church, VA, American Society of Photogrammetry, 1980. 552 p. \$10.

Consideration is given to such topics as digital classification accuracy, hydrometeorology, computational photogrammetry, digital image processing and rectification, the role of remote sensing in continuing education and professional development, digital displays, and the application of orthophotography in highway planning and construction. Also examined are the analysis of Landsat MSS data, remote sensor systems, close-range photogrammetry, the use of aerial photography in remote sensing, photogrammetric instruments, and automated cartography. B.J.

A82-10038 Applications of digital displays in photo-interpretation and digital mapping. B. L. Schrock (U.S. Army, Computer Sciences Laboratory, Fort Belvoir, VA). In: American Society of Photogrammetry, Annual Meeting, 46th, St. Louis, MO, March 9-14, 1980, ASP Technical Papers. Falls Church, VA, American Society of Photogrammetry, 1980, p. 201-212.

The Digital Image Analysis Laboratory (DIAL) at USAETL is a large-scale interactive system designed for research and development activities in digital image processing. The system has been successfully applied to a variety of investigations in both digital mapping and photointerpretation as described in this presentation. Recently a Demonstration Image Processing System (DEMONS) has been added to the DIAL system to serve as a high-speed work station for processing very large digital images. Although DEMONS has been reasonably successful in manipulating large images, its limitations indicate that future such systems might be hybrid systems combining the best features of both hardcopy (film) and softcopy (cathode ray tube) exploitation systems. (Author)

A82-10860 Two-dimensional resampling of line scan imagery by one-dimensional processing. D. E. Friedmann (MacDonald, Dettwiller and Associates, Ltd., Richmond, British Columbia, Canada). *Photogrammetric Engineering and Remote Sensing*, vol. 47, Oct. 1981, p. 1459-1467. 33 refs. Research supported by the Department of Industry, Trade and Commerce.

Geometric correction of remote sensing data, such as Landsat MSS data, requires two-dimensional resampling. The resampling operation is typically carried out in two one-dimensional operations: along and across scan lines. The usual reasons given for validating the procedure are lower cost and higher speed. The theoretical assumptions under which one-dimensional processing is valid are presented in the light of current and future remote sensing sensors. It is shown that the assumptions are violated when a substantial amount of image rotation is incorporated into the precision processing. A method to perform image rotation with an additional step using one-dimensional processing is presented. The method makes precision correction and alignment of remote sensing data, to a map projection, both possible and accurate with one-dimensional processing. (Author)

A82-10861 Estimation of atmospheric path-radiance by the covariance matrix method. P. Switzer, W. S. Kowalik, and R. J. P. Lyon (Stanford University, Stanford, CA). *Photogrammetric Engineering and Remote Sensing*, vol. 47, Oct. 1981, p. 1469-1476. 16 refs.

A new method has been developed as an extension of Chavez's Regression Technique (Chavez, 1975) to provide estimates of the atmospheric path-radiance in the four Landsat MSS bands. The extension uses the correlation between all four bands of data

simultaneously instead of in pairs. The Regression Method and this extension do not require auxiliary data, but operate solely upon the digital numbers recorded on the Landsat tapes. Furthermore, they do not require the presence of sites of low reflectance (basalt flows, clear lakes) or sites of low irradiance (shadows due to topography or clouds) in the Landsat data, or topographic slope data. Instead, we use Landsat data from areas of homogeneous reflectance in hilly terrain as test areas for estimation of the band-specific atmospheric path-radiances. The method has been applied to Landsat data from diverse terrain types and atmospheric conditions using three different Landsat images covering semi-arid western Nevada, temperate eastern Pennsylvania, and tropical central New Guinea. The method yields reasonable results from each area. (Author)

A82-12757 A theory of wave scattering from an inhomogeneous layer with an irregular interface. A. K. Fung and H. J. Eom (Kansas, University, Lawrence, KS). *IEEE Transactions on Antennas and Propagation*, vol. AP-29, Nov. 1981, p. 899-910. 10 refs. NSF Grant No. ENG-79-09374; Grant No. DAAG29-80-K-0018.

Bistatic wave scattering from a layer of Rayleigh scatterers with an irregular interface is studied by combining the doubling method in volume scattering with the Kirchhoff method in rough surface scattering. Theoretical results are presented illustrating the effect of the rough interface. It is found that for scattered and incident angles near the vertical, the rough interface brings about a substantial increase relative to the plane interface in both the like and cross-scattering coefficients over all azimuth angles. For large scattered and incident angles, however, the reverse is true, except for azimuth angles around the specular direction. C.R.

A82-12882 Digital mapping using entities - A new concept. S. E. Masry (New Brunswick, University, Fredericton, Canada). *Photogrammetric Engineering and Remote Sensing*, vol. 47, Nov. 1981, p. 1561-1565.

An approach to digital mapping using aerial or satellite photography is presented which is based on the use of linear features to establish the relationship between an image and a ground coordinate system in lieu of or in addition to individual control points. The concept is based on entity-to-entity correspondence, an entity being defined as a set of points describing part or the whole of a feature. It involves the transformation of the mathematical functions defining the observed entities in order that they become identical to the corresponding functions describing control entities obtained from a topographic data base or map. The concept has successfully been applied to carry out the absolute orientation of a stereomodel, and perform analytical space resection of an aerial photograph, with precision and convergence comparable to those derived from conventional control. S.C.S.

A82-12913 † Aspects in the development of aerial-photography tasks (Voprosy razvitiia aerofotos'emochnykh rabot). Iu. I. Poletaev. *Geodeziia i Kartografiia*, Sept. 1981, p. 32-34. In Russian.

Recent developments in aerial photography in the Soviet Union are briefly reviewed. Attention is given to calibration methods, ways to improve the quality of negatives, optimal exposure techniques, scaling, and automated processing. B.J.

A82-13121 Interactive techniques for estimating precipitation from GOES imagery. J. F. Moses, L. E. Spayd, Jr., R. S. Gird, and A. L. Siebers (NOAA, National Earth Satellite Service, Washington, DC). In: Joint Automatic Control Conference, Charlottesville, VA, June 17-19, 1981, Proceedings. Volume 2. New York, American Institute of Chemical Engineers, 1981. 9 p. (TP-6C). 6 refs.

Recent development of an interactive computer technique aids meteorologists in using geostationary satellite imagery to estimate precipitation. The interactive technique utilizes the interpretive abilities and experience of the meteorologist with the speed and accuracy of the computer to reduce the time and effort required by the previously developed manual method. An analysis of a precipitation event in Kansas on July 4-5, 1979, illustrates the technique. A comparison of satellite estimates to ground truth reports shows that the estimates indicate the areas of maximum observed precipitation accumulation. (Author)

A82-13633 † Calculation of the decrease in the contrast of objects of a place due to light scattering in the atmosphere (O vychislenii padeniia kontrasta ob'ektov mestnosti iz-za rasseianiia sveta v atmosfere). Iu. L. Biriukov and E. G. Markarian (Moskovskii Institut Inzhenerov Geodezii, Aerofotos'emki i Kartografii, Moscow, USSR). *Geodeziia i Aerofotos'emka*, no. 4, 1981, p. 80-86. 9 refs. In Russian.

With reference to aerial photography, an analytical method is presented for calculating the decrease in the image contrast of small-scale objects on the earth's surface due to light scattering in the atmosphere. An analysis is presented of the dependence of the contrast of the object and background, observed through the optical medium, on the optical thickness of the atmosphere, the solar zenith distance, the angles of sight, and the albedo of the object and background. Numerical results are presented. B.J.

A82-13634 † Concerning the geometric accuracy of infrared scanner photographs (K voprosu o geometricheskoi tochnosti infrakrasnykh skanernykh snimkov). O. I. Egorova (Moskovskii Institut Inzhenerov Geodezii, Aerofotos'emki i Kartografii, Moscow, USSR). *Geodeziia i Aerofotos'emka*, no. 4, 1981, p. 113-116. In Russian.

The sources of geometric errors of infrared scanner images are examined along with methods to eliminate these errors. Experimental results concerning the accuracy of infrared scanner photographs are presented. B.J.

A82-14860 Reflectivity and emissivity of snow and ground at mm waves. R. D. Hayes, N. C. Currie, and J. A. Scheer (Georgia Institute of Technology, Atlanta, GA). In: International Radar Conference, Arlington, VA, April 28-30, 1980, Record. New York, Institute of Electrical and Electronics Engineers, Inc., 1980, p. 67-72.

A summary is provided of the results of a test program conducted to determine the backscatter and emissivity characteristics of background clutter at millimeter wavelengths. The test was conducted during the late winter time frame to include snow and wet terrain as background types. It is pointed out that active and passive millimeter wave RF sensors are prime candidates for the role of air-to-surface anti-armor weapons applications because of certain advantages compared to microwave sensors and electro-optical sensors. However, the design, development, and evaluation of systems for such an application requires an extensive understanding of the millimeter wavelength reflectivity and emissivity characteristics of clutter and targets. It was found in the investigation that the radar reflectivity of the snow varies strongly with the diurnal freeze-melt cycle. Radar cross sections for short and tall grass are also considered. G.R.

A82-14870 * A digital fast correlation approach to produce SEASAT SAR imagery. C. Wu (California Institute of Technology, Jet Propulsion Laboratory, Pasadena, CA). In: International Radar Conference, Arlington, VA, April 28-30, 1980, Record.

New York, Institute of Electrical and Electronics Engineers, Inc., 1980, p. 153-160. 9 refs. Contract No. NAS7-100.

This paper describes a digital processing algorithm and its associated system design for producing images from SEASAT Synthetic Aperture Radar (SAR) data. The proposed system uses the fast Fourier transform approach to perform the two-dimensional correlation process. The range migration problem, which is often a major obstacle to efficient processing, can be alleviated by approximating the locus of echoes from a point target by several linear segments. SAR data corresponding to each segment is correlated separately, and the results are coherently summed to produce full-resolution images. This processing approach exhibits high computation efficiency and simple processing control functions. It is particularly attractive for software implementation based on general purpose computer. Results of this implementation and examples of digitally correlated SEASAT SAR imagery are discussed. B.J.

A82-15003 # Investigations concerning the image-controlled segmentation of objects in multispectral imagery data (Untersuchungen zur bildgesteuerten Separierung von Objekten in multispektralen Bilddaten). R. Schärf. Karlsruhe, Universität, Fakultät für Elektrotechnik, Dr.-Ing. Dissertation, 1981. 157 p. 74 refs. In German.

The automatic segmentation of objects in an image represents an essential step in a procedure for the interpretation of images. The considered investigation is concerned with image-controlled process-

es, based on sequential operations, for the extraction of areal objects from real multispectral imagery. A survey is presented of various operational principles used for image segmentation, and a description is provided of the characteristics of multispectral imagery data. Problems of data compression are examined, and different segmentation procedures are compared. This comparison leads to the development of a two-stage procedure for the segmentation of objects on the basis of region growing. Important aspects of the new procedure are related to sequential iterative processing and the initial control of the processing steps by means of automatically extracted structural image elements. At a later stage, the characteristics and the position of the segmented objects provide additional control elements. G.R.

A82-15029 Two-dimensional model variability in thermal inertia surveys. D. A. Pratt (Newcastle, University, Newcastle, Australia). *Remote Sensing of Environment*, vol. 9, June 1980, p. 325-338. 20 refs. Research supported by the Australian Research Grants Committee.

Calibration of thermal inertia surveys requires the production of a numerical model where thermal inertia is expressed as a function of the diurnal ground surface temperature range and albedo. The model is calculated for a given set of local meteorological and surface conditions which must be assumed constant over the whole of the surveyed area. This paper reports the results of an investigation which estimates the magnitudes of thermal inertia errors as a function of the departure of the local conditions from those assumed. The parameters under investigation are wind speed, average air temperature, air-temperature fluctuations, surface roughness, slope and changes in the thermal inertia profile. (Author)

A82-15034 * Texture transforms of remote sensing data. J. R. Irons (NASA, Goddard Space Flight Center, Earth Resources Branch, Greenbelt, MD) and G. W. Petersen (Pennsylvania State University, University Park, PA). *Remote Sensing of Environment*, vol. 11, Nov. 1981, p. 359-370. 16 refs.

Tone and texture are fundamental interrelated visual concepts. The concepts are used for the digital analysis of remotely sensed image data. The reported investigation had the objective to develop software for the quantification of image texture and to apply the texture information to both image enhancement and thematic classification of remotely sensed data. The quantitative texture information was applied to the analysis of Landsat-2 Multispectral Scanner Subsystem (MSS) data. Attention is given to the characterization of image texture, textured transformations, the subtext program, and a description of methods and results. It is pointed out that the inability to use the texture transforms of the Landsat MSS data for the thematic mapping of the study area's land cover contrasts sharply with the reported results of the textural analysis of digitized aerial photography by Hsu (1978). G.R.

A82-15125 * Optically processed Seasat radar mosaic of Florida. M. L. Bryan (California Institute of Technology, Jet Propulsion Laboratory, Pasadena, CA). *Photogrammetric Engineering and Remote Sensing*, vol. 47, Sept. 1981, p. 1335-1337.

An uncontrolled mosaic of optically correlated Seasat radar imagery of Florida is presented to illustrate the data and the large area synoptic coverage made possible by combining multiple data sets. The images were taken from a total of 12 passes over 33 days from July 24, 1978 to August 27, 1978. The mosaic is controlled geometrically and with respect to image tone (representing radar backscatter). The SAR data was obtained at an L-band frequency (1.275 GHz, 23.5 cm) and in a horizontal transmit/receive mode, resulting in a 25 m resolution in 100 km swath widths. M.S.K.

A82-15764 Compensation of systematic errors in bundle adjustment. E. Kilpela, J. Heikkilä, and K. Inkilä (Helsinki University of Technology, Esbo, Finland). *Photogrammetria*, vol. 37, Nov. 1981, p. 1-13. 7 refs.

Results of the application of a bundle program to study the effects of weighted additional parameters on the accuracy and reliability of self-calibration are examined. Six additional parameter sets used with and without weighting, as well as a comparison of simultaneous and a posteriori self-calibration are studied. General features of the program are outlined, and the program is applied to photography of test areas at 1:4000 and 1:12,000 scales. Root mean

square errors in planimetry and height are used as quantities for determining the effectiveness of compensation of systematic errors. Best results were obtained by employing weights corresponding to image point displacements of less than five micrometers, and weights equal to zero, especially in cases of minor side overlap. Simultaneous self-calibrations proved more efficient than a posteriori self-calibration. M.S.K.

A82-15765 Compensation of systematic errors of image and model coordinates. E. Kilpela (Helsinki University of Technology, Esbo, Finland). *Photogrammetria*, vol. 37, Nov. 1981, p. 15-44. 9 refs.

Compensation for systematic errors of image and model coordinates in different aerotriangulation methods is studied. Four test fields in Australia and Finland used for the photogrammetric adjustments were coordinated by a ground survey. Flight programs and measurements are outlined, and compensation procedures comprised reference adjustment, component calibration, test field calibration, and self calibration. Blockwise vs stripwise parameters, significance testing of additional parameters, weighting of additional parameters, correlations, and a priori data refinements, as well as side overlap, single vs double block, control point pattern, and the use of a reseau to correct film distortion were considered. Calibration improved the triangulation by 20%, self calibration produced results superior to test field calibration, and the introduction of strip invariant additional parameters was found to be ineffective. M.S.K.

A82-15970 Cost effective computer processing of airborne scanner data for regional level mapping. S. Thiruvengadachari (National Remote Sensing Agency, Hyderabad, India). *Photogrammetric Engineering and Remote Sensing*, vol. 47, Dec. 1981, p. 1705-1708.

The reported investigation concerning an optimization of the computer analysis of multispectral data was conducted in connection with an airborne scanner survey over an area of approximately 750 sq km in the northeastern part of India. The survey was conducted to obtain information with regard to flood inundation along a selected range of a major river system. Digital analysis was performed on the interactive Multispectral Data Analysis System, operated at the National Remote Sensing Agency facility at Hyderabad. An 11 channel scanner mounted on a DC-3 Dakota aircraft was used in the survey. Attention is given to the study background, analysis methodology, categorical analysis, and categorization accuracy. It was found that the computer analysis of 11-channel airborne scanner data can be made cost effective by the use of fewer channels, when regional selection of level information is to be obtained. G.R.

A82-15971 * The Control Point Library Building System. W. Niblack (IBM France, S.A., Paris, France). *Photogrammetric Engineering and Remote Sensing*, vol. 47, Dec. 1981, p. 1709-1715. 7 refs. Contracts No. NAS5-22999; No. NAS5-23790.

The Earth Resources Observation System (EROS) Data Center in Sioux Falls, South Dakota distributes precision corrected Landsat MSS and RBV data. These data are derived from master data tapes produced by the Master Data Processor (MDP), NASA's system for computing and applying corrections to the data. Included in the MDP is the Control Point Library Building System (CPLBS), an interactive, menu-driven system which permits a user to build and maintain libraries of control points. The control points are required to achieve the high geometric accuracy desired in the output MSS and RBV data. This paper describes the processing performed by CPLBS, the accuracy of the system, and the host computer and special image viewing equipment employed. (Author)

A82-15973 Orientation and construction of models. III - Mathematical basis of the orientation problem of one-dimensional central perspective photographs. A. Okamoto (Kyoto University, Kyoto, Japan). *Photogrammetric Engineering and Remote Sensing*, vol. 47, Dec. 1981, p. 1739-1752. 9 refs.

The reported analysis of the general orientation problem of one-dimensional central perspective photographs makes use of the mathematical basis employed in the orientation problem of two-dimensional (conventional) central perspective pictures. The general orientation problem of a stereoscopic pair of one-dimensional photographs is considered, taking into account also the special case in which the interior orientation parameters are known. Attention is given to the photogrammetric orientation problem of one-

dimensional central-perspective photographs, and the orientation problem in the case of individual one-dimensional photographs. G.R.

A82-16160 Spectral correlation filters and natural colour coding. N. J. Mulder (International Institute for Aerial Survey and Earth Sciences, Enschede, Netherlands). *ITC Journal*, no. 3, 1981, p. 237-252.

A system utilizing spectral correlation filters and natural color coding has been developed for remote sensing. Studies of principal components (Mulder and Hempenius, 1974) have shown that there are only two or three independent factors in reflectance spectra of natural materials. Filters have thus been designed to store reflection spectra of water, dense green vegetation, and bare soil using a natural color coding scheme. Nearly all other natural reflection spectra can be described as a linear combination of these three spectra. The method has been tested for a simulation using Landsat data. S.C.S.

A82-16163 Theoretical reliability of elementary photogrammetric procedures. I. F. A. A. F. Amer (International Institute for Aerial Survey and Earth Sciences, Enschede, Netherlands). *ITC Journal*, no. 3, 1981, p. 278-307. 10 refs.

The reliability of elementary photogrammetric procedures for production photogrammetrists is presented. The derivation of the weight coefficient matrix of the residuals is obtained, noting its structure and the significance of its main and off-diagonal elements. For high homogeneous reliability, the main diagonal elements should be close to unity and equal. When all the main diagonal elements are equal the reference boundary value is achieved. The difference between detection and location of gross errors is illustrated. It is shown that a rejection matrix may be employed to evaluate the possibility of locating gross errors. S.C.S.

A82-16601 Airborne and spaceborne multispectral photography of the earth (Mnogozonal'nye aerokosmicheskie s'emki zemli). R. Z. Sagdeev. Moscow, Izdatel'stvo Nauka, 1981. 304 p. In Russian.

Multispectral scanning of earth resources is considered, with attention given to the Soyuz-22 Raduga experiment, optical scanning, remote spectroscopy, polarimetry methods, analog processing, and digital processing. Particular consideration is given to such topics as the parameter optimization of spaceborne photography systems, the instrumental interpretation of multispectral aerial and space photographs, a special-purpose optoelectronic system for the operational acquisition of multispectral image data, the energy calibration of multispectral scanner systems, and the maximum mean accuracy of classification of remote-sensing objects. B.J.

A82-16605 † Evaluation of the information content of the channels of spaceborne multispectral photography of the Fergana region by the MKF-6 camera from Soyuz-22 (Otsenka i informativnosti kanalov mnogozonal'noi kosmicheskoi fotos'emki Ferganskogo uchastka kamerai MKF-6 s kosmicheskogo korablia 'Soyuz-22'). G. B. Gonin and V. P. Koroleva. In: Airborne and spaceborne multispectral photography of the earth. Moscow, Izdatel'stvo Nauka, 1981, p. 24-37. 10 refs. In Russian.

A82-16606 † Geometric quality of MKF-6 photographs (Geometricheskoe kachestvo snimkov MKF-6). Ia. L. Ziman, V. A. Krasikov, and V. I. Iurov. In: Airborne and spaceborne multispectral photography of the earth. Moscow, Izdatel'stvo Nauka, 1981, p. 37-43. In Russian.

The photogrammetric calibration and digital processing of multispectral photographs obtained with the MKF-6 camera in the Raduga experiment aboard Soyuz-22 are considered. It is shown that the MKF-6 photographs are topographic ones and can be used to solve many kinds of photogrammetric problem. B.J.

A82-16607 † Methods of instrumental interpretation of multispectral aerial and space photographs (Metody izmeritel'nogo deshifirovaniia mnogozonal'nykh aerokosmicheskikh snimkov). I. A. Labutina and Iu. I. Fivenskii. In: Airborne and spaceborne multispectral photography of the earth. Moscow, Izdatel'stvo Nauka, 1981, p. 43-55. 7 refs. In Russian.

A82-16612 † Spectrometric studies of the earth's surface (Spektrometricheskie issledovaniia zemnoi poverkhnosti). G. A.

07 DATA PROCESSING AND DISTRIBUTION SYSTEMS

Avanesov and N. I. Snetkova. In: Airborne and spaceborne multi-spectral photography of the earth. Moscow, Izdatel'stvo Nauka, 1981, p. 100-117. 95 refs. In Russian.

A review of the literature on the remote spectroscopy of earth resources is presented. A classification of terrestrial features on the basis of spectral characteristics is considered. B.J.

A82-16614 † The application of holographic gratings in spectrometers for the spatial-spectral analysis of the earth's surface from aerial and space platforms in the visible and near-infrared spectral regions (K voprosu o primenenii golograficheskikh reshetok v spektrometrah dlia prostranstvenno-spektral'nogo analiza zemnoi poverkhnosti s aerokosmicheskikh platform v vidimom i blizhnem ik-diapazonakh spektra). E. G. Lykashva. In: Airborne and spaceborne multispectral photography of the earth. Moscow, Izdatel'stvo Nauka, 1981, p. 128-135. 6 refs. In Russian.

A82-16615 † The maximum mean accuracy of classification of remote-sensing objects and the influence on this accuracy of data acquisition and processing methods (Dostizhimaia sredniaia tochnost' klassifikatsii ob'ektov distantsionnogo zondirovaniia i vliianie na nee metodov sbora i obrabotki dannykh). B. M. Balter. In: Airborne and spaceborne multispectral photography of the earth. Moscow, Izdatel'stvo Nauka, 1981, p. 135-151. In Russian.

A review of the literature on the classification of remote-sensing objects is used to investigate the mean accuracy of classification. This accuracy was found to be 82% and (with a probability of 0.95) not lower than 55%. Current methods of automatic classification produce an increase of 8% compared with nonautomatic methods. The mean accuracy in the period 1972-1977 was found to increase by 1% every year. Such factors as type of sensor, platform, and data processing do not have an appreciable influence on the mean accuracy. B.J.

A82-16616 † Characteristics of the photometry of small objects from aerial and space photographs (Osobennosti fotometrirovaniia malykh ob'ektov po aerokosmicheskim fotosnimkam). Iu. I. Fivenskii and Iu. N. Kuznetsov. In: Airborne and spaceborne multispectral photography of the earth. Moscow, Izdatel'stvo Nauka, 1981, p. 152-164. 8 refs. In Russian.

The current status of the method of microphotometric determinations from remotely sensed images is described, and results of a laboratory experiment are presented. It is shown that the photometric properties are invariant to the geometry and distribution characteristics of small details on the photograph. Requirements on the photometric calibration of aerial and space photography systems are examined. B.J.

A82-16617 † Estimation of the brightness field from results of multispectral photography of the earth from space (Otsenka iarkostnogo polia po rezul'tatam mnogozonol'nogo fotografirovaniia zemli iz kosmosa). V. A. Kotsov. In: Airborne and spaceborne multispectral photography of the earth. Moscow, Izdatel'stvo Nauka, 1981, p. 165-169. In Russian.

A method for the statistical estimation of brightness and spectral contrasts for the territory of the USSR on the basis of data from the Soyuz-22 Raduga experiment is presented. The statistical characteristics of the contrasts are given. B.J.

A82-16618 † The use of a priori information in the remote sensing of the earth from space (Ispol'zovanie apriornoj informatsii pri izuchenii zemli iz kosmosa). V. A. Kottsov and I. B. Prokuronov. In: Airborne and spaceborne multispectral photography of the earth. Moscow, Izdatel'stvo Nauka, 1981, p. 170-174. 5 refs. In Russian.

The relationship between the concept of an object in remote sensing and the characteristics of a priori information is examined in the framework of pattern recognition theory. The improvement of remote sensing methods by using the representation of localized factors is considered. B.J.

A82-16621 † The choice of the orientation of the analyzer in polarimetric surveys (O vybore orientatsii analizatora pri polarizatsionnoi s'emke). V. V. Egorov and B. S. Zhukov. In: Airborne and spaceborne multispectral photography of the earth.

Moscow, Izdatel'stvo Nauka, 1981, p. 197-202. In Russian.

An analysis is presented of the conditions of achieving maximum contrast in polarimetric remote-sensing surveys. It is found that for surveys of soil-vegetation objects the maximum contrast is generally attained when the analyzer is oriented parallel to the solar-vertical plane. Experimental results on such surveys are presented. B.J.

A82-16623 † Analog methods for processing multispectral photographs (Ob analogovykh metodakh obrabotki mnogozonal'nykh fotosnimkov). Iu. M. Chesnokov. In: Airborne and spaceborne multispectral photography of the earth. Moscow, Izdatel'stvo Nauka, 1981, p. 211-216. In Russian.

The possibilities of analog techniques for the processing of multispectral photographs are reviewed. Particular attention is given to the development of laser-based analog optoelectronic devices for the conversion of multispectral images into color images. B.J.

A82-16625 † Structural analysis of aerial and space images (Strukturnyi analiz aerokosmicheskikh snimkov). K. A. Kraush. In: Airborne and spaceborne multispectral photography of the earth. Moscow, Izdatel'stvo Nauka, 1981, p. 224-234. 10 refs. In Russian.

The theoretical principles of the structural analysis of remote sensing images are presented. A block diagram of an optoelectronic device for performing the structural analysis is given, and possible variants of the optical system are examined. The calculation of the intensity of the components of the spatial-frequency spectrum is considered, and the influence of noise is assessed. B.J.

A82-16626 † Investigation of the spatial structure of space images of the earth's surface (Izuchenie prostranstvennoi struktury kosmicheskikh izobrazhenii zemnoi poverkhnosti). V. V. Egorov and G. P. Arumov. In: Airborne and spaceborne multispectral photography of the earth. Moscow, Izdatel'stvo Nauka, 1981, p. 235-243. In Russian.

Aspects of the texture analysis of space photographs of the earth's surface are discussed. The analysis of the spatial structure was carried out by two methods: an analog technique for the formation of spatial-frequency spectra (Wiener spectra) and an analytic method for the component separation of mixtures of natural objects. Examples of analysis are presented. B.J.

A82-16627 † Processing of multispectral image data on special-purpose computer systems (Obrabotka mnogozonal'noi video-informatsii na spetsializirovannykh vychislitel'nykh kompleksakh). V. A. Krasikov and V. A. Shamis. In: Airborne and spaceborne multispectral photography of the earth. Moscow, Izdatel'stvo Nauka, 1981, p. 244-248. In Russian.

The development of special-purpose operational systems for processing multispectral earth-resources data is considered. A Soviet system is described that assures effective access to the image. The library of application programs ensures effective thematic processing. B.J.

A82-16628 † Programs for the statistical analysis of multispectral photographs (Programmy statisticheskogo analiza mnogozonal'nykh snimkov). V. A. Krasikov, V. G. Sobchuk, V. A. Shamis, and M. V. Khatuntseva. In: Airborne and spaceborne multispectral photography of the earth. Moscow, Izdatel'stvo Nauka, 1981, p. 248-253. In Russian.

Minicomputer-implemented algorithms for the statistical analysis of multispectral photographs of earth resources are described. Particular attention is given to the computation and construction of brightness-distribution histograms, and to the computation of the vectors of mean and covariant matrices. B.J.

A82-16629 † Linear combinations of multispectral images (Lineinye kombinatsii mnogozonal'nykh snimkov). M. V. Khatuntseva. In: Airborne and spaceborne multispectral photography of the earth. Moscow, Izdatel'stvo Nauka, 1981, p. 253-261. In Russian.

The use of linear combinations of multispectral images in the thematic analysis and interpretation of multispectral photographs of the earth's surface is considered. Particular attention is given to the

machine implementation of the method of principal components.

B.J.

A82-16630 † Coordinate referencing of MKF-6 photographs and their transformation to the cartographic projection (Koodinatnaia priviazka snimkov MKF-6 i preobrazovanie ikh v kartografi-cheskuiu proektsiiu). Ia. L. Ziman, V. A. Krasikov, V. G. Sobchuk, and V. A. Shamis. In: Airborne and spaceborne multispectral photography of the earth. Moscow, Izdatel'stvo Nauka, 1981, p. 261-266. In Russian.

An analysis is presented of the use of affine transformations in the processing of multispectral photographs of earth resources and their transformation to the Kavraiskii cartographic projection. The optimization of access to the images is assured by a programmable virtual memory. B.J.

A82-18167 Photo inertial positioning system development at the Canada Centre for Remote Sensing. J. R. Gibson and J. E. Smyth (Canada Centre for Remote Sensing, Ottawa, Canada). In: PLANS '80 - Position Location and Navigation Symposium, Atlantic City, NJ, December 8-11, 1980, Record. New York, Institute of Electrical and Electronics Engineers, Inc., 1980, p. 436-438.

The system and projects described form part of the continuing development work on the Photo Inertial Positioning System at the Canada Centre for Remote Sensing. The system consists of an aerial camera having navigation systems and sensors hard-mounted to it. A general-purpose data acquisition system is used in time-correlating the data from these and other sensors. It is noted that during the past several years, the system development has been slanted toward the application of shallow water charting. The system is at present capable of providing postflight position accuracies of the order of 1 meter and attitude accuracies of 1 arcmin. C.R.

N82-10072*# General Electric Co., Lanham, Md. Space Div. **COMPUTATIONAL ASPECTS OF GEOMETRIC CORRECTION DATA GENERATION IN THE LANDSAT-D IMAGERY PROCESSING**

I. Levine /in NASA. Goddard Space Flight Center Sixth Ann. Flight Mech./Estimation Theory Symp. Oct. 1981 16 p ref

(Contract NAS5-25300)

Avail: NTIS HC A13/MF A01 CSCL 05B

A method is presented for systematic and geodetic correction data calculation. It is based on presentation of image distortions as a sum of nominal distortions and linear effects caused by variation of the spacecraft position and attitude variables from their nominals. The method may be used for both MSS and TM image data and it is incorporated into the processing by means of mostly offline calculations. Modeling shows that the maximal of the method are of the order of 5m at the worst point in a frame; the standard deviations of the average errors less than .8m. Author

N82-10466* National Aeronautics and Space Administration. Ames Research Center, Moffett Field, Calif.

MATE VAN: MOBILE ANALYSIS AND TRAINING EXTENSION

[1981] 7 p

(NASA-TM-84056) Avail: NASA Scientific and Technical Information Facility, P. O. Box 8757, B.W.I. Airport, Md. 21240 CSCL 05B

A modified 30-foot motor coach was equipped with modern data processing equipment in order to train personnel and demonstrate useful techniques and capabilities for analyzing and applying LANDSAT imagery in the western regional area. A block diagram of the interactive digital image manipulation system is presented and its processing features itemized. Specifications for the van and the equipment are listed. False color composites used to interpret and identify many LANDSAT technological applications are included. A.R.H.

N82-10469*# Martin Marietta Corp., Denver, Colo. **ONBOARD UTILIZATION OF GROUND CONTROL POINTS FOR IMAGE CORRECTION. VOLUME 1: EXECUTIVE SUMMARY Final Report**

May 1981 30 p refs 4 Vol.

(Contract NAS5-26094)

(NASA-CR-166731; MCR-81-576-Vol-1) Avail: NTIS

HC A03/MF A01 CSCL 05B

Operation of a navigation system, centered around image correction, was simulated and the system performance was analyzed. Onboard utilization of ground control points for image correction is summarized. Simulation results, and recommendations for future mission requirements are presented. E.A.K.

N82-10470*# Martin Marietta Corp., Denver, Colo. **ONBOARD UTILIZATION OF GROUND CONTROL POINTS FOR IMAGE CORRECTION. VOLUME 2: ANALYSIS AND SIMULATION RESULTS Final Report**

May 1981 183 p refs 4 Vol.

(Contract NAS5-26094)

(NASA-CR-166732; MCR-81-576-Vol-2) Avail: NTIS HC A09/MF A01 CSCL 05B

An approach to remote sensing that meets future mission requirements was investigated. The deterministic acquisition of data and the rapid correction of data for radiometric effects and image distortions are the most critical limitations of remote sensing. The following topics are discussed: onboard image correction systems, GCP navigation system simulation, GCP analysis, and image correction analysis measurement. E.A.K.

N82-10471*# Martin Marietta Corp., Denver, Colo. **ONBOARD UTILIZATION OF GROUND CONTROL POINTS FOR IMAGE CORRECTION. VOLUME 3: GROUND CONTROL POINT SIMULATION SOFTWARE DESIGN Final Report**

May 1981 409 p refs 4 Vol.

(Contract NAS5-26094)

(NASA-CR-166733; MCR-81-576-Vol-3) Avail: NTIS HC A18/MF A01 CSCL 05B

The software developed to simulate the ground control point navigation system is described. The Ground Control Point Simulation Program (GCPsim) is designed as an analysis tool to predict the performance of the navigation system. The system consists of two star trackers, a global positioning system receiver, a gyro package, and a landmark tracker. E.A.K.

N82-10472*# Martin Marietta Corp., Denver, Colo. **ONBOARD UTILIZATION OF GROUND CONTROL POINTS FOR IMAGE CORRECTION. VOLUME 4: CORRELATION ANALYSIS SOFTWARE DESIGN Final Report**

May 1981 86 p refs 4 Vol.

(Contract NAS5-26094)

(NASA-CR-166734; MCR-81-576-Vol-4) Avail: NTIS HC A05/MF A01 CSCL 05B

The software utilized for image correction accuracy measurement is described. The correlation analysis program is written to allow the user various tools to analyze different correlation algorithms. The algorithms were tested using LANDSAT imagery in two different spectral bands. Three classification algorithms are implemented. E.A.K.

N82-10485# Technical Research Centre of Finland, Espoo. Maankaeytoen Lab.

SMALL-SCALE TERRAIN MAPPING BASED ON NUMERICAL INTERPRETATION OF LANDSAT IMAGERY [LANDSAT-KUVIEN NUMEERISEEN TULIKINTAAN PERUSTUVA PIENKAAVAINEN MAASTOKARTOITUS]

Esa Franssila 1981 75 p refs In FINNISH; ENGLISH summary Original contains color illustrations

(VTT-40; ISBN-951-38-1180-8; ISSN-0355-3477) Avail: NTIS HC A04/MF A01

The usability of digital LANDSAT imagery for producing terrain data, the general map of Finland (1: 400,000) and other small-scale terrain maps was investigated. The image processing was based on numerical processing of: image correction to map projection; image interpretation; data generalization; and graphic output along with statistical summary data. In order to achieve an automated cartographic generalization, the scale caused details were effaced by applying alternative rules. Compared with the conventional generalization, the result is defective. Figure lines for cartographic presentation were produced. Author (ESA)

N82-11103*# Computer Sciences Corp., El Segundo, Calif. **MAGNETIC FIELD SATELLITE (MAGSAT) DATA PROCESSING SYSTEM SPECIFICATIONS**

D. Berman, R. Gomez, and A. Miller Oct. 1980 136 p refs (Contract NAS5-24391)

(NASA-CR-166737; CSC/TM-80/6214) Avail: NTIS HC A07/MF A01 CSCL 22B

07 DATA PROCESSING AND DISTRIBUTION SYSTEMS

The software specifications for the MAGSAT data processing system (MDPS) are presented. The MDPS is divided functionally into preprocessing of primary input data, data management, chronicle processing, and postprocessing. Data organization and validity, and checks of spacecraft and instrumentation are discussed. Output products of the MDPS, including various plots and data tapes, are described. Formats for important tapes are presented. Discussions and mathematical formulations for coordinate transformations and field model coefficients are included. S.L.

N82-11509 Washington Univ., Seattle.
IDENTIFICATION OF LITHOLOGIC UNITS USING MULTI-CHANNEL IMAGING SYSTEMS Ph.D. Thesis
Diane Louise Evans 1981 129 p
Avail: Univ. Microfilms Order No. 8121194

It is shown that it is possible to compare laboratory reflectance spectra directly with multispectral images. The signal that would be produced if a particular laboratory sample were in a detector's field of view was calculated and converted into a digital number of DN value. Stacks of spatially registered multispectral images were then searched for materials that had spectral characteristics similar to the laboratory samples. When laboratory reflectance spectra of a suite of Hawaiian samples were compared to Viking Lander images of Mars, a weathered basaltic tephra from a Hawaiian cinder cone was found to have spectral characteristics that were similar in all bandpasses to surficial deposit at the Viking 1 site. When the reflectance spectra of the suite of samples were compared to Viking Orbiter images, the same Hawaiian tephra was found to correspond to a regional spectral unit in the low latitudes of Mars. It was also possible to compare laboratory reflectance spectra to Landsat images of the Earth. Comparison of laboratory reflectance spectra with multispectral images make it possible to derive compositional information from the images. Dissert. Abstr.

N82-13470* Environmental Research and Technology, Inc., Concord, Mass.
ANALYSIS OF SOIL MOISTURE EXTRACTION ALGORITHM USING DATA FROM AIRCRAFT EXPERIMENTS Final Report
Hsiao-hua K. Burke and Jean-Hsien Ho Jun. 1981 37 p refs (Contract NAS5-26361)
(NASA-CR-166719; P-A826) Avail: NTIS HC A03/MF A01 CSCL 08M

A soil moisture extraction algorithm is developed using a statistical parameter inversion method. Data sets from two aircraft experiments are utilized for the test. Multifrequency microwave radiometric data surface temperature, and soil moisture information are contained in the data sets. The surface and near surface (< or = 5 cm) soil moisture content can be extracted with accuracy of approximately 5% to 6% for bare fields and fields with grass cover by using L, C, and X band radiometer data. This technique is used for handling large amounts of remote sensing data from space. S.L.

N82-14548* Applied Physics Lab., Johns Hopkins Univ., Laurel, Md.
RADAR CORRELATION WITH ICE DEPOLARIZATION MEASUREMENTS OF THE 28.56 GHz COMSTAR BEACON AND ASSOCIATED CROSS POLARIZATION STATISTICS
Julius Goldhirsh Aug. 1980 51 p refs
(NASA-CR-166717; JHU/APL-SIR-80U-026)
HC A04/MF A01 CSCL 08L

Two cases of radar correlation with significant ice depolarization events accompanied by low copolarization fades of the 28.56 GHz COMSTAR beacon signal are described. The copol and cross polarization levels of the 28.56 GHz beacon signal were sequentially monitored. A nearby high resolution S band radar pointing along the Earth satellite path monitored the simultaneous ice and rain reflectivity. For the first case, excellent correlation is noted between the cross polarization events and relatively large and extended ice reflectivities along a segment of the Earth satellite path at altitudes near and above the 0 C isotherm. In the second case, the radar and receiver data strongly suggest the cross polarization mechanism is due to a hailshaft which intersects the path at altitudes well below the 0 C isotherm. Extracted depolarization signals were statistically characterized for the 1979 data base in terms of a cumulative distribution as well as monthly and time of day statistics under the given condition that the copol fade is less than 2 dB. B.W.

N82-14568* Centre National d'Etudes Spatiales, Paris (France).
SPOT DATA SIMULATIONS: LITTORAL APPLICATIONS
N. Lannelongue In ESA Appl. of Remote Sensing Data on the Continental Shelf Jul. 1981 p 129-130

Avail: NTIS HC A13/MF A01; ESA, Paris FF 125

Remote sensing SPOT imagery was simulated. User plans for taking advantage of the data are elaborated and the adequacy of SPOT specifications is assessed. Since actual satellite data are not available, a set of aerial remote sensing images with a photographic camera and multispectral scanner was used. The Loire estuary is being studied. Data in the visible and near infrared, of high resolution and good accessibility, are being collected. Simulations show that images can be used immediately after launch. Author (ESA)

N82-14578* Consiglio Nazionale delle Ricerche, Venice (Italy).
MULTITEMPORAL CALIBRATION OF LANDSAT IMAGES: A METHOD FOR IMPROVING THE MARINE PHENOMENA RECOGNITION, WITH AS EXAMPLE THE VENICE LAGOON

L. Alberotanza and A. Zandonella (Telespazio S.p.a.) In ESA Appl. of Remote Sensing Data on the Continental Shelf Jul. 1981 p 205-209 refs

Avail: NTIS HC A13/MF A01; ESA, Paris FF 125

A method for LANDSAT data multitemporal calibration, developed during work on pollution diffusion in the Venice lagoon, was examined. The method consists of a projection, onto a like signal feature space, of images recorded in different time periods, with the aim of enhancing and analyzing the common features. An application in marine phenomena recognition (discrimination between water brightness image and haze image) is discussed together with the results. Author (ESA)

N82-14584* Norwegian Defence Research Establishment, Kjeller.
SEASAT SAR PROCESSING AT THE NORWEGIAN DEFENCE RESEARCH ESTABLISHMENT
E. A. Herland In ESA Appl. of Remote Sensing Data on the Continental Shelf Jul. 1981 p 247-253 refs

Avail: NTIS HC A13/MF A01; ESA, Paris FF 125

A digital processor which processes synthetic aperture radar (SAR) images from raw data gathered by a satellite platform is described. The basic principles of SAR are explained; the algorithms for the digital processor are given in terms of a block diagram, the different parts of which are considered separately. A routine for achieving automatic focusing in azimuth compression without satellite orbit information is discussed. Examples of imagery obtained by applying the algorithms to raw data from the Seasat-1 SAR system are shown. These indicate that it is possible to detect ships and that the system can be used for maritime surveillance purposes. Author (ESA)

N82-15484* Energy Information Administration, Washington, D.C. Geomagnetic Service.
THE REDUCTION, VERIFICATION AND INTERPRETATION OF MAGSAT MAGNETIC DATA OVER CANADA Progress Report
R. L. Coles, Principal Investigator, E. Dawson, G. V. Haines, G. Jansen vanBeek, J. K. Walker, and L. R. Newitt Jul. 1981 3 p Sponsored by NASA ERTS
(E82-10006; NASA-CR-164904; PR-3) Avail: NTIS HC A02/MF A01 CSCL 05B

Magnetic anomalies of lithospheric origin are weak at Magsat altitudes (20 to 30 nT at most), and are easily masked by much larger effects caused by field-aligned and other currents at high latitudes. Most of Canada lies under the influence of ionospheric currents in the auroral zone and polar cap. A more refined selection of quiet Magsat data allowed a revised scalar magnetic anomaly map of the whole region north of about 40 deg N latitude. Very preliminary vector anomaly maps and absolute vector component maps were derived. The scalar magnitudes show great promise for mapping the total force and anomaly fields. The Z vector data also appear to be good. The horizontal X and Y vector data are seriously contaminated with external fields and maybe other effects. A.R.H.

N82-15502# Marconi Co. Ltd., Chelmsford (England). Communications Research Div.

SQUINTEd SAR SYSTEM Final Report

In its Additional Studies of Earth Resources Syn. Aperture Radar Payload Oct. 1980 32 p refs

Avail: NTIS HC A06/MF A01

It is found that for conventional SAR systems pointing broadside to the satellite track it is impossible to obtain the required swath width at several incidence angles with the same antenna design. It is suggested that the swath width might be increased by 'squinting' the beam forwards or backwards. A feasibility study of such a system is discussed. J.M.S.

N82-15503# Deutsche Forschungs- und Versuchsanstalt fuer Luft- und Raumfahrt, Oberpfaffenhofen (West Germany). Inst. fuer Hochfrequenztechnik.

VISUAL EVALUATION OF E-SLAR IMAGERY

Juergen Nithack Feb. 1981 52 p refs In GERMAN; ENGLISH summary Report will also be announced as translation (ESA-TT-734)

(DFVLR-FB-81-11) Avail: NTIS HC A04/MF A01; DFVLR, Cologne DM 13,10

Flights were conducted E-SLAR (side looking airborne radar) for remote sensing experiments with active microwave techniques (X-band). The analog recorded data were mainly evaluated by visual methods to judge the system and its usefulness to solve Earth scientific questions. J.M.S.

N82-15504# Naval Postgraduate School, Monterey, Calif. Dept. of Oceanography.

BIOLOGICAL PATCHINESS IN RELATION TO SATELLITE THERMAL IMAGERY AND ASSOCIATED CHEMICAL MESOSCALE FEATURES M.S. Thesis

Ronald Wayne Phoebus Jun. 1981 63 p refs

(AD-A105757) Avail: NTIS HC A04/MF A01 CSCL 08/1

The presence of biological patches, or communities, can have a direct effect on Naval operations, scientific research, and fisheries. It is shown that remote infrared satellite sensing may be used as a real-time tool to accurately locate thermally and biologically significant features. Several physical, chemical, and biological variables were sampled in the surface layer of mesoscale thermal features which were located using satellite imagery. The bio-chemical sampling produced replicate results from which the distribution of biomass could be inferred. Possible explanations are advanced for patch forming mechanisms and biomass distribution. Author (GRA)

N82-15698# National Oceanic and Atmospheric Administration, Washington, D. C.

ENVIRONMENTAL SATELLITE IMAGERY, MARCH 1981

May 1981 69 p refs

(PB81-248049; KMRD-5.4-8103) Avail: NTIS HC A04/MF A01 CSCL 04B

Current cloud data obtained by operational environmental satellites was documented. Daily global satellite imagery is recorded in condensed form as a guide to data stored in the NOAA archives and is designed to help users select data for research and climatological use. The polar hemispheric mosaics reproduced in this catalog are derived from the advanced very high resolution radiometer (AVHRR (GSC)) data, and prepared daily by high speed computers. Visible and infrared swaths obtained while the satellite is northbound are used in the 15L mosaics from TIROS-N and the infrared channel only in the 17L mosaics from NOAA-6, NOAA-7 will include both the infrared and visible mosaics from the 14L pass. Infrared data swaths obtained during southbound passage of TIROS-N are labeled 03L, NOAA-6 are labeled 07L and NOAA-7 will be labeled 02L. GRA

Page intentionally left blank

Page intentionally left blank

INSTRUMENTATION AND SENSORS

Includes data acquisition and camera systems and remote sensors.

A82-10045 **Data compression and reconstruction for mixed resolution multispectral sensors.** R. A. Schowengerdt (Arizona, University, Tucson, AZ). In: American Society of Photogrammetry, Annual Meeting, 46th, St. Louis, MO, March 9-14, 1980, ASP Technical Papers. Falls Church, VA, American Society of Photogrammetry, 1980, p. 318-328. 13 refs. Research supported by the U.S. Geological Survey.

A data compression technique that utilizes a mixture of spatial resolutions for a multispectral scanner is described. The complementary reconstruction procedure that extrapolates edge information from the high resolution band(s) to the low resolution bands is also discussed. Examples of Landsat MSS imagery that have been compressed and reconstructed to the original resolution are presented. Error rates are calculated for two types of scenes, one containing prominent topographic effects, the other of an agricultural area. Improvement in radiometric quality of up to 40% is achieved by application of the reconstruction procedure to the compressed data.

A82-10051 * **Absolute image registration for geosynchronous satellites.** R. Nankervis, D. Koch (NASA, Goddard Space Flight Center, Greenbelt, MD), H. Sielski (Computer Sciences Corp., Silver Spring, MD), and D. Hall (HRB Singer, Inc., State College, PA). In: American Society of Photogrammetry, Annual Meeting, 46th, St. Louis, MO, March 9-14, 1980, ASP Technical Papers.

Falls Church, VA, American Society of Photogrammetry, 1980, p. 438-446. 6 refs.

A procedure for the absolute registration of earth images acquired by cameras on geosynchronous satellites is described. A conventional least squares process is used to estimate navigational parameters and camera pointing biases from observed minus computed landmark line and element numbers. These estimated parameters along with orbit and attitude dynamic models are used to register images, employing an automated grey-level correlation technique, inside the span represented by the landmark data. Experimental results obtained from processing the SMS-2 observation data base covering May 2, 1979 through May 20, 1979 show registration accuracies with a standard deviation of less than two pixels if the registration is within the landmark data span. It is also found that accurate registration can be expected for images obtained up to 48 hours outside of the landmark data span. B.J.

A82-10858 **Orientation and construction of models. I - The orientation problem in close-range photogrammetry.** A. Okamoto (Kyoto University, Kyoto, Japan). *Photogrammetric Engineering and Remote Sensing*, vol. 47, Oct. 1981, p. 1437-1454. 14 refs.

The orientation problem of a stereoscopic pair of photographs taken with nonmetric cameras is considered, first algebraically and then geometrically. Also, some orientation techniques are presented. The orientation theory given here is quite fundamental and is applicable to various photogrammetric problems such as the calibration problem of nonmetric cameras and the orientation problem of stereo-strip imagery. In particular, one promising calibration method can be developed to provide interior orientation parameters for each of a stereoscopic pair of photographs, respectively, by using only distances in the object space as control. (Author)

A82-11406 **A mathematical model of an over-sea airborne UHF radio link.** T. Slator. *Marconi Review*, vol. 44, 2nd Quarter, 1981, p. 101-118. 9 refs.

A mathematical model is described which enables the performance of an over-the-sea airborne UHF radio link to be estimated as a function of terminal height and separation distance taking account statistically of variations of signal level caused by such factors as irregular antenna radiation patterns and a rough sea surface. (Author)

A82-11533 * **Radiative transfer theory for passive microwave remote sensing of random media.** S. L. Chuang and J. A. Kong

(MIT, Cambridge, MA). In: Research topics in electromagnetic wave theory. New York, Wiley-Interscience, 1981, p. 136-160. 14 refs. NSF Grant No. ENG-78-23145; Grant No. NAG5-16; Contract No. F19628-80-C-0052.

The radiative transfer theory is applied to a random medium for the case of passive remote sensing. A general numerical solution with Gaussian quadrature method is studied. For a medium with laminar structure or a medium with cylindrical structure, closed form solutions are obtained by solving the radiative transfer equations of a two-layer random medium. Numerical results for the general case and the two limiting cases are compared. V.L.

A82-12127 * # **Repeatability and measurement uncertainty of the United States meteorological rocketsonde.** F. J. Schmidlin (NASA, Wallops Flight Center, Wallops Island, VA). (*International Symposium on Middle Atmosphere Dynamics and Transport, University of Illinois, Urbana, IL, July 28-Aug. 1, 1980.*) *Journal of Geophysical Research*, vol. 86, Oct. 20, 1981, p. 9599-9603. 11 refs.

It is pointed out that rocketsondes provide the only in situ 'ground truth' data for altitudes above 30 km. The need for precise temperature information has, therefore, led to a study of rocketsonde instrument repeatability and measurement uncertainty. Results obtained from root-mean-square difference and linear regression techniques are consistent and strongly suggest that the Datasonde precision is better than 1 C up to an altitude of 53 or 54 km. This result excludes atmospheric variability, which may occur within 5 min, and effects owing to spatial differences, which are small for paired measurements. At altitudes of 55 km and higher it is possible that sensor and flight-related anomalies, differences in radiation corrections owing to differing solar angles because of varying launch times, or even seasonal variations may create conditions that affect the magnitude of the standard corrections. G.R.

A82-12600 * **Airborne laser acquisition of cross-section data.** J. G. Collins (U.S. Army, Engineer Waterways Experiment Station, Vicksburg, MS) and W. B. Krabill (NASA, Wallops Flight Center, Wallops Island, VA). In: Civil engineering applications of remote sensing; Proceedings of the Specialty Conference, Madison, WI, August 13, 14, 1980. New York, American Society of Civil Engineers, 1980, p. 175-181.

The feasibility of obtaining cross-section data from airborne remote sensing systems is investigated. Eleven test profiles in the Wolf River Basin, near Memphis, Tennessee, are selected. Each profile is characterized using conventional ground survey methods; under 'leaves-off' conditions, photogrammetric, airborne laser, and airborne radar data are obtained. Results indicate that valley profiles can be accurately characterized with an airborne laser system. C.R.

A82-13293 * **Intercalibration of Landsat 1-3 and NOAA 6 and 7 scanner data.** M. J. Duggin (New York, State University, Syracuse, NY). *Applied Optics*, vol. 20, Nov. 15, 1981, p. 3815, 3816. 14 refs. Contract No. JPL-916331.

A82-13547 **The influence of gravity waves on radiometric measurements - A case study.** M. T. Decker (NOAA, Wave Propagation Laboratory, Boulder, CO), F. Einaudi (Georgia Institute of Technology, Atlanta, GA), and J. J. Finnigan (Cooperative Institute for Research in Environmental Sciences, Boulder, CO; Commonwealth Scientific and Industrial Research Organization, Div. of Environmental Mechanics, Canberra, Australia). *Journal of Applied Meteorology*, vol. 20, Oct. 1981, p. 1231-1238. 26 refs.

During the 1978 PHOENIX experiment at the Boulder Atmospheric Observatory in Colorado, the presence of atmospheric gravity waves was detected by various independent remote sensing instruments. Fluctuations in the zenith atmospheric radiation were measured at 22.235 and 55.45 GHz in the water vapor and oxygen absorption bands and compared with corresponding fluctuations of surface pressure and the height of FM-CW radar echo returns. These fluctuations are explained, qualitatively and quantitatively, in terms of an internal gravity wave generated by wind shear above the boundary layer. The analysis shows that the oscillations at 22.235 GHz are essentially due to fluctuations of water vapor in the antenna beam while those at 55.45 GHz are due to temperature variations. (Author)

A82-13738 **Block adjustment with additional parameters.** F. Ackermann (Stuttgart, Universität, Stuttgart, West Germany).

08 INSTRUMENTATION AND SENSORS

Photogrammetria, vol. 36, Oct. 1981, p. 217-227. 25 refs.

The current status of the technique of systematic image error correction by block adjustment with additional parameters is reviewed. The technique, which has proven to be highly effective and widely applicable, is defined as based on the principle of aerial triangulation, with the parameters being additional unknowns, the magnitudes of which are estimated from observational data for a prefixed type of image deformation. Current research and development has centered on problems of the selection, reliability, determinability and statistical assessment of the additional parameters. Available results have shown that carefully applied additional parameters almost always give improved accuracy, depending on overlap, redundancy and control. The basic limitation of the method lies in the fact that additional parameters belong to the functional part of the mathematical adjustment model, and so are based on the erroneous assumption that image deformations are constant for a large group of photographs. S.C.S.

A82-14299 Characteristics of westward travelling surges during magnetospheric substorms. W. G. Tighe and G. Rostoker (Alberta, University, Edmonton, Canada). *Journal of Geophysics Zeitschrift für Geophysik*, vol. 50, no. 1, 1981, p. 51-67. 19 refs. Research supported by the Natural Sciences and Engineering Research Council of Canada.

Data from arrays of magnetometers along lines of constant magnetic latitude and longitude, supplemented with all-sky camera and riometer data, are used to study the temporal development and typical scale size of westward traveling surges which occur during magnetospheric substorms. It is found that the motion of the head of the surge can be quite irregular, and in extreme cases, the surge form may grow and decay in a confined longitudinal sector without any significant westward displacement. The positive D-component perturbation, the characteristic signature of a surge, is generally confined within a longitude range of 6-10 deg at about 70 deg N, and is believed to be generated by a filamentary southward ionospheric current flowing at the edge of the surge. A comprehensive model of the three-dimensional current system is presented by a detailed comparison of model and observed latitude and longitude profiles of the magnetic disturbance. It is found that the best agreement is obtained when the entire electrojet system flows from southeast to northwest relative to the lines of constant magnetic latitude. J.F.

A82-15039 * Availability of Seasat synthetic aperture radar imagery. B. Holt (California Institute of Technology, Jet Propulsion Laboratory, Pasadena, CA). *Remote Sensing of Environment*, vol. 11, Nov. 1981, p. 413-417. NASA-supported research.

One of the sensors of the Seasat satellite was a synthetic aperture radar (SAR), which was operated over both oceanic and land areas. The Seasat SAR was an active imaging microwave system which transmitted and received horizontally polarized radiation at L-band frequency (1.275 GHz, 23-cm wavelength). Extensive coverage was obtained over North America, Europe, the Eastern Pacific Ocean, the Western and Northern Atlantic Ocean, and the Beaufort Sea. Surface coverage was also acquired over limited portions of Central America, the Gulf of Mexico, and the Caribbean Sea. The majority of the data has been optically processed in a so-called survey mode. Each optically processed Seasat pass has a swath width of 100 km at a scale of 1:500,000. A subset of the SAR data has been digitally processed in a so-called high-resolution mode. Digital processing has been performed upon selected scenes with dimensions of 100 x 100 km. Digitally processed imagery has a nominal ground resolution of 25 m. G.R.

A82-15655 † Current aerial cameras (Sovremennye aerofotoapparaty). V. G. Afremov and V. B. Il'in. *Geodeziya i Kartografiya*, Oct. 1981, p. 40-42. 6 refs. In Russian.

The paper considers the development and operation of the TE and TES aerial cameras, having focal distances of 350, 100, 70, and 50 mm and FOV angles of 40, 103, 120, and 136.5 deg, respectively, for 18 x 18 cm frames. The basic technical characteristics and some applications of these cameras are presented. B.J.

A82-15920 Three bearing method for passive triangulation in systems with unknown deterministic biases. M. Mangel and C. R. Carter (California, University, Davis, CA). *IEEE Transactions on Aerospace and Electronic Systems*, vol. AES-17, Nov. 1981, p. 814-819. 5 refs. Contract No. N00014-81-K-0030.

The paper presents an operationally simple method for triangulation in systems with strong biases, which requires three bearing measurements and two turns of the aircraft. The triangulation problem is considered in the search for a stationary target, in which deterministic and random terms enter into the observed bearing. Numerical and flight testing are reported, and it is shown how the method can be modified to include random fluctuation and confidence contours about the point of triangulation. D.L.G.

A82-15951 † Satellites of the Meteor series, intended for earth studies from space (Sputniki serii 'Meteor', prednaznachennye dlia izuchenii zemli iz kosmosa). Iu. V. Trifonov. *Issledovanie Zemli iz Kosmosa*, Sept.-Oct. 1981, p. 8-20. 8 refs. In Russian.

The objectives and main results of the Soviet experimental program for the operational study of the earth from space by means of Meteor satellites are presented. Examples of the effective use of multispectral wide-angle television data of low and medium resolution in the fields of geology, hydrology, weather modification, hydrometeorology, forestry, and navigation are given. The specific features of the Meteor program for remote sensing are described. The ballistic design of the experimental remote sensing system is characterized, indicating a sun-synchronous orbit for the system. The advantage of using a low-thrust electrojet engine in the Meteor program is discussed. J.F.

A82-15952 † Technical equipment of an experiment for remote sensing of the earth from space (Kompleks tekhnicheskikh sredstv eksperimenta po distantsionnomu zondirovaniu zemli iz kosmosa). Iu. V. Trifonov. *Issledovanie Zemli iz Kosmosa*, Sept.-Oct. 1981, p. 21-27. In Russian.

The equipment used in an experiment (1980-1981) to obtain multispectral television data of medium and high resolution using a second-generation Meteor satellite is described. The prospects of developing a continuously active space system for earth resources studies are characterized. The design features and structural characteristics of the spacecraft used in the experiment are noted. These features include the improved accuracy of three-axis attitude control and stabilization of the angular velocity; structural and weight improvements, and the increased possibilities for automatic control in transmitting and receiving data. J.F.

A82-15955 † Experimental telemetry system based on the Fragment multispectral scanning system (Eksperimental'nyi informatsionno-izmeritel'nyi kompleks na osnove mnogoazonal'noi skaniruiushchei sistemy 'Fragment'). G. A. Avanesov (Akademiia Nauk SSSR, Institut Kosmicheskikh Issledovani, Moscow, USSR). *Issledovanie Zemli iz Kosmosa*, Sept.-Oct. 1981, p. 40-44. 8 refs. In Russian.

The structure and functions of the main system of the experimental telemetry complex, based on the Fragment multispectral scanning system are considered. A preliminary analysis of the results of an experiment involving the operational acquisition and machine processing of multispectral data is given. The system is shown to be useful for the development of operational methods of earth-resources study. J.F.

A82-15958 † Metrological support of measurements of earth-surface brightness by the Fragment multispectral scanning system (Metrologicheskoe obespechenie izmerenii iarkosti zemnoi poverkhnosti mnogoazonal'noi skaniruiushchei sistemoi 'Fragment'). G. A. Avanesov, Ia. L. Ziman, A. G. Sychev, and V. I. Tarnopol'skii (Akademiia Nauk SSSR, Institut Kosmicheskikh Issledovani, Moscow, USSR). *Issledovanie Zemli iz Kosmosa*, Sept.-Oct. 1981, p. 65-77. 12 refs. In Russian.

A82-16164 The application of programmable pocket calculators for computations during survey flights. H. C. Zorn (International Institute for Aerial Survey and Earth Sciences, Enschede, Netherlands). *ITC Journal*, no. 3, 1981, p. 308-333.

Computation during survey flights can be effectively achieved using a programmable pocket calculator such as the Hewlett-Packard C41 model. Using this calculator, formulas and programs have been developed for computing survey turns; wind star; heading and ground speed, given wind vector and required course; pressure altitude required to reach required true altitude; and true airspeed given indicated airspeed, air temperature, and pressure altitude. Other potential applications include the conversion of latitude and longi-

tude to UTM zone and coordinates, and great circle and loxodrome computations. S.C.S.

A82-16447 * **Magnetic field observations on DE-A and -B.** W. H. Farthing, M. Sugiura, B. G. Ledley (NASA, Goddard Space Flight Center, Greenbelt, MD), and L. J. Cahill, Jr. (Minnesota, University, Minneapolis, MN). *Space Science Instrumentation*, vol. 5, Dec. 1981, p. 551-560. 14 refs.

Magnetic field observations are conducted on each of the DE-A and -B satellites by a triaxial fluxgate magnetometer. In the basic mode the instrumental resolution is + or - 1.5 nT; in addition, the DE-A magnetometer has two modes of higher resolution: + or - 0.25 nT and + or - 20 pT. The sampling rate is 16 vector samples per second in all modes. The experiment objectives include observations of field-aligned currents, magnetospheric equatorial currents, and ULF waves. These observations, taking full advantage of the specifically selected orbits of the two spacecraft and of the unique combination of instruments, are performed to achieve a better understanding of the electrodynamic coupling within the atmosphere-ionosphere-magnetosphere system and of wave-particle interactions which contribute to the coupling processes. (Author)

A82-16602 † **Main results of the Raduga experiment (Osnovnnye itogi eksperimenta 'Raduga').** Ia. L. Ziman, Iu. M. Chesnokov, and V. V. Aksenov. In: *Airborne and spaceborne multispectral photography of the earth.* Moscow, Izdatel'stvo Nauka, 1981, p. 5-13. In Russian.

The Raduga experiment, involving the multispectral photography of earth resources from Soyuz-22, is described. Attention is given to the preflight testing and calibration of the multispectral cameras, the operational characteristics of the equipment, results of photointerpretation, and the success with which the goals of the experiment were carried out. It has been concluded that the MKF-6 and MSP-4 multispectral instrumentation is suitable for practical implementation in the remote sensing of earth resources. B.J.

A82-16613 † **Methodology and practice of spectroscopic measurements of landscape elements in the preparation and carrying out of down-looking experiments (Metodika i praktika spektrometri-cheskikh izmerenii elementov landshafta pri obespechenii i provedenii podsputnikovyykh eksperimentov).** G. B. Gonin, A. A. Bartashevich, N. V. Kravchuk, N. N. Mozgov, and Iu. V. Ponomarenko. In: *Airborne and spaceborne multispectral photography of the earth.* Moscow, Izdatel'stvo Nauka, 1981, p. 118-128. 7 refs. In Russian.

Various aspects concerning the preparation and carrying out of down-looking experiments associated with multispectral scanning of landscape elements are considered. Particular consideration is given to the mathematical modeling of the earth-atmosphere system (with allowance for the scattering and turbulence properties of the atmosphere), and to calibration specifications in aerial spectroscopy experiments. B.J.

A82-17165 * **Global satellite measurements of water vapour, wind speed and wave height.** D. B. Chelton, K. J. Hussey, and M. E. Parke (California Institute of Technology, Jet Propulsion Laboratory, Pasadena, CA). *Nature*, vol. 294, Dec. 10, 1981, p. 529-532. 6 refs. NASA-supported research.

The results of global measurements of atmospheric water vapor by the Seasat Scanning Multichannel Microwave Radiometer and wave height and wind speed by the Seasat altimeter (ALT) are reported. The 13.5 GHz ALT has a 3.125 ns pulsewidth and 1022 Hz repetition rate, and measures surface height to a resolution exceeding 10 cm relative to a reference ellipsoid. Full ALT data comprise 135 km equatorial groundtracks, with about a 50 cm difference of sea wave height compared to buoy reference measurements, and wind-speed accuracy to within 0.25-1.58 m/sec up to 20 m/sec. Highest water vapor concentrations were observed in the tropics and the lowest at high latitudes. Wind speeds were highest for the north-east and south-east tradewinds in both the Atlantic and Pacific oceans. Average wave height is small in the summer North Hemisphere and the largest waves are in the winter Southern ocean, and lowest in western Atlantic and Pacific ocean areas where winds are lightest. D.H.K.

A82-17918 # **User needs and the future of operational meteorological satellites.** D. B. Miller and J. R. Silverman (NOAA,

Advanced Systems Concepts Group, Washington, DC). *American Institute of Aeronautics and Astronautics, Aerospace Sciences Meeting, 20th, Orlando, FL, Jan. 11-14, 1982, Paper 82-0388.* 9 p.

Applications of the TIROS-N and GOES satellites are reviewed, and requirements for the next generation of meteorological satellites are discussed. TIROS N spacecraft were a joint effort of the U.S., U.K., and France, and carried instrumentation which provided information on oceanographic and hydrologic processes, agricultural products, meteorology, and digital imaging. The GOES satellites give continuous viewing of weather features and collect and relay meteorological data from remote platforms such as buoys, ships, stations, aircraft, and balloons. The next generation of GOES spacecraft are also intended for GEO, and instruments will provide imaging in the IR and visual with 1-2 and 0.5 km resolution, respectively, multispectral imaging, vertical temperature resolution in the troposphere to 1-5 km, and have solar X ray sensing capabilities, as well as for the atmospheric electron density. Further instrumentation additions and choice of orbits are examined, noting that a careful consideration of the capital return on investment will be required before any decision to fly new meteorological spacecraft. M.S.K.

N82-10071*# Scientific Analysts and Consultants, Inc., Rockville, Md.

DISTORTION-FREE MAPPING OF VISSR IMAGERY DATA FROM GEOSYNCHRONOUS SATELLITES

F. K. Chan /In NASA, Goddard Space Flight Center Sixth Ann. Flight Mech./Estimation Theory Symp. Oct. 1981 35 p ref

(Contracts NOAA-01-8-MO1-1864; NOAA-NA79-KA-C-00026) Avail: NTIS HC A13/MF A01 CSCL 22A

The formulation is rigorous and includes all misalignment angles of the VISSR, the sun sensor and the instantaneous spin axis with the satellite's body axis. It also includes the effects due to the motion of the satellite's suborbital point. All the mapping equations for distortion removal were reduced to simplest forms, and all the algorithms were optimized as much as possible. An approach was then formulated for implementing these algorithms for in-line operational use. It is concluded that in-line distortion removal is possible in real-time processing of infra-red but not visible VISSR imagery data. T.M.

N82-10073*# General Electric Co., Lanham, Md. Space Div. **THE MSS CONTROL POINT LOCATION ERROR FILTER FOR LANDSAT-D**

I. Levine /In NASA, Goddard Space Flight Center Sixth Ann. Flight Mech./Estimation Theory Symp. Oct. 1981 18 p refs

(Contract NAS5-25300)

Avail: NTIS HC A13/MF A01 CSCL 05B

The filter produces the maximum likelihood estimates for average values of the spacecraft position and attitude errors during a single scene. The quality of the filter performance is characterized by the maximal cross and along track residual errors for which probability distributions can be calculated analytically for a given pattern of control points. The filter with an automatic selection of the best set of estimates provides geodetic correction at 90% of pixels with residual errors less than 40 m for four or more control points and the mean squared measurement errors of the order of 20-25 m. The same accuracy can be preserved for eight or more control points and measurement errors of 30-35 m. T.M.

N82-10468*# National Aeronautics and Space Administration, Goddard Space Flight Center, Greenbelt, Md.

MAGSAT: VECTOR MAGNETOMETER ABSOLUTE SENSOR ALIGNMENT DETERMINATION

M. H. Acuna Sep. 1981 39 p refs

(NASA-TM-79648) Avail: NTIS HC A03/MF A01 CSCL 14B

A procedure is described for accurately determining the absolute alignment of the magnetic axes of a triaxial magnetometer sensor with respect to an external, fixed, reference coordinate system. The method does not require that the magnetic field vector orientation, as generated by a triaxial calibration field system, be known to better than a few degrees from its true position, and minimizes the number of positions through which a sensor assembly must be rotated to obtain a solution. Computer simulations show that accuracies of better than 0.4 seconds of arc can be achieved under typical test conditions associated with existing magnetic test facilities. The basic approach is similar

08 INSTRUMENTATION AND SENSORS

in nature to that presented by McPherron and Snare (1978) except that only three sensor positions are required and the system of equations to be solved is considerably simplified. Applications of the method to the case of the MAGSAT Vector Magnetometer are presented and the problems encountered discussed. A.R.H.

N82-10481# Research Inst. of National Defence, Linköping (Sweden). Huvudavdelning 3.

USE OF RADAR AND MICROWAVE RADIOMETRY FOR RECONNAISSANCE SATELLITES [ANVAENDNING AV RADAR OCH MIKROVAAGSRADIOMETRIE VID SPANINGSSATELLITER]

Hans Lok Oct. 1980 28 p refs In SWEDISH (FOA-C-30204-E1) Avail: NTIS HC A03/MF A01

The advantages and disadvantages of side-looking radar and microwave radiometers for observations of Earth by satellite are discussed. Each system is examined with regards to field of view and instrument sensitivity. Microwave attenuation is also discussed. A.R.H.

N82-10484# Kiruna Geophysical Inst. (Sweden).

A SWEDISH PROPOSAL FOR AN EISCAT/GEOS-2 EXPERIMENT

Svante Westerlund, Georg Gustafsson, Aake Steen, John Murdin, Gudmund Wannberg, Rolf Bostrom (Uppsala Ionospheric Obs., Sweden), Aake Hedberg (Uppsala Ionospheric Obs., Sweden), Hermann Oppenorth (Uppsala Ionospheric Obs., Sweden), Erling Nielsen (Max-Planck Inst. fuer Aeronomie, Katlenburg-Lindau, West Germany), Carl-Gunne Faeltthamar (Royal Inst. of Technol., Stockholm) et al Mar. 1981 28 p refs (KGI-175; ISSN-0347-6405) Avail: NTIS HC A03/MF A01

An experiment that uses GEOS to measure in the equatorial plane at the same time as EISCAT and other ground based instrumentation are monitoring the ionosphere is described. The generation, acceleration and loss of auroral particles are studied. Signatures of particle precipitation in the ionosphere and properties of the plasma and electric field in the equatorial plane are correlated. The position of the conjugate point of GEOS is determined during various conditions. Such data in conjunction with magnetic field models, make it feasible to identify and estimate the various effects that contribute to the field during disturbances. i.e. to improve geomagnetic field models. Author (ESA)

N82-10488# University Coll., Dublin (Ireland). Dept. of Physics.

STUDY ON CALIBRATION METHODS FOR EARTH OBSERVATION OPTICAL IMAGING INSTRUMENTS Final Report

E. O. Mongain Paris ESA Nov. 1980 230 p refs

(Contract ESA-4237/80/NL-PP(SC)) (UCD-207/1/80; ESA-CR(P)-1443) Avail: NTIS HC A11/MF A01

The properties and calibration of lamps diffusors, and detectors are considered. Measurements of solar irradiance from ground level are illustrated and the NASA solar spectral irradiance experiments are discussed with respect to the possibility of image striping as an inherent property of imaging arrays. Author (ESA)

N82-11512*# Research and Data Systems, Inc., Lanham, Md. SMMR DATA SET DEVELOPMENT FOR GARP

John Kogut May 1981 60 p

(Contract NAS5-25781) (NASA-CR-166721) Avail: NTIS HC A04/MF A01 CSCL 05B

The NIMBUS 7 Scanning Multichannel Microwave Radiometer (SMMR) data are analyzed. The impact of cross polarization and Faraday rotation on SMMR derived brightness temperatures is evaluated. The algorithms used to retrieve the geophysical parameters are tested, refined, and compared with values derived by other techniques. The technical approach taken is described and the results presented. S.L.

N82-12447*# EG & G Washington Analytical Services Center, Inc., Riverdale, Md.

IONOSPHERIC PROPAGATION CORRECTION MODELING FOR SATELLITE ALTIMETERS

George Nesterzuk Nov. 1981 14 p refs

(Contract NAS6-3075) (NASA-CR-156881) Avail: NTIS HC A02/MF A01 CSCL 20D

The theoretical basis and available accuracy verifications were reviewed and compared for ionospheric correction procedures

based on a global ionospheric model driven by solar flux, and a technique in which measured electron content (using Faraday rotation measurements) for one path is mapped into corrections for a hemisphere. For these two techniques, RMS errors for correcting satellite altimeters data (at 14 GHz) are estimated to be 12 cm and 3 cm, respectively. On the basis of global accuracy and reliability after implementation, the solar flux model is recommended. Author

N82-13465* National Aeronautics and Space Administration, Goddard Space Flight Center, Greenbelt, Md.

SCANNER Patent

Robert F. Hummer (Santa Barbara Research Center) and Deane T. Upton, inventors (to NASA) (Santa Barbara Research Center) Issued 10 Nov. 1981 12 p Filed 19 May 1975 Supersedes N76-19408 (14 - 10, p 1252) Continuation of abandoned US Patent Appl. SN-583219, filed 30 Sep. 1966 Sponsored by NASA

(NASA-Case-GSC-12032-2; US-Patent-4,300,159;

US-Patent-Appl-SN-578700; US-Patent-Appl-SN-583219;

US-Patent-Class-358-109; US-Patent-Class-250-235;

US-Patent-Class-250-236) Avail: US Patent and Trademark Office CSCL 20F

An aerial vehicle rotating in gyroscopic fashion about one of its axes has an optical system which scans an area below the vehicle in determined relation to vehicle rotation. A sensing device is provided to sense the physical condition of the area of scan and optical means are associated to direct the physical intelligence received from the scan area to the sensing means. Means are provided to incrementally move the optical means through a series of steps to effect sequential line scan of the area being viewed keyed to the rotational rate of the vehicle.

Official Gazette of the U.S. Patent and Trademark Office

N82-13469*# National Aeronautics and Space Administration, Goddard Space Flight Center, Greenbelt, Md.

INTERPOLATING FOR THE LOCATION OF REMOTE SENSOR DATA

Edward F. Puccinelli and Jack Kornfield (NSF) Jul. 1981 23 p refs

(NASA-TM-82169) Avail: NTIS HC A02/MF A01 CSCL 05B

An interpolation algorithm is presented as a practical alternative to common interpolation and approximation methods when applied to the problem of determining the location of remote sensor data. This algorithm is based upon knowledge of the geometry of the problem and is shown to be inherently more accurate than common interpolation schemes which may be applied to all types of data. A practical location problem is used to demonstrate its accuracy and computational cost. Author

N82-14171# Officine Galileo S.p.A., Florence (Italy).

INFRARED RADIANCE MODEL VARIATION BY SENSOR FLIGHT MEASUREMENTS

R. Baldassini Fontana, D. Sciacovelli (ESTEC, Noordwijk, Netherlands), and L. Fraiture (ESOC, Darmstadt, West Germany) In ESA Spacecraft Flight Dyn. Aug. 1981 p 461-478 refs

Avail: NTIS HC A22/MF A01; ESA, Paris FF 160 Member States, AU, CN and NO (+20% others)

The NASA and BAC-ESR 4 IR radiance models of Earth, applied to attitude sensor calibration, are compared. The sensors are IR pencil beams on spinning satellites. Flight measurements of Geos 2 and OTS transfer orbits were compared to simulations from a model which describes the optics, detector and electronics of the beam, based on directly measured parameters and laboratory test data. The models performed equally well. It is shown that anomalies in preflight calibration can be detected. A small mismatch of the optical axis inclination of a Geos 2 IR telescope was observed. Author (ESA)

N82-14560# Centre National d'Etudes Spatiales, Toulouse (France).

STATE-OF-THE-ART IN USING A SPACEBORNE ALTIMETER AND SCATTEROMETER FOR THE DETERMINATION OF WIND, SEA STATE, AND MARINE AND ICE DYNAMICS

M. Lefebvre and J.-L. Hyacinthe (Centre National pour l'Exploitation des Oceans, Paris) In ESA Appl. of Remote Sensing Data on the Continental Shelf Jul. 1981 p 57-58

Avail: NTIS HC A13/MF A01; ESA, Paris FF 125

The accuracy of Seasat altimeter and scatterometer data is discussed. Sea state obtained through altimeter pulse shape and wind data obtained by altimeter pulse amplitude or, with direction by the scatterometer backscatter, are compared with model and map values. The altimeter performs well, but not the scatterometer. Altimeter data can be used to investigate marine and ice dynamics on a large scale, e.g., a sea. For seasonal and interannual fluctuation of oceanic circulation, a few cm accuracy on the relative satellite trajectory without geoid accuracy is needed. For the mean ocean circulation and the absolute determination of current, a 10 cm accurate geoid is needed. Author (ESA)

N82-14563# Canada Centre for Remote Sensing, Ottawa (Ontario).

A RECOMMENDED SENSOR PACKAGE FOR THE DETECTION AND TRACKING OF OIL SPILLS

H. H. Zwick, R. A. Neville, and R. A. O'Neil /n ESA Appl. of Remote Sensing Data on the Continental Shelf Jul. 1981 p 77-88 refs

Avail: NTIS HC A13/MF A01; ESA, Paris FF 125

Oil on open water under clear skies is a relatively easy target, oil under ice is very difficult. Results of remote sensing experiments acquiring data for system specification are discussed. Instruments assessed include active microwave sensors for the measurement of backscatter from oil slicks, scanners for oil thickness determination from the spectral character of reflected radiation and solar heating effects, and laser fluorosensors for oil-specific detection in oil and water and/or ice mixtures and for Raman scattering from the surface. The most effective system for the wide variety of conditions experienced in Canada consists of a laser fluorosensor, an ultraviolet/infrared line scanner, a side-looking airborne radar, low light level television and photographic cameras. These sensors are supported by real time data annotation, display, and analysis systems. Author (ESA)

N82-14577# Belfotop P.v.b.a., Wemmel (Belgium).

AIRBORNE REMOTE SENSING OF THE COASTAL ZONE
J. L. vanGenderen and G. DeMan /n ESA Appl. of Remote Sensing Data on the Continental Shelf Jul. 1981 p 197-202

Avail: NTIS HC A13/MF A01; ESA, Paris FF 125

Using the European remote sensing aircraft platform, equipped with a digital multispectral scanner, two metric cameras, a realtime imaging system, and a digital navigation system, coastal zones were studied. The airborne platform and its operation are described. Practical problems associated with coastal airborne remote sensing are discussed (position fixing over water; day-night imaging; film processing; digital multispectral data processing) and examples from oil pollution monitoring, thermal discharge studies, coastal erosion, and surface wave direction analysis are given.

Author (ESA)

N82-14599# Carson Helicopters, Inc., Perkasi, Pa. Geoscience Div.

NURE AERIAL GAMMA-RAY AND MAGNETIC RECONNAISSANCE SURVEY OF MAINE AND PORTIONS OF NEW YORK. VOLUME 1: DATA ACQUISITION, REDUCTION AND INTERPRETATION Final Report

Aug. 1981 273 p refs
(Contract DE-AC13-76GJ-01664)

(DE82-000650; GJBX-327-81-Vol-1)

Avail: NTIS

HC A12/MF A01

A rotary wing high sensitivity radiometric and magnetic survey of the State of Maine and of Binghamton, Ogdensburg and Utica in New York State was performed. The survey was flown with a Sikorsky S58T helicopter equipped with a high sensitivity calibrated gamma ray spectrometer. The radiometric data were processed to compensate for Compton scattering effects and altitude variations. The data were normalized to 400 feet terrain clearance. The reduced data are presented in the form of stacked profiles, standard deviation anomaly plots, histogram plots and microfiche listings. DOE

N82-14616# Royal Aircraft Establishment, Farnborough (England). Remote Sensing Unit.

REMOTE SENSING INFORMATION BULLETIN; ISSUE NUMBER 6

Jul. 1981 33 p

Avail: NTIS HC A03/MF A01

The activities of the Center up to July 1981 are reported. Topics include: the United Kingdom report to the seventh Earthnet meeting, in June 1981; satellite status reports for LANDSAT 1, 2, 3, and D; microwave remote sensing, including Seasat synthetic aperture radar; Mapsat feasibility study; Eros field office; and symposia and conferences organized by the Center, including a summer school on remote sensing applications in marine science and technology. Author (ESA)

N82-14779# National Oceanic and Atmospheric Administration, Seattle, Wash. Pacific Marine Environmental Lab.

GEM: A SIMPLE METEOROLOGICAL BUOY WITH SATELLITE TELEMETRY

R. Michael Reynolds /n ESA Nowcasting: Mesoscale Observations and Short-Range Prediction Jun. 1981 p 401-404 refs

Avail: NTIS HC A19/MF A01; ESA, Paris FF 160 Member States, AU, CN and NO (+20% others)

A small, easily deployable and inexpensive buoy was developed for mesoscale research. The synthesis of the detailed parameter fields necessary for mesometeorology necessitates the deployment of a network of buoys that are less expensive than most standard designs. Vector averaged winds, scalar winds, air temperature, water temperature, and gusts are measured. Compass readings provide surface current direction. The buoy transmits data via the GOES satellite which eliminates the need for internal tape recording. Computer processing of the data is described. Proper counterbalancing and vector averaging are shown to reduce the effects of buoy motion. Author (ESA)

N82-15110# Air Force Systems Command, Wright-Patterson AFB, Ohio.

METEOROLOGICAL SATELLITES

16 Oct. 1981 7 p refs Transl. into ENGLISH from Skrzydlata Polska (Poland) no. 27, 1979 21 p

(AD-A107427; FTD-ID(RS)T-1059-81)

Avail: NTIS

HC A02/MF A01 CSCL 22B

Meteor-2 (second generation meteorological satellite) and an experimental satellite on which instruments are being tested and modified for the requirements of hydrometeorology and a determination of natural resources are presently operational in the U.S.S.R. Television devices with a 1-10 km terrain image resolution operating in the visible and infrared region are used to determine the space system, velocity and direction of cloud movements and provide information about the snow and ice cover, cyclones, storms, vortices in the atmosphere, and velocity and direction of wind. Images with a 50-1000 m resolution make possible geological and hydrological surveys, an evaluation of the state of vegetation and crops, detection of forest fires, determination of pollution of the atmosphere and sea and determination of optimal fishing regions in the ocean. Measurement of the intensity of atmospheric radiation in narrow infrared regions and very high frequencies allows remote evaluation of the temperature and humidity distribution in the vertical cross section of the Earth's atmosphere. Author

N82-15483# General Electric Co., Philadelphia, Pa. Space Div.

LANDSAT-2 AND LANDSAT-3 FLIGHT EVALUATION REPORT, 23 APRIL TO 23 JULY 1979

1 Aug. 1979 258 p ERTS

(Contract NAS5-21808)

(E82-10005; NASA-CR-163348; Doc-79SDS4242)

Avail: NTIS HC A12/MF A01 CSCL 05B

The performance of satellite subsystems and the response of in-orbit payload systems are summarized. Graphs and tables show the values of the various parameters of these systems. A spacecraft orbit reference table is included. A.R.H.

N82-15493# IBM Federal Systems Div., Houston, Texas.
ERSYS-SPP ACCESS METHOD SUBSYSTEM DESIGN SPECIFICATION

R. C. Weise, Principal Investigator Sep. 1980 74 p Sponsored by NASA, USDA, Dept. of Commerce, Dept. of Interior, and Agency for International Development ERTS

(Contract NAS9-14350; Proj. AgRISTARS)

(E82-10015; NASA-CR-161039; MU-11-00300; JSC-16918)

Avail: NTIS HC A04/MF A01 CSCL 02C

The STARAN special purpose processor (SPP) is a machine allowing the same operation to be performed on up to 512 different data elements simultaneously. In the ERSYS system,

08 INSTRUMENTATION AND SENSORS

it is to be attached to a 4341 plug compatible machine (PCM) to do certain existing algorithms and, at a later date, to perform other to be specified algorithms. That part of the interface between the 4341 PCM and the SPP located in the 4341 PCM is known as the SPP access method (SPPAM). Access to the SPPAM will be obtained by use of the NQUEUE and DQUEUE commands. The subsystem design specification is to incorporate all applicable design considerations from the ERSYS system design specification and the Level B requirements documents relating to the SPPAM. It is intended as a basis for the preliminary design review and will expand into the subsystem detailed design specification. Author

N82-15495*# General Electric Co., Philadelphia, Pa. Space Div.

LANDSAT-2 AND LANDSAT-3 FLIGHT EVALUATION REPORT, 23 OCTOBER 1978 TO 23 JANUARY 1979

1 Feb. 1979 236 p ERTS

(Contract NAS5-21808)

(E82-10017; NASA-CR-166640; Doc-79SDS4201) Avail: NTIS HC A11/MF A01 CSCL 05B

Orbital parameters and adjustments are discussed and tabulated. The performance of the various subsystems and payloads on the two satellites is documented in tables. A.R.H.

N82-15500# Marconi Co. Ltd., Chelmsford (England). Communications Research Div.

ADDITIONAL STUDIES OF EARTH RESOURCES SYNTHETIC APERTURE RADAR PAYLOADS Final Report

A. P. Luscombe Paris ESA Oct. 1980 105 p refs

(Contract ESA-6225/80-F-CG(SC))

(MTR-80/90; ESA-CR(P)-1469) Avail: NTIS HC A06/MF A01

Results of design studies on the synthetic aperture radar payload are discussed. A new baseline system for an incidence angle of about 45 deg was specified, and its performance at smaller angles is assessed. A feasibility study of a squinted SAR system is described. For individual titles, see N82-15501 through N82-15502.

N82-15501# Marconi Co. Ltd., Chelmsford (England). Communications Research Div.

NEW BASELINE SYSTEM Final Report

In its Additional Studies of Earth Resources Syn. Aperture Radar Payload Oct. 1980 46 p refs

Avail: NTIS HC A06/MF A01

A baseline system with an incidence angle of around 45 deg was specified for the Earth resources SAR payload and its operation at smaller angles was investigated. The basic system design and method of analysis are described. The choices of pulse repetition frequency (PRF) for different incidence angles, the problem of ambiguities and their evaluation and the antenna beam patterns are covered along with the selection of major system parameters (beam pattern, PRF's and incidence angles). The detail and the baseline system suggested is analyzed in terms of the image quality specifications. Two more aspects of the SAR system, the transmitter power requirements and the variation in ground range resolution with incidence angle, are discussed. A listing of the basic results for four different incidence angles is given. J.M.S.

09
GENERAL

Includes economic analysis.

A82-12530 Remote sensing contributions to the management of renewable resources. C. Sheffield (Earth Satellite Corp., Washington, DC). In: The year of the Shuttle; Proceedings of the Eighteenth Space Congress, Cocoa Beach, FL, April 29-May 1, 1981. Cocoa Beach, FL, Canaveral Council of Technical Societies, 1981, p. 2-7 to 2-14. 9 refs.

Present and future contributions of space-derived remotely sensed data, obtained from observations of five major areas of renewable resources, are discussed. The data needs for the five resource areas - agriculture, forestry, rangeland management, coastal zones, and the ocean harvest - are described, and the principal satellites and sensors flown in space to cover these areas since 1972 are presented. Data sources and data needs are compared, and areas of data deficiency and limitation are identified. A profile of earth sensing satellites to fill these gaps in a 1985-1995 time frame is given. Cooperative international efforts to develop future earth resource satellites are suggested. J.F.

A82-12541 The 1981 RCA space constellation. A. Schnapf (RCA, Astro-Electronics Div., Princeton, NJ). In: The year of the Shuttle; Proceedings of the Eighteenth Space Congress, Cocoa Beach, FL, April 29-May 1, 1981. Cocoa Beach, FL, Canaveral Council of Technical Societies, 1981, p. 5-43 to 5-53.

The eight spacecraft scheduled for launch in 1981 are described. These are the RCA Satcom D and E commercial communication satellites, the U.S. Navy NOVA 1 and 2 navigation satellites, NASA's Dynamics Explorer A and B scientific satellites, the U.S. Department of Commerce NOAA-C operational meteorological satellite, and the Department of Defense DMSP Block 5D-2 operational meteorological satellite. It is noted that in addition a number of RCA color television camera systems will be carried on the Space Transportation System for aiding the astronauts in inspecting and deploying cargo from the cargo bay and for providing video transmissions of engineering and public relations activity in the Shuttle crew compartment. C.R.

A82-17307 # ISRO satellite mission support facilities - Scope and future plans. M. K. Sundararaman, V. S. Iyengar, and K. V. Venkatachary (Indian Space Research Organization, Sriharikota, India). In: Space tracking and data systems; Proceedings of the Symposium, Arlington, VA, June 16-18, 1981. New York, American Institute of Aeronautics and Astronautics, 1981, p. 51-63.

It is the objective of the Indian Space Research Organization (ISRO) to provide communication and education to widely dispersed rural communities in India, and to survey and manage the country's natural resources with the aid of satellite technology. India maintains also a modest scientific research program which employs satellite missions. A brief overview is provided of the Indian space program, giving attention to the network's current capabilities for satellite data acquisition, tracking activities, and data dissemination. A description is given of plans for the coming decade. G.R.

N82-10087*# National Aeronautics and Space Administration. Goddard Space Flight Center, Greenbelt, Md. **REPORT ON ACTIVE AND PLANNED SPACECRAFT AND EXPERIMENTS**

Robert W. Vostreys, ed. and Harriet H. Maitson, ed. Aug. 1981 310 p refs (NASA-TM-84025; NSSDC/WDC-A-R&S-81-10) Avail: NTIS HC A14/MF A01 CSCL 22A

Active and planned spacecraft activity and experiments between June 1, 1980 and May 31, 1981 known to the National Space Science Data Center are described. The information covers a wide range of disciplines: astronomy, Earth sciences, meteorology, planetary sciences, aeronomy, particles and fields, solar physics, life sciences, and material sciences. Each spacecraft and experiment is described and its current status presented. Descriptions of navigational and communications satellites and

of spacecraft that contain only continuous radio beacons used for ionospheric studies are specifically excluded. J.D.H.

N82-10102*# National Aeronautics and Space Administration. Washington, D. C.

MISSION OPERATION REPORT: OSTA-1

26 Oct. 1981 28 p (NASA-TM-84053; S-420-81-01) Avail: NTIS HC A03/MF A01 CSCL 22B

The Office of Space and Terrestrial Applications (OSTA 1) payload was designed to demonstrate shuttle's capability as a space research platform and the potential application of techniques for future remote sensing. Because thermal tests planned for STS-2 flight require that the payload bay to be pointed towards Earth, the experiments selected for OSTA 1 emphasize terrestrial sciences and are concerned with remote sensing for Earth resources, environmental quality, ocean conditions, meteorological phenomena, and life sciences. Characteristics of the STS-2 flight, the major events timeline, geographical areas coverage, pallet experiments ground coverages, and experiment operating modes are described. The OSTA-1 pallet configuration, payload interface, and the instruments comprising each of the experiments are described and illustrated. Mission support stations, and the payload team are listed. Mission cost data are included. A.R.H.

N82-13010# Eurosat S.A., Geneva (Switzerland).

OVERALL ECONOMIC IMPACT OF AN OPERATIONAL METEOSAT SYSTEM Final Report

J. B. Lagarde, P. Brendle (BETA/ULP), C. Miller, and P. Cohendet (BETA/ULP) Paris ESA Jan. 1981 70 p refs (Contract ESA-4421/80/F-FC(SC)) (ESA-CR(P)-1457) Avail: NTIS HC A04/MF A01

The METEOSAT concept through its development and well into its expected operational mode, up to 1990 was analyzed. Account was taken of the disturbance introduced by the METEOSAT 1 failure in November 1979, of the delay in the launch of METEOSAT 2, and of the uncertainties arising from the lack of decision, at the end of 1980, on the operational METEOSAT follow-on. Results show important positive economic effects both for the users community (direct benefits) and for the contracting industry concerned (induced benefits).

Author (ESA)

N82-14555# European Space Agency, Paris (France).

THE NEED FOR INTEGRATED OFF-SHORE, REAL-TIME INFORMATION AND MANAGEMENT SYSTEMS

L. W. Morley In: *Its Appl. of Remote Sensing Data on the Continental Shelf* Jul. 1981 p 17-21 refs

Avail: NTIS HC A13/MF A01; ESA, Paris FF 125

Integrated planning, in which data from ships, aircraft, data buoys, and shore or satellite-borne radar are used for ocean surveillance is urged. The Atlantic coast of Canada is used as an example of the inefficiency of current management methods. Traffic control, search and rescue missions, pollution control, weather forecasting, and fisheries management are directed by separate government agencies, each with its own information system. A coordinated approach would reduce waste and allow full advantage to be taken of technological developments, e.g., satellites, unknown when the agencies were created.

Author (ESA)

N82-14615# Erno Raumfahrttechnik G.m.b.H., Bremen (West Germany). Abteilung Satelliten und Sonden PRV-1.

STUDY OF A COMBINED SATELLITE SYSTEM FOR REMOTE SENSING AND EARTH-ORIENTED RESEARCH (LOCSS) Final Report, Jul. 1980

HansJuergen Guenther, Wolfgang Gericke, Hansjoerg Klotz, Rainer Krieger, Birgit Metzgar, Joachim Nauck, Klaus Plate, Rudolf Rohr, Gernot Schmidt, and Gerhard Schneider Bonn Bundesministerium fuer Forschung und Technologie Jan. 1981 222 p refs in GERMAN; ENGLISH summary Sponsored by Bundesministerium fuer Forschung und Technologie (BMFT-FB-W-81-002; ISSN-0170-1339) Avail: NTIS HC A10/MF A01; Fachinformationszentrum, Karlsruhe, West Germany DM 38,60

The suitability of three European satellite platforms (ERD-SAT, SPAS, SPOT) for a combined satellite system (remote sensing and Earth-oriented research) is discussed. The system consists of two Sun-synchronous orbiting satellites with a combined remote

09 GENERAL

sensing and Earth-oriented research payload and of a pure climatography satellite on a drift orbit. All platforms can accommodate the basic payload, but SPAS offers some advantages and is the only platform able to accommodate the extended payload. The combined three-satellite system offers cost advantages over the four-satellite system only if the space shuttle is used as launcher. Hence, SPAS should be given preference over the other platforms for such a system. The subsystem design is presented and problem areas are discussed. Data acquisition and data processing of image and climatic data are the bottlenecks in existing systems. Author (ESA)

N82-16496* # Mississippi State Univ., Mississippi State. Remote Sensing Center.

A PROPOSAL FOR CONTINUATION OF SUPPORT FOR THE APPLICATION OF REMOTELY SENSED DATA TO STATE AND REGIONAL PROBLEMS. PART 1: TECHNICAL PROPOSAL

Jun. 1981 114 p ERTS

(Grant NGL-25-001-054)

(E82-10018; NASA-CR-164817)

Avail: NTIS

HC A06/MF A01 CSCL 05A

The objectives, procedures, accomplishments, plans, and ultimate uses of information from current projects at the Mississippi Remote Sensing Center are discussed for the following applications: (1) land use planning; (2) strip mine inventory and reclamation; (3) biological management for white tailed deer; (4) forest habitats in potential lignite areas; (5) change discrimination in gravel operations; (6) discrimination of freshwater wetlands for inventory and monitoring; and (7) remote sensing data analysis support systems. The initiation of a conceptual design for a LANDSAT based, state wide information system is proposed.

A.R.H.

N82-15497 # Committee on Science and Technology (U. S. House).

CIVIL LAND REMOTE SENSING SYSTEMS

Washington GPO 1981 370 p Joint hearings before the Subcomm. on Space Sci. and Appl. of the Comm. on Sci. and Technol. and the Subcomm. on Sci., Technol., and Space of the Comm. on Com., Sci., and Transportation, 97th Congr., 1st Sess., No. 40, 22-23 Jul. 1981

(GPO-35-265) Avail: Subcommittee on Space Science and Applications

Steps taken to facilitate NOAA assumption of responsibility for operating LANDSAT D and LANDSAT D prime are reviewed and institutional alternatives for transferring operational responsibility for the program to the private sector are examined. These include: (1) an existing private corporation; (2) a legislatively established for profit private corporation; (3) a government corporation; and (4) Federal agency ownership with private sector operation. The advantages and disadvantages of each of these options are considered as well as user participation.

A.R.H.

N82-15499 # Cologne Univ. (West Germany). Inst. fuer Geophysik und Meteorologie.

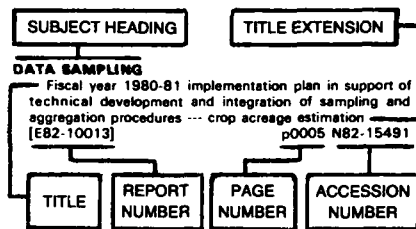
ANALYSIS OF SATELLITE OBSERVATIONS: THEORETICAL STUDIES ON THE SAMPLING PROBLEM [ANALYSE VON SATELLITENBEOBACHTUNGEN - THEORETISCHE UNTERSUCHUNGEN ZUM SAMPLING PROBLEM]

Hans Joachim Preuss 1981 68 p refs In GERMAN; ENGLISH summary

(Mitt-31; ISSN-0069-5882) Avail: NTIS HC A04/MF A01

In a general mission analysis, some orbital and measuring characteristics are simulated and their influence on the sampling investigated. The important role of a satellite with a moderate inclination (approximately 60 deg) is shown; with the drifting orbit homogeneous sampling of diurnal variations and of radiance distributions is possible in a global scale within about 15 days. More complex scan modes (off track, rotary or conical) may improve the angular sampling, especially in case of Sun synchronous satellites, but for studies in small temporal and spatial scales a system with at least three satellites is necessary. The general results are applied on the determination of the radiation balance. By means of models for the diurnal variations and anisotropic behavior, measurements are created and sampling errors demonstrated. Author

Typical Subject Index Listing



The subject heading is a key to the subject content of the document. The title is used to provide a description of the subject matter. When the title is insufficiently descriptive of the document content, the title extension is added, separated from the title by three hyphens. The (NASA or AIAA) accession number and the page number are included in each entry to assist the user in locating the abstract in the abstract section (of this supplement). If applicable, a report number is also included as an aid in identifying the document. Under any one subject heading, the accession numbers are arranged in sequence with the AIAA accession numbers appearing first.

A

ACID RAIN
 Role of remote sensing in the study of acid rain impact on aquatic systems p0036 A82-17892
 [AIAA PAPER 82-0336]
 Investigation of the application of remote sensing technology to environmental monitoring p0013 N82-15488
 [E82-10010]

ACIDITY
 Role of remote sensing in the study of acid rain impact on aquatic systems p0036 A82-17892
 [AIAA PAPER 82-0336]

AERIAL PHOTOGRAPHY
 Aspects in the development of aerial-photography tasks p0041 A82-12913
 Current aerial cameras p0050 A82-15655
 Photo inertial positioning system development at the Canada Centre for Remote Sensing p0045 A82-18167

AERIAL RECONNAISSANCE
 A history of flying and photography: In the Photogrammetry Division of the National Ocean Survey 1919 - 1979 p0017 N82-15520
 [PB81-246738]

AEROSOLS
 Study of stack emissions by combination of lidar and correlation spectrometer p0008 A82-12818
 Radiative heating rates and some optical properties of the St. Louis aerosol, as inferred from aircraft measurements p0008 A82-14320
 Results from the July 1981 Workshop on Passive Remote Sensing of the Troposphere p0009 A82-17841
 [AIAA PAPER 82-0207]

AEROSPACE TECHNOLOGY TRANSFER
 Civil land remote sensing systems p0056 N82-15497
 [GPO-35-265]

AFRICA
 Skylab 4 observations of Volcanoes. Part A: Volcanoes and volcanic landforms. Part B: Summit eruption of Fernandina Caldera, Galapagos Islands, Ecuador p0020 N82-12496
 p0004 N82-12500
 Report on Skylab 4 African drought and arid land experiment p0037 N82-12501
 Necessity of remote sensing for ocean studies. Part 1: Northwest African missions, Sahara-1 and Atlor-1 --- sea truth/remote sensing correlation of offshore upwelling p0032 N82-14582
 The mineralogy of global magnetic anomalies [E82-10009] p0021 N82-15487

AGRICULTURE
 Remote sensing techniques in the study of the agricultural potential of soils under the Cerrado vegetation /Brazil/ p0001 A82-10040
 Remote sensing contributions to the management of renewable resources p0055 A82-12530
 Study and mapping of agricultural land use, based on space images p0003 A82-15963
 Rural development in the humid tropics p0003 A82-16162
 Cultural features imaged and observed from Skylab 4. Application of remote sensing to selected problems within the state of California [E82-10004] p0004 N82-15482

AGROCLIMATOLOGY
 Wheat cultivation: Identification and estimation of areas using LANDSAT data [E82-10007] p0004 N82-15485

AGROMETEOROLOGY
 Winterkill indicator model. Crop Condition Assessment Division (CCAD) data base interface driver, user's manual [E82-10014] p0005 N82-15492

AIR LAND INTERACTIONS
 Thermal inertia, thermal admittance, and the effect of layers p0008 A82-15027

AIR POLLUTION
 Trace pollutant concentrations in a multiday smog episode in the California South Coast Air Basin by long path length Fourier transform infrared spectroscopy p0007 A82-10700
 Spacelab-research of European regions with strong negative environmental influences, based on AVHRR-data of the satellites Tiros-N and NOAA p0007 A82-12517
 Study of stack emissions by combination of lidar and correlation spectrometer p0008 A82-12818
 Radiative heating rates and some optical properties of the St. Louis aerosol, as inferred from aircraft measurements p0008 A82-14320
 Results from the July 1981 Workshop on Passive Remote Sensing of the Troposphere [AIAA PAPER 82-0207] p0009 A82-17841
 Proof of concept study [AD-A104338] p0010 N82-11839
 Quantitative analysis of atmospheric pollution phenomena p0010 N82-12505

AIR QUALITY
 Shuttle applications in tropospheric air quality observations [NASA-CR-145374] p0010 N82-11635
 Aircraft data summaries of the SURE intensives, volume 4 [DE82-900311] p0012 N82-13569

AIR SAMPLING
 Automated analyzer for aircraft measurements of atmospheric methane and total hydrocarbons p0007 A82-11949

AIR WATER INTERACTIONS
 Analysis of SEASAT wind observations over the Indian Ocean p0023 A82-10671
 Annual and nonseasonal variability of monthly low-level wind fields over the Southeastern Tropical Pacific p0025 A82-17494
 Variations in upper ocean heat storage determined from satellite data p0025 A82-17567
 Anomalous wind estimates from the Seasat scatterometer p0026 A82-18724
 Meteorological lab applications of Skylab handheld-camera photographs p0011 N82-12506
 Determination of surface wind speed from remotely measured whitecap coverage, a feasibility assessment p0030 N82-14565
 The Norwegian remote sensing experiment (Norsex) in a marginal ice zone p0031 N82-14566
 A preliminary evaluation of Seasat performance over the area of JASIN and its relevance to ERS-1 p0031 N82-14567

AIR WATER INTERACTIONS GREAT LAKES (US)
 Project Noordwijk. Part 1: Measurements of the radar backscatter coefficient gamma (sigma deg) in 1977 and 1978 --- on a sea platform [PHL-1979-49-PT-1] p0032 N82-14817
 Project Noordwijk. Part 2: Results of North Sea clutter measurements in the I-band performed from the platform Noordwijk in September/October 1977 [PHL-1980-28-PT-2] p0033 N82-14618
 Meteorological and oceanographic observations on board Netherlands lightvessels and the lightplatform 'Goeree' in the North Sea p0033 N82-15684
 [KNMI-141-28]

Mesoscale cloud features observed from Skylab p0011 N82-12509

AIR SPEED
 The application of programmable pocket calculators for computations during survey flights p0050 A82-18164

ALASKA
 Application of satellite Doppler techniques to the national mapping program p0015 A82-10056
 Bureau of Land Management satellite Doppler positioning techniques p0015 A82-10057
 Geophysical monitoring for climatic change, number 8: Summary Report, 1979 [PB81-233355] p0012 N82-13631

ALBEDO
 The near-infrared radiation received by satellites from clouds p0025 A82-17492
 Use of environmental satellite data for input to energy balance snowmelt models [PB81-227795] p0039 N82-15673

ALGAE
 Remote sensing that motivated community action p0008 A82-12594
 Remote sensing of benthic microalgal biomass with a tower-mounted multispectral scanner p0024 A82-15031

ALGORITHMS
 Analysis of soil moisture extraction algorithm using data from aircraft experiments [NASA-CR-166719] p0046 N82-13470

ALIGNMENT
 MAGSAT: Vector magnetometer absolute sensor alignment determination [NASA-TM-79648] p0051 N82-10468

ALTIMETERS
 Seasat altimetry adjustment model including tidal and other sea surface effects [AD-A104188] p0026 N82-10473
 Ionospheric propagation correction modeling for satellite altimeters [NASA-CR-156881] p0052 N82-12447

AMAZON REGION (SOUTH AMERICA)
 Remote sensing in forestry: Application to the Amazon region [E82-10012] p0005 N82-15490

ANGULAR RESOLUTION
 The effect of angular factors on popularly used indicators of vegetative vigor p0001 A82-10039

ANNUAL VARIATIONS
 Annual and nonseasonal variability of monthly low-level wind fields over the Southeastern Tropical Pacific p0025 A82-17494

ANTARCTIC REGIONS
 Geophysical monitoring for climatic change, number 8: Summary Report, 1979 [PB81-233355] p0012 N82-13631

ANTENNA RADIATION PATTERNS
 Additional studies of Earth resources synthetic aperture radar payloads [MTR-80/90] p0054 N82-15500
 New baseline system p0054 N82-15501
 Squinted SAR system p0047 N82-15502

ARABIAN SEA
 Detection of monsoon inversion by TIROS-N satellite p0024 A82-17168

ARCHAEOLOGY
 Radar mapping, archaeology, and ancient land use in the Maya lowlands [NASA-CR-164931] p0010 N82-11514

ARCTIC OCEAN
 The ice-conditions in the Greenland waters, 1965. Coastal maps [ISBN-87-7478-183-9] p0026 N82-10467
 The ice conditions in the Greenland waters [ISBN-87-7478-183-9] p0028 N82-12533
 The Norwegian remote sensing experiment (Norsex) in a marginal ice zone p0031 N82-14566
 Measurements of radar backscatter from Arctic Sea ice in the summer [AD-A105586] p0032 N82-14592
 Measurements of radar backscatter from Arctic Sea ice in the summer. Appendices A and B [AD-A105736] p0032 N82-14593

ARGENTINA
 Vegetation patterns p0004 N82-12500

ARID LANDS
 Satellite sensing of irrigation patterns in semiarid areas An Indian study p0002 A82-10864
 Space photographs obtained with the Fragment system as a base for landscape mapping and physical-geographical classification of arid territories p0009 A82-15967
 Report on Skylab 4 African drought and arid land experiment p0037 N82-12501

ARIZONA

- Geological features of southwestern North America
p0020 N82-12495
- Meteorological lab applications of Skylab
handheld-camera photographs p0011 N82-12506
- ASTRONOMICAL COORDINATES**
Coordinates of features on the Galilean satellites
p0019 A82-12366

ATLANTIC OCEAN

- An investigation of a polar low with a spiral cloud
structure p0007 A82-10616
- Synoptic thermal and oceanographic parameter
distributions in the New York Bight Apex
p0023 A82-12885
- Comparison of polar and geostationary satellite infrared
observations of sea surface temperatures in the Gulf of
Maine p0024 A82-15030
- Upper tropospheric cyclonic vortices in the tropical South
Atlantic p0009 A82-16325
- Global satellite measurements of water vapour, wind
speed and wave height p0051 A82-17165
- Remote sensing of the Chesapeake Bay plume salinity
via microwave radiometry p0027 N82-10670
- Preliminary analysis of ocean color scanner data from
Superflux III p0027 N82-10672
- Analysis of testbed airborne multispectral scanner data
from Superflux II --- Chesapeake Bay plume and James
Shelf data p0027 N82-10682
- An assessment of the potential contributions to
oceanography from Skylab visual observations and
handheld-camera photographs p0028 N82-12503
- Meteorological lab applications of Skylab
handheld-camera photographs p0011 N82-12506
- The need for integrated off-shore, real-time information
and management systems p0055 N82-14555
- An evaluation of Seasat-A data in relation to optimum
track ship weather routing and site specific forecasting for
the offshore oil industry p0030 N82-14564
- A short review of an oceanographic use of Meteosat
data by the ORSTOM remote sensing service
p0031 N82-14570
- Necessity of remote sensing for ocean studies. Part 1:
Northwest African missions, Sahara-1 and Atlor-1 --- sea
truth/remote sensing correlation of offshore upwelling
p0032 N82-14582

ATLANTIC OCEAN PACIFIC OCEAN

- Availability of Seasat synthetic aperture radar imagery
p0050 A82-15039

ATMOSPHERIC ATTENUATION

- Water vapour absorption in the 3.5-4.2 micron
atmospheric window p0023 A82-14586
- The radiowave propagation environment - Science and
technology objectives for the 80's p0009 A82-18052

ATMOSPHERIC CHEMISTRY

- Trace pollutant concentrations in a multiday smog episode
in the California South Coast Air Basin by long path length
Fourier transform infrared spectroscopy p0007 A82-10700

- Automated analyzer for aircraft measurements of
atmospheric methane and total hydrocarbons
p0007 A82-11949

- Results from the July 1981 Workshop on Passive Remote
Sensing of the Troposphere
[AIAA PAPER 82-0207] p0009 A82-17841

ATMOSPHERIC CIRCULATION

- An investigation of a polar low with a spiral cloud
structure p0007 A82-10616

ATMOSPHERIC MODELS

- Ionospheric propagation correction modeling for satellite
altimeters
[NASA-CR-156881] p0052 N82-12447

ATMOSPHERIC MOISTURE

- Global satellite measurements of water vapour, wind
speed and wave height p0051 A82-17165
- Scientific studies using Bhaskara satellite microwave
radiometer (SAMIR) data: A short overview --- calibration
of the instrument and its use in the study of oceanographic
parameters p0032 N82-14587
- Sensitivity analysis of a mesoscale moisture model
[AD-A101528] p0012 N82-14590

ATMOSPHERIC OPTICS

- Radiative heating rates and some optical properties of
the St. Louis aerosol, as inferred from aircraft
measurements p0008 A82-14320
- Spectral atmospheric observations at Nantucket Island,
May 7-14, 1981
[NASA-TM-83196] p0029 N82-14550

ATMOSPHERIC PRESSURE

- Oceanic wind and balanced pressure-height fields derived
from satellite measurements p0023 A82-13214

ATMOSPHERIC RADIATION

- Estimation of atmospheric path-radiance by the
covariance matrix method p0041 A82-10861
- The influence of gravity waves on radiometric
measurements - A case study p0049 A82-13547
- Environmental Monitoring Report, Sandia National Labs.,
Albuquerque, New Mexico, 180
[DE81-027839] p0010 N82-11649

ATMOSPHERIC SCATTERING

- Calculation of the decrease in the contrast of objects of
a place due to light scattering in the atmosphere
p0042 A82-13633

ATMOSPHERIC SOUNDING

- Repeatability and measurement uncertainty of the United
States meteorological rocketsonde p0049 A82-12127

- Microwave limb sounder --- measuring trace gases in
the upper atmosphere
[NASA-CASE-NPO-14544-1] p0011 N82-12685

ATMOSPHERIC TEMPERATURE

- Repeatability and measurement uncertainty of the United
States meteorological rocketsonde p0049 A82-12127
- Thermal inertia, thermal admittance, and the effect of
layers p0008 A82-15027

AURORAL ZONES

- Characteristics of westward travelling surges during
magnetospheric substorms p0050 A82-14299

AUSTRALIA

- Use of visible and thermal satellite data to monitor an
intermittently flooding marshland p0036 A82-15037
- Compensation of systematic errors of image and model
coordinates p0043 A82-15765
- Vegetation patterns p0004 N82-12500

B

BACKSCATTERING

- A theory of wave scattering from an inhomogeneous
layer with an irregular interface p0041 A82-12757
- Radar backscattering from ocean waves at low grazing
angles p0023 A82-14730
- The surface albedo of the earth in the near ultraviolet
/330-340 nm/ p0016 A82-15032
- Measurement of sea and ice backscatter reflectivity using
an OTH radar system p0025 A82-18074
- Evaluation of the Seasat wind scatterometer
p0025 A82-18716
- Anomalous wind estimates from the Seasat
scatterometer p0026 A82-18724
- Progress in radar snow research --- Brookings, South
Dakota
[NASA-CR-166709] p0038 N82-12510
- State-of-the-art in using a spaceborne altimeter and
scatterometer for the determination of wind, sea state, and
marine and ice dynamics --- Seasat instruments
p0052 N82-14560
- Measurements of radar backscatter from Arctic Sea ice
in the summer. Appendices A and B
[AD-A105736] p0032 N82-14593
- Project Noordwijk. Part 1: Measurements of the radar
backscatter coefficient gamma (sigma deg) in 1977 and
1978 --- on a sea platform
[PHL-1979-49-PT-1] p0032 N82-14617

BALTIC SEA

- Maritime applications of image processing at DFVLR,
Oberpfaffenhofen, West Germany --- LANDSAT
multispectral scanner images, digital interactive image
analysis p0032 N82-14585

BARLEY

- US/Canada wheat and barley crop calendar exploratory
experiment implementation plan
[E82-10016] p0005 N82-15494

BAYS (TOPOGRAPHIC FEATURES)

- Field study for Landsat water quality verification
p0036 A82-12597
- Synoptic thermal and oceanographic parameter
distributions in the New York Bight Apex
p0023 A82-12885
- Visual observations of floating ice from Skylab
p0037 N82-12504

BEACHES

- A method for using aerial photos in delineating historic
patterns of beach accretion and retreat
[PB81-223836] p0010 N82-11536

BEARING (DIRECTION)

- Three bearing method for passive triangulation in systems
with unknown deterministic biases p0050 A82-15920

BERING SEA

- Ice conditions in the eastern Bering Sea from NOAA
and LANDSAT imagery: Winter conditions 1974, 1976,
1977, 1979
[PB81-220188] p0028 N82-11537

BIAS

- Three bearing method for passive triangulation in systems
with unknown deterministic biases p0050 A82-15920

BIBLIOGRAPHIES

- Report on Active and Planned Spacecraft and
experiments
[NASA-TM-84025] p0055 N82-10087

BIOMASS

- Remote sensing of benthic microalgal biomass with a
tower-mounted multispectral scanner p0024 A82-15031
- Biological patchiness in relation to satellite thermal
imagery and associated chemical mesoscale features
[AD-A105757] p0047 N82-15504

BIRDS

- Remote sensing applications to resource problems in
South Dakota
[E82-10002] p0004 N82-15481

BLIGHT

- Evaluation of digital photographic enhancement for Dutch
elm disease detection p0002 A82-12884

BLUE GREEN ALGAE

- Maritime applications of image processing at DFVLR,
Oberpfaffenhofen, West Germany --- LANDSAT
multispectral scanner images, digital interactive image
analysis p0032 N82-14585

BRAZIL

- Remote sensing techniques in the study of the agricultural
potential of soils under the Cerrado vegetation /Brazil/
p0001 A82-10040

- Wheat cultivation: Identification and estimation of areas
using LANDSAT data
[E82-10007] p0004 N82-15485
- Quantitative analysis of drainage obtained from aerial
photographs and RBV/LANDSAT images
[E82-10008] p0039 N82-15486
- Remote sensing in forestry: Application to the Amazon
region
[E82-10012] p0005 N82-15490

BRIGHTNESS

- Metrological support of measurements of earth-surface
brightness by the Fragment multispectral scanning
system p0050 A82-15958

BRIGHTNESS DISCRIMINATION

- Multitemporal calibration of LANDSAT images: A
method for improving the marine phenomena recognition,
with as example the Venice lagoon ---
brightness/green/yellow feature space, image
enhancement p0046 N82-14578

BRIGHTNESS DISTRIBUTION

- Estimation of the brightness field from results of
multispectral photography of the earth from space
p0044 A82-16617

- Programs for the statistical analysis of multispectral
photographs p0044 A82-16628

BRIGHTNESS TEMPERATURE

- A comparison of radiative transfer models for predicting
the microwave emission from soils p0035 A82-10694
- Water vapour absorption in the 3.5-4.2 micron
atmospheric window p0023 A82-14586
- Remote sensing of the Chesapeake Bay plume salinity
via microwave radiometry p0027 N82-10670
- SMMR data set development for GARP --- impact of
cross polarization and Faraday rotation on SMMR derived
brightness temperatures
[NASA-CR-166721] p0052 N82-11512
- Limit on remote FTIR detection of trace gases
[AD-A104842] p0011 N82-12511
- Determination of surface wind speed from remotely
measured whitecap coverage, a feasibility assessment
p0030 N82-14565

BUOYS

- GEM: A simple meteorological buoy with satellite
telemetry p0053 N82-14779

C

CALCULATORS

- The application of programmable pocket calculators for
computations during survey flights p0050 A82-16164

CALDERAS

- Skylab 4 observations of Volcanoes. Part A: Volcanoes
and volcanic landforms. Part B: Summit eruption of
Fernandian Caldera, Galapagos Islands, Ecuador
p0020 N82-12496

CALIBRATING

- Aspects in the development of aerial-photography tasks
p0041 A82-12913

A new method for computing distortion

- p0016 A82-12914
- Intercalibration of Landsat 1-3 and NOAA 6 and 7 scanner
data p0049 A82-13293
- Compensation of systematic errors of image and model
coordinates p0043 A82-15765
- Main results of the Raduga experiment
p0051 A82-16602

Geometric quality of MKF-6 photographs

- p0043 A82-16606

- Characteristics of the photometry of small objects from
aerial and space photographs p0044 A82-16616

- Measurement of sea and ice backscatter reflectivity using
an OTH radar system p0025 A82-18074

- Study on calibration methods for Earth observation optical
imaging instruments
[UCD-207/1/80] p0052 N82-10488

- Infrared radiance model variation by sensor flight
measurements p0052 N82-14171

- Coastal zone research using remote sensing techniques
--- calibration of coastal zone color scanner
p0031 N82-14571

CALIFORNIA

- Spectral behavior of wheat yield variety trials
p0002 A82-10863

- Landsat imagery for hydrologic modeling
p0036 A82-12592

- Identification of conifer species groupings from Landsat
digital classifications p0002 A82-12887

- The use of satellite infrared imagery for describing ocean
processes in relation to spawning of the northern anchovy
/Engraulis mordax/ p0025 A82-17565

- Geological features of southwestern North America
p0020 N82-12495

- Vegetation patterns p0004 N82-12500

- Application of remote sensing to selected problems within
the state of California
[E82-10004] p0004 N82-15482

CAMERAS

- A new method for computing distortion
p0016 A82-12914

- Current aerial cameras p0050 A82-15655

SUBJECT INDEX

A history of flying and photography: In the Photogrammetry Division of the National Ocean Survey 1919 - 1979 [PB81-246738] p0017 N82-15520

CANADA

The Manicouagan impact structure observed from Skylab [CONTRIB-544] p0020 N82-12497

The need for integrated off-shore, real-time information and management systems p0055 N82-14555

The reduction, verification and interpretation of Magsat magnetic data over Canada [E82-10006] p0046 N82-15484

US/Canada wheat and barley crop calendar exploratory experiment implementation plan [E82-10016] p0005 N82-15494

CANOPIES (VEGETATION)

An improvement in land cover classification achieved by merging microwave data with Landsat multispectral scanner data p0007 A82-10043

Stand density estimation on panoramic transparencies p0002 A82-10862

Spectral behavior of wheat yield variety trials p0002 A82-10863

Temporal spectral response of a corn canopy p0002 A82-12886

Temporal relationships between spectral response and agronomic variables of a corn canopy p0002 A82-15038

In situ spectral reflectance studies of tidal wetland grasses p0036 A82-15969

Inclusion of a simple vegetation layer in terrain temperature models for thermal infrared (IR) signature prediction [AD-A104469] p0003 N82-11910

CARBON MONOXIDE

A new method for inferring carbon monoxide concentrations from gas filter radiometer data p0009 A82-16837

CENTRAL AMERICA

Availability of Seasat synthetic aperture radar imagery p0050 A82-15039

Radar mapping, archaeology, and ancient land use in the Maya lowlands [NASA-CR-164931] p0010 N82-11514

CENTRAL PROCESSING UNITS

ERSYS-SPP access method subsystem design specification [E82-10015] p0053 N82-15493

CHESAPEAKE BAY (US)

Chesapeake Bay Plume Study: Superflux 1980 [NASA-CP-2188] p0026 N82-10661

Superflux I, II, and III experiment design: Remote sensing aspects p0027 N82-10664

Superflux I, II, and III experiment designs: Water sampling and analyses --- Chesapeake Bay, environmental monitoring and remote sensing p0027 N82-10665

Monitoring the Chesapeake Bay using satellite data for Superflux III p0027 N82-10668

Remote sensing of the Chesapeake Bay plume salinity via microwave radiometry p0027 N82-10670

Preliminary analysis of ocean color scanner data from Superflux III p0027 N82-10672

Analysis of testbed airborne multispectral scanner data from Superflux II --- Chesapeake Bay plume and James Shelf data p0027 N82-10682

Application of the NASA airborne oceanographic lidar to the mapping of chlorophyll and other organic pigments p0027 N82-10684

Assessment of Superflux relative to remote sensing --- airborne remote sensing of the Chesapeake Bay plume and shelf regions p0028 N82-10694

CHILE

Global Tectonics: Some Geologic analyses of observations and photographs from Skylab p0020 N82-12494

CHLOROPHYLLS

Synoptic thermal and oceanographic parameter distributions in the New York Bight Apex p0023 A82-12885

Remote sensing of benthic microalgal biomass with a tower-mounted multispectral scanner p0024 A82-15031

Temporal relationships between spectral response and agronomic variables of a corn canopy p0002 A82-15038

Role of remote sensing in the study of acid rain impact on aquatic systems p0036 A82-17892

Application of the NASA airborne oceanographic lidar to the mapping of chlorophyll and other organic pigments p0027 N82-10684

Assessment of Superflux relative to remote sensing --- airborne remote sensing of the Chesapeake Bay plume and shelf regions p0028 N82-10694

Development of the coastal zone color scanner for NIMBUS 7, Volume 1: Mission objectives and instrument description [NASA-CR-166720-VOL-1] p0028 N82-11511

The color of the sea and its relation to surface chlorophyll and depth of the euphotic zone p0030 N82-14562

Coastal zone research using remote sensing techniques --- calibration of coastal zone color scanner p0031 N82-14571

Recent work in passive optical imaging of water --- space and aircraft derived data p0038 N82-14575

The feasibility of using remotely sensed color as an index of Irish coastal water properties --- statistical correlation of sea truth data p0032 N82-14581

Necessity of remote sensing for ocean studies. Part 1: Northwest African missions, Sahara-1 and Atlor-1 --- sea truth/remote sensing correlation of offshore upwelling p0032 N82-14582

CITIES

Cultural features imaged and observed from Skylab 4 p0010 N82-12499

CLASSIFICATIONS

Phytoecozonation of Sevier Lake region of Utah using digitized Landsat MSS data p0001 A82-10042

An improvement in land cover classification achieved by merging microwave data with Landsat multispectral scanner data p0007 A82-10043

Spectrometric studies of the earth's surface p0043 A82-16612

The maximum mean accuracy of classification of remote-sensing objects and the influence on this accuracy of data acquisition and processing methods p0044 A82-16615

Fiscal year 1980-81 implementation plan in support of technical development and integration of sampling and aggregation procedures --- crop acreage estimation [E82-10013] p0005 N82-15491

CLIMATOLOGY

Upper tropospheric cyclonic vortices in the tropical South Atlantic p0009 A82-16325

CTD/O2 measurements during the Equatorial Pacific Ocean Climate Study (EPOCS) in 1979 [PB81-211203] p0026 N82-10461

Study on satellite radar altimetry in climatological and oceanographic research, volume 1 [SP/153/06/01/FR(80)-VOL-1] p0026 N82-10486

Study on satellite radar altimetry in climatological and oceanographic research, volume 2 [SP/153/06/01/FR(80)-VOL-2] p0026 N82-10487

Geophysical monitoring for climatic change, number 8: Summary Report, 1979 [PB81-233355] p0012 N82-13631

Environmental satellite imagery, March 1981 [PB81-248049] p0047 N82-15698

CLOUD COVER

The near-infrared radiation received by satellites from clouds p0025 A82-17492

CLOUD PHOTOGRAPHY

An investigation of a polar low with a spiral cloud structure p0007 A82-10616

Meteorological lab applications of Skylab handheld-camera photographs p0011 N82-12506

Some aspects of tropical storm structure revealed by handheld-camera photographs from space p0011 N82-12507

Mesoscale wake clouds in Skylab photographs p0011 N82-12508

Mesoscale cloud features observed from Skylab p0011 N82-12509

CLOUDS

Limit on remote FTIR detection of trace gases [AD-A104842] p0011 N82-12511

COASTAL CURRENTS

Operational use of remote sensing for coastal zone management and possible contribution of specialized satellites --- aerial photography p0031 N82-14574

Mapping of surface currents in Greenland fiords by means of LANDSAT images --- multispectral photography p0038 N82-14579

Necessity of remote sensing for ocean studies. Part 1: Northwest African missions, Sahara-1 and Atlor-1 --- sea truth/remote sensing correlation of offshore upwelling p0032 N82-14582

COASTAL ECOLOGY

Data sources for analyses of Great Lakes wetlands p0035 A82-10054

A marine environmental monitoring and assessment program p0027 N82-10663

A method for using aerial photos in delineating historic patterns of beach accretion and retreat [PB81-223836] p0010 N82-11536

Requirements in pollution monitoring and coastal management p0030 N82-14558

Studies of the Indian continental shelf: Application of remote sensing data p0031 N82-14569

Operational use of remote sensing for coastal zone management and possible contribution of specialized satellites --- aerial photography p0031 N82-14574

COASTAL WATER

Satellite imagery and shoreline erosion prediction p0036 A82-12595

Clear water radiances for atmospheric correction of coastal zone color scanner imagery p0025 A82-17292

The use of satellite infrared imagery for describing ocean processes in relation to spawning of the northern anchovy /Engraulis mordax/ p0025 A82-17565

An inertially-aided aircraft track recovery system for coastal mapping p0037 A82-18166

The ice-conditions in the Greenland waters, 1965. Coastal maps [ISBN-87-7478-183-9] p0026 N82-10467

Analysis of testbed airborne multispectral scanner data from Superflux II --- Chesapeake Bay plume and James Shelf data p0027 N82-10682

COMPUTER TECHNIQUES

The need for integrated off-shore, real-time information and management systems p0055 N82-14555

The color of the sea and its relation to surface chlorophyll and depth of the euphotic zone p0030 N82-14562

SPOT data simulations: Littoral applications p0046 N82-14568

A short review of an oceanographic use of Meteorosat data by the ORSTOM remote sensing service p0031 N82-14570

Coastal zone research using remote sensing techniques --- calibration of coastal zone color scanner p0031 N82-14571

Marine activities in Sweden for which remote sensing data may be of interest --- oceanography, weather forecasting, and analysis p0031 N82-14576

Airborne remote sensing of the coastal zone p0053 N82-14577

The use of LANDSAT MSS to observe sediment distribution and movement in the Solent coastal area --- multispectral scanner (MSS) p0038 N82-14580

The feasibility of using remotely sensed color as an index of Irish coastal water properties --- statistical correlation of sea truth data p0032 N82-14581

Use of Side Looking Airborne Radar (SLAR) for oil pollution monitoring in Norway p0012 N82-14588

COASTAL ZONE COLOR SCANNER

Clear water radiances for atmospheric correction of coastal zone color scanner imagery p0025 A82-17292

Development of the coastal zone color scanner for NIMBUS 7, Volume 1: Mission objectives and instrument description [NASA-CR-166720-VOL-1] p0028 N82-11511

Coastal zone research using remote sensing techniques --- calibration of coastal zone color scanner p0031 N82-14571

COASTS

Remote sensing contributions to the management of renewable resources p0055 A82-12530

Development of a coastal relief of the Gulf of Riga, based on results of an analysis of space images p0024 A82-15962

Application of remote sensing data on the continental shelf: Proceedings of an EAReL-ESA Symposium [ESA-SP-167] p0029 N82-14553

COLOR CODING

Spectral correlation filters and natural colour coding p0043 A82-16160

COLOR INFRARED PHOTOGRAPHY

Area-wide soil loss predictions using CIR airphotos p0007 A82-12591

COLOR TELEVISION

The 1981 RCA space constellation p0055 A82-12541

COLORADO

Preliminary results of mapping urban land cover with Seasat SAR imagery p0007 A82-10044

COLORADO PLATEAU (US)

Morphostructural analyses of space imagery in the central Colorado Plateau p0019 N82-10465

Geological features of southwestern North America p0020 N82-12495

COMPUTER GRAPHICS

Digital image technology - MC&G impact --- Mapping, Charting, & Geodesy p0015 A82-10028

Applications of digital displays in photointerpretation and digital mapping p0041 A82-10038

Digitizing and automated output mapping errors p0015 A82-10859

Interactive techniques for estimating precipitation from GOES imagery p0041 A82-13121

Small-scale terrain mapping based on numerical interpretation of LANDSAT imagery [VT-40] p0045 N82-10485

COMPUTER PROGRAMS

Compensation of systematic errors in bundle adjustment p0042 A82-15764

The application of programmable pocket calculators for computations during survey flights p0050 A82-16164

Programs for the statistical analysis of multispectral photographs p0044 A82-16628

Onboard utilization of ground control points for image correction. Volume 3: Ground control point simulation software design [NASA-CR-166733] p0045 N82-10471

Onboard utilization of ground control points for image correction. Volume 4: Correlation analysis software design [NASA-CR-166734] p0045 N82-10472

Magnetic Field Satellite (Magsat) data processing system specifications [NASA-CR-166737] p0045 N82-11103

COMPUTER SYSTEMS DESIGN

ERSYS-SPP access method subsystem design specification [E82-10015] p0053 N82-15493

COMPUTER TECHNIQUES

Mapping of the 1978 Kentucky River Flood from NOAA-5 satellite thermal infrared data p0035 A82-10033

Water temperature mapping by infrared scanner p0036 A82-12598

- Identification of conifer species groupings from Landsat digital classifications p0002 A82-12887
A new method for computing distortion p0016 A82-12914
- Cost effective computer processing of airborne scanner data for regional level mapping p0043 A82-15970
Analog methods for processing multispectral photographs p0044 A82-16623
Processing of multispectral image data on special-purpose computer systems p0044 A82-16627
- COMPUTERIZED SIMULATION**
SPOT data simulations: Littoral applications p0046 A82-14568
- CONFERENCES**
American Society of Photogrammetry, Annual Meeting, 46th, St. Louis, MO, March 9-14, 1980, ASP Technical Papers p0041 A82-10027
Civil engineering applications of remote sensing: Proceedings of the Specialty Conference, University of Wisconsin, Madison, WI, August 13, 14, 1980 p0035 A82-12589
Chesapeake Bay Plume Study: Superflux 1980 [NASA-CP-2188] p0026 A82-10661
Application of remote sensing data on the continental shelf: Proceedings of an EARL-ESA Symposium [ESA-SP-167] p0029 A82-14553
- CONGRESSIONAL REPORTS**
Civil land remote sensing systems [GPO-35-265] p0056 A82-15497
- CONIFERS**
Identification of conifer species groupings from Landsat digital classifications p0002 A82-12887
- CONTINENTAL SHELVES**
Analysis of testbed airborne multispectral scanner data from Superflux II --- Chesapeake Bay plume and James Shelf data p0027 A82-10682
Assessment of Superflux relative to remote sensing --- airborne remote sensing of the Chesapeake Bay plume and shelf regions p0028 A82-10694
Application of remote sensing data on the continental shelf: Proceedings of an EARL-ESA Symposium [ESA-SP-167] p0029 A82-14553
Studies of the Indian continental shelf: Application of remote sensing data p0031 A82-14569
- COORDINATE TRANSFORMATIONS**
Coordinate referencing of MKF-6 photographs and their transformation to the cartographic projection p0045 A82-16630
- COORDINATES**
MAGSAT: Vector magnetometer absolute sensor alignment determination [NASA-TM-79648] p0051 A82-10468
- CORN**
Temporal spectral response of a corn canopy p0002 A82-12886
Temporal relationships between spectral response and agronomic variables of a corn canopy p0002 A82-15038
Remote sensing of crop moisture status p0003 A82-17997
- COST EFFECTIVENESS**
Landsat imagery for hydrologic modeling p0036 A82-12592
- COVARIANCE**
Estimation of atmospheric path-radiance by the covariance matrix method p0041 A82-10861
- CROP CALENDARS**
Development and evaluation of an automatic labeling technique for spring small grains [EB2-10001] p0004 A82-15480
US/Canada wheat and barley crop calendar exploratory experiment implementation plan [EB2-10016] p0005 A82-15494
- CROP GROWTH**
Spectral behavior of wheat yield variety trials p0002 A82-10863
The discrimination of winter wheat using a growth-state signature p0002 A82-15026
- CROP IDENTIFICATION**
Limitations in the spectral discrimination of the Landsat MSS p0001 A82-10046
Temporal spectral response of a corn canopy p0002 A82-12886
Methods of instrumental interpretation of multispectral aerial and space photographs p0043 A82-16607
- CROP INVENTORIES**
Remote sensing for vineyard management p0001 A82-10047
Temporal relationships between spectral response and agronomic variables of a corn canopy p0002 A82-15038
Development and evaluation of an automatic labeling technique for spring small grains [EB2-10001] p0004 A82-15480
Wheat cultivation: Identification and estimation of areas using LANDSAT data [EB2-10007] p0004 A82-15485
Fiscal year 1980-81 implementation plan in support of technical development and integration of sampling and aggregation procedures --- crop acreage estimation [EB2-10013] p0005 A82-15491
- CROP VIGOR**
The effect of angular factors on popularly used indicators of vegetative vigor p0001 A82-10039
Remote sensing for vineyard management p0001 A82-10047
- Remote sensing of crop moisture status p0003 A82-17997
- Winterkill indicator model, Crop Condition Assessment Division (CCAD) data base interface driver, user's manual [EB2-10014] p0005 A82-15492
- CROSS POLARIZATION**
SMRM data set development for GARP --- impact of cross polarization and Faraday rotation on SMRM derived brightness temperatures [NASA-CR-166721] p0052 A82-11512
Radar correlation with ice depolarization measurements of the 28.56 GHz COMSTAR beacon and associated cross polarization statistics [NASA-CR-166717] p0046 A82-14548
- CRUSTAL FRACTURES**
Remote structural study of sinkhole occurrence p0019 A82-12590
Morphostructural analyses of space imagery in the central Colorado Plateau p0019 A82-10465
- CURRENT SHEETS**
Distant magnetic field effects associated with Birkeland currents /made possible by the evaluation of TRIAD's attitude oscillations/ p0015 A82-12215
- CYCLONES**
An investigation of a polar low with a spiral cloud structure p0007 A82-10616
Upper tropospheric cyclonic vortices in the tropical South Atlantic p0009 A82-16325
Meteorological lab applications of Skylab handheld-camera photographs p0011 A82-12506
- D**
- DAMS**
Application of Landsat to the inventory of DAMS p0036 A82-12593
- DATA ACQUISITION**
LANDSAT-2 and LANDSAT-3 flight evaluation report, 23 April to 23 July 1979 [EB2-10005] p0053 A82-15483
LANDSAT-2 and LANDSAT-3 flight evaluation report, 23 October 1978 to 23 January 1979 [EB2-10017] p0054 A82-15495
- DATA BASES**
The SACLANTCEN oceanographic data base. Volume 1: Design criteria and data structure and content [AD-A103277] p0029 A82-13639
- DATA COMPRESSION**
Data compression and reconstruction for mixed resolution multispectral sensors p0049 A82-10045
- DATA CORRELATION**
Factorial analysis of terrain feature positioning parameters used in combining radar and digital terrain model data p0015 A82-10029
A digital fast correlation approach to produce SEASAT SAR imagery p0042 A82-14870
Interpolating for the location of remote sensor data [NASA-TM-82169] p0052 A82-13469
- DATA PROCESSING**
U.S. Navy planning for satellite oceanographic data exploitation [AAS 81-072] p0024 A82-16341
Magnetic Field Satellite (Magsat) data processing system specifications [NASA-CR-166737] p0045 A82-11103
Analysis of soil moisture extraction algorithm using data from aircraft experiments [NASA-CR-166719] p0046 A82-13470
Development and evaluation of an automatic labeling technique for spring small grains [EB2-10001] p0004 A82-15480
ERSYS-SPP access method subsystem design specification [EB2-10015] p0053 A82-15493
- DATA PROCESSING EQUIPMENT**
MATE VAN: Mobile analysis and training extension --- analyzing LANDSAT digital data [NASA-TM-84056] p0045 A82-10466
- DATA REDUCTION**
Bureau of Land Management satellite Doppler positioning techniques p0015 A82-10057
A closer examination of the reduction of satellite magnetometer data for geological studies p0019 A82-11039
A new method for inferring carbon monoxide concentrations from gas filter radiometer data p0009 A82-16837
MATE VAN: Mobile analysis and training extension --- analyzing LANDSAT digital data [NASA-TM-84056] p0045 A82-10466
Seasat altimetry adjustment model including tidal and other sea surface effects [AD-A104188] p0026 A82-10473
Statistical Techniques Applied to Aerial Radiometric Surveys (STAARS): Series introduction and the principal-components-analysis method --- National Uranium Resource Evaluation Program [DEB1-029177] p0019 A82-10476
The reduction, verification and interpretation of Magsat magnetic data over Canada [EB2-10006] p0046 A82-15484
- DATA SAMPLING**
Fiscal year 1980-81 implementation plan in support of technical development and integration of sampling and aggregation procedures --- crop acreage estimation [EB2-10013] p0005 A82-15491
Analysis of satellite observations: Theoretical studies on the sampling problem [MITT-31] p0056 A82-15499
- DATA SYSTEMS**
The Control Point Library Building System --- for Landsat MSS and RBV geometric image correction p0043 A82-15971
U.S. Navy planning for satellite oceanographic data exploitation [AAS 81-072] p0024 A82-16341
- DECIDUOUS TREES**
Evaluation of digital photographic enhancement for Dutch elm disease detection p0002 A82-12884
- DEER**
A proposal for continuation of support for the application of remotely sensed data to state and regional problems. Part 1: Technical proposal [EB2-10018] p0056 A82-15496
- DEForestation**
Remote sensing in forestry: Application to the Amazon region [EB2-10012] p0005 A82-15490
- DELAWARE**
In situ spectral reflectance studies of tidal wetland grasses p0036 A82-15969
- DELAWARE BAY (US)**
Remote sensing of the Chesapeake Bay plume salinity via microwave radiometry p0027 A82-10670
- DELTA**
Study of the dynamics of the Danube delta using space images p0036 A82-15961
- DEPOLARIZATION**
Radar correlation with ice depolarization measurements of the 28.56 GHz COMSTAR beacon and associated cross polarization statistics [NASA-CR-166717] p0046 A82-14548
- DESERTS**
Study of the anthropogenic influence on the environment, based on multispectral scanning images p0008 A82-15965
Space photographs obtained with the Fragment system as a base for landscape mapping and physical-geographical classification of arid territories p0009 A82-15967
Desert sand seas p0020 A82-12493
- DIGITAL DATA**
Factorial analysis of terrain feature positioning parameters used in combining radar and digital terrain model data p0015 A82-10029
Phytocoenozation of Sevier Lake region of Utah using digitized Landsat MSS data p0001 A82-10042
Wheat cultivation: Identification and estimation of areas using LANDSAT data [EB2-10007] p0004 A82-15485
- DIGITAL TECHNIQUES**
American Society of Photogrammetry, Annual Meeting, 46th, St. Louis, MO, March 9-14, 1980, ASP Technical Papers p0041 A82-10027
Digital image technology - MC&G impact --- Mapping, Charting, & Geodesy p0015 A82-10028
Applications of digital displays in photointerpretation and digital mapping p0041 A82-10038
Digitizing and automated output mapping errors p0015 A82-10859
Digital mapping using entities - A new concept p0041 A82-12882
Evaluation of digital photographic enhancement for Dutch elm disease detection p0002 A82-12884
A digital fast correlation approach to produce SEASAT SAR imagery p0042 A82-14870
The use of digitally processed Landsat imagery for vegetation mapping in Sulawesi, Indonesia p0003 A82-17998
Small-scale terrain mapping based on numerical interpretation of LANDSAT imagery [VTT-40] p0045 A82-10485
Some aspects of tropical storm structure revealed by handheld-camera photographs from space p0011 A82-12507
Seasat SAR processing at the Norwegian Defence Research Establishment --- design and operation of a digital process p0046 A82-14584
Maritime applications of image processing at DFVLR, Oberpfaffenhofen, West Germany --- LANDSAT multispectral scanner images, digital interactive image analysis p0032 A82-14585
- DISTORTION**
A new method for computing distortion p0016 A82-12914
- DISTRICT OF COLUMBIA**
Adaptation of land use to surficial geology in metropolitan Washington, D.C. p0010 A82-11718
- DOMESTIC SATELLITE COMMUNICATIONS SYSTEMS**
ISRO satellite mission support facilities - Scope and future plans p0055 A82-17307
- DOPPLER EFFECT**
Report of survey for McDonald Observatory, Harvard Radio Astronomy Station, and vicinity [PB81-234338] p0016 A82-13606

DOPPLER RADAR

- Application of satellite Doppler techniques to the national mapping program p0015 A82-10056
- Bureau of Land Management satellite Doppler positioning techniques p0015 A82-10057

DRAINAGE PATTERNS

- Morphostructural analyses of space imagery in the central Colorado Plateau p0019 N82-10465
- Report on Skylab 4 African drought and arid land experiment p0037 N82-12501
- Quantitative analysis of drainage obtained from aerial photographs and RBV/LANDSAT images [E82-10008] p0039 N82-15486

DROUGHT

- Report on Skylab 4 African drought and arid land experiment p0037 N82-12501

DUNES

- Desert sand seas p0020 N82-12493

DYNAMICS EXPLORER SATELLITES

- Magnetic field observations on DE-A and -B --- Dynamics Explorer A and B satellites p0051 A82-16447

E**EARTH ALBEDO**

- The surface albedo of the earth in the near ultraviolet /330-340 nm/ p0016 A82-15032

EARTH ATMOSPHERE

- Nitric oxide delta band emission in the earth's atmosphere
- Comparison of a measurement and a theory p0008 A82-13268

EARTH CRUST

- Space techniques to monitor movements in the earth's crust p0016 A82-18797
- The mineralogy of global magnetic anomalies [E82-10009] p0021 N82-15487

EARTH MOVEMENTS

- Space techniques to monitor movements in the earth's crust p0016 A82-18797

EARTH OBSERVATIONS (FROM SPACE)

- Skylab explores the Earth [NASA-SP-380] p0019 N82-12492

EARTH RESOURCES INFORMATION SYSTEM

- Civil land remote sensing systems [GPO-35-265] p0056 N82-15497

EARTH SURFACE

- Thermal inertia, thermal admittance, and the effect of layers p0008 A82-15027
- The surface albedo of the earth in the near ultraviolet /330-340 nm/ p0016 A82-15032
- Metrological support of measurements of earth-surface brightness by the Fragment multispectral scanning system p0050 A82-15958

ECOLOGY

- Use of visible and thermal satellite data to monitor an intermittently flooding marshland p0036 A82-15037
- A proposal for continuation of support for the application of remotely sensed data to state and regional problems. Part 1: Technical proposal [E82-10018] p0056 N82-15496

ECONOMIC IMPACT

- Overall economic impact of an operational Meteorosat system [ESA-CR(P)-1457] p0055 N82-13010

ECOSYSTEMS

- Phytoecozonation of Sevier Lake region of Utah using digitized Landsat MSS data p0001 A82-10042
- Chesapeake Bay Plume Study: Superflux 1980 [NASA-CP-2188] p0026 N82-10661
- Superflux I, II, and III experiment design: Remote sensing aspects p0027 N82-10664
- Superflux I, II, and III experiment designs: Water sampling and analyses --- Chesapeake Bay, environmental monitoring and remote sensing p0027 N82-10665
- Deep Ocean Mining Environmental Study. Environmental effects of commercial-scale mining [PB81-227753] p0029 N82-13484

ECUADOR

- Skylab 4 observations of Volcanoes. Part A: Volcanoes and volcanic landforms. Part B: Summit eruption of Fernandian Caldera, Galapagos Islands, Ecuador p0020 N82-12496

EDUCATIONAL TELEVISION

- ISRO satellite mission support facilities - Scope and future plans p0055 A82-17307

EISCAT RADAR SYSTEM (EUROPE)

- A Swedish proposal for an EISCAT/GEOS-2 experiment --- geomagnetic field models [KGI-175] p0052 N82-10484

EJECTA

- Satellite observations of the Mt. St. Helens' eruption of 18 May 1980 [AD-A105784] p0012 N82-14591

ELECTROMAGNETIC FIELDS

- Radiative transfer theory for passive microwave remote sensing of random media p0049 A82-11533

EMISSION SPECTRA

- Nitric oxide delta band emission in the earth's atmosphere
- Comparison of a measurement and a theory p0008 A82-13268

EMISSIVITY

- Reflectivity and emissivity of snow and ground at mm waves p0042 A82-14860

ENGLAND

- The use of LANDSAT MSS to observe sediment distribution and movement in the Solent coastal area --- multispectral scanner (MSS) p0038 N82-14580

ENVIRONMENTAL EFFECTS

- Deep Ocean Mining Environmental Study. Environmental effects of commercial-scale mining [PB81-227753] p0029 N82-13484

ENVIRONMENTAL MANAGEMENT

- Requirements in pollution monitoring and coastal management p0030 N82-14558

ENVIRONMENTAL MONITORING

- Civil engineering applications of remote sensing; Proceedings of the Specialty Conference, University of Wisconsin, Madison, WI, August 13, 14, 1980 p0035 A82-12589
- Use of visible and thermal satellite data to monitor an intermittently flooding marshland p0036 A82-15037
- Study of the anthropogenic influence on the environment, based on multispectral scanning images p0008 A82-15965
- ISRO satellite mission support facilities - Scope and future plans p0055 A82-17307
- User needs and the future of operational meteorological satellites p0051 A82-17918

- [AIAA PAPER 82-0388] p0051 A82-17918
- The radiowave propagation environment - Science and technology objectives for the 80's p0009 A82-18052
- A marine environmental monitoring and assessment program p0027 N82-10663
- Superflux I, II, and III experiment design: Remote sensing aspects p0027 N82-10664
- Superflux I, II, and III experiment designs: Water sampling and analyses --- Chesapeake Bay, environmental monitoring and remote sensing p0027 N82-10665
- Monitoring the Chesapeake Bay using satellite data for Superflux III p0027 N82-10668

- Shuttle applications in tropospheric air quality observations [NASA-CR-145374] p0010 N82-11635
- Environmental Monitoring Report, Sandia National Labs., Albuquerque, New Mexico, 180 p0010 N82-11649

- Snow-mapping experiment p0037 N82-12498
- Quantitative analysis of atmospheric pollution phenomena p0010 N82-12505
- Limit on remote FTIR detection of trace gases [AD-A104842] p0011 N82-12511

- Environmental data for sites in the National Solar Data Network [DE82-000071] p0011 N82-12707
- Special observations by the Hohenpeissenberg Meteorological Observatory. Number 42: Results of aerological and surface ozone measurements during the first semester of 1980 p0012 N82-12714

- Aircraft data summaries of the SURE intensives, volume 4 [DE82-900311] p0012 N82-13569

- ERS-1: Mission objectives and system concept p0029 N82-14554
- The need for integrated off-shore, real-time information and management systems p0055 N82-14555

- Offshore petroleum industry environmental data requirements: Emphasis on remote sensing p0030 N82-14557
- Fisheries investigations and management benefits from remote sensing --- fish tracking p0030 N82-14559

- A look at nonsatellite remote sensing systems for marine use --- together with satellite systems, overall view of the technology p0032 N82-14586
- Study of a combined satellite system for remote sensing and earth-oriented research (LOCSS) --- ESA satellite [BMFT-FB-W-81-002] p0055 N82-14615

- Meteorological satellites [AD-A107427] p0053 N82-15110
- Investigation of the application of remote sensing technology to environmental monitoring [E82-10010] p0013 N82-15488
- National Hurricane operations plan [PB81-247231] p0013 N82-15697

- Environmental satellite imagery, March 1981 [PB81-248049] p0047 N82-15698

EQUATORIAL REGIONS

- CTD/O2 measurements during the Equatorial Pacific Ocean Climate Study (EPOCS) in 1979 [PB81-211203] p0026 N82-10461

EROSION

- Satellite imagery and shoreline erosion prediction p0036 A82-12595
- A method for using aerial photos in delineating historic patterns of beach accretion and retreat [PB81-223836] p0010 N82-11536
- Airborne remote sensing of the coastal zone p0053 N82-14577

ERROR ANALYSIS

- Factorial analysis of terrain feature positioning parameters used in combining radar and digital terrain model data p0015 A82-10029
- Digitizing and automated output mapping errors p0015 A82-10859
- Concerning the geometric accuracy of infrared scanner photographs p0042 A82-13634
- Some problem areas in the field of quality control for aerotriangulation p0016 A82-16161

ERROR CORRECTING DEVICES

- Block adjustment with additional parameters p0049 A82-13738
- The MSS control point location error filter for LANDSAT-D p0051 N82-10073

ERS-1 (ESA SATELLITE)

- ERS-1: Mission objectives and system concept p0029 N82-14554

ESA SATELLITES

- Study of a combined satellite system for remote sensing and earth-oriented research (LOCSS) --- ESA satellite [BMFT-FB-W-81-002] p0055 N82-14615

ESTUARIES

- Field study for Landsat water quality verification p0036 A82-12597
- Remote sensing of benthic microalgal biomass with a tower-mounted multispectral scanner p0024 A82-15031
- Chesapeake Bay Plume Study: Superflux 1980 [NASA-CP-2188] p0026 N82-10661
- Superflux I, II, and III experiment design: Remote sensing aspects p0027 N82-10664
- Remote sensing of the Chesapeake Bay plume salinity via microwave radiometry p0027 N82-10670
- Preliminary analysis of ocean color scanner data from Superflux III p0027 N82-10672
- SPOT data simulations: Littoral applications p0046 A82-14568

- The use of LANDSAT MSS to observe sediment distribution and movement in the Solent coastal area --- multispectral scanner (MSS) p0038 N82-14580

EUROPE

- Spacelab-research of European regions with strong negative environmental influences, based on AVHRR data of the satellites Tiros-N and NOAA p0007 A82-12517
- Availability of Seasat synthetic aperture radar imagery p0050 A82-15039

EUTROPHICATION

- The operational use of Landsat for lake quality assessment p0036 A82-12596

EVAPOTRANSPIRATION

- A simulation study of the recession coefficient for antecedent precipitation index --- soil moisture and water runoff estimation [NASA-TM-83860] p0038 N82-14549

F**FARADAY EFFECT**

- SMMR data set development for GARP --- impact of cross polarization and Faraday rotation on SMMR derived brightness temperatures [NASA-CR-166721] p0052 N82-11512

FARMLANDS

- Satellite sensing of irrigation patterns in semiarid areas - An Indian study p0002 A82-10864
- Study and mapping of agricultural land use, based on space images p0003 A82-15963
- Aircraft radar response to soil moisture p0003 A82-17564
- Vegetation patterns p0004 A82-12500

FIELD OF VIEW

- The choice of the orientation of the analyzer in polarimetric surveys p0044 A82-16621
- Scanner --- photography from a spin stabilized synchronous satellite [NASA-CASE-GSC-12032-2] p0052 N82-13465
- Interpolating for the location of remote sensor data [NASA-TM-82169] p0052 N82-13469

FINLAND

- Compensation of systematic errors of image and model coordinates p0043 A82-15765
- Small-scale terrain mapping based on numerical interpretation of LANDSAT imagery [VTT-40] p0045 N82-10485

FLOODS

- Mapping of surface currents in Greenland fiords by means of LANDSAT images --- multispectral photography p0038 N82-14579

FIRES

- Quantitative analysis of atmospheric pollution phenomena p0010 N82-12505

FISHERIES

- The use of satellite infrared imagery for describing ocean processes in relation to spawning of the northern anchovy /Engraulis mordax/ p0025 A82-17565
- Application of remote sensing data on the continental shelf: Proceedings of an EARL-ESA Symposium [ESA-SP-167] p0029 N82-14553
- Fisheries investigations and management benefits from remote sensing --- fish tracking p0030 N82-14559
- The Seasat commercial demonstration program p0030 N82-14561
- A short review of an oceanographic use of Meteorosat data by the ORSTOM remote sensing service p0031 N82-14570

FLIGHT TESTS

- Three bearing method for passive triangulation in systems with unknown deterministic biases p0050 A82-15920

FLOOD PLAINS

- Mapping of the 1978 Kentucky River Flood from NOAA-S satellite thermal infrared data p0035 A82-10033

FLOOD PREDICTIONS

- Satellite rainfall estimation for hydrologic forecasting p0035 A82-10032

A systems approach to the real-time runoff analysis with a deterministic rainfall-runoff model
[PB81-224495] p0037 N82-11530
Analysis of rainfall from flash flood producing thunderstorms, using GOES data p0038 N82-14724

FLOODS

Use of visible and thermal satellite data to monitor an intermittently flooding marshland p0036 A82-15037
Cost effective computer processing of airborne scanner data for regional level mapping p0043 A82-15970

FLORIDA

Field study for Landsat water quality verification p0036 A82-12597
Optically processed Seasat radar mosaic of Florida p0042 A82-15125

FLUORESCENCE

Application of the NASA airborne oceanographic lidar to the mapping of chlorophyll and other organic pigments p0027 N82-10684
A recommended sensor package for the detection and tracking of oil spills p0053 N82-14563

FOREST FIRES

Quantitative analysis of atmospheric pollution phenomena p0010 N82-12505

FOREST MANAGEMENT

A VHF homing system with VHF radiotelephony for area-representative strip-survey flights conducted, as part of combined forest inventories, with light aircraft carrying 70 mm and 35 mm cameras p0003 A82-15748
Rural development in the humid tropics p0003 A82-16162
Large-scale color aerial photography as a tool in sampling for mortality rates p0003 N82-10489
[PB81-214777]

FORESTS

Mapping vegetation association boundaries with Landsat MSS data - An Oklahoma example p0001 A82-10041
Stand density estimation on panoramic transparencies p0002 A82-10862
Remote sensing contributions to the management of renewable resources p0055 A82-12530
Identification of conifer species groupings from Landsat digital classifications p0002 A82-12887
Mapping of forest vegetation on the basis of space images p0003 A82-15964
Study of the anthropogenic influence on the environment, based on multispectral scanning images p0008 A82-15965

The use of digitally processed Landsat imagery for vegetation mapping in Sulawesi, Indonesia p0003 A82-17998
Vegetation patterns p0004 N82-12500
Application of remote sensing to selected problems within the state of California p0004 N82-15482

Remote sensing in forestry: Application to the Amazon region p0005 N82-15490
[E82-10012]

FRAMING CAMERAS

Orientation and construction of models. I - The orientation problem in close-range photogrammetry p0049 A82-10858

FRANCE

The operational oil pollution surveillance system being used in France: Forecasted future developments in consideration of the NATO/CCMS remote sensing pilot study conclusions p0012 N82-14573

FRESH WATER

Recent work in passive optical imaging of water --- space and aircraft derived data p0038 N82-14575

FRONTS (METEOROLOGY)

An investigation of a polar low with a spiral cloud structure p0007 A82-10616

G**GALEIAN SATELLITES**

Coordinates of features on the Galilean satellites p0019 A82-12366

GAS ANALYSIS

A new method for inferring carbon monoxide concentrations from gas filter radiometer data p0009 A82-16837
Proof of concept study [AD-A104338] p0010 N82-11639

GEOCHRONOLOGY

Study of the time evolution of the lithosphere [NASA-CR-164968] p0016 N82-11696

GEODESY

Digital image technology - MC&G impact --- Mapping, Charting, & Geodesy p0015 A82-10028
Space techniques to monitor movements in the earth's crust p0016 A82-18797
Study of the time evolution of the lithosphere [NASA-CR-164968] p0016 N82-11696
Reports of Planetary Geology Program, 1981 [NASA-TM-84211] p0016 N82-14041
Description and comparison of algorithms for solving large sets of sparse matrix normal equations in geodesy and photogrammetry [SER-C-261] p0017 N82-15812

GEODETTIC SURVEYS

Application of satellite Doppler techniques to the national mapping program p0015 A82-10056

Bureau of Land Management satellite Doppler positioning techniques p0015 A82-10057

GPS application to mapping, charting and geodesy p0015 A82-10645

Phototriangulation with map referencing of photographs in linear surveys p0016 A82-12912

Some problem areas in the field of quality control for aerotriangulation p0016 A82-16161

Theoretical reliability of elementary photogrammetric procedures. I p0043 A82-16163

Report of survey for McDonald Observatory, Harvard Radio Astronomy Station, and vicinity [PB81-234338] p0016 N82-13606

A history of flying and photography: In the Photogrammetry Division of the National Ocean Survey 1919 - 1979 p0017 N82-15520
[PB81-246738]

GEOLOGICAL FAULTS

Morphostructural analyses of space imagery in the central Colorado Plateau p0019 N82-10465

Global Tectonics: Some Geologic analyses of observations and photographs from Skylab p0020 N82-12494

GEOLOGICAL SURVEYS

A closer examination of the reduction of satellite magnetometer data for geological studies p0019 A82-11039

Coordinates of features on the Galilean satellites p0019 A82-12366

Statistical Techniques Applied to Aerial Radiometric Surveys (STAARS): Series introduction and the principal-components-analysis method --- National Uranium Resource Evaluation Program p0019 N82-10476

Skylab explores the Earth [NASA-SP-380] p0019 N82-12492

Global Tectonics: Some Geologic analyses of observations and photographs from Skylab p0020 N82-12494

Geological features of southwestern North America p0020 N82-12495

Skylab 4 observations of Volcanoes. Part A: Volcanoes and volcanic landforms. Part B: Summit eruption of Fernandian Caldera, Galapagos Islands, Ecuador p0020 N82-12496

The Manicouagan impact structure observed from Skylab [CONTRIB-544] p0020 N82-12497

Geologic applications of thermal-inertia mapping from satellite --- Powder River, Wyoming; Cubeza Prieta, Arizona, and Yellowstone National Park [E82-10011] p0021 N82-15489

Preliminary analysis of gravity and aeromagnetic surveys of the Timber Mountain area, southern Nevada [DE81-029462] p0022 N82-15506

Geology and linears of Libya p0019 N82-10618

Adaptation of land use to surficial geology in metropolitan Washington, D.C. p0010 N82-11718

Geomagnetism

A closer examination of the reduction of satellite magnetometer data for geological studies p0019 A82-11039

Magnetic field-aligned electron distributions in the dayside cusp p0015 A82-12186

Distant magnetic field effects associated with Birkeland currents /made possible by the evaluation of TRIAD's attitude oscillations/ p0015 A82-12215

Magnetic field observations on DE-A and -B --- Dynamics Explorer A and B satellites p0051 A82-16447

Use of hydromagnetic waves to map geomagnetic field lines p0016 A82-16868

A Swedish proposal for an EISCAT/GEOS-2 experiment --- geomagnetic field models [KGI-175] p0052 N82-10484

Magnetic Field Satellite (Magsat) data processing system specifications [NASA-CR-166737] p0045 N82-11103

The mineralogy of global magnetic anomalies [E82-10009] p0021 N82-15487

Geometric Rectification (IMAGERY)

Factorial analysis of terrain feature positioning parameters used in combining radar and digital terrain model data p0015 A82-10029

Two-dimensional resampling of line scan imagery by one-dimensional processing p0041 A82-10860

Digital mapping using entities - A new concept p0041 A82-12882

A new method for computing distortion p0016 A82-12914

Concerning the geometric accuracy of infrared scanner photographs p0042 A82-13634

Block adjustment with additional parameters p0049 A82-13738

Compensation of systematic errors in bundle adjustment p0042 A82-15764

Compensation of systematic errors of image and model coordinates p0043 A82-15765

The Control Point Library Building System --- for Landsat MSS and RBV geometric image correction p0043 A82-15971

Computational aspects of geometric correction data generation in the LANDSAT-D imagery processing p0045 N82-10072

GEOMORPHOLOGY

Development of a coastal relief of the Gulf of Riga, based on results of an analysis of space images p0024 A82-15962

Investigation and mapping of the erosion relief of the Kalachkaia upland on the basis of multispectral scanner images p0008 A82-15966

Space photographs obtained with the Fragment system as a base for landscape mapping and physical-geographical classification of arid territories p0009 A82-15967

Morphostructural analyses of space imagery in the central Colorado Plateau p0019 N82-10465

Desert sand seas p0020 N82-12493

GEOPHYSICS

Analysis of satellite observations: Theoretical studies on the sampling problem [MITT-31] p0056 N82-15499

GEO THERMAL RESOURCES

Geologic applications of thermal-inertia mapping from satellite --- Powder River, Wyoming; Cubeza Prieta, Arizona, and Yellowstone National Park [E82-10011] p0021 N82-15489

GLACIOLOGY

Study on satellite radar altimetry in climatological and oceanographic research, volume 1 [SP/153/06/01/FR(80)-VOL-1] p0026 N82-10486

Study on satellite radar altimetry in climatological and oceanographic research, volume 2 [SP/153/06/01/FR(80)-VOL-2] p0026 N82-10487

GLOBAL AIR POLLUTION

A new method for inferring carbon monoxide concentrations from gas filter radiometer data p0009 A82-16837

GLOBAL ATMOSPHERIC RESEARCH PROGRAM

SMMR data set development for GARP --- impact of cross polarization and Faraday rotation on SMMR derived brightness temperatures [NASA-CR-166721] p0052 N82-11512

GLOBAL POSITIONING SYSTEM

GPS application to mapping, charting and geodesy p0015 A82-10645

Onboard utilization of ground control points for image correction. Volume 1: Executive summary [NASA-CR-166731] p0045 N82-10469

Onboard utilization of ground control points for image correction. Volume 2: Analysis and simulation results [NASA-CR-166732] p0045 N82-10470

Onboard utilization of ground control points for image correction. Volume 3: Ground control point simulation software design [NASA-CR-166733] p0045 N82-10471

Onboard utilization of ground control points for image correction. Volume 4: Correlation analysis software design [NASA-CR-166734] p0045 N82-10472

GOES SATELLITES

User needs and the future of operational meteorological satellites [AIAA PAPER 82-0388] p0051 A82-17918

Government/Industry Relations

The Seasat commercial demonstration program p0030 N82-14561

Grains (Food)

Development and evaluation of an automatic labeling technique for spring small grains [E82-10001] p0004 N82-15480

GRASSES

In situ spectral reflectance studies of tidal wetland grasses p0036 A82-15969

GRASSHOPPERS

Remote sensing applications to resource problems in South Dakota [E82-10002] p0004 N82-15481

GRASSLANDS

The effect of angular factors on popularly used indicators of vegetative vigor p0001 A82-10039

Mapping vegetation association boundaries with Landsat MSS data - An Oklahoma example p0001 A82-10041

GRATINGS (SPECTRA)

The application of holographic gratings in spectrometers for the spatial-spectral analysis of the earth's surface from aerial and space platforms in the visible and near-infrared spectral regions p0044 A82-16614

GRAVELS

Remote sensing studies of some ironstone gravels and plinthite in Thailand p0019 N82-12491

GRAVIMETRY

Preliminary analysis of gravity and aeromagnetic surveys of the Timber Mountain area, southern Nevada [DE81-029462] p0022 N82-15506

GRAVITY WAVES

The influence of gravity waves on radiometric measurements - A case study p0049 A82-13547

GRAZING INCIDENCE

Radar backscattering from ocean waves at low grazing angles p0023 A82-14730

GREAT BASIN (US)

Phytocoenozation of Sevier Lake region of Utah using digitized Landsat MSS data p0001 A82-10042

GREAT LAKES (NORTH AMERICA)

Data sources for analyses of Great Lakes wetlands p0035 A82-10054

GREAT PLAINS CORRIDOR (NORTH AMERICA)

- US/Canada wheat and barley crop calendar exploration experiment implementation plan [E82-10016] p0005 N82-15494

GREENLAND

- Measurement of sea and ice backscatter reflectivity using an OTH radar system p0025 A82-18074
The ice-conditions in the Greenland waters, 1965. Coastal maps [ISBN-87-7478-183-9] p0026 N82-10467
The ice conditions in the Greenland waters [ISBN-87-7478-183-9] p0028 N82-12533
Mapping of surface currents in Greenland fiords by means of LANDSAT images --- multispectral photography p0038 N82-14579

GROUND TRUTH

- The mineralogy of global magnetic anomalies [E82-10009] p0021 N82-15487

GUATEMALA

- Radar mapping, archaeology, and ancient land use in the Maya lowlands [NASA-CR-164931] p0010 N82-11514
Global Tectonics: Some Geologic analyses of observations and photographs from Skylab p0020 N82-12494

GULF OF ALASKA

- An evaluation of Seasat-A data in relation to optimum track ship weather routing and site specific forecasting for the offshore oil industry p0030 N82-14564

GULFS

- Comparison of polar and geostationary satellite infrared observations of sea surface temperatures in the Gulf of Maine p0024 A82-15030
Development of a coastal relief of the Gulf of Riga, based on results of an analysis of space images p0024 A82-15962
Visual observations of floating ice from Skylab p0037 N82-12504

H**HABITATS**

- Repetitive aerial photography for assessing marsh vegetation changes p0001 A82-10048
A proposal for continuation of support for the application of remotely sensed data to state and regional problems. Part 1: Technical proposal [E82-10018] p0056 N82-15496

HAWAII

- A method for using aerial photos in delineating historic patterns of beach accretion and retreat [PB81-223836] p0010 N82-11536
Skylab 4 observations of Volcanoes. Part A: Volcanoes and volcanic landforms. Part B: Summit eruption of Fernandian Caldera, Galapagos Islands, Ecuador p0020 N82-12496

HAZE

- Multitemporal calibration of LANDSAT images: A method for improving the marine phenomena recognition, with as example the Venice lagoon --- brightness/green/yellow feature space, image enhancement p0046 N82-14578

HEAT FLUX

- Thermal inertia, thermal admittance, and the effect of layers p0008 A82-15027

HEAT STORAGE

- Variations in upper ocean heat storage determined from satellite data p0025 A82-17567

HOLOGRAPHY

- The application of holographic gratings in spectrometers for the spatial-spectral analysis of the earth's surface from aerial and space platforms in the visible and near-infrared spectral regions p0044 A82-16614

HOMING DEVICES

- A VHF homing system with VHF radiotelephony for area-representative strip-survey flights conducted, as part of combined forest inventories, with light aircraft carrying 70 mm and 35 mm cameras p0003 A82-15748

HURRICANES

- National Hurricane operations plan [PB81-247231] p0013 N82-15697

HYDROCARBONS

- Automated analyzer for aircraft measurements of atmospheric methane and total hydrocarbons p0007 A82-11949

HYDROGRAPHY

- Application of Landsat to the inventory of DAMS p0036 A82-12593
Study of the dynamics of the Danube delta using space images p0036 A82-15961
Quantitative analysis of drainage obtained from aerial photographs and RBV/LANDSAT images [E82-10008] p0039 N82-15486

HYDROLOGY

- Satellite rainfall estimation for hydrologic forecasting p0035 A82-10032
Civil engineering applications of remote sensing: Proceedings of the Specialty Conference, University of Wisconsin, Madison, WI, August 13, 14, 1980 p0035 A82-12589
Landsat imagery for hydrologic modeling p0036 A82-12592
Field study for Landsat water quality verification p0036 A82-12597

- Operational use of remote sensing for coastal zone management and possible contribution of specialized satellites --- aerial photography p0031 N82-14574
The effect of spatial variability in precipitation on streamflow [AD-A105955] p0038 N82-14589

HYDROLOGY MODELS

- Civil engineering applications of remote sensing: Proceedings of the Specialty Conference, University of Wisconsin, Madison, WI, August 13, 14, 1980 p0035 A82-12589
An application of Landsat derived data to a regional hydrologic model p0037 A82-17999

HYDROMETEOROLOGY

- A systems approach to the real-time runoff analysis with a deterministic rainfall-runoff model [PB81-224495] p0037 N82-11530
A simulation study of the recession coefficient for antecedent precipitation index --- soil moisture and water runoff estimation [NASA-TM-83860] p0038 N82-14549
Meteorological satellites [AD-A107427] p0053 N82-15110

ICE

- Radar correlation with ice depolarization measurements of the 28.56 GHz COMSTAR beacon and associated cross polarization statistics [NASA-CR-166717] p0046 N82-14548

ICE MAPPING

- The ice-conditions in the Greenland waters, 1965. Coastal maps [ISBN-87-7478-183-9] p0026 N82-10467
Ice conditions in the eastern Bering Sea from NOAA and LANDSAT imagery: Winter conditions 1974, 1976, 1977, 1979 [PB81-220188] p0028 N82-11537
The Norwegian remote sensing experiment (Norsex) in a marginal ice zone p0031 N82-14566

ICE REPORTING

- Visual observations of floating ice from Skylab p0037 N82-12504
The ice conditions in the Greenland waters [ISBN-87-7478-183-9] p0028 N82-12533
Marine activities in Sweden for which remote sensing data may be of interest --- oceanography, weather forecasting, and analysis p0031 N82-14576

ILLINOIS

- The effect of spatial variability in precipitation on streamflow [AD-A105955] p0038 N82-14589

IMAGE CONTRAST

- Calculation of the decrease in the contrast of objects of a place due to light scattering in the atmosphere p0042 A82-13633
Estimation of the brightness field from results of multispectral photography of the earth from space p0044 A82-16617
Polarimetric surveys of oil slicks p0009 A82-16619
Images of sea waves obtained in polarimetric surveys p0024 A82-16620
The choice of the orientation of the analyzer in polarimetric surveys p0044 A82-16621

IMAGE ENHANCEMENT

- Evaluation of digital photographic enhancement for Dutch elm disease detection p0002 A82-12884
Multitemporal calibration of LANDSAT images: A method for improving the marine phenomena recognition, with as example the Venice lagoon --- brightness/green/yellow feature space, image enhancement p0046 N82-14578

IMAGE FILTERS

- Spectral correlation filters and natural colour coding p0043 A82-16160

IMAGE PROCESSING

- American Society of Photogrammetry, Annual Meeting, 46th, St. Louis, MO, March 9-14, 1980, ASP Technical Papers p0041 A82-10027
Digital image technology - MC&G impact --- Mapping, Charting, & Geodesy p0015 A82-10028
Mapping of the 1978 Kentucky River Flood from NOAA-5 satellite thermal infrared data p0035 A82-10033
Applications of digital displays in photointerpretation and digital mapping p0041 A82-10038
An improvement in land cover classification achieved by merging microwave data with Landsat multispectral scanner data p0007 A82-10043
Preliminary results of mapping urban land cover with Seasat SAR imagery p0007 A82-10044
Absolute image registration for geosynchronous satellites p0049 A82-10051
Two-dimensional resampling of line scan imagery by one-dimensional processing p0041 A82-10860
Intercalibration of Landsat 1-3 and NOAA 6 and 7 scanner data p0049 A82-13293
Investigations concerning the image-controlled segmentation of objects in multispectral imagery data --- German thesis p0042 A82-15003
Texture transforms of remote sensing data p0042 A82-15034
Optically processed Seasat radar mosaic of Florida p0042 A82-15125

- Analysis of variance of thematic mapping experiment data p0009 A82-15968
Cost effective computer processing of airborne scanner data for regional level mapping p0043 A82-15970
The Control Point Library Building System --- for Landsat MSS and RBV geometric image correction p0043 A82-15971

- Airborne and spaceborne multispectral photography of the earth --- Russian book p0043 A82-16601
Geometric quality of MKF-6 photographs p0043 A82-16606

- The maximum mean accuracy of classification of remote-sensing objects and the influence on this accuracy of data acquisition and processing methods p0044 A82-16615

- Analog methods for processing multispectral photographs p0044 A82-16623
Structural analysis of aerial and space images p0044 A82-16625

- Processing of multispectral image data on special-purpose computer systems p0044 A82-16627
Programs for the statistical analysis of multispectral photographs p0044 A82-16628
Coordinate referencing of MKF-6 photographs and their transformation to the cartographic projection p0045 A82-16630

- The use of digitally processed Landsat imagery for vegetation mapping in Sulawesi, Indonesia p0003 A82-17998

- Distortion-free mapping of VISSR imagery data from geosynchronous satellites p0051 N82-10071
Computational aspects of geometric correction data generation in the LANDSAT-D imagery processing p0045 N82-10072

- MATE VAN: Mobile analysis and training extension --- analyzing LANDSAT digital data [NASA-TM-84056] p0045 N82-10466

- Onboard utilization of ground control points for image correction. Volume 1: Executive summary [NASA-CR-166731] p0045 N82-10469

- Onboard utilization of ground control points for image correction. Volume 2: Analysis and simulation results [NASA-CR-166732] p0045 N82-10470

- Onboard utilization of ground control points for image correction. Volume 3: Ground control point simulation software design [NASA-CR-166733] p0045 N82-10471

- Onboard utilization of ground control points for image correction. Volume 4: Correlation analysis software design [NASA-CR-166734] p0045 N82-10472

- Small-scale terrain mapping based on numerical interpretation of LANDSAT imagery [VT-40] p0045 N82-10485

- Identification of lithologic units using multichannel imaging systems p0046 N82-11509

- Airborne remote sensing of the coastal zone p0053 N82-14577

- Seasat SAR processing at the Norwegian Defence Research Establishment --- design and operation of a digital process p0046 N82-14584

- Maritime applications of image processing at DFVLR, Oberpfaffenhofen, West Germany --- LANDSAT multispectral scanner images, digital interactive image analysis p0032 N82-14585

IMAGE RECONSTRUCTION

- Data compression and reconstruction for mixed resolution multispectral sensors p0049 A82-10045

IMAGE RESOLUTION

- Data compression and reconstruction for mixed resolution multispectral sensors p0049 A82-10045
Aspects in the development of aerial-photography tasks p0041 A82-12913

- A new method for computing distortion p0016 A82-12914

- Characteristics of the photometry of small objects from aerial and space photographs p0044 A82-16616

- Distortion-free mapping of VISSR imagery data from geosynchronous satellites p0051 N82-10071

IMAGE ROTATION

- Two-dimensional resampling of line scan imagery by one-dimensional processing p0041 A82-10860

IMAGING TECHNIQUES

- SAR imaging of ocean waves - Theory p0023 A82-11202

- Study on calibration methods for Earth observation optical imaging instruments [UCD-207/1/80] p0052 N82-10488

- A recommended sensor package for the detection and tracking of oil spills p0053 N82-14563

IN-FLIGHT MONITORING

- Infrared radiance model variation by sensor flight measurements p0052 A82-14171

INCIDENCE

- New baseline system p0054 N82-15501
Squinted SAR system p0047 N82-15502

INDIA

- Satellite sensing of irrigation patterns in semiarid areas An Indian study p0002 A82-10864

- Cost effective computer processing of airborne scanner data for regional level mapping p0043 A82-15970

- Detection of monsoon inversion by TIROS-N satellite p0024 A82-17168

- Studies of the Indian continental shelf: Application of remote sensing data p0031 N82-14569

INDIAN OCEAN
 Analysis of SEASAT wind observations over the Indian Ocean p0023 A82-10671
 ICAPS oceanographic data for the Indian Ocean [AD-A103173] p0029 N82-13641
 An evaluation of Seasat-A data in relation to optimum track ship weather routing and site specific forecasting for the offshore oil industry p0030 N82-14564

INDIAN SPACE PROGRAM
 ISRO satellite mission support facilities - Scope and future plans p0055 A82-17307

INDIAN SPACECRAFT
 Scientific studies using Bhaskara satellite microwave radiometer (SAMIR) data: A short overview --- calibration of the instrument and its use in the study of oceanographic parameters p0032 N82-14587

INDONESIA
 Rural development in the humid tropics p0003 A82-16162
 The use of digitally processed Landsat imagery for vegetation mapping in Sulawesi, Indonesia p0003 A82-17998

INERTIAL NAVIGATION
 Photo inertial positioning system development at the Canada Centre for Remote Sensing p0045 A82-18167

INFESTATION
 Vegetation patterns p0004 N82-12500
 Remote sensing applications to resource problems in South Dakota [E82-10002] p0004 N82-15481

INFRARED ASTRONOMY
 Infrared spectroscopy of microorganisms near 3.4 microns in relation to geology and astronomy [PREPRINT-69] p0020 N82-12713

INFRARED IMAGERY RADIOMETRIC RESOLUTION
 Water temperature mapping by infrared scanner p0036 A82-12598

INFRARED PHOTOGRAPHY
 Concerning the geometric accuracy of infrared scanner photographs p0042 A82-13634

INFRARED RADIATION
 Biological patchiness in relation to satellite thermal imagery and associated chemical mesoscale features [AD-A105757] p0047 N82-15504

INFRARED REFLECTION
 Mapping of the 1978 Kentucky River Flood from NOAA-5 satellite thermal infrared data p0035 A82-10033
 Effect of grain size and snowpack water equivalence on visible and near-infrared satellite observations of snow p0035 A82-12553

INFRARED SPECTRA
 Proof of concept study [AD-A104338] p0010 N82-11639
 Inclusion of a simple vegetation layer in terrain temperature models for thermal infrared (IR) signature prediction [AD-A104469] p0003 N82-11910
 Satellite observations of the Mt. St. Helens' eruption of 18 May 1980 [AD-A105784] p0012 N82-14591

INFRARED SPECTROSCOPY
 Trace pollutant concentrations in a midday smog episode in the California South Coast Air Basin by long path length Fourier transform infrared spectroscopy p0007 A82-10700
 Infrared spectroscopy of microorganisms near 3.4 microns in relation to geology and astronomy [PREPRINT-69] p0020 N82-12713

INFRARED TRACKING
 Satellite observations of the Mt. St. Helens' eruption of 18 May 1980 [AD-A105784] p0012 N82-14591

INLAND WATERS
 The operational use of Landsat for lake quality assessment p0036 A82-12596
 An inertially-aided aircraft track recovery system for coastal mapping p0037 A82-18166

INSOLATION
 Environmental data for sites in the National Solar Data Network [DE82-000071] p0011 N82-12707

INSTRUMENT ERRORS
 Ionospheric propagation correction modeling for satellite altimeters [NASA-CR-156881] p0052 N82-12447

INSTRUMENT ORIENTATION
 Orientation and construction of models. III - Mathematical basis of the orientation problem of one-dimensional central perspective photographs p0043 A82-15973
 Images of sea waves obtained in polarimetric surveys p0024 A82-16620
 The choice of the orientation of the analyzer in polarimetric surveys p0044 A82-16621
 An inertially-aided aircraft track recovery system for coastal mapping p0037 A82-18166

MAGSAT: Vector magnetometer absolute sensor alignment determination [NASA-TM-79648] p0051 N82-10468
 Infrared radiance model variation by sensor flight measurements p0052 N82-14171

INTERNAL WAVES
 Visual observations of the ocean p0028 N82-12502
 An assessment of the potential contributions to oceanography from Skylab visual observations and handheld-camera photographs p0028 N82-12503

Surface signs of internal ocean dynamics [AD-A101380] p0029 N82-13642

INTERPOLATION
 Interpolating for the location of remote sensor data [NASA-TM-82169] p0052 N82-13469

IONOSPHERE
 A Swedish proposal for an EISCAT/GEOS-2 experiment --- geomagnetic field models [KGI-175] p0052 N82-10484

IONOSPHERIC CURRENTS
 Characteristics of westward travelling surges during magnetospheric substorms p0050 A82-14299

IONOSPHERIC DRIFT
 Use of hydromagnetic waves to map geomagnetic field lines p0016 A82-16868

IONOSPHERIC ELECTRON DENSITY
 Magnetic field-aligned electron distributions in the dayside cusp p0015 A82-12186

IONOSPHERIC PROPAGATION
 The radiowave propagation environment - Science and technology objectives for the 80's p0009 A82-18052
 Ionospheric propagation correction modeling for satellite altimeters [NASA-CR-156881] p0052 N82-12447

IRELAND
 The feasibility of using remotely sensed color as an index of Irish coastal water properties --- statistical correlation of sea truth data p0032 N82-14581

IRON COMPOUNDS
 Remote sensing studies of some ironstone gravels and plinthite in Thailand p0019 N82-12491

IRRADIANCE
 The color of the sea and its relation to surface chlorophyll and depth of the euphotic zone p0030 N82-14562

IRRIGATION
 Satellite sensing of irrigation patterns in semiarid areas - An Indian study p0002 A82-10864

ISLANDS
 Mesoscale wake clouds in Skylab photographs p0011 N82-12508
 Boundary detection criteria for satellite altimeters [NASA-CR-156880] p0028 N82-12734

ITALY
 Study of stack emissions by combination of lidar and correlation spectrometer p0008 A82-12816
 Skylab 4 observations of Volcanoes. Part A: Volcanoes and volcanic landforms. Part B: Summit eruption of Fernandian Caldera, Galapagos Islands, Ecuador p0020 N82-12496

J

JAPAN
 Skylab 4 observations of Volcanoes. Part A: Volcanoes and volcanic landforms. Part B: Summit eruption of Fernandian Caldera, Galapagos Islands, Ecuador p0020 N82-12496

JET STREAMS (METEOROLOGY)
 Meteorological lab applications of Skylab handheld-camera photographs p0011 N82-12506

KANSAS
 Interactive techniques for estimating precipitation from GOES imagery p0041 A82-13121
 The discrimination of winter wheat using a growth-state signature p0002 A82-15026
 Aircraft radar response to soil moisture p0003 A82-17564

KENTUCKY
 Mapping of the 1978 Kentucky River Flood from NOAA-5 satellite thermal infrared data p0035 A82-10033

L

LAGOONS
 Multitemporal calibration of LANDSAT images: A method for improving the marine phenomena recognition, with as example the Venice lagoon --- brightness/green/yellow feature space, image enhancement p0046 N82-14578

LAKE ICE
 The development of the Tiros Global Environmental Satellite System [AIAA PAPER 82-0383] p0025 A82-17915
 Visual observations of floating ice from Skylab p0037 N82-12504

LAKE ONTARIO
 Visual observations of floating ice from Skylab p0037 N82-12504
 Recent work in passive optical imaging of water --- space and aircraft derived data p0038 N82-14575

LAKES
 Remote sensing that motivated community action p0008 A82-12594
 The operational use of Landsat for lake quality assessment p0038 A82-12596
 Role of remote sensing in the study of acid rain impact on aquatic systems [AIAA PAPER 82-0336] p0036 A82-17892

The Manicouagan impact structure observed from Skylab [CONTRIB-544] p0020 N82-12497

LAND ICE
 Measurement of sea and ice backscatter reflectivity using an OTH radar system p0025 A82-18074

LAND MANAGEMENT
 Remote sensing for vineyard management p0001 A82-10047
 Bureau of Land Management satellite Doppler positioning techniques p0015 A82-10057
 Civil engineering applications of remote sensing: Proceedings of the Specialty Conference, University of Wisconsin, Madison, WI, August 13, 14, 1980 p0035 A82-12589
 Adaptation of land use to surficial geology in metropolitan Washington, D.C. p0010 N82-11718

LAND USE
 Introducing remote sensing to county-level agencies in Michigan through the Cooperative Extension Service p0007 A82-10034
 Remote sensing techniques in the study of the agricultural potential of soils under the Cerrado vegetation /Brazil/ p0001 A82-10040
 Preliminary results of mapping urban land cover with Seasat SAR imagery p0007 A82-10044
 Areawide soil loss predictions using CIR airphotos p0007 A82-12591
 Study of the dynamics of the Danube delta using space images p0036 A82-15961
 Study and mapping of agricultural land use, based on space images p0003 A82-15983
 Study of the anthropogenic influence on the environment, based on multispectral scanning images p0008 A82-15965
 Analysis of variance of thematic mapping experiment data p0009 A82-15968
 An evaluation of the spatial resolution of soil moisture information [NASA-CR-166724] p0009 N82-11513
 Radar mapping, archaeology, and ancient land use in the Maya lowlands [NASA-CR-164931] p0010 N82-11514
 Adaptation of land use to surficial geology in metropolitan Washington, D.C. p0010 N82-11718
 Cultural features imaged and observed from Skylab 4 p0010 N82-12499
 Vegetation patterns p0004 N82-12500
 Report on Skylab 4 African drought and arid land experiment p0037 N82-12501
 A proposal for continuation of support for the application of remotely sensed data to state and regional problems. Part 1: Technical proposal [E82-10018] p0056 N82-15496

LANDSAT D
 Computational aspects of geometric correction data generation in the LANDSAT-D imagery processing p0045 A82-10072
 The MSS control point location error filter for LANDSAT-D p0051 N82-10073

LANDSAT 2
 LANDSAT-2 and LANDSAT-3 flight evaluation report, 23 April to 23 July 1979 [E82-10005] p0053 N82-15483
 LANDSAT-2 and LANDSAT-3 flight evaluation report, 23 October 1978 to 23 January 1979 [E82-10017] p0054 N82-15495

LANDSAT 3
 LANDSAT-2 and LANDSAT-3 flight evaluation report, 23 April to 23 July 1979 [E82-10005] p0053 N82-15483
 LANDSAT-2 and LANDSAT-3 flight evaluation report, 23 October 1978 to 23 January 1979 [E82-10017] p0054 N82-15495

LASER APPLICATIONS
 Airborne laser acquisition of cross-section data p0049 A82-12600
 Analog methods for processing multispectral photographs p0044 A82-16623
 Space techniques to monitor movements in the earth's crust p0016 A82-18797
 Remote sensing of sea state by laser altimeters [NASA-CR-165049] p0033 N82-14789

LIBERIA
 A history of flying and photography: In the Photogrammetry Division of the National Ocean Survey 1919 - 1979 [PBB1-246738] p0017 N82-15520

LIBRARIAN
 Distant magnetic field effects associated with Birkeland currents /made possible by the evaluation of TRIAD's attitude oscillations/ p0015 A82-12215

LIBYA
 Geology and linears of Libya p0019 N82-10618

LIGHT SCATTERING
 Calculation of the decrease in the contrast of objects of a place due to light scattering in the atmosphere p0042 A82-13633

LIMNOLOGY
 Data sources for analyses of Great Lakes wetlands p0035 A82-10054
 Remote sensing that motivated community action p0008 A82-12594
 The operational use of Landsat for lake quality assessment p0038 A82-12596

LINEAR FILTERS

The MSS control point location error filter for LANDSAT-D p0051 N82-10073

LITHOSPHERE

Study of the time evolution of the lithosphere [NASA-CR-164968] p0016 N82-11696
The reduction, verification and interpretation of Magsat magnetic data over Canada [E82-10006] p0046 N82-15484

LOWER CALIFORNIA (MEXICO)

The use of satellite infrared imagery for describing ocean processes in relation to spawning of the northern anchovy /Engraulis mordax/ p0025 A82-17565
Geological features of southwestern North America p0020 N82-12495

M

MAGNETIC ANOMALIES

A closer examination of the reduction of satellite magnetometer data for geological studies p0019 A82-11039

The reduction, verification and interpretation of Magsat magnetic data over Canada [E82-10006] p0046 N82-15484

The mineralogy of global magnetic anomalies [E82-10009] p0021 N82-15487

MAGNETIC EFFECTS

Distant magnetic field effects associated with Birkeland currents /made possible by the evaluation of TRIAD's attitude oscillations/ p0015 A82-12215

MAGNETIC FIELDS

Magnetic field-aligned electron distributions in the dayside cusp p0015 A82-12186

MAGSAT: Vector magnetometer absolute sensor alignment determination [NASA-TM-79648] p0051 N82-10468

MAGNETIC MEASUREMENT

Magnetic field observations on DE-A and B --- Dynamics Explorer A and B satellites p0051 A82-16447

MAGNETIC STORMS

Characteristics of westward travelling surges during magnetospheric substorms p0050 A82-14299

MAGNETIC SURVEYS

Use of hydromagnetic waves to map geomagnetic field lines p0016 A82-16868

Space techniques to monitor movements in the earth's crust p0016 A82-18797

Magnetic Field Satellite (Magsat) data processing system specifications [NASA-CR-166737] p0045 N82-11103

NURE aerial gamma-ray and magnetic reconnaissance survey of Maine and portions of New York, Volume 1: Data acquisition, reduction and interpretation [E82-000650] p0053 N82-14599

NURE aerial gamma-ray and magnetic reconnaissance survey of Maine and portions of New York, volume 2 [E82-000781] p0020 N82-14600

NURE aerial gamma-ray and magnetic reconnaissance survey of Maine and portions of New York, volume 2 [E82-000401] p0020 N82-14601

NURE aerial gamma-ray and magnetic reconnaissance survey of Maine and portions of New York, volume 2 [E82-000780] p0021 N82-14602

NURE aerial gamma-ray and magnetic reconnaissance survey of Maine and portions of New York, volume 2 [E82-000872] p0021 N82-14603

NURE aerial gamma-ray and magnetic reconnaissance survey of Maine and portions of New York, volume 2 [E82-000772] p0021 N82-14604

NURE aerial gamma-ray and magnetic reconnaissance survey of Maine and portions of New York, volume 2 [E82-000785] p0021 N82-14605

NURE aerial gamma-ray and magnetic reconnaissance survey of Maine and portions of New York, volume 2 [E82-000869] p0021 N82-14606

NURE aerial gamma-ray and magnetic reconnaissance survey of Maine and portions of New York, volume 2 [E82-000794] p0021 N82-14607

NURE aerial gamma-ray and magnetic reconnaissance survey of Maine and portions of New York, volume 2 [E82-000784] p0021 N82-14608

Preliminary analysis of gravity and aeromagnetic surveys of the Timber Mountain area, southern Nevada [E81-029462] p0022 N82-15506

MAGNETOHYDRODYNAMIC WAVES

Use of hydromagnetic waves to map geomagnetic field lines p0016 A82-16868

MAGNETOMETERS

Magnetic field observations on DE-A and B --- Dynamics Explorer A and B satellites p0051 A82-16447

MAGSAT: Vector magnetometer absolute sensor alignment determination [NASA-TM-79648] p0051 N82-10468

MAGNETOSPHERE

Characteristics of westward travelling surges during magnetospheric substorms p0050 A82-14299

Use of hydromagnetic waves to map geomagnetic field lines p0016 A82-16868

MAGSAT SATELLITES

Magnetic Field Satellite (Magsat) data processing system specifications [NASA-CR-166737] p0045 N82-11103

MAINE

NURE aerial gamma-ray and magnetic reconnaissance survey of Maine and portions of New York, Volume 1: Data acquisition, reduction and interpretation [E82-000650] p0053 N82-14599

NURE aerial gamma-ray and magnetic reconnaissance survey of Maine and portions of New York, volume 2 [E82-000781] p0020 N82-14600

NURE aerial gamma-ray and magnetic reconnaissance survey of Maine and portions of New York, volume 2 [E82-000401] p0020 N82-14601

NURE aerial gamma-ray and magnetic reconnaissance survey of Maine and portions of New York, volume 2 [E82-000780] p0021 N82-14602

NURE aerial gamma-ray and magnetic reconnaissance survey of Maine and portions of New York, volume 2 [E82-000872] p0021 N82-14603

NURE aerial gamma-ray and magnetic reconnaissance survey of Maine and portions of New York, volume 2 [E82-000772] p0021 N82-14604

NURE aerial gamma-ray and magnetic reconnaissance survey of Maine and portions of New York, volume 2 [E82-000785] p0021 N82-14605

NURE aerial gamma-ray and magnetic reconnaissance survey of Maine and portions of New York, volume 2 [E82-000869] p0021 N82-14606

NURE aerial gamma-ray and magnetic reconnaissance survey of Maine and portions of New York, volume 2 [E82-000794] p0021 N82-14607

NURE aerial gamma-ray and magnetic reconnaissance survey of Maine and portions of New York, volume 2 [E82-000784] p0021 N82-14608

MALAYA

Vegetation patterns p0004 N82-12500

MAN ENVIRONMENT INTERACTIONS

Spacelab-research of European regions with strong negative environmental influences, based on AVHRR-data of the satellites Tiros-N and NOAA p0007 A82-12517

Study of the anthropogenic influence on the environment, based on multispectral scanning images p0008 A82-15965

Cultural features imaged and observed from Skylab 4 p0010 N82-12499

MAPPING

Digital image technology - MC&G impact --- Mapping, Charting, & Geodesy p0015 A82-10028

Applications of digital displays in photointerpretation and digital mapping p0041 A82-10038

Application of satellite Doppler techniques to the national mapping program p0015 A82-10056

Bureau of Land Management satellite Doppler positioning techniques p0015 A82-10057

Cost effective computer processing of airborne scanner data for regional level mapping p0043 A82-15970

Small-scale terrain mapping based on numerical interpretation of LANDSAT imagery [VTT-40] p0045 N82-10485

Reports of Planetary Geology Program, 1981 [NASA-TM-84211] p0016 N82-14041

The reduction, verification and interpretation of Magsat magnetic data over Canada [E82-10006] p0046 N82-15484

MAPS

A global atlas of GEOS-3 significant waveheight and comparison of the data with national buoy data p0026 N82-10660

MARINE BIOLOGY

Fisheries investigations and management benefits from remote sensing --- fish tracking p0030 N82-14559

MARINE ENVIRONMENTS

A marine environmental monitoring and assessment program p0027 N82-10663

Monitoring the Chesapeake Bay using satellite data for Superflux III p0027 N82-10668

A look at nonsatellite remote sensing systems for marine use --- together with satellite systems, overall view of the technology p0032 N82-14586

MARINE METEOROLOGY

An investigation of a polar low with a spiral cloud structure p0007 A82-10616

Analysis of SEASAT wind observations over the Indian Ocean p0023 A82-10671

Oceanic wind and balanced pressure-height fields derived from satellite measurements p0023 A82-13214

Upper tropospheric cyclonic vortices in the tropical South Atlantic p0009 A82-16325

Detection of monsoon inversion by TIROS-N satellite p0024 A82-17168

CTD/O2 measurements during the Equatorial Pacific Ocean Climate Study (EPOCS) in 1979 [PB81-211203] p0026 N82-10461

The potential and requirements for space oceanography --- National Oceanic Satellite system and U.S. Navy requirements p0029 N82-14556

Offshore petroleum industry environmental data requirements: Emphasis on remote sensing p0030 N82-14557

The Seasat commercial demonstration program p0030 N82-14561

Determination of surface wind speed from remotely measured whitecap coverage, a feasibility assessment p0030 N82-14565

Marine activities in Sweden for which remote sensing data may be of interest --- oceanography, weather forecasting, and analysis p0031 N82-14576

Scientific studies using Bhaskara satellite microwave radiometer (SAMIR) data: A short overview --- calibration of the instrument and its use in the study of oceanographic parameters p0032 N82-14587

GEM: A simple meteorological buoy with satellite telemetry p0053 N82-14779

Meteorological and oceanographic observations on board Netherlands lightvessels and the lightplatform 'Goeree' in the North Sea [KNMI-141-28] p0033 N82-15684

MARINE RESOURCES

Remote sensing contributions to the management of renewable resources p0055 A82-12530

Chesapeake Bay Plume Study: Superflux 1980 [NASA-CP-2188] p0026 N82-10661

Superflux I, II, and III experiment design: Remote sensing aspects p0027 N82-10664

Superflux I, II, and III experiment designs: Water sampling and analyses --- Chesapeake Bay, environmental monitoring and remote sensing p0027 N82-10665

Application of the NASA airborne oceanographic lidar to the mapping of chlorophyll and other organic pigments p0027 N82-10684

Studies of the Indian continental shelf: Application of remote sensing data p0031 N82-14569

MARINE TRANSPORTATION

An evaluation of Seasat-A data in relation to optimum track ship weather routing and site specific forecasting for the offshore oil industry p0030 N82-14564

MARKING

Development and evaluation of an automatic labeling technique for spring small grains [E82-10001] p0004 N82-15480

MARSHLANDS

Repetitive aerial photography for assessing marsh vegetation changes p0001 A82-10448

Use of visible and thermal satellite data to monitor an intermittently flooding marshland p0036 A82-15037

MASSACHUSETTS

Spectral atmospheric observations at Nantucket Island, May 7-14, 1981 [NASA-TM-83196] p0029 N82-14550

MATHEMATICAL MODELS

A mathematical model of an over-sea airborne UHF radio link p0049 A82-11406

A Swedish proposal for an EISCAT/GEOS-2 experiment --- geomagnetic field models [KGI-175] p0052 N82-10484

Ionospheric propagation correction modeling for satellite altimeters [NASA-CR-156881] p0052 N82-12447

Sensitivity analysis of a mesoscale moisture model [AD-A101528] p0012 N82-14590

Winterkill indicator model, Crop Condition Assessment Division (CCAD) data base interface driver, user's manual [E82-10014] p0005 N82-15492

Use of environmental satellite data for input to energy balance snowmelt models [PB81-227795] p0039 N82-15673

MEDITERRANEAN SEA

Requirements in pollution monitoring and coastal management p0030 N82-14558

Oil spills: Large scale monitoring by LANDSAT p0012 N82-14572

Operational use of remote sensing for coastal zone management and possible contribution of specialized satellites --- aerial photography p0031 N82-14574

MESOMETEOROLOGY

GEM: A simple meteorological buoy with satellite telemetry p0053 N82-14779

MESOSCALE PHENOMENA

Visual observations of the ocean p0028 N82-12502

Mesoscale wake clouds in Skylab photographs p0011 N82-12508

Mesoscale cloud features observed from Skylab p0011 N82-12509

Sensitivity analysis of a mesoscale moisture model [AD-A101528] p0012 N82-14590

METEORITE CRATERS

The Manicouagan impact structure observed from Skylab [CONTRIB-544] p0020 N82-12497

METEOROLOGICAL PARAMETERS

Two-dimensional model variability in thermal inertia surveys p0042 A82-15029

The determination of navigational and meteorological variables measured by NOAA/RFC WP3D aircraft [PB81-225468] p0028 N82-11743

METEOROLOGICAL RADAR

Analysis of bright bands from 3-D radar data --- for snow/rain delineation p0035 A82-10208

METEOROLOGY

Meteorological lab applications of Skylab handheld-camera photographs p0011 N82-12506

Analysis of satellite observations: Theoretical studies on the sampling problem [MITT-31] p0056 N82-15499

METEOSAT SATELLITE

Overall economic impact of an operational Meteosat system [ESA-CR(P)-1457] p0055 N82-13010

METHANE

Automated analyzer for aircraft measurements of atmospheric methane and total hydrocarbons p0007 A82-11949

MEXICO

Radar mapping, archaeology, and ancient land use in the Maya lowlands
[NASA-CR-164931] p0010 N82-11514
Global Tectonics: Some Geologic analyses of observations and photographs from Skylab p0020 N82-12494
Geological features of southwestern North America p0020 N82-12495

MICHIGAN

Introducing remote sensing to county-level agencies in Michigan through the Cooperative Extension Service p0007 A82-10034
Data sources for analyses of Great Lakes wetlands p0035 A82-10054

MICROORGANISMS

Infrared spectroscopy of microorganisms near 3.4 microns in relation to geology and astronomy [PREPRINT-69] p0020 N82-12713

MICROWAVE EMISSION

A comparison of radiative transfer models for predicting the microwave emission from soils p0035 A82-10694
SMMR data set development for GARP --- impact of cross polarization and Faraday rotation on SMMR derived brightness temperatures [NASA-CR-166721] p0052 N82-11512

MICROWAVE IMAGERY

An improvement in land cover classification achieved by merging microwave data with Landsat multispectral scanner data p0007 A82-10043
A preliminary evaluation of Seasat performance over the area of JASIN and its relevance to ERS-1 p0031 N82-14567
Visual Evaluation of E-SLAR imagery [DFVLR-FB-81-11] p0047 N82-15503

MICROWAVE RADIOMETERS

Use of radar and microwave radiometry for reconnaissance satellites [FOA-C-30204-E1] p0052 N82-10481
Microwave limb sounder --- measuring trace gases in the upper atmosphere [NASA-CASE-NPO-14544-1] p0011 N82-12685
Scientific studies using Bhaskara satellite microwave radiometer (SAMIR) data: A short overview --- calibration of the instrument and its use in the study of oceanographic parameters p0032 N82-14587

MICROWAVE SCATTERING

Radiative transfer theory for passive microwave remote sensing of random media p0049 A82-11533
Reflectivity and emissivity of snow and ground at mm waves p0042 A82-14860
Ocean surface height-slope probability density function from SEASAT altimeter echo p0024 A82-15076
An analysis of short pulse and dual frequency radar techniques for measuring ocean wave spectra from satellites p0024 A82-15318
State-of-the-art in using a spaceborne altimeter and scatterometer for the determination of wind, sea state, and marine and ice dynamics --- Seasat instruments p0052 N82-14560

MICROWAVE SENSORS

Technology transfer of NASA microwave remote sensing system [NASA-CR-165791] p0028 N82-11515
Remote Sensing Information Bulletin: Issue number 6 p0053 N82-14616

MILLIMETER WAVES

Reflectivity and emissivity of snow and ground at mm waves p0042 A82-14860

MINERAL DEPOSITS

Deep Ocean Mining Environmental Study. Environmental effects of commercial-scale mining [PB81-227753] p0029 N82-13484

MINERAL EXPLORATION

Statistical Techniques Applied to Aerial Radiometric Surveys (STAARS): Series introduction and the principal-components-analysis method --- National Uranium Resource Evaluation Program p0019 N82-10476
NURE aerial gamma-ray and magnetic reconnaissance survey of Maine and portions of New York. Volume 1: Data acquisition, reduction and interpretation [DE82-000650] p0053 N82-14599
NURE aerial gamma-ray and magnetic reconnaissance survey of Maine and portions of New York, volume 2 [DE82-000781] p0020 N82-14600
NURE aerial gamma-ray and magnetic reconnaissance survey of Maine and portions of New York, volume 2 [DE82-000401] p0020 N82-14601
NURE aerial gamma-ray and magnetic reconnaissance survey of Maine and portions of New York, volume 2 [DE82-000780] p0021 N82-14602
NURE aerial gamma-ray and magnetic reconnaissance survey of Maine and portions of New York, volume 2 [DE82-000872] p0021 N82-14603
NURE aerial gamma-ray and magnetic reconnaissance survey of Maine and portions of New York, volume 2 [DE82-000772] p0021 N82-14604
NURE aerial gamma-ray and magnetic reconnaissance survey of Maine and portions of New York, volume 2 [DE82-000785] p0021 N82-14605
NURE aerial gamma-ray and magnetic reconnaissance survey of Maine and portions of New York, volume 2 [DE82-000869] p0021 N82-14606

NURE aerial gamma-ray and magnetic reconnaissance survey of Maine and portions of New York, volume 2 [DE82-000794] p0021 N82-14607

NURE aerial gamma-ray and magnetic reconnaissance survey of Maine and portions of New York, volume 2 [DE82-000784] p0021 N82-14608

Geologic applications of thermal-inertia mapping from satellite --- Powder River, Wyoming; Cubeza Prieta, Arizona, and Yellowstone National Park [E82-10011] p0021 N82-15489

An investigation into the applicability of thermal infrared scanning for exploration [BMFT-FB-T-81-087] p0022 N82-15925

MINERALOGY

The mineralogy of global magnetic anomalies [E82-10009] p0021 N82-15487

MINES (EXCAVATION)

A proposal for continuation of support for the application of remotely sensed data to state and regional problems. Part 1: Technical proposal [E82-10018] p0056 N82-15496

MINING

Deep Ocean Mining Environmental Study. Environmental effects of commercial-scale mining [PB81-227753] p0029 N82-13484

MISSISSIPPI

A proposal for continuation of support for the application of remotely sensed data to state and regional problems. Part 1: Technical proposal [E82-10018] p0056 N82-15496

MISSOURI

Radiative heating rates and some optical properties of the St. Louis aerosol, as inferred from aircraft measurements p0008 A82-14320

MISSOURI RIVER BASIN (US)

The potential for use of Landsat data in water resources planning for the Missouri River Basin p0037 A82-18000

MODULATION TRANSFER FUNCTION

Wave orbital velocity, fade, and SAR response to azimuth waves p0023 A82-11203

MOISTURE CONTENT

Effect of grain size and snowpack water equivalence on visible and near-infrared satellite observations of snow p0035 A82-12553

Remote sensing of crop moisture status p0003 A82-17997

Progress in radar snow research --- Brookings, South Dakota [NASA-CR-166709] p0038 N82-12510

MOLECULAR SPECTROSCOPY

Nitric oxide delta band emission in the earth's atmosphere Comparison of a measurement and a theory p0008 A82-13268

MONSOONS

Detection of monsoon inversion by TIROS-N satellite p0024 A82-17168

MOUNTAINS

Snow-mapping experiment p0037 N82-12498
Preliminary analysis of gravity and aeromagnetic surveys of the Timber Mountain area, southern Nevada [DE81-029462] p0022 N82-15506

Use of environmental satellite data for input to energy balance snowmelt models [PB81-227795] p0039 N82-15673

MULTIPATH TRANSMISSION

A mathematical model of an over-sea airborne UHF radio link p0049 A82-11406

MULTISPECTRAL BAND CAMERAS

Main results of the Raduga experiment p0051 A82-16602

MULTISPECTRAL BAND SCANNERS

Data compression and reconstruction for mixed resolution multispectral sensors p0049 A82-10045
Limitations in the spectral discrimination of the Landsat MSS p0001 A82-10046

Computational aspects of geometric correction data generation in the LANDSAT-D imagery processing p0045 N82-10072

The MSS control point location error filter for LANDSAT-D p0051 N82-10073

MULTISPECTRAL PHOTOGRAPHY

Investigations concerning the image-controlled segmentation of objects in multispectral imagery data --- German thesis p0042 A82-15003

Experimental telemetry system based on the Fragment multispectral scanning system p0050 A82-15955

Study and mapping of agricultural land use, based on space images p0003 A82-15963

Airborne and spaceborne multispectral photography of the earth --- Russian book p0043 A82-16601

Main results of the Raduga experiment p0051 A82-16602

Evaluation of the information content of the channels of spaceborne multispectral photography of the Fergana region by the MKF-6 camera from Soyuz-22 p0043 A82-16605

Geometric quality of MKF-6 photographs p0043 A82-16606

Methods of instrumental interpretation of multispectral aerial and space photographs p0043 A82-16607

Characteristics of the photometry of small objects from aerial and space photographs p0044 A82-16616

Estimation of the brightness field from results of multispectral photography of the earth from space p0044 A82-16617

Analog methods for processing multispectral photographs p0044 A82-16623

Processing of multispectral image data on special-purpose computer systems p0044 A82-16627

Programs for the statistical analysis of multispectral photographs p0044 A82-16628

Linear combinations of multispectral images p0044 A82-16629

Coordinate referencing of MKF-6 photographs and their transformation to the cartographic projection p0045 A82-16630

Identification of lithologic units using multichannel imaging systems p0046 N82-11509

Multitemporal calibration of LANDSAT images: A method for improving the marine phenomena recognition, with as example the Venice lagoon --- brightness/green/yellow feature space, image enhancement p0046 N82-14578

Mapping of surface currents in Greenland fiords by means of LANDSAT images --- multispectral photography p0038 N82-14579

The use of LANDSAT MSS to observe sediment distribution and movement in the Solent coastal area --- multispectral scanner (MSS) p0038 N82-14580

Maritime applications of image processing at DFVLR, Oberpfaffenhofen, West Germany --- LANDSAT multispectral scanner images, digital interactive image analysis p0032 N82-14585

MULTIVARIATE STATISTICAL ANALYSIS

Statistical Techniques Applied to Aerial Radiometric Surveys (STAARS): Series introduction and the principal-components-analysis method --- National Uranium Resource Evaluation Program [DE81-029177] p0019 N82-10476

Fiscal year 1980-81 implementation plan in support of technical development and integration of sampling and aggregation procedures --- crop acreage estimation [E82-10013] p0005 N82-15491

N

NASA PROGRAMS

Reports of Planetary Geology Program, 1981 [NASA-TM-84211] p0016 N82-14041

NATIONAL OCEANIC SATELLITE SYSTEM

The potential and requirements for space oceanography --- National Oceanic Satellite system and U.S. Navy requirements p0029 N82-14556

NATIONAL SEVERE STORMS PROJECT

National Hurricane operations plan, [PB81-247231] p0013 N82-15697

NAVIGATION AIDS

The application of programmable pocket calculators for computations during survey flights p0050 A82-16164

NEAR INFRARED RADIATION

Effect of grain size and snowpack water equivalence on visible and near-infrared satellite observations of snow p0035 A82-12553

The near-infrared radiation received by satellites from clouds p0025 A82-17492

NEARSHORE WATER

Synoptic thermal and oceanographic parameter distributions in the New York Bight Apex p0023 A82-12885

NEBRASKA

Remote sensing of crop moisture status p0003 A82-17997

The potential for use of Landsat data in water resources planning for the Missouri River Basin p0037 A82-18000

NEVADA

Estimation of atmospheric path-radiance by the covariance matrix method p0041 A82-10861

Preliminary analysis of gravity and aeromagnetic surveys of the Timber Mountain area, southern Nevada [DE81-029462] p0022 N82-15506

NEW ENGLAND (US)

Meteorological lab applications of Skylab handheld-camera photographs p0011 N82-12506

NEW GUINEA (ISLAND)

Estimation of atmospheric path-radiance by the covariance matrix method p0041 A82-10861

NEW MEXICO

Environmental Monitoring Report, Sandia National Labs., Albuquerque, New Mexico, 180 [DE81-027839] p0010 N82-11649

Meteorological lab applications of Skylab handheld-camera photographs p0011 N82-12506

NEW YORK

Synoptic thermal and oceanographic parameter distributions in the New York Bight Apex p0023 A82-12885

Role of remote sensing in the study of acid rain impact on aquatic systems [AIAA PAPER 82-0336] p0036 A82-17892

Meteorological lab applications of Skylab handheld-camera photographs p0011 N82-12506

NURE aerial gamma-ray and magnetic reconnaissance survey of Maine and portions of New York. Volume 1: Data acquisition, reduction and interpretation [DE82-000650] p0053 N82-14599

NURE aerial gamma-ray and magnetic reconnaissance survey of Maine and portions of New York, volume 2 [DE82-000781] p0020 N82-14600

SUBJECT INDEX

NURE aerial gamma-ray and magnetic reconnaissance survey of Maine and portions of New York, volume 2 [DEB2-000401] p0020 N82-14601

NURE aerial gamma-ray and magnetic reconnaissance survey of Maine and portions of New York, volume 2 [DEB2-000780] p0021 N82-14602

NURE aerial gamma-ray and magnetic reconnaissance survey of Maine and portions of New York, volume 2 [DEB2-000872] p0021 N82-14603

NURE aerial gamma-ray and magnetic reconnaissance survey of Maine and portions of New York, volume 2 [DEB2-000772] p0021 N82-14604

NURE aerial gamma-ray and magnetic reconnaissance survey of Maine and portions of New York, volume 2 [DEB2-000785] p0021 N82-14605

NURE aerial gamma-ray and magnetic reconnaissance survey of Maine and portions of New York, volume 2 [DEB2-000889] p0021 N82-14606

NURE aerial gamma-ray and magnetic reconnaissance survey of Maine and portions of New York, volume 2 [DEB2-000794] p0021 N82-14607

NURE aerial gamma-ray and magnetic reconnaissance survey of Maine and portions of New York, volume 2 [DEB2-000784] p0021 N82-14608

NEW ZEALAND

Global Tectonics: Some Geologic analyses of observations and photographs from Skylab p0020 N82-12494

Vegetation patterns p0004 N82-12500

NITRIC OXIDE

Nitric oxide delta band emission in the earth's atmosphere Comparison of a measurement and a theory p0008 A82-13268

NORTH AMERICA

Availability of Seasat synthetic aperture radar imagery p0050 A82-15039

Geological features of southwestern North America p0020 N82-12495

Skylab 4 observations of Volcanoes. Part A: Volcanoes and volcanic landforms. Part B: Summit eruption of Fernandian Caldera, Galapagos Islands, Ecuador p0020 N82-12496

NORTH CAROLINA

Satellite imagery and shoreline erosion prediction p0036 A82-12595

Aircraft data summaries of the SURE intensives, volume 4 [DEB2-900311] p0012 N82-13569

NORTH SEA

An evaluation of Seasat-A data in relation to optimum track ship weather routing and site specific forecasting for the offshore oil industry p0030 N82-14564

Coastal zone research using remote sensing techniques --- calibration of coastal zone color scanner p0031 N82-14571

Project Noordwijk. Part 1: Measurements of the radar backscatter coefficient gamma (sigma deg) in 1977 and 1978 --- on a sea platform [PHL-1979-49-PT-1] p0032 N82-14617

Project Noordwijk. Part 2: Results of North Sea clutter measurements in the l-band performed from the platform Noordwijk in September/October 1977 [PHL-1980-28-PT-2] p0033 N82-14618

Meteorological and oceanographic observations on board Netherlands lightvessels and the lightplatform 'Goeree' in the North Sea [KNMI-141-28] p0033 N82-15684

NORWAY

The Norwegian remote sensing experiment (Norsex) in a marginal ice zone p0031 N82-14566

O

OCEAN BOTTOM

Deep Ocean Mining Environmental Study. Environmental effects of commercial-scale mining [PBB1-227753] p0029 N82-13484

Operational use of remote sensing for coastal zone management and possible contribution of specialized satellites --- aerial photography p0031 N82-14574

OCEAN COLOR SCANNER

Preliminary analysis of ocean color scanner data from Superflux III p0027 N82-10672

OCEAN CURRENTS

The observation of tidal patterns, currents, and bathymetry with SLAR imagery of the sea p0023 A82-11201

A short review of an oceanographic use-of Meteosat data by the ORSTOM remote sensing service p0031 N82-14570

Marine activities in Sweden for which remote sensing data may be of interest --- oceanography, weather forecasting, and analysis p0031 N82-14576

OCEAN DATA ACQUISITIONS SYSTEMS

U. S. Navy planning for satellite oceanographic data exploitation [AAS 81-072] p0024 A82-16341

Technology transfer of NASA microwave remote sensing system [NASA-CR-165791] p0028 N82-11515

The need for integrated off-shore, real-time information and management systems p0055 N82-14555

The potential and requirements for space oceanography

--- National Oceanic Satellite system and U.S. Navy requirements p0029 N82-14556

Requirements in pollution monitoring and coastal management p0030 N82-14558

A look at nonsatellite remote sensing systems for marine use --- together with satellite systems, overall view of the technology p0032 N82-14586

GEM: A simple meteorological buoy with satellite telemetry p0053 N82-14779

OCEAN DYNAMICS

Surface signs of internal ocean dynamics [AD-A101380] p0029 N82-13642

State-of-the-art in using a spaceborne altimeter and scatterometer for the determination of wind, sea state, and marine and ice dynamics --- Seasat instruments p0052 N82-14560

OCEAN SURFACE

Analysis of SEASAT wind observations over the Indian Ocean p0023 A82-10671

Wave orbital velocity, fade, and SAR response to azimuth waves p0023 A82-11203

Water vapour absorption in the 3.5-4.2 micron atmospheric window p0023 A82-14586

Radar backscattering from ocean waves at low grazing angles p0023 A82-14730

Ocean surface height-slope probability density function from SEASAT altimeter echo p0024 A82-15076

Determination of the length of sea waves by an airborne radar technique p0024 A82-15213

An analysis of short pulse and dual frequency radar techniques for measuring ocean wave spectra from satellites p0024 A82-15318

Investigation of survey conditions for the ocean surface in the 0.4-1.1 micron spectral range p0024 A82-15960

Clear water radiances for atmospheric correction of coastal zone color scanner imagery p0025 A82-17292

The near-infrared radiation received by satellites from clouds p0025 A82-17492

Variations in upper ocean heat storage determined from satellite data p0025 A82-17567

Measurement of sea and ice backscatter reflectivity using an OTH radar system p0025 A82-18074

Seasat altimetry adjustment model including tidal and other sea surface effects p0026 N82-10473

A global atlas of GEOS-3 significant waveheight and comparison of the data with national buoy data p0026 N82-10660

Surface signs of internal ocean dynamics [AD-A101380] p0029 N82-13642

Determination of surface wind speed from remotely measured whitecap coverage, a feasibility assessment p0030 N82-14565

A preliminary evaluation of Seasat performance over the area of JASIN and its relevance to ERS-1 p0031 N82-14567

Oil spills: Large scale monitoring by LANDSAT p0012 N82-14572

Airborne remote sensing of the coastal zone p0053 N82-14577

Multitemporal calibration of LANDSAT images: A method for improving the marine phenomena recognition, with as example the Venice lagoon --- brightness/green/yellow feature space, image enhancement p0046 N82-14578

The feasibility of using remotely sensed color as an index of Irish coastal water properties --- statistical correlation of sea truth data p0032 N82-14581

Project Noordwijk. Part 1: Measurements of the radar backscatter coefficient gamma (sigma deg) in 1977 and 1978 --- on a sea platform [PHL-1979-49-PT-1] p0032 N82-14617

Project Noordwijk. Part 2: Results of North Sea clutter measurements in the l-band performed from the platform Noordwijk in September/October 1977 [PHL-1980-28-PT-2] p0033 N82-14618

Remote sensing of sea state by laser altimeters [NASA-CR-165049] p0033 N82-14789

OCEAN TEMPERATURE

Comparison of polar and geostationary satellite infrared observations of sea surface temperatures in the Gulf of Maine p0024 A82-15030

Detection of monsoon inversion by TIROS-N satellite p0024 A82-17168

The use of satellite infrared imagery for describing ocean processes in relation to spawning of the northern anchovy /Engraulis mordax/ p0025 A82-17565

ICAPS oceanographic data for the Indian Ocean [AD-A103173] p0029 N82-13641

OCEANOGRAPHIC PARAMETERS

Fisheries investigations and management benefits from remote sensing --- fish tracking p0030 N82-14559

OCEANOGRAPHY

SAR imaging of ocean waves - Theory p0023 A82-11202

Synoptic thermal and oceanographic parameter distributions in the New York Bight Apex p0023 A82-12885

Investigation of survey conditions for the ocean surface in the 0.4-1.1 micron spectral range p0024 A82-15960

Study on satellite radar altimetry in climatological and oceanographic research, volume 1 [SP/153/06/01/FR(80)-VOL-1] p0026 N82-10486

OPERATIONAL PROBLEMS

Study on satellite radar altimetry in climatological and oceanographic research, volume 2 [SP/153/06/01FR(80)-VOL-2] p0026 N82-10487

Application of the NASA airborne oceanographic lidar to the mapping of chlorophyll and other organic pigments p0027 N82-10684

Assessment of Superflux relative to remote sensing --- airborne remote sensing of the Chesapeake Bay plume and shelf regions p0028 N82-10694

Visual observations of the ocean p0028 N82-12502

An assessment of the potential contributions to oceanography from Skylab visual observations and handheld-camera photographs p0028 N82-12503

Boundary detection criteria for satellite altimeters [NASA-CR-156880] p0028 N82-12734

The SACLANTCEN oceanographic data base. Volume 1: Design criteria and data structure and content [AD-A103277] p0029 N82-13639

ICAPS oceanographic data for the Indian Ocean [AD-A103173] p0029 N82-13641

Application of remote sensing data on the continental shelf: Proceedings of an EAReL-ESA Symposium [ESA-SP-167] p0029 N82-14553

ERS-1: Mission objectives and system concept p0029 N82-14554

Offshore petroleum industry environmental data requirements: Emphasis on remote sensing p0030 N82-14557

An evaluation of Seasat-A data in relation to optimum track ship weather routing and site specific forecasting for the offshore oil industry p0030 N82-14564

Studies of the Indian continental shelf: Application of remote sensing data p0031 N82-14569

Scientific studies using Bhaskara satellite microwave radiometer (SAMIR) data: A short overview --- calibration of the instrument and its use in the study of oceanographic parameters p0032 N82-14587

A global atlas of GEOS-3 significant waveheight data and comparison of the data with national buoy data [NASA-CR-156882] p0033 N82-15498

Biological patchiness in relation to satellite thermal imagery and associated chemical mesoscale features [AD-A105757] p0047 N82-15504

Meteorological and oceanographic observations on board Netherlands lightvessels and the lightplatform 'Goeree' in the North Sea [KNMI-141-28] p0033 N82-15684

OFFSHORE ENERGY SOURCES

Offshore petroleum industry environmental data requirements: Emphasis on remote sensing p0030 N82-14557

The Seasat commercial demonstration program p0030 N82-14561

OHIO

Aircraft data summaries of the SURE intensives, volume 4 [DEB2-900311] p0012 N82-13569

OIL EXPLORATION

Offshore petroleum industry environmental data requirements: Emphasis on remote sensing p0030 N82-14557

Geologic applications of thermal-inertia mapping from satellite --- Powder River, Wyoming; Cuzco Prieta, Arizona, and Yellowstone National Park [EB2-10011] p0021 N82-15489

OIL POLLUTION

Oil spills: Large scale monitoring by LANDSAT p0012 N82-14572

The operational oil pollution surveillance system being used in France: Forecasted future developments in consideration of the NATO/CCMS remote sensing pilot study conclusions p0012 N82-14573

Use of Side Looking Airborne Radar (SLAR) for oil pollution monitoring in Norway p0012 N82-14588

OIL SLICKS

Polarimetric surveys of oil slicks p0009 A82-16619

A recommended sensor package for the detection and tracking of oil spills p0053 N82-14563

OKLAHOMA

Mapping vegetation association boundaries with Landsat MSS data - An Oklahoma example p0001 A82-10041

ONBOARD DATA PROCESSING

Application of satellite Doppler techniques to the national mapping program p0015 A82-10056

GPS application to mapping, charting and geodesy p0015 A82-10645

Onboard utilization of ground control points for image correction. Volume 2: Analysis and simulation results [NASA-CR-166732] p0045 N82-10470

Onboard utilization of ground control points for image correction. Volume 3: Ground control point simulation software design [NASA-CR-166733] p0045 N82-10471

Onboard utilization of ground control points for image correction. Volume 4: Correlation analysis software design [NASA-CR-166734] p0045 N82-10472

OPERATIONAL PROBLEMS

LANDSAT-2 and LANDSAT-3 flight evaluation report, 23 April to 23 July 1979 [EB2-10005] p0053 N82-15483

LANDSAT-2 and LANDSAT-3 flight evaluation report, 23 October 1978 to 23 January 1979 [EB2-10017] p0054 N82-15495

OPTICAL CORRECTION PROCEDURE

OPTICAL CORRECTION PROCEDURE

A new method for computing distortion
p0016 A82-12914

OPTICAL EQUIPMENT

Study on calibration methods for Earth observation optical imaging instruments
[UCD-207/1/80] p0052 N82-10488

OPTICAL PATHS

Estimation of atmospheric path-radiance by the covariance matrix method
p0041 A82-10861

OPTICAL POLARIZATION

Analysis of the information content of the polarimetric method of remote sensing
p0003 A82-16622

OPTICAL RADAR

Application of the NASA airborne oceanographic lidar to the mapping of chlorophyll and other organic pigments
p0027 N82-10684

OSTA-1 PAYLOAD

Mission operation report: OSTA-1
[NASA-TM-84053] p0055 N82-10102

OVER-THE-HORIZON RADAR

Measurement of sea and ice backscatter reflectivity using an OTH radar system
p0025 A82-18074

OXYGEN

CTD/O2 measurements during the Equatorial Pacific Ocean Climate Study (EPOCS) in 1979
[PB81-211203] p0026 N82-10461

OZONOMETRY

Trace pollutant concentrations in a multiday smog episode in the California South Coast Air Basin by long path length Fourier transform infrared spectroscopy
p0007 A82-10700

Special observations by the Hohenpeissenberg Meteorological Observatory, Number 42: Results of aerological and surface ozone measurements during the first semester of 1980
[SONDERBOB-42] p0012 N82-12714

P

PACIFIC OCEAN

Oceanic wind and balanced pressure-height fields derived from satellite measurements
p0023 A82-13214
Global satellite measurements of water vapour, wind speed and wave height
p0051 A82-17165
Annual and nonseasonal variability of monthly low-level wind fields over the Southeastern Tropical Pacific
p0025 A82-17494

The use of satellite infrared imagery for describing ocean processes in relation to spawning of the northern anchovy (*Engraulis mordax*)
p0025 A82-17565
CTD/O2 measurements during the Equatorial Pacific Ocean Climate Study (EPOCS) in 1979
[PB81-211203] p0026 N82-10461

An assessment of the potential contributions to oceanography from Skylab visual observations and handheld-camera photographs
p0028 N82-12503
Deep Ocean Mining Environmental Study. Environmental effects of commercial-scale mining
[PB81-227753] p0029 N82-13484

An evaluation of Seasat-A data in relation to optimum track ship weather routing and site specific forecasting for the offshore oil industry
p0030 N82-14564

PARAMETER IDENTIFICATION

Absolute image registration for geosynchronous satellites
p0049 A82-10051

PATENT POLICY

Microwave limb sounder --- measuring trace gases in the upper atmosphere
[NASA-CASE-NPO-14544-1] p0011 N82-12685

PATTERN RECOGNITION

American Society of Photogrammetry, Annual Meeting, 46th, St. Louis, MO, March 9-14, 1980, ASP Technical Papers
p0041 A82-10027

Digital image technology - MC&G impact --- Mapping, Charting, & Geodesy
p0015 A82-10028
Investigations concerning the image-controlled segmentation of objects in multispectral imagery data --- German thesis
p0042 A82-15003

The use of a priori information in the remote sensing of the earth from space
p0044 A82-16618

Identification of lithologic units using multichannel imaging systems
p0046 N82-11509

Vegetation patterns
p0004 N82-12500

Development and evaluation of an automatic labeling technique for spring small grains
p0004 N82-15480

Wheat cultivation: Identification and estimation of areas using LANDSAT data
[E82-10007] p0004 N82-15485

PATTERN REGISTRATION

An improvement in land cover classification achieved by merging microwave data with Landsat multispectral scanner data
p0007 A82-10043

Absolute image registration for geosynchronous satellites
p0049 A82-10051

PAYLOADS

LANDSAT-2 and LANDSAT-3 flight evaluation report, 23 April to 23 July 1979
[E82-10005] p0053 N82-15483

LANDSAT-2 and LANDSAT-3 flight evaluation report, 23 October 1978 to 23 January 1979
[E82-10017] p0054 N82-15495

PENNSYLVANIA

Comparison of conventional and remotely sensed estimates of runoff curve numbers in southeastern Pennsylvania
p0035 A82-10031
Estimation of atmospheric path-radiance by the covariance matrix method
p0041 A82-10861

PETROGRAPHY

The mineralogy of global magnetic anomalies
[E82-10009] p0021 N82-15487

PHENOLOGY

The discrimination of winter wheat using a growth-state signature
p0002 A82-15026
US/Canada wheat and barley crop calendar exploratory experiment implementation plan
[E82-10016] p0005 N82-15494

PHILIPPINES

Rural development in the humid tropics
p0003 A82-16162

PHOTO GEOLOGY

Remote sensing study of sinkhole occurrence
p0019 A82-12590

Development of a coastal relief of the Gulf of Riga, based on results of an analysis of space images
p0024 A82-15962

Investigation and mapping of the erosion relief of the Kalachskia upland on the basis of multispectral scanner images
p0008 A82-15966

Space techniques to monitor movements in the earth's crust
p0016 A82-18797

Geology and linears of Libya
p0019 N82-10618

Remote sensing studies of some ironstone gravels and plinthite in Thailand
p0019 N82-12491

Skylab explores the Earth
[NASA-SP-380] p0019 N82-12492

Global Tectonics: Some Geologic analyses of observations and photographs from Skylab
p0020 N82-12494

Geological features of southwestern North America
p0020 N82-12495

Skylab 4 observations of Volcanoes. Part A: Volcanoes and volcanic landforms. Part B: Summit eruption of Fernandian Caldera, Galapagos Islands, Ecuador
p0020 N82-12496

The Manicouagan impact structure observed from Skylab
[CONTRIB-544] p0020 N82-12497

PHOTOGRAMMETRY

American Society of Photogrammetry, Annual Meeting, 46th, St. Louis, MO, March 9-14, 1980, ASP Technical Papers
p0041 A82-10027

Orientation and construction of models. I - The orientation problem in close-range photogrammetry
p0049 A82-10858

Digital mapping using entities - A new concept
p0041 A82-12882

Phototriangulation with map referencing of photographs in linear surveys
p0016 A82-12912

Aspects in the development of aerial-photography tasks
p0041 A82-12913

Block adjustment with additional parameters
p0049 A82-13738

Compensation of systematic errors in bundle adjustment
p0042 A82-15764

Compensation of systematic errors of image and model coordinates
p0043 A82-15765

Orientation and construction of models. III - Mathematical basis of the orientation problem of one-dimensional central perspective photographs
p0043 A82-15973

Theoretical reliability of elementary photogrammetric procedures. I
p0043 A82-16163

Geometric quality of MKF-6 photographs
p0043 A82-16606

A history of flying and photography: In the Photogrammetry Division of the National Ocean Survey 1919 - 1979
[PB81-246738] p0017 N82-15520

Description and comparison of algorithms for solving large sets of sparse matrix normal equations in geodesy and photogrammetry
[SER-C-261] p0017 N82-15812

PHOTOINTERPRETATION

Applications of digital displays in photointerpretation and digital mapping
p0041 A82-10038

Remote sensing for vineyard management
p0001 A82-10047

Repetitive aerial photography for assessing marsh vegetation changes
p0001 A82-10048

Identification of conifer species groupings from Landsat digital classifications
p0002 A82-12887

Interactive techniques for estimating precipitation from GOES imagery
p0041 A82-13121

Investigations concerning the image-controlled segmentation of objects in multispectral imagery data --- German thesis
p0042 A82-15003

The discrimination of winter wheat using a growth-state signature
p0002 A82-15026

Space photographs obtained with the Fragment system as a base for landscape mapping and physical-geographical classification of arid territories
p0009 A82-15967

Airborne and spaceborne multispectral photography of the earth --- Russian book
p0043 A82-16601

Main results of the Raduga experiment
p0051 A82-16602

Methods of instrumental interpretation of multispectral aerial and space photographs
p0043 A82-16607

SUBJECT INDEX

The maximum mean accuracy of classification of remote-sensing objects and the influence on this accuracy of data acquisition and processing methods
p0044 A82-16615

Characteristics of the photometry of small objects from aerial and space photographs
p0044 A82-16616

The use of a priori information in the remote sensing of the earth from space
p0044 A82-16618

Analog methods for processing multispectral photographs
p0044 A82-16623

Investigation of the spatial structure of space images of the earth's surface
p0044 A82-16626

Processing of multispectral image data on special-purpose computer systems
p0044 A82-16627

Linear combinations of multispectral images
p0044 A82-16629

A method for using aerial photos in delineating historic patterns of beach accretion and retreat
[PB81-223836] p0010 N82-11536

Skylab explores the Earth
[NASA-SP-380] p0019 N82-12492

Visual observations of floating ice from Skylab
p0037 N82-12504

Mesoscale wake clouds in Skylab photographs
p0011 N82-12508

Mesoscale cloud features observed from Skylab
p0011 N82-12509

Quantitative analysis of drainage obtained from aerial photographs and RBV/LANDSAT images
[E82-10008] p0039 N82-15486

Visual Evaluation of E-SLAR imagery
[DFVLR-FB-81-11] p0047 N82-15503

PHOTOMAPPING

Comparison of conventional and remotely sensed estimates of runoff curve numbers in southeastern Pennsylvania
p0035 A82-10031

Date sources for analyses of Great Lakes wetlands
p0035 A82-10054

GPS application to mapping, charting and geodesy
p0015 A82-10645

Digitizing and automated output mapping errors
p0015 A82-10859

Coordinates of features on the Galilean satellites
p0019 A82-12366

Area-wide soil loss predictions using CIR airphotos
p0007 A82-12591

Satellite imagery and shoreline erosion prediction
p0036 A82-12595

Digital mapping using entities - A new concept
p0041 A82-12882

Phototriangulation with map referencing of photographs in linear surveys
p0016 A82-12912

Aerial and space methods in cartography
p0016 A82-12915

Investigations concerning the image-controlled segmentation of objects in multispectral imagery data --- German thesis
p0042 A82-15003

A VHF homing system with VHF radiotelephony for area-representative strip-survey flights conducted, as part of combined forest inventories, with light aircraft carrying 70 mm and 35 mm cameras
p0003 A82-15748

Aerial-photography flights over Upper Franconia in 1980 - Operation and first application-related experience
p0008 A82-15749

Study and mapping of agricultural land use, based on space images
p0003 A82-15963

Mapping of forest vegetation on the basis of space images
p0003 A82-15964

Study of the anthropogenic influence on the environment, based on multispectral scanning images
p0008 A82-15965

Space photographs obtained with the Fragment system as a base for landscape mapping and physical-geographical classification of arid territories
p0009 A82-15967

Analysis of variance of thematic mapping experiment data
p0009 A82-15968

Orientation and construction of models. III - Mathematical basis of the orientation problem of one-dimensional central perspective photographs
p0043 A82-15973

Coordinate referencing of MKF-6 photographs and their transformation to the cartographic projection
p0045 A82-16630

The development of the Tiros Global Environmental Satellite System
[AIAA PAPER 82-0383] p0025 A82-17915

The use of digitally processed Landsat imagery for vegetation mapping in Sulawesi, Indonesia
p0003 A82-17998

An inertially-aided aircraft track recovery system for coastal mapping
p0037 A82-18166

Photo inertial positioning system development at the Canada Centre for Remote Sensing
p0045 A82-18167

Large-scale color aerial photography as a tool in sampling for mortality rates
[PB81-214777] p0003 N82-10489

Desert sand seas
p0020 N82-12493

Snow-mapping experiment
p0037 N82-12498

An assessment of the potential contributions to oceanography from Skylab visual observations and handheld-camera photographs
p0028 N82-12503

Mapping of surface currents in Greenland fiords by means of LANDSAT images --- multispectral photography
p0038 N82-14579

SUBJECT INDEX

PHOTOMETRY

Characteristics of the photometry of small objects from aerial and space photographs p0044 A82-16616

PHOTORECONNAISSANCE

Current aerial cameras p0050 A82-15655
Quantitative analysis of atmospheric pollution phenomena p0010 N82-12505
Some aspects of tropical storm structure revealed by handheld-camera photographs from space p0011 N82-12507

PLAINS

Investigation and mapping of the erosion relief of the Kalachkaia upland on the basis of multispectral scanner images p0008 A82-15966

PLANETARY GEOLOGY

Reports of Planetary Geology Program, 1981 [NASA-TM-84211] p0016 N82-14041

PLANKTON

Development of the coastal zone color scanner for NIMBUS 7. Volume 1: Mission objectives and instrument description [NASA-CR-166720-VOL-1] p0028 N82-11511
Spectral atmospheric observations at Nantucket Island, May 7-14, 1981 [NASA-TM-83196] p0029 N82-14550
The color of the sea and its relation to surface chlorophyll and depth of the euphotic zone p0030 N82-14562
The feasibility of using remotely sensed color as an index of Irish coastal water properties --- statistical correlation of sea truth data p0032 N82-14581

PLANT STRESS

Remote sensing of crop moisture status p0003 A82-17997
Investigation of the application of remote sensing technology to environmental monitoring [E82-10010] p0013 N82-15488

PLANTS (BOTANY)

Phytoecozonation of Sevier Lake region of Utah using digitized Landsat MSS data p0001 A82-10042

POLAR CAPS

The ice conditions in the Greenland waters [ISBN-87-7478-183-9] p0028 N82-12533

POLAR METEOROLOGY

An investigation of a polar low with a spiral cloud structure p0007 A82-10616

POLAR REGIONS

ERS-1: Mission objectives and system concept p0029 N82-14554

POLARIMETRY

Polarimetric surveys of oil slicks p0009 A82-16619
Images of sea waves obtained in polarimetric surveys p0024 A82-16620
The choice of the orientation of the analyzer in polarimetric surveys p0044 A82-16621
Analysis of the information content of the polarimetric method of remote sensing p0003 A82-16622

POLARIZATION

Aircraft radar response to soil moisture p0003 A82-17564

POLLUTION MONITORING

Trace pollutant concentrations in a multiday smog episode in the California South Coast Air Basin by long path length Fourier transform infrared spectroscopy p0007 A82-10700
Automated analyzer for aircraft measurements of atmospheric methane and total hydrocarbons p0007 A82-11949
Space-lab-research of European regions with strong negative environmental influences, based on AVHRR-data of the satellites Tiros-N and NOAA p0007 A82-12517
Remote sensing that motivated community action p0008 A82-12594
Study of stack emissions by combination of lidar and correlation spectrometer p0008 A82-12816
Polarimetric surveys of oil slicks p0009 A82-16619
A new method for inferring carbon monoxide concentrations from gas filter radiometer data p0009 A82-16837
Role of remote sensing in the study of acid rain impact on aquatic systems [AIAA PAPER 82-0336] p0036 A82-17892
Shuttle applications in tropospheric air quality observations [NASA-CR-145374] p0010 N82-11635
Proof of concept study [AD-A104338] p0010 N82-11639
Quantitative analysis of atmospheric pollution phenomena p0010 N82-12505
Geophysical monitoring for climatic change, number 8: Summary Report, 1979 [PB81-233355] p0012 N82-13631
Application of remote sensing data on the continental shelf: Proceedings of an EAReL-ESA Symposium [ESA-SP-167] p0029 N82-14553
Requirements in pollution monitoring and coastal management p0030 N82-14558
A recommended sensor package for the detection and tracking of oil spills p0053 N82-14563
Studies of the Indian continental shelf: Application of remote sensing data p0031 N82-14569
Oil spills: Large scale monitoring by LANDSAT p0012 N82-14572

The operational oil pollution surveillance system being used in France: Forecasted future developments in consideration of the NATO/CCMS remote sensing pilot study conclusions p0012 N82-14573
Airborne remote sensing of the coastal zone p0053 N82-14577
Multitemporal calibration of LANDSAT images: A method for improving the marine phenomena recognition, with as example the Venice lagoon --- image brightness/green/yellow feature space, image enhancement p0046 N82-14578
Use of Side Looking Airborne Radar (SLAR) for oil pollution monitoring in Norway p0012 N82-14588
Investigation of the application of remote sensing technology to environmental monitoring [E82-10010] p0013 N82-15488

POLLUTION TRANSPORT

Results from the July 1981 Workshop on Passive Remote Sensing of the Troposphere [AIAA PAPER 82-0207] p0009 A82-17841

POSITION (LOCATION)

Interpolating for the location of remote sensor data [NASA-TM-82169] p0052 N82-13469

POSITION ERRORS

Digitizing and automated output mapping errors p0015 A82-10859
Some problem areas in the field of quality control for aerotriangulation p0016 A82-16161
Theoretical reliability of elementary photogrammetric procedures. I p0043 A82-16163

POSITION INDICATORS

Photo inertial positioning system development at the Canada Centre for Remote Sensing p0045 A82-18167

PRECIPITATION (METEOROLOGY)

Interactive techniques for estimating precipitation from GOES imagery p0041 A82-13121
A simulation study of the recession coefficient for antecedent precipitation index --- soil moisture and water runoff estimation [NASA-TM-83860] p0038 N82-14549
The effect of spatial variability in precipitation on streamflow [AD-A105955] p0038 N82-14589
PREDICTION ANALYSIS TECHNIQUES
A comparison of radiative transfer models for predicting the microwave emission from soils p0035 A82-10694
PROJECT PLANNING
U.S. Navy planning for satellite oceanographic data exploitation [AAS 81-072] p0024 A82-16341

Q

QUALITY CONTROL

Some problem areas in the field of quality control for aerotriangulation p0016 A82-16161

QUEBEC

The Manicouagan impact structure observed from Skylab [CONTRIB-544] p0020 N82-12497

R

RADAR ATTENUATION

Radar correlation with ice depolarization measurements of the 28.56 GHz COMSTAR beacon and associated cross polarization statistics [NASA-CR-166717] p0046 N82-14548

RADAR BEACONS

Radar correlation with ice depolarization measurements of the 28.56 GHz COMSTAR beacon and associated cross polarization statistics [NASA-CR-166717] p0046 N82-14548

RADAR DATA

Analysis of bright bands from 3-D radar data --- for snow/rain delineation p0035 A82-10208

RADAR ECHOES

The influence of gravity waves on radiometric measurements - A case study p0049 A82-13547
Study on satellite radar altimetry in climatological and oceanographic research, volume 1 [SP/153/06/01/FR(80)-VOL-1] p0026 N82-10486
Study on satellite radar altimetry in climatological and oceanographic research, volume 2 [SP/153/06/01/FR(80)-VOL-2] p0026 N82-10487

RADAR IMAGERY

Factorial analysis of terrain feature positioning parameters used in combining radar and digital terrain model data p0015 A82-10029
Remote sensing techniques in the study of the agricultural potential of soils under the Cerrado vegetation /Brazil/ p0001 A82-10040
Preliminary results of mapping urban land cover with Seasat SAR imagery p0007 A82-10044
The observation of tidal patterns, currents, and bathymetry with SLAR imagery of the sea p0023 A82-11201
SAR imaging of ocean waves - Theory p0023 A82-11202
Wave orbital velocity, fade, and SAR response to azimuth waves p0023 A82-11203

RADIO ALTIMETERS

A digital fast correlation approach to produce SEASAT SAR imagery p0042 A82-14870
Availability of Seasat synthetic aperture radar imagery p0050 A82-15039

Optically processed Seasat radar mosaic of Florida p0042 A82-15125

A preliminary evaluation of Seasat processing of the area of JASIN and its relevance to ERS-1 p0031 N82-14567

Seasat SAR processing at the Norwegian Defence Research Establishment --- design and operation of a digital process p0046 N82-14584

Visual Evaluation of E-SLAR imagery [DFVLR-FB-81-11] p0047 N82-15503

RADAR MAPS

Radar mapping, archaeology, and ancient land use in the Maya lowlands [NASA-CR-164931] p0010 N82-11514

RADAR MEASUREMENT

Determination of the length of sea waves by an airborne radar technique p0024 A82-15213
An analysis of short pulse and dual frequency radar techniques for measuring ocean wave spectra from satellites p0024 A82-15318
Measurement of sea and ice backscatter reflectivity using an OTH radar system p0025 A82-18074

RADAR RESOLUTION

Additional studies of Earth resources synthetic aperture radar payloads [MTR-80/90] p0054 N82-15500
New baseline system p0054 N82-15501
Squinted SAR system p0047 N82-15502

RADAR SCATTERING

Radar backscattering from ocean waves at low grazing angles p0023 A82-14730
Aircraft radar response to soil moisture p0003 A82-17564
Measurement of sea and ice backscatter reflectivity using an OTH radar system p0025 A82-18074
Anomalous wind estimates from the Seasat scatterometer p0026 A82-18724
Progress in radar snow research --- Brookings, South Dakota [NASA-CR-166709] p0038 N82-12510
Project Noordwijk. Part 1: Measurements of the radar backscatter coefficient gamma (sigma deg) in 1977 and 1978 --- on a sea platform [PHL-1979-49-PT-1] p0032 N82-14617
Project Noordwijk. Part 2: Results of North Sea clutter measurements in the L-band performed from the platform Noordwijk in September/October 1977 [PHL-1980-28-PT-2] p0033 N82-14618

RADAR SIGNATURES

The determination of navigational and meteorological variables measured by NOAA/RFC WP3D aircraft [PBB1-225468] p0028 N82-11743
Measurements of radar backscatter from Arctic Sea ice in the summer [AD-A105586] p0032 N82-14592
Measurements of radar backscatter from Arctic Sea ice in the summer, Appendices A and B [AD-A105736] p0032 N82-14593

RADAR TRACKING

The operational oil pollution surveillance system being used in France: Forecasted future developments in consideration of the NATO/CCMS remote sensing pilot study conclusions p0012 N82-14573

RADIANCE

Limitations in the spectral discrimination of the Landsat MSS p0001 A82-10046
Estimation of atmospheric path-radiance by the covariance matrix method p0041 A82-10861
Clear water radiances for atmospheric correction of coastal zone color scanner imagery p0025 A82-17292
The near-infrared radiation received by satellites from clouds p0025 A82-17492
Infrared radiance model variation by sensor flight measurements p0052 N82-14171

RADIATION ABSORPTION

Water vapour absorption in the 3.5-4.2 micron atmospheric window p0023 A82-14586

RADIATIVE HEAT TRANSFER

Radiative heating rates and some optical properties of the St. Louis aerosol, as inferred from aircraft measurements p0008 A82-14320

RADIATIVE TRANSFER

A comparison of radiative transfer models for predicting the microwave emission from soils p0035 A82-10694
Radiative transfer theory for passive microwave remote sensing of random media p0049 A82-11533
An evaluation of the spatial resolution of soil moisture information [NASA-CR-166724] p0009 N82-11513

RADIO ALTIMETERS

Ocean surface height-slope probability density function from SEASAT altimeter echo p0024 A82-15076
Seasat altimetry adjustment model including tidal and other sea surface effects [AD-A104188] p0026 N82-10473
Study on satellite radar altimetry in climatological and oceanographic research, volume 1 [SP/153/06/01/FR(80)-VOL-1] p0026 N82-10486
Study on satellite radar altimetry in climatological and oceanographic research, volume 2 [SP/153/06/01/FR(80)-VOL-2] p0026 N82-10487

State-of-the-art in using a spaceborne altimeter and scatterometer for the determination of wind, sea state, and marine and ice dynamics --- Seasat instruments p0052 N82-14560

RADIO ATTENUATION

The radiowave propagation environment - Science and technology objectives for the 80's p0009 A82-18052

RADIO DIRECTION FINDERS

Three bearing method for passive triangulation in systems with unknown deterministic biases p0050 A82-15920

RADIO RELAY SYSTEMS

A mathematical model of an over-sea airborne UHF radio link p0049 A82-11406

RADIOACTIVE CONTAMINANTS

Environmental Monitoring Report, Sandia National Labs., Albuquerque, New Mexico, 180 [DB81-027839] p0010 N82-11649

RADIOMETRIC CORRECTION

Clear water radiances for atmospheric correction of coastal zone color scanner imagery p0025 A82-17292

RADIOMETRIC RESOLUTION

The effect of angular factors on popularly used indicators of vegetative vigor p0001 A82-10039

Data compression and reconstruction for mixed resolution multispectral sensors p0049 A82-10045

The influence of gravity waves on radiometric measurements - A case study p0049 A82-13547

Onboard utilization of ground control points for image correction. Volume 2: Analysis and simulation results [NASA-CR-166732] p0045 N82-10470

Recent work in passive optical imaging of water --- space and aircraft derived data p0038 N82-14575

Use of environmental satellite data for input to energy balance snowmelt models [PB81-227795] p0039 N82-15673

RADIOTELEPHONES

A VHF homing system with VHF radiotelephony for area-representative strip-survey flights conducted, as part of combined forest inventories, with light aircraft carrying 70 mm and 35 mm cameras p0003 A82-15748

RAIN

Satellite rainfall estimation for hydrologic forecasting p0035 A82-10032

Analysis of bright bands from 3-D radar data --- for snow/rain delineation p0035 A82-10208

An evaluation of the spatial resolution of soil moisture information [NASA-CR-166724] p0009 N82-11513

A systems approach to the real-time runoff analysis with a deterministic rainfall-runoff model [PB81-224495] p0037 N82-11530

Scientific studies using Bhaskara satellite microwave radiometer (SAMIR) data: A short overview --- calibration of the instrument and its use in the study of oceanographic parameters p0032 N82-14587

Analysis of rainfall from flash flood producing thunderstorms, using GOES data p0038 N82-14724

RANGELANDS

Remote sensing contributions to the management of renewable resources p0055 A82-12530

Vegetation patterns p0004 N82-12500

RAYLEIGH SCATTERING

A theory of wave scattering from an inhomogeneous layer with an irregular interface p0041 A82-12757

RECLAMATION

A proposal for continuation of support for the application of remotely sensed data to state and regional problems. Part 1: Technical proposal [E82-10018] p0056 N82-15496

RECONNAISSANCE AIRCRAFT

The determination of navigational and meteorological variables measured by NOAA/RFC WP3D aircraft [PB81-225468] p0028 N82-11743

REFLECTANCE

Effect of grain size and snowpack water equivalence on visible and near-infrared satellite observations of snow p0035 A82-12553

Oil spills: Large scale monitoring by LANDSAT p0012 N82-14572

REGIONAL PLANNING

Introducing remote sensing to county-level agencies in Michigan through the Cooperative Extension Service p0007 A82-10034

Aerial-photography flights over Upper Franconia in 1980 Operation and first application-related experience p0008 A82-15749

The potential for use of Landsat data in water resources planning for the Missouri River Basin p0037 A82-18000

RELIEF MAPS

Development of a coastal relief of the Gulf of Riga, based on results of an analysis of space images p0024 A82-15962

RESOURCES MANAGEMENT

Remote sensing for vineyard management p0001 A82-10047

Remote sensing contributions to the management of renewable resources p0055 A82-12530

Study of the anthropogenic influence on the environment, based on multispectral scanning images p0008 A82-15965

The potential for use of Landsat data in water resources planning for the Missouri River Basin p0037 A82-18000

Application of remote sensing data on the continental shelf. Proceedings of an EAReL-ESA Symposium [ESA-SP-167] p0029 N82-14553

Fisheries investigations and management benefits from remote sensing --- fish tracking p0030 N82-14559

Application of remote sensing to selected problems within the state of California [E82-10004] p0004 N82-15482

RIVER BASINS

Airborne laser acquisition of cross-section data p0049 A82-12600

Cost effective computer processing of airborne scanner data for regional level mapping p0043 A82-15970

RIVERS

Satellite rainfall estimation for hydrologic forecasting p0035 A82-10032

Study of the dynamics of the Danube delta using space images p0036 A82-15961

Visual observations of floating ice from Skylab p0037 N82-12504

Quantitative analysis of drainage obtained from aerial photographs and RBV/LANDSAT images [E82-10008] p0039 N82-15486

ROADS

Cultural features imaged and observed from Skylab 4 p0010 N82-12499

ROCKET SOUNDING

Repeatability and measurement uncertainty of the United States meteorological rocketsonde p0049 A82-12127

ROCKY MOUNTAINS (NORTH AMERICA)

An application of Landsat derived data to a regional hydrologic model p0037 A82-17999

ROUTES

An evaluation of Seasat-A data in relation to optimum track ship weather routing and site specific forecasting for the offshore oil industry p0030 N82-14564

RURAL AREAS

Cultural features imaged and observed from Skylab 4 p0010 N82-12499

RURAL LAND USE

Rural development in the humid tropics p0003 A82-16162

S

S MATRIX THEORY

A theory of wave scattering from an inhomogeneous layer with an irregular interface p0041 A82-12757

SALINITY

Remote sensing of the Chesapeake Bay plume salinity via microwave radiometry p0028 N82-10670

Operational use of remote sensing for coastal zone management and possible contribution of specialized satellites --- aerial photography p0031 N82-14574

The feasibility of using remotely sensed color as an index of Irish coastal water properties --- statistical correlation of sea truth data p0032 N82-14581

Measurements of radar backscatter from Arctic Sea ice in the summer. Appendices A and B [AD-A105736] p0032 N82-14593

SAN ANDREAS FAULT

Geological features of southwestern North America p0020 N82-12495

SANDS

Desert sand seas p0020 N82-12493

SATELLITE OBSERVATION

Magnetic field-aligned electron distributions in the dayside cusp p0015 A82-12186

The potential and requirements for space oceanography --- National Oceanic Satellite system and U.S. Navy requirements p0029 N82-14556

Analysis of satellite observations: Theoretical studies on the sampling problem [MITT-31] p0056 N82-15499

SATELLITE ORBITS

Distant magnetic field effects associated with Birkeland currents /made possible by the evaluation of TRIAD's attitude oscillations/ p0015 A82-12215

LANDSAT-2 and LANDSAT-3 flight evaluation report, 23 April to 23 July 1979 p0053 N82-15483

LANDSAT-2 and LANDSAT-3 flight evaluation report, 23 October 1978 to 23 January 1979 [E82-10017] p0054 N82-15495

SATELLITE SURFACES

Coordinates of features on the Galilean satellites p0019 A82-12366

SATELLITE TELEVISION

The 1981 RCA space constellation p0055 A82-12541

Satellites of the Meteor series, intended for earth studies from space p0050 A82-15951

Technical equipment of an experiment for remote sensing of the earth from space p0050 A82-15952

SATELLITE-BORNE INSTRUMENTS

Metrological support of measurements of earth-surface brightness by the Fragment multispectral scanning system p0050 A82-15958

Magnetic field observations on DE-A and -B --- Dynamics Explorer A and B satellites p0051 A82-16447

SATELLITE-BORNE PHOTOGRAPHY

Coordinates of features on the Galilean satellites p0019 A82-12366

Satellites of the Meteor series, intended for earth studies from space p0050 A82-15951

Technical equipment of an experiment for remote sensing of the earth from space p0050 A82-15952

Study of the anthropogenic influence on the environment, based on multispectral scanning images p0008 A82-15965

Processing of multispectral image data on special-purpose computer systems p0044 A82-16627

Computational aspects of geometric correction data generation in the LANDSAT-D imagery processing p0045 N82-10072

Scanner --- photography from a spin stabilized synchronous satellite [NASA-CASE-GSC-12032-2] p0052 N82-13465

SATELLITE-BORNE RADAR

Study on satellite radar altimetry in climatological and oceanographic research, volume 2 [SP/153/06/01FR(80)-VOL-2] p0026 N82-10487

SAUDI ARABIA

A history of flying and photography: In the Photogrammetry Division of the National Ocean Survey 1919 - 1979 [PB81-246738] p0017 N82-15520

SCANNERS

Scanner --- photography from a spin stabilized synchronous satellite [NASA-CASE-GSC-12032-2] p0052 N82-13465

SCANNING

Airborne and spaceborne multispectral photography of the earth --- Russian book p0043 A82-16601

SCATTERING CROSS SECTIONS

Airborne laser acquisition of cross-section data p0049 A82-12600

SCATTEROMETERS

Evaluation of the Seasat wind scatterometer p0025 A82-18716

SCENE ANALYSIS

Data compression and reconstruction for mixed resolution multispectral sensors p0049 A82-10045

MATE VAN: Mobile analysis and training extension --- analyzing LANDSAT digital data [NASA-TM-84056] p0045 N82-10466

Application of remote sensing to selected problems within the state of California [E82-10004] p0004 N82-15482

SEA ICE

The development of the Tiros Global Environmental Satellite System [AIAA PAPER 82-0383] p0025 A82-17915

Measurement of sea and ice backscatter reflectivity using an OTH radar system p0025 A82-18074

The ice-conditions in the Greenland waters, 1965. Coastal maps [ISBN-87-7478-183-9] p0026 N82-10467

Study on satellite radar altimetry in climatological and oceanographic research, volume 1 [SP/153/06/01/FR(80)-VOL-1] p0026 N82-10486

Ice conditions in the eastern Bering Sea from NOAA and LANDSAT imagery: Winter conditions 1974, 1976, 1977, 1979 [PB81-220188] p0028 N82-11537

Visual observations of floating ice from Skylab p0037 N82-12504

The ice conditions in the Greenland waters [ISBN-87-7478-183-9] p0028 N82-12533

Boundary detection criteria for satellite altimeters [NASA-CR-156880] p0028 N82-12734

ERS-1: Mission objectives and system concept p0029 N82-14554

The Norwegian remote sensing experiment (Norx) in a marginal ice zone p0031 N82-14566

Marine activities in Sweden for which remote sensing data may be of interest --- oceanography, weather forecasting, and analysis p0031 N82-14576

Measurements of radar backscatter from Arctic Sea ice in the summer [AD-A105586] p0032 N82-14592

Measurements of radar backscatter from Arctic Sea ice in the summer. Appendices A and B [AD-A105736] p0032 N82-14593

SEA ROUGHNESS

SAR imaging of ocean waves - Theory p0023 A82-11202

A mathematical model of an over-sea airborne UHF radio link p0049 A82-11406

Ocean surface height-slope probability density function from SEASAT altimeter echo p0024 A82-15076

Images of sea waves obtained in polarimetric surveys p0024 A82-16620

Evaluation of the Seasat wind scatterometer p0025 A82-18716

Anomalous wind estimates from the Seasat scatterometer p0026 A82-18724

Visual observations of the ocean p0028 N82-12502

Determination of surface wind speed from remotely measured whitecap coverage, a feasibility assessment p0030 N82-14565

A preliminary evaluation of Seasat performance over the area of JASIN and its relevance to ERS-1 p0031 N82-14567

Oil spills: Large scale monitoring by LANDSAT p0012 N82-14572

Project Noordwijk. Part 1: Measurements of the radar backscatter coefficient gamma (sigma deg) in 1977 and 1978 --- on a sea platform [PHL-1979-49-PT-1] p0032 N82-14617

Project Noordwijk. Part 2: Results of North Sea clutter measurements in the I-band performed from the platform Noordwijk in September/October 1977 [PHL-1980-28-PT-2] p0033 N82-14618

SEA STATES

Analysis of SEASAT wind observations over the Indian Ocean p0023 A82-10671
 Radar backscattering from ocean waves at low grazing angles p0023 A82-14730
 Investigation of survey conditions for the ocean surface in the 0.4-1.1 micron spectral range p0024 A82-15960
 Global satellite measurements of water vapour, wind speed and wave height p0051 A82-17165
 A global atlas of GEOS-3 significant waveheight and comparison of the data with national buoy data p0026 N82-10660

State-of-the-art in using a spaceborne altimeter and scatterometer for the determination of wind, sea state, and marine and ice dynamics --- Seasat instruments p0052 N82-14560

An evaluation of Seasat-A data in relation to optimum track ship weather routing and site specific forecasting for the offshore oil industry p0030 N82-14564

Scientific studies using Bhaskara satellite microwave radiometer (SAMIR) data: A short overview --- calibration of the instrument and its use in the study of oceanographic parameters p0032 N82-14587

Remote sensing of sea state by laser altimeters [NASA-CR-165049] p0033 N82-14789

A global atlas of GEOS-3 significant waveheight data and comparison of the data with national buoy data [NASA-CR-156882] p0033 N82-15498

SEA TRUTH

The Norwegian remote sensing experiment (Norsex) in a marginal ice zone p0031 N82-14566

Coastal zone research using remote sensing techniques --- calibration of coastal zone color scanner p0031 N82-14571

The feasibility of using remotely sensed color as an index of Irish coastal water properties --- statistical correlation of sea truth data p0032 N82-14581

Necessity of remote sensing for ocean studies. Part 1: Northwest African missions, Sahara-1 and Atlor-1 --- sea truth/remote sensing correlation of offshore upwelling p0032 N82-14582

A look at nonsatellite remote sensing systems for marine use --- together with satellite systems, overall view of the technology p0032 N82-14586

GEM: A simple meteorological buoy with satellite telemetry p0053 N82-14779

A global atlas of GEOS-3 significant waveheight data and comparison of the data with national buoy data [NASA-CR-156882] p0033 N82-15498

SEA WATER

Variations in upper ocean heat storage determined from satellite data p0025 A82-17567

CTD/O2 measurements during the Equatorial Pacific Ocean Climate Study (EPOCS) in 1979 [PBB1-211203] p0026 N82-10461

Preliminary analysis of ocean color scanner data from Superflux III p0027 N82-10672

Development of the coastal zone color scanner for NIMBUS 7. Volume 1: Mission objectives and instrument description [NASA-CR-166720-VOL-1] p0028 N82-11511

The color of the sea and its relation to surface chlorophyll and depth of the euphotic zone p0030 N82-14562

SEAMOUNTS

Visual observations of the ocean p0028 N82-12502

SEARCH RADAR

Three bearing method for passive triangulation in systems with unknown deterministic biases p0050 A82-15920

SEAS

Availability of Seasat synthetic aperture radar imagery p0050 A82-15039

Global Tectonics: Some Geologic analyses of observations and photographs from Skylab p0020 N82-12494

SEASAT SATELLITES

State-of-the-art in using a spaceborne altimeter and scatterometer for the determination of wind, sea state, and marine and ice dynamics --- Seasat instruments p0052 N82-14560

The Seasat commercial demonstration program p0030 N82-14561

SEDIMENT TRANSPORT

Mapping of surface currents in Greenland fiords by means of LANDSAT images --- multispectral photography p0038 N82-14579

The use of LANDSAT MSS to observe sediment distribution and movement in the Solent coastal area --- multispectral scanline (MSS) p0038 N82-14580

Maritime applications of image processing at DFVLR, Oberpfaffenhofen, West Germany --- LANDSAT multispectral scanner images, digital interactive image analysis p0032 N82-14585

SEDIMENTARY ROCKS

Remote sensing studies of some ironstone gravels and plinthite in Thailand p0019 N82-12491

SEDIMENTS

Recent work in passive optical imaging of water --- space and aircraft derived data p0038 N82-14575

The use of LANDSAT MSS to observe sediment distribution and movement in the Solent coastal area --- multispectral scanline (MSS) p0038 N82-14580

SENSITIVITY

Evaluation of the Seasat wind scatterometer p0025 A82-18716

Assessment of Superflux relative to remote sensing --- airborne remote sensing of the Chesapeake Bay plume and shelf regions p0028 N82-10694

SEWAGE

A marine environmental monitoring and assessment program p0027 N82-10663

Operational use of remote sensing for coastal zone management and possible contribution of specialized satellites --- aerial photography p0031 N82-14574

SHALLOW WATER

An inertially-aided aircraft track recovery system for coastal mapping p0037 A82-18166

Photo inertial positioning system development at the Canada Centre for Remote Sensing p0045 A82-18167

SHIP TERMINALS

A mathematical model of an over-sea airborne UHF radio link p0049 A82-11406

SHORELINES

Satellite imagery and shoreline erosion prediction p0036 A82-12595

SPOT data simulations: Littoral applications p0046 N82-14568

SIBERIA

Investigation of the spatial structure of space images of the earth's surface p0044 A82-16626

SIDE-LOOKING RADAR

The observation of tidal patterns, currents, and bathymetry with SLAR imagery of the sea p0023 A82-11201

Use of radar and microwave radiometry for reconnaissance satellites [FOA-C-30204-E1] p0052 N82-10481

Use of Side Looking Airborne Radar (SLAR) for oil pollution monitoring in Norway p0012 N82-14588

SIGNAL PROCESSING

A digital fast correlation approach to produce SEASAT SAR imagery p0042 A82-14870

SINKHOLES

Remote sensing study of sinkhole occurrence p0019 A82-12590

SKY RADIATION

Spectral atmospheric observations at Nantucket Island, May 7-14, 1981 [NASA-TM-83196] p0029 N82-14550

SKYLAB 4

Skylab explores the Earth [NASA-SP-380] p0019 N82-12492

SMOKE

Quantitative analysis of atmospheric pollution phenomena p0010 N82-12505

SNOW

Analysis of bright bands from 3-D radar data --- for snow/rain delineation p0035 A82-10208

SNOW COVER

Effect of grain size and snowpack water equivalence on visible and near-infrared satellite observations of snow p0035 A82-12553

Reflectivity and emissivity of snow and ground at mm waves p0042 A82-14860

Snow-mapping experiment [PBB1-227795] p0037 N82-12498

Progress in radar snow research --- Brookings, South Dakota [NASA-CR-166709] p0038 N82-12510

Use of environmental satellite data for input to energy balance snowmelt models [PBB1-227795] p0039 N82-15673

SOIL EROSION

Area-wide soil loss predictions using CIR airphotos p0007 A82-12591

Investigation and mapping of the erosion relief of the Kalachkaia upland on the basis of multispectral scanner images p0008 A82-15966

Report on Skylab 4 African drought and arid land experiment p0037 N82-12501

SOIL MAPPING

Remote sensing techniques in the study of the agricultural potential of soils under the Cerrado vegetation /Brazil/ p0001 A82-10040

Limitations in the spectral discrimination of the Landsat MSS p0001 A82-10046

A comparison of radiative transfer models for predicting the microwave emission from soils p0035 A82-10694

Space photographs obtained with the Fragment system as a base for landscape mapping and physical-geographical classification of arid territories p0009 A82-15967

Aircraft radar response to soil moisture p0003 A82-17564

SOIL MOISTURE

Aircraft radar response to soil moisture p0003 A82-17564

Remote sensing of crop moisture status p0003 A82-17997

An evaluation of the spatial resolution of soil moisture information [NASA-CR-186724] p0009 N82-11513

Analysis of soil moisture extraction algorithm using data from aircraft experiments [NASA-CR-166719] p0046 N82-13470

A simulation study of the recession coefficient for antecedent precipitation index --- soil moisture and water runoff estimation [NASA-TM-83860] p0038 N82-14549

Quantitative analysis of drainage obtained from aerial photographs and RBV/LANDSAT images [E82-10008] p0039 N82-15486

SOILS

The choice of the orientation of the analyzer in polarimetric surveys p0044 A82-16621

Analysis of the information content of the polarimetric method of remote sensing p0003 A82-16622

Remote sensing studies of some ironstone gravels and plinthite in Thailand p0019 N82-12491

SOLAR FLUX DENSITY

Ionospheric propagation correction modeling for satellite altimeters [NASA-CR-156881] p0052 N82-12447

SOLAR RADIATION

The surface albedo of the earth in the near ultraviolet /330-340 nm/ p0016 A82-15032

Use of environmental satellite data for input to energy balance snowmelt models [PBB1-227795] p0039 N82-15673

SORGHUM

Remote sensing of crop moisture status p0003 A82-17997

SOUNDING ROCKETS

Repeatability and measurement uncertainty of the United States meteorological rocketsonde p0049 A82-12127

SOUTH AMERICA

Upper tropospheric cyclonic vortices in the tropical South Atlantic p0009 A82-16325

Skylab 4 observations of Volcanoes. Part A: Volcanoes and volcanic landforms. Part B: Summit eruption of Fernandina Caldera, Galapagos Islands, Ecuador p0020 N82-12496

Mesoscale cloud features observed from Skylab p0011 N82-12509

SOUTH CAROLINA

Remote sensing of benthic microalgal biomass with a tower-mounted multispectral scanner p0024 A82-15031

SOUTH DAKOTA

Progress in radar snow research --- Brookings, South Dakota [NASA-CR-166709] p0038 N82-12510

Remote sensing applications to resource problems in South Dakota [E82-10002] p0004 N82-15481

SOUTHEAST ASIA

Rural development in the humid tropics p0003 A82-16162

SOUTHERN CALIFORNIA

Trace pollutant concentrations in a midday smog episode in the California South Coast Air Basin by long path length Fourier transform infrared spectroscopy p0007 A82-10700

SOVIET SPACECRAFT

Satellites of the Meteor series, intended for earth studies from space p0050 A82-15951

Technical equipment of an experiment for remote sensing of the earth from space p0050 A82-15952

SOYBEANS

Limitations in the spectral discrimination of the Landsat MSS p0001 A82-10046

SPACE MISSIONS

Report on Active and Planned Spacecraft and experiments [NASA-TM-84025] p0055 N82-10087

SPACE SHUTTLE ORBITERS

Mission operation report: OSTA-1 [NASA-TM-84053] p0055 N82-10102

Shuttle applications in tropospheric air quality observations [NASA-CR-145374] p0010 N82-11635

SPACE SHUTTLES

The 1981 RCA space constellation p0055 A82-12541

SPACEBORNE EXPERIMENTS

Report on Active and Planned Spacecraft and experiments [NASA-TM-84025] p0055 N82-10087

Mission operation report: OSTA-1 [NASA-TM-84053] p0055 N82-10102

SPACECRAFT LAUNCHING

The 1981 RCA space constellation p0055 A82-12541

SPACECRAFT PERFORMANCE

LANDSAT-2 and LANDSAT-3 flight evaluation report, 23 April to 23 July 1979 [E82-10005] p0053 N82-15483

LANDSAT-2 and LANDSAT-3 flight evaluation report, 23 October 1978 to 23 January 1979 [E82-10017] p0054 N82-15495

SPACELAB

Spacelab-research of European regions with strong negative environmental influences, based on AVHRR-data of the satellites Tiros-N and NOAA p0007 A82-12517

SPATIAL DISTRIBUTION

The effect of spatial variability in precipitation on streamflow [AD-A105955] p0038 N82-14589

SPATIAL RESOLUTION

Data compression and reconstruction for mixed resolution multispectral sensors p0049 A82-10045

Structural analysis of aerial and space images p0044 A82-16625

Investigation of the spatial structure of space images of the earth's surface p0044 A82-16626

SPECTRAL CORRELATION

An evaluation of the spatial resolution of soil moisture information
[NASA-CR-166724] p0009 N82-11513

SPECTRAL CORRELATION

In situ spectral reflectance studies of tidal wetland grasses p0036 A82-15969
Spectral correlation filters and natural colour coding p0043 A82-16160

SPECTRAL EMISSION

Nitric oxide delta band emission in the earth's atmosphere
Companion of a measurement and a theory p0008 A82-13268

SPECTRAL RECONNAISSANCE

Spectrometric studies of the earth's surface p0043 A82-16612
Methodology and practice of spectroscopic measurements of landscape elements in the preparation and carrying out of down-looking experiments p0051 A82-16613

The application of holographic gratings in spectrometers for the spatial-spectral analysis of the earth's surface from aerial and space platforms in the visible and near-infrared spectral regions p0044 A82-16614

Use of radar and microwave radiometry for reconnaissance satellites
[FOA-C-30204-E1] p0052 N82-10481

NURE aerial gamma-ray and magnetic reconnaissance survey of Maine and portions of New York. Volume 1: Data acquisition, reduction and interpretation [DE82-000650] p0053 N82-14599

NURE aerial gamma-ray and magnetic reconnaissance survey of Maine and portions of New York, volume 2 [DE82-000781] p0020 N82-14600

NURE aerial gamma-ray and magnetic reconnaissance survey of Maine and portions of New York, volume 2 [DE82-000401] p0020 N82-14601

NURE aerial gamma-ray and magnetic reconnaissance survey of Maine and portions of New York, volume 2 [DE82-000780] p0021 N82-14602

NURE aerial gamma-ray and magnetic reconnaissance survey of Maine and portions of New York, volume 2 [DE82-000872] p0021 N82-14603

NURE aerial gamma-ray and magnetic reconnaissance survey of Maine and portions of New York, volume 2 [DE82-000772] p0021 N82-14604

NURE aerial gamma-ray and magnetic reconnaissance survey of Maine and portions of New York, volume 2 [DE82-000785] p0021 N82-14605

NURE aerial gamma-ray and magnetic reconnaissance survey of Maine and portions of New York, volume 2 [DE82-000869] p0021 N82-14606

NURE aerial gamma-ray and magnetic reconnaissance survey of Maine and portions of New York, volume 2 [DE82-000794] p0021 N82-14607

NURE aerial gamma-ray and magnetic reconnaissance survey of Maine and portions of New York, volume 2 [DE82-000784] p0021 N82-14608

SPECTRAL REFLECTANCE

The effect of angular factors on popularly used indicators of vegetative vigor p0001 A82-10039
Limitations in the spectral discrimination of the Landsat MSS p0001 A82-10046
Spectral behavior of wheat yield variety trials p0002 A82-10863

Intercalibration of Landsat 1-3 and NOAA 6 and 7 scanner data p0049 A82-13293

Reflectivity and emissivity of snow and ground at mm waves p0042 A82-14860

Temporal relationships between spectral response and agronomic variables of a corn canopy p0002 A82-15038

Metrological support of measurements of earth-surface brightness by the Fragment multispectral scanning system p0050 A82-15958

Investigation of survey conditions for the ocean surface in the 0.4-1.1 micron spectral range p0024 A82-15960

In situ spectral reflectance studies of tidal wetland grasses p0036 A82-15969

Measurement of sea and ice backscatter reflectivity using an OTH radar system p0025 A82-18074

Identification of lithologic units using multichannel imaging systems p0046 N82-11509

SPECTRAL RESOLUTION

Estimation of the brightness field from results of multispectral photography of the earth from space p0044 A82-16617

SPECTRAL SENSITIVITY

An improvement in land cover classification achieved by merging microwave data with Landsat multispectral scanner data p0007 A82-10043

Evaluation of the information content of the channels of spaceborne multispectral photography of the Fergana region by the MKF-6 camera from Soyuz-22 p0043 A82-16605

SPOT data simulations: Littoral applications p0046 N82-14568

SPECTRAL SIGNATURES

The discrimination of winter wheat using a growth-state signature p0002 A82-15026

Inclusion of a simple vegetation layer in terrain temperature models for thermal infrared (IR) signature prediction [AD-A104469] p0003 N82-11910

A recommended sensor package for the detection and tracking of oil spills p0053 N82-14563

SPECTROMETERS

The application of holographic gratings in spectrometers for the spatial-spectral analysis of the earth's surface from aerial and space platforms in the visible and near-infrared spectral regions p0044 A82-16614

SPECTROPHOTOMETRY

Spectral atmospheric observations at Nantucket Island, May 7-14, 1981 [NASA-TM-83196] p0029 N82-14550

SPECTROSCOPY

Spectrometric studies of the earth's surface p0043 A82-16612

Methodology and practice of spectroscopic measurements of landscape elements in the preparation and carrying out of down-looking experiments p0051 A82-16613

SPOT (FRENCH SATELLITE)

SPOT data simulations: Littoral applications p0046 N82-14568

SPRINGS (WATER)

Remote sensing that motivated community action p0008 A82-12594

STACKS

Study of stack emissions by combination of lidar and correlation spectrometer p0008 A82-12816

STATISTICAL ANALYSIS

Factorial analysis of terrain feature positioning parameters used in combining radar and digital terrain model data p0015 A82-10029

Analysis of variance of thematic mapping experiment data p0009 A82-15968

Estimation of the brightness field from results of multispectral photography of the earth from space p0044 A82-16617

Programs for the statistical analysis of multispectral photographs p0044 A82-16628

STEREOPHOTOGRAPHY

Orientation and construction of models. I - The orientation problem in close-range photogrammetry p0049 A82-10858

Aerial-photography flights over Upper Franconia in 1980 Operation and first application-related experience p0008 A82-15749

Orientation and construction of models. III - Mathematical basis of the orientation problem of one-dimensional central perspective photographs p0043 A82-15973

An inertially-aided aircraft track recovery system for coastal mapping p0037 A82-18166

STORMS

An evaluation of the spatial resolution of soil moisture information [NASA-CR-166724] p0009 N82-11513

STREAMS

An application of Landsat derived data to a regional hydrologic model p0037 A82-17999

STRIP MINING

Investigation of the application of remote sensing technology to environmental monitoring [EB2-10010] p0013 N82-15488

STRUCTURAL BASINS

An application of Landsat derived data to a regional hydrologic model p0037 A82-17999

STRUCTURAL PROPERTIES (GEOLOGY)

Morphostructural analyses of space imagery in the central Colorado Plateau p0019 N82-10465

Geology and linears of Libya p0019 N82-10618

The Manicouagan impact structure observed from Skylab [CONTRIB-544] p0020 N82-12497

Reports of Planetary Geology Program, 1981 [NASA-TM-84211] p0016 N82-14041

SULFUR DIOXIDES

Study of stack emissions by combination of lidar and correlation spectrometer p0008 A82-12816

Aircraft data summaries of the SURE intensives, volume 4 [DE82-900311] p0012 N82-13569

SUPPORT SYSTEMS

ISRO satellite mission support facilities - Scope and future plans p0055 A82-17307

SURFACE LAYERS

Thermal inertia, thermal admittance, and the effect of layers p0008 A82-15027

SURFACE PROPERTIES

Metrological support of measurements of earth-surface brightness by the Fragment multispectral scanning system p0050 A82-15958

Investigation of survey conditions for the ocean surface in the 0.4-1.1 micron spectral range p0024 A82-15960

SURFACE ROUGHNESS

Airborne laser acquisition of cross-section data p0049 A82-12600

A theory of wave scattering from an inhomogeneous layer with an irregular interface p0041 A82-12757

A global atlas of GEOS-3 significant waveheight and comparison of the data with national buoy data p0025 N82-10660

Progress in radar snow research --- Brookings, South Dakota [NASA-CR-166709] p0038 N82-12510

SURFACE TEMPERATURE

Two-dimensional model variability in thermal inertia surveys p0042 A82-15029

SUBJECT INDEX

Comparison of polar and geostationary satellite infrared observations of sea surface temperatures in the Gulf of Maine p0024 A82-15030

Inclusion of a simple vegetation layer in terrain temperature models for thermal infrared (IR) signature prediction [AD-A104469] p0003 N82-11910

Analysis of soil moisture extraction algorithm using data from aircraft experiments [NASA-CR-166719] p0046 N82-13470

Necessity of remote sensing for ocean studies. Part 1: Northwest African missions, Sahara-1 and Altor-1 --- see truth/remote sensing correlation of offshore upwelling p0032 N82-14582

An investigation into the applicability of thermal infrared scanning for exploration [BMFT-FB-T-81-087] p0022 N82-15925

SURFACE WATER

Application of Landsat to the inventory of DAMS p0036 A82-12593

SURGES

Characteristics of westward travelling surges during magnetospheric substorms p0050 A82-14299

SUSQUEHANNA RIVER BASIN (MD-NY-PA)

Texture transforms of remote sensing data p0042 A82-15034

SWEDEN

Marine activities in Sweden for which remote sensing data may be of interest --- oceanography, weather forecasting, and analysis p0031 N82-14576

SYNOPTIC METEOROLOGY

An investigation of a polar low with a spiral cloud structure p0007 A82-10816

Analysis of SEASAT wind observations over the Indian Ocean p0023 A82-10671

SYNTHETIC APERTURE RADAR

Preliminary results of mapping urban land cover with Seasat SAR imagery p0007 A82-10044

SAR imaging of ocean waves - Theory p0023 A82-11202

Wave orbital velocity, fade, and SAR response to azimuth waves p0023 A82-11203

A digital fast correlation approach to produce SEASAT SAR imagery p0042 A82-14870

Availability of Seasat synthetic aperture radar imagery p0050 A82-15039

Optically processed Seasat radar mosaic of Florida p0042 A82-15125

Seasat SAR processing at the Norwegian Defence Research Establishment --- design and operation of a digital process p0046 N82-14584

Remote Sensing Information Bulletin: Issue number 6 p0053 N82-14616

Additional studies of Earth resources synthetic aperture radar payloads [MTR-80/90] p0054 N82-15500

New baseline system p0054 N82-15501

Squinted SAR system p0047 N82-15502

SYSTEMS SIMULATION

Onboard utilization of ground control points for image correction. Volume 1: Executive summary [NASA-CR-166731] p0045 N82-10469

T

TECHNOLOGY TRANSFER

Introducing remote sensing to county-level agencies in Michigan through the Cooperative Extension Service p0007 A82-10034

MATE VAN: Mobile analysis and training extension --- analyzing LANDSAT digital data [NASA-TM-84056] p0045 N82-10466

Technology transfer of NASA microwave remote sensing system [NASA-CR-165791] p0028 N82-11515

TECTONIC PLATES

Global Tectonics: Some Geological analyses of observations and photographs from Skylab p0020 N82-12494

TECTONICS

Space techniques to monitor movements in the earth's crust p0016 A82-18797

TELEMETRY

Technical equipment of an experiment for remote sensing of the earth from space p0050 A82-15952

Experimental telemetry system based on the Fragment multispectral scanning system p0050 A82-15955

TEMPERATURE INVERSIONS

Detection of monsoon inversion by TIROS-N satellite p0024 A82-17168

TENNESSEE

Airborne laser acquisition of cross-section data p0049 A82-12600

TERRAIN ANALYSIS

Factorial analysis of terrain feature positioning parameters used in combining radar and digital terrain model data p0015 A82-10029

Airborne laser acquisition of cross-section data p0049 A82-12600

Investigation and mapping of the erosion relief of the Kalachskia upland on the basis of multispectral scanner images p0008 A82-15968

- Space photographs obtained with the Fragment system as a base for landscape mapping and physical-geographical classification of arid territories p0009 A82-15967
- Description and comparison of algorithms for solving large sets of sparse matrix normal equations in geodesy and photogrammetry [SER-C-261] p0017 N82-15812
- TERRESTRIAL RADIATION**
- Metrological support of measurements of earth-surface brightness by the Fragment multispectral scanning system p0050 A82-15958
- Infrared radiance model variation by sensor flight measurements p0052 N82-14171
- Analysis of satellite observations: Theoretical studies on the sampling problem [MITT-31] p0056 N82-15499
- TEXAS**
- Areawide soil loss predictions using CIR airphotos p0007 A82-12591
- Statistical Techniques Applied to Aerial Radiometric Surveys (STAARS): Series introduction and the principal-components-analysis method --- National Uranium Resource Evaluation Program [DEB1-029177] p0019 N82-10476
- Report of survey for McDonald Observatory, Harvard Radio Astronomy Station, and vicinity [PBB1-234338] p0016 N82-13606
- TEXTURES**
- Texture transforms of remote sensing data p0042 A82-15034
- Investigation of the spatial structure of space images of the earth's surface p0044 A82-16626
- THAILAND**
- Rural development in the humid tropics p0003 A82-16162
- Remote sensing studies of some ironstone gravels and pinitite in Thailand p0019 N82-12491
- THEMATIC MAPPING**
- Mapping vegetation association boundaries with Landsat MSS data - An Oklahoma example p0001 A82-10041
- An improvement in land cover classification achieved by merging microwave data with Landsat multispectral scanner data p0007 A82-10043
- Preliminary results of mapping urban land cover with Seasat SAR imagery p0007 A82-10044
- Repetitive aerial photography for assessing marsh vegetation changes p0001 A82-10048
- Satellite studies of irrigation patterns in semiarid areas An Indian study p0002 A82-10864
- Temporal spectral response of a corn canopy p0002 A82-12886
- Aerial and space methods in cartography p0016 A82-12915
- Investigations concerning the image-controlled segmentation of objects in multispectral imagery data --- German thesis p0042 A82-15003
- Analysis of variance of thematic mapping experiment data p0009 A82-15968
- Processing of multispectral image data on special-purpose computer systems p0044 A82-16627
- Linear combinations of multispectral images p0044 A82-16629
- Application of the NASA airborne oceanographic lidar to the mapping of chlorophyll and other organic pigments p0027 N82-10684
- The operational oil pollution surveillance system being used in France: Forecasted future developments in consideration of the NATO/CCMS remote sensing pilot study conclusions p0012 N82-14573
- Remote sensing in forestry: Application to the Amazon region [E82-10012] p0005 N82-15490
- A global atlas of GEOS-3 significant waveheight data and comparison of the data with national buoy data [NASA-CR-156882] p0033 N82-15498
- THERMAL CONDUCTIVITY**
- Thermal inertia, thermal admittance, and the effect of layers p0008 A82-15027
- THERMAL MAPPING**
- Mapping of the 1978 Kentucky River Flood from NOAA-5 satellite thermal infrared data p0035 A82-10033
- Civil engineering applications of remote sensing: Proceedings of the Specialty Conference, University of Wisconsin, Madison, WI, August 13, 14, 1980 p0035 A82-12589
- Water temperature mapping by infrared scanner p0036 A82-12598
- Synoptic thermal and oceanographic parameter distributions in the New York Bight Apex p0023 A82-12885
- Two-dimensional model variability in thermal inertia surveys p0042 A82-15029
- Use of visible and thermal satellite data to monitor an intermittently flooding marshland p0036 A82-15037
- The use of satellite infrared imagery for describing ocean processes in relation to spawning of the northern anchovy *Engraulis mordax* p0025 A82-17565
- Remote sensing of crop moisture status p0003 A82-17997
- Inclusion of a simple vegetation layer in terrain temperature models for thermal infrared (IR) signature prediction [AD-A104469] p0003 N82-11910
- A recommended sensor package for the detection and tracking of oil spills p0053 N82-14563
- A short review of an oceanographic use of Meteorat data by the ORSTOM remote sensing service p0031 N82-14570
- Geologic applications of thermal-inertia mapping from satellite --- Powder River, Wyoming; Cubeza Prieta, Arizona, and Yellowstone National Park [E82-10011] p0021 N82-15489
- Biological patchiness in relation to satellite thermal imagery and associated chemical mesoscale features [AD-A105757] p0047 N82-15504
- An investigation into the applicability of thermal infrared scanning for exploration [BMFT-FB-T-81-087] p0022 N82-15925
- THERMAL POLLUTION**
- Airborne remote sensing of the coastal zone p0053 N82-14577
- THERMAL RESISTANCE**
- Two-dimensional model variability in thermal inertia surveys p0042 A82-15029
- THUNDERSTORMS**
- Analysis of rainfall from flash flood producing thunderstorms, using GOES data p0038 N82-14724
- TIDAL FLATS**
- Remote sensing of benthic microalgal biomass with a tower-mounted multispectral scanner p0024 A82-15031
- In situ spectral reflectance studies of tidal wetland grasses p0036 A82-15969
- TIDAL WAVES**
- The observation of tidal patterns, currents, and bathymetry with SLAR imagery of the sea p0023 A82-11201
- TIDES**
- Seasat altimetry adjustment model including tidal and other sea surface effects [AD-A104188] p0026 N82-10473
- TIMBER IDENTIFICATION**
- An improvement in land cover classification achieved by merging microwave data with Landsat multispectral scanner data p0007 A82-10043
- Identification of conifer species groupings from Landsat digital classifications p0002 A82-12887
- Remote sensing in forestry: Application to the Amazon region [E82-10012] p0005 N82-15490
- TIMBER INVENTORY**
- A VHF homing system with VHF radiotelephony for area-representative strip-survey flights conducted, as part of combined forest inventories, with light aircraft carrying 70 mm and 35 mm cameras p0003 A82-15748
- Mapping of forest vegetation on the basis of space images p0003 A82-15964
- TIMBER VIGOR**
- Evaluation of digital photographic enhancement for Dutch elm disease detection p0002 A82-12884
- Large-scale color aerial photography as a tool in sampling for mortality rates [PBB1-214777] p0003 N82-10489
- Remote sensing applications to resource problems in South Dakota [E82-10002] p0004 N82-15481
- TIROS N SERIES SATELLITES**
- User needs and the future of operational meteorological satellites [AIAA PAPER 82-0388] p0051 A82-17918
- TIROS SATELLITES**
- The development of the Tiros Global Environmental Satellite System [AIAA PAPER 82-0383] p0025 A82-17915
- TOPOGRAPHY**
- A new method for computing distortion p0016 A82-12914
- Geometric quality of MKF-6 photographs p0043 A82-16606
- Small-scale terrain mapping based on numerical interpretation of LANDSAT imagery [VTT-40] p0045 N82-10485
- TRACE CONTAMINANTS**
- Trace pollutant concentrations in a multiday smog episode in the California South Coast Air Basin by long path length Fourier transform infrared spectroscopy p0007 A82-10700
- TRACE ELEMENTS**
- Proof of concept study [AD-A104338] p0010 N82-11639
- Limit on remote FTIR detection of trace gases [AD-A104842] p0011 N82-12511
- TRACKING NETWORKS**
- ISRO satellite mission support facilities - Scope and future plans p0055 A82-17307
- TRAINING DEVICES**
- MATE VAN: Mobile analysis and training extension --- analyzing LANDSAT digital data [NASA-TM-84056] p0045 N82-10466
- TRANSFORMATIONS (MATHEMATICS)**
- Texture transforms of remote sensing data p0042 A82-15034
- TRANSIT TIME DATA PROCESSING**
- Boundary detection criteria for satellite altimeters [NASA-CR-156880] p0028 N82-12734
- TREES (PLANTS)**
- Large-scale color aerial photography as a tool in sampling for mortality rates [PBB1-214777] p0003 N82-10489
- TRIANGULATION**
- Phototriangulation with map referencing of photographs in linear surveys p0016 A82-12912
- Block adjustment with additional parameters p0049 A82-13738
- Compensation of systematic errors of image and model coordinates p0043 A82-15765
- Three bearing method for passive triangulation in systems with unknown deterministic biases p0050 A82-15920
- Some problem areas in the field of quality control for aerotriangulation p0016 A82-16161
- TROPICAL METEOROLOGY**
- Upper tropospheric cyclonic vortices in the tropical South Atlantic p0009 A82-16325
- Detection of monsoon inversion by TIROS-N satellite p0024 A82-17168
- Annual and nonseasonal variability of monthly low-level wind fields over the Southeastern Tropical Pacific p0025 A82-17494
- National Hurricane operations plan [PBB1-247231] p0013 N82-15697
- TROPICAL REGIONS**
- Rural development in the humid tropics p0003 A82-16162
- The use of digitally processed Landsat imagery for vegetation mapping in Sulawesi, Indonesia p0003 A82-17998
- TROPICAL STORMS**
- Some aspects of tropical storm structure revealed by handheld-camera photographs from space p0011 N82-12507
- TROPOSPHERE**
- Results from the July 1981 Workshop on Passive Remote Sensing of the Troposphere [AIAA PAPER 82-0207] p0009 A82-17841
- Shuttle applications in tropospheric air quality observations [NASA-CR-145374] p0010 N82-11635
- U**
- U.S.S.R.**
- Study of the anthropogenic influence on the environment, based on multispectral scanning images p0008 A82-15965
- Space photographs obtained with the Fragment system as a base for landscape mapping and physical-geographical classification of arid territories p0009 A82-15967
- Evaluation of the information content of the channels of spaceborne multispectral photography of the Fergana region by the MKF-6 camera from Soyuz-22 p0043 A82-16605
- Spectrometric studies of the earth's surface p0043 A82-16612
- Estimation of the brightness field from results of multispectral photography of the earth from space p0044 A82-16617
- Linear combinations of multispectral images p0044 A82-16629
- Skylab 4 observations of Volcanoes. Part A: Volcanoes and volcanic landforms. Part B: Summit eruption of Fernandian Caldera, Galapagos Islands, Ecuador p0020 N82-12496
- U.S.S.R. SPACE PROGRAM**
- Satellites of the Meteor series, intended for earth studies from space p0050 A82-15951
- Technical equipment of an experiment for remote sensing of the earth from space p0050 A82-15952
- Experimental telemetry system based on the Fragment multispectral scanning system p0050 A82-15955
- Metrological support of measurements of earth-surface brightness by the Fragment multispectral scanning system p0050 A82-15958
- Investigation of survey conditions for the ocean surface in the 0.4-1.1 micron spectral range p0024 A82-15960
- Study of the dynamics of the Danube delta using space images p0036 A82-15961
- Development of a coastal relief of the Gulf of Riga, based on results of an analysis of space images p0024 A82-15962
- Study and mapping of agricultural land use, based on space images p0003 A82-15963
- Mapping of forest vegetation on the basis of space images p0003 A82-15964
- Main results of the Raduga experiment p0051 A82-16602
- U.S.S.R. THEMATIC MAPPING**
- Investigation and mapping of the erosion relief of the Kalachkaia upland on the basis of multispectral scanner images p0008 A82-15966
- ULTRAHIGH FREQUENCIES**
- A mathematical model of an over-sea airborne UHF radio link p0049 A82-11406
- UNDERWATER RESOURCES**
- Deep Ocean Mining Environmental Study. Environmental effects of commercial-scale mining [PBB1-227753] p0029 N82-13484
- UNITED STATES OF AMERICA**
- Snow-mapping experiment p0037 N82-12498
- UPPER ATMOSPHERE**
- Microwave limb sounder --- measuring trace gases in the upper atmosphere [NASA-CASE-NPO-14544-1] p0011 N82-12685.

UPWELLING WATER

The use of satellite infrared imagery for describing ocean processes in relation to spawning of the northern anchovy /Engraulis mordax/ p0025 A82-17565
A short review of an oceanographic use of Meteosat data by the ORSTOM remote sensing service p0031 N82-14570
Necessity of remote sensing for ocean studies. Part 1: Northwest African missions, Sahara-1 and Atlor-1 --- sea truth/remote sensing correlation of offshore upwelling p0032 N82-14582

URANIUM

Statistical Techniques Applied to Aerial Radiometric Surveys (STAARS): Series introduction and the principal-components-analysis method --- National Uranium Resource Evaluation Program p0019 N82-10476
NURE aerial gamma-ray and magnetic reconnaissance survey of Maine and portions of New York. Volume 1: Data acquisition, reduction and interpretation [DE82-000650] p0053 N82-14599
NURE aerial gamma-ray and magnetic reconnaissance survey of Maine and portions of New York, volume 2 [DE82-000781] p0020 N82-14600
NURE aerial gamma-ray and magnetic reconnaissance survey of Maine and portions of New York, volume 2 [DE82-000401] p0020 N82-14600
NURE aerial gamma-ray and magnetic reconnaissance survey of Maine and portions of New York, volume 2 [DE82-000780] p0021 N82-14602
NURE aerial gamma-ray and magnetic reconnaissance survey of Maine and portions of New York, volume 2 [DE82-000872] p0021 N82-14603
NURE aerial gamma-ray and magnetic reconnaissance survey of Maine and portions of New York, volume 2 [DE82-000772] p0021 N82-14604
NURE aerial gamma-ray and magnetic reconnaissance survey of Maine and portions of New York, volume 2 [DE82-000785] p0021 N82-14605
NURE aerial gamma-ray and magnetic reconnaissance survey of Maine and portions of New York, volume 2 [DE82-000869] p0021 N82-14606
NURE aerial gamma-ray and magnetic reconnaissance survey of Maine and portions of New York, volume 2 [DE82-000794] p0021 N82-14607
NURE aerial gamma-ray and magnetic reconnaissance survey of Maine and portions of New York, volume 2 [DE82-000784] p0021 N82-14608

URBAN RESEARCH

Preliminary results of mapping urban land cover with Seasat SAR imagery p0007 A82-10044
Radiative heating rates and some optical properties of the St. Louis aerosol, as inferred from aircraft measurements p0008 A82-14320
Adaptation of land use to surficial geology in metropolitan Washington, D.C. p0010 N82-11718

USER MANUALS (COMPUTER PROGRAMS)

Winterkill indicator model, Crop Condition Assessment Division (CCAD) data base interface driver, user's manual [E82-10014] p0005 N82-15492

USER REQUIREMENTS

Technology transfer of NASA microwave remote sensing system [NASA-CR-165791] p0028 N82-11515

UTAH

Phytocozonation of Sevier Lake region of Utah using digitized Landsat MSS data p0001 A82-10042

V

VEGETATION

The effect of angular factors on popularly used indicators of vegetative vigor p0001 A82-10039
Remote sensing techniques in the study of the agricultural potential of soils under the Cerrado vegetation /Brazil/ p0001 A82-10040
Mapping vegetation association boundaries with Landsat MSS data - An Oklahoma example p0001 A82-10041
Mapping of forest vegetation on the basis of space images p0003 A82-15964
Methodology and practice of spectroscopic measurements of landscape elements in the preparation and carrying out of down-looking experiments p0051 A82-16613
The choice of the orientation of the analyzer in polarimetric surveys p0044 A82-16621
Analysis of the information content of the polarimetric method of remote sensing p0003 A82-16622
The use of digitally processed Landsat imagery for vegetation mapping in Sulawesi, Indonesia p0003 A82-17998
Inclusion of a simple vegetation layer in terrain temperature models for thermal infrared (IR) signature prediction [AD-A104469] p0003 N82-11910
Vegetation patterns p0004 N82-12500
Remote sensing in forestry: Application to the Amazon region [E82-10012] p0005 N82-15490

VEGETATION GROWTH
Repetitive aerial photography for assessing marsh vegetation changes p0001 A82-10048

VERY LONG BASE INTERFEROMETRY

Space techniques to monitor movements in the earth's crust p0016 A82-18797

VIDEO DATA

Investigations concerning the image-controlled segmentation of objects in multispectral imagery data --- German thesis p0042 A82-15003

VINEYARDS

Remote sensing for vineyard management p0001 A82-10047

VIRGINIA

Repetitive aerial photography for assessing marsh vegetation changes p0001 A82-10048
Analysis of testbed airborne multispectral scanner data from Superflux II --- Chesapeake Bay plume and James Shelf data p0027 N82-10682

VISIBLE INFRARED SPIN SCAN RADIOMETRY

Distortion-free mapping of VISSR imagery data from geosynchronous satellites p0051 N82-10071

VISIBLE SPECTRUM

Effect of grain size and snowpack water equivalence on visible and near-infrared satellite observations of snow p0035 A82-12553

VISUAL OBSERVATION

Desert sand seas p0020 N82-12493
Global Tectonics: Some Geologic analyses of observations and photographs from Skylab p0020 N82-12494
Geological features of southwestern North America p0020 N82-12495
Skylab 4 observations of Volcanoes. Part A: Volcanoes and volcanic landforms. Part B: Summit eruption of Fernandian Caldera, Galapagos Islands, Ecuador p0020 N82-12496
Snow-mapping experiment p0037 N82-12498
Visual observations of the ocean p0028 N82-12502
An assessment of the potential contributions to oceanography from Skylab visual observations and handheld-camera photographs p0028 N82-12503
Visual observations of floating ice from Skylab p0037 N82-12504

VOLCANOES

Skylab 4 observations of Volcanoes. Part A: Volcanoes and volcanic landforms. Part B: Summit eruption of Fernandian Caldera, Galapagos Islands, Ecuador p0020 N82-12496
Quantitative analysis of atmospheric pollution phenomena p0010 N82-12505
Satellite observations of the Mt. St. Helens' eruption of 18 May 1980 [AD-A105784] p0012 N82-14591

W

WASHINGTON

Satellite observations of the Mt. St. Helens' eruption of 18 May 1980 [AD-A105784] p0012 N82-14591

WATER COLOR

Field study for Landsat water quality verification p0036 A82-12597
Preliminary analysis of ocean color scanner data from Superflux III p0027 N82-10672
Development of the coastal zone color scanner for NIMBUS 7. Volume 1: Mission objectives and instrument description [NASA-CR-166720-VOL-1] p0028 N82-11511
The color of the sea and its relation to surface chlorophyll and depth of the euphotic zone p0030 N82-14562
Coastal zone research using remote sensing techniques --- calibration of coastal zone color scanner p0031 N82-14571
The feasibility of using remotely sensed color as an index of Irish coastal water properties --- statistical correlation of sea truth data p0032 N82-14581

WATER CURRENTS

Maritime applications of image processing at DFVLR, Oberpfaffenhofen, West Germany --- LANDSAT multispectral scanner images, digital interactive image analysis p0032 N82-14585

WATER DEPTH

The observation of tidal patterns, currents, and bathymetry with SLAR imagery of the sea p0023 A82-11201
An inertially-aided aircraft track recovery system for coastal mapping p0037 A82-18166
Recent work in passive optical imaging of water --- space and aircraft derived data p0038 N82-14575

WATER FLOW

The effect of spatial variability in precipitation on streamflow [AD-A105955] p0038 N82-14589

WATER MANAGEMENT

Civil engineering applications of remote sensing: Proceedings of the Specialty Conference, University of Wisconsin, Madison, WI, August 13, 14, 1980 p0035 A82-12589
The potential for use of Landsat data in water resources planning for the Missouri River Basin p0037 A82-18000
Remote sensing applications to resource problems in South Dakota [E82-10002] p0004 N82-15481

WATER POLLUTION

Spacelab-research of European regions with strong negative environmental influences, based on AVHRR-data of the satellites Tiros-N and NOAA p0007 A82-12517
Remote sensing that motivated community action p0008 A82-12594
Polarimetric surveys of oil slicks p0009 A82-16619
Chesapeake Bay Plume Study: Superflux 1980 [NASA-CP-2188] p0026 N82-10661
Multitemporal calibration of LANDSAT images: A method for improving the marine phenomena recognition, with as example the Venice lagoon --- brightness/green/yellow feature space, image enhancement p0046 N82-14578

WATER QUALITY

The operational use of Landsat for lake quality assessment p0036 A82-12596
Field study for Landsat water quality verification p0036 A82-12597
Role of remote sensing in the study of acid rain impact on aquatic systems p0036 A82-17892
[AIAA PAPER 82-0336] Superflux I, II, and III experiment designs: Water sampling and analyses --- Chesapeake Bay, environmental monitoring and remote sensing p0027 N82-10665
Application of the NASA airborne oceanographic lidar to the mapping of chlorophyll and other organic pigments p0027 N82-10684
Recent work in passive optical imaging of water --- space and aircraft derived data p0038 N82-14575

WATER RESOURCES

Landsat imagery for hydrologic modeling p0036 A82-12592
The potential for use of Landsat data in water resources planning for the Missouri River Basin p0037 A82-18000

WATER RUNOFF

Comparison of conventional and remotely sensed estimates of runoff curve numbers in southeastern Pennsylvania p0035 A82-10031
A systems approach to the real-time runoff analysis with a deterministic rainfall-runoff model [PB81-224495] p0037 N82-11530
A simulation study of the recession coefficient for antecedent precipitation index --- soil moisture and water runoff estimation [NASA-TM-83860] p0038 N82-14549

WATER TEMPERATURE

Water temperature mapping by infrared scanner p0036 A82-12598
Synoptic thermal and oceanographic parameter distributions in the New York Bight Apex p0023 A82-12885
Variations in upper ocean heat storage determined from satellite data p0025 A82-17567
The development of the Tiros Global Environmental Satellite System [AIAA PAPER 82-0383] p0025 A82-17915
ICAPS oceanographic data for the Indian Ocean [AD-A103173] p0029 N82-13641
Fisheries investigations and management benefits from remote sensing --- fish tracking p0030 N82-14559
A short review of an oceanographic use of Meteosat data by the ORSTOM remote sensing service p0031 N82-14570
Operational use of remote sensing for coastal zone management and possible contribution of specialized satellites --- aerial photography p0031 N82-14574

WATER VAPOR

Water vapour absorption in the 3.5-4.2 micron atmospheric window p0023 A82-14586

WATER WAVES

SAR imaging of ocean waves - Theory p0023 A82-11202
Wave orbital velocity, fade, and SAR response to azimuth waves p0023 A82-11203
Radar backscattering from ocean waves at low grazing angles p0023 A82-14730
Ocean surface height-slope probability density function from SEASAT altimeter echo p0024 A82-15076
Determination of the length of sea waves by an airborne radar technique p0024 A82-15213
An analysis of short pulse and dual frequency radar techniques for measuring ocean wave spectra from satellites p0024 A82-15318
Images of sea waves obtained in polarimetric surveys p0024 A82-16620
Global satellite measurements of water vapour, wind speed and wave height p0051 A82-17165
A global atlas of GEOS-3 significant waveheight and comparison of the data with national buoy data p0026 N82-10660
Surface signs of internal ocean dynamics [AD-A101380] p0029 N82-13642
Determination of surface wind speed from remotely measured whitecap coverage, a feasibility assessment p0030 N82-14565
Airborne remote sensing of the coastal zone p0053 N82-14577
A global atlas of GEOS-3 significant waveheight data and comparison of the data with national buoy data [NASA-CR-156882] p0033 N82-15498

WATERSHEDS

Comparison of conventional and remotely sensed estimates of runoff curve numbers in southeastern Pennsylvania p0035 A82-10031

SUBJECT INDEX

YELLOWSTONE NATIONAL PARK (ID-MT-WY)

Areawide soil loss predictions using CIR airphotos
p0007 A82-12591

Landsat imagery for hydrologic modeling
p0036 A82-12592

An application of Landsat derived data to a regional hydrologic model
p0037 A82-17999

A simulation study of the recession coefficient for antecedent precipitation index --- soil moisture and water runoff estimation
[NASA-TM-83860] p0038 N82-14549

Remote sensing applications to resource problems in South Dakota
[E82-10002] p0004 N82-15481

WAVE REFLECTION

Wave orbital velocity, fade, and SAR response to azimuth waves
p0023 A82-11203

WAVE SCATTERING

A theory of wave scattering from an inhomogeneous layer with an irregular interface
p0041 A82-12757

WEATHER FORECASTING

A systems approach to the real-time runoff analysis with a deterministic rainfall-runoff model
[PBB1-224495] p0037 N82-11530

Some aspects of tropical storm structure revealed by handheld-camera photographs from space
p0011 N82-12507

The Seasat commercial demonstration program
p0030 N82-14561

National Hurricane operations plan
[PBB1-247231] p0013 N82-15697

WEST GERMANY

Aerial-photography flights over Upper Franconia in 1980 - Operation and first application-related experience
p0008 A82-15749

WETLANDS

An improvement in land cover classification achieved by merging microwave data with Landsat multispectral scanner data
p0007 A82-10043

Data sources for analyses of Great Lakes wetlands
p0035 A82-10054

In situ spectral reflectance studies of tidal wetland grasses
p0036 A82-15969

A proposal for continuation of support for the application of remotely sensed data to state and regional problems. Part 1: Technical proposal
[E82-10018] p0056 N82-15496

WHEAT

Spectral behavior of wheat yield variety trials
p0002 A82-10863

The discrimination of winter wheat using a growth-state signature
p0002 A82-15026

Vegetation patterns
p0004 N82-12500

Wheat cultivation: Identification and estimation of areas using LANDSAT data
[E82-10007] p0004 N82-15485

Winterkill indicator model, Crop Condition Assessment Division (CCAD) data base interface driver, user's manual
[E82-10014] p0005 N82-15492

US/Canada wheat and barley crop calendar exploratory experiment implementation plan
[E82-10016] p0005 N82-15494

WILDERNESS

Application of remote sensing to selected problems within the state of California
[E82-10004] p0004 N82-15482

WIND DIRECTION

Evaluation of the Seasat wind scatterometer
p0025 A82-18716

Anomalous wind estimates from the Seasat scatterometer
p0026 A82-18724

WIND MEASUREMENT

Analysis of SEASAT wind observations over the Indian Ocean
p0023 A82-10671

WIND PROFILES

Annual and nonseasonal variability of monthly low-level wind fields over the Southeastern Tropical Pacific
p0025 A82-17494

WIND VELOCITY

Annual and nonseasonal variability of monthly low-level wind fields over the Southeastern Tropical Pacific
p0025 A82-17494

State-of-the-art in using a spaceborne altimeter and scatterometer for the determination of wind, sea state, and marine and ice dynamics --- Seasat instruments
p0052 N82-14560

WIND VELOCITY MEASUREMENT

Oceanic wind and balanced pressure-height fields derived from satellite measurements
p0023 A82-13214

Global satellite measurements of water vapour, wind speed and wave height
p0051 A82-17165

Evaluation of the Seasat wind scatterometer
p0025 A82-18716

Anomalous wind estimates from the Seasat scatterometer
p0026 A82-18724

Determination of surface wind speed from remotely measured whitecap coverage, a feasibility assessment
p0030 N82-14565

WINTER

Ice conditions in the eastern Bering Sea from NOAA and LANDSAT imagery: Winter conditions 1974, 1976, 1977, 1979
[PBB1-220188] p0028 N82-11537

Winterkill indicator model, Crop Condition Assessment Division (CCAD) data base interface driver, user's manual
[E82-10014] p0005 N82-15492

WISCONSIN

Remote sensing that motivated community action
p0008 A82-12594

The operational use of Landsat for lake quality assessment
p0036 A82-12596

A simulation study of the recession coefficient for antecedent precipitation index --- soil moisture and water runoff estimation
[NASA-TM-83860] p0038 N82-14549

WYOMING

Geologic applications of thermal-inertia mapping from satellite --- Powder River, Wyoming; Cubeza Prieta, Arizona, and Yellowstone National Park
[E82-10011] p0021 N82-15489

Y

YELLOWSTONE NATIONAL PARK (ID-MT-WY)

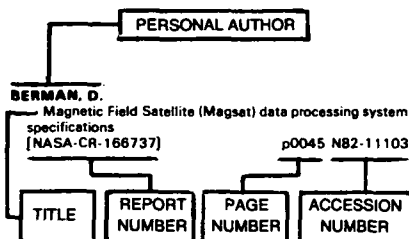
Geologic applications of thermal-inertia mapping from satellite --- Powder River, Wyoming; Cubeza Prieta, Arizona, and Yellowstone National Park
[E82-10011] p0021 N82-15489

PERSONAL AUTHOR INDEX

EARTH RESOURCES / A Continuing Bibliography (Issue 33)

APRIL 1982

Typical Personal Author Index Listing



Listings in this index are arranged alphabetically by personal author. The title of the document provides the user with a brief description of the subject matter. The report number helps to indicate the type of document listed (e.g., NASA report, translation, NASA contractor report). The page and accession numbers are located beneath and to the right of the title, e.g., p0045 N82-11103. Under any one author's name the accession numbers are arranged in sequence with the AIAA accession numbers appearing first.

A

- AARONS, J.**
The radiowave propagation environment - Science and technology objectives for the 80's p0009 A82-18052
- ABRAMS, R. B.**
The surface albedo of the earth in the near ultraviolet /330-340 nm/ p0016 A82-15032
- ACKERMANN, F.**
Block adjustment with additional parameters p0049 A82-13738
- ACUNA, M. H.**
MAGSAT: Vector magnetometer absolute sensor alignment determination [NASA-TM-79648] p0051 N82-10468
- ADAMS, R. E. W.**
Radar mapping, archaeology, and ancient land use in the Maya lowlands [NASA-CR-164931] p0010 N82-11514
- AFREMOV, V. G.**
Current aerial cameras p0050 A82-15655
- AHMADJIAN, M.**
Proof of concept study [AD-A104338] p0010 N82-11639
Limit on remote FTIR detection of trace gases [AD-A104842] p0011 N82-12511
- AKEY, N. D.**
Technology transfer of NASA microwave remote sensing system [NASA-CR-165791] p0028 N82-11515
- AKSENOV, V. V.**
Main results of the Raduga experiment p0051 A82-16602
- AL-MUFTI, S.**
Infrared spectroscopy of microorganisms near 3.4 microns in relation to geology and astronomy [PREPRINT-69] p0020 N82-12713
- ALBERTANZA, L.**
Multitemporal calibration of LANDSAT images: A method for improving the marine phenomena recognition, with as example the Venice lagoon p0046 N82-14578
- ALBUISSON, M.**
Oil spills: Large scale monitoring by LANDSAT p0012 N82-14572
- ALEXANDER, R. H.**
Adaptation of land use to surficial geology in metropolitan Washington, D.C. p0010 N82-11718
- ALLAN, T. D.**
A preliminary evaluation of Seasat performance over the area of JASIN and its relevance to ERS-1 p0031 N82-14567
- AMER, F. A. A. F.**
Theoretical reliability of elementary photogrammetric procedures. I p0043 A82-16163

B

- ANAEJIONU, P.**
Report on Skylab 4 African drought and arid land experiment p0037 N82-12501
- ANDERSON, H. N.**
Stand density estimation on panoramic transparencies p0002 A82-10862
- ANDERSON, J. A.**
Aircraft data summaries of the SURE intensives, volume 4 [DE82-900311] p0012 N82-13569
- ANDERSON, T. H.**
Geological features of southwestern North America p0020 N82-12495
- ARNAL, B.**
Aerial-photography flights over Upper Franconia in 1980 - Operation and first application-related experience p0008 A82-15749
- ARUMOV, G. P.**
Investigation of the spatial structure of space images of the earth's surface p0044 A82-16626
- ASCE, M.**
Remote sensing study of sinkhole occurrence p0019 A82-12590
- ASLAM, A.**
Progress in radar snow research [NASA-CR-166709] p0038 N82-12510
- AUSTIN, G. L.**
Analysis of bright bands from 3-D radar data p0035 A82-10208
- AVANESOV, G. A.**
Experimental telemetry system based on the Fragment multispectral scanning system p0050 A82-15955
Metrological support of measurements of earth-surface brightness by the Fragment multispectral scanning system p0050 A82-15958
Spectrometric studies of the earth's surface p0043 A82-16612
- BAHN, G. S.**
Synoptic thermal and oceanographic parameter distributions in the New York Bight Apex p0023 A82-12885
- BALDASSINIFONTANA, R.**
Infrared radiance model variation by sensor flight measurements p0052 A82-14171
- BALICK, L. K.**
Inclusion of a simple vegetation layer in terrain temperature models for thermal infrared (IR) signature prediction [AD-A104469] p0003 N82-11910
- BALL, W. E., JR.**
Bureau of Land Management satellite Doppler positioning techniques p0015 A82-10057
- BALTER, B. M.**
The maximum mean accuracy of classification of remote-sensing objects and the influence on this accuracy of data acquisition and processing methods p0044 A82-16615
- BARNES, J. C.**
Snow-mapping experiment p0037 N82-12498
- BARRICK, D. E.**
Ocean surface height-slope probability density function from SEASAT altimeter echo p0024 A82-15076
- BARTASHEVICH, A. A.**
Methodology and practice of spectroscopic measurements of landscape elements in the preparation and carrying out of down-looking experiments p0051 A82-16613
- BARTLETT, D. S.**
In situ spectral reflectance studies of tidal wetland grasses p0036 A82-15969
- BARTON, I. J.**
Water vapour absorption in the 3.5-4.2 micron atmospheric window p0023 A82-14586
- BARTSCHI, B.**
Limit on remote FTIR detection of trace gases [AD-A104842] p0011 N82-12511
- BEFORT, W. A.**
Stand density estimation on panoramic transparencies p0002 A82-10862
- BELL, G. J.**
The near-infrared radiation received by satellites from clouds p0025 A82-17492
- BENSON, A. S.**
Application of remote sensing to selected problems within the state of California [E82-10004] p0004 N82-15482
- BERG, C. P.**
Mapping of the 1978 Kentucky River Flood from NOAA-5 satellite thermal infrared data p0035 A82-10033
- BERMAN, D.**
Magnetic Field Satellite (Magsat) data processing system specifications [NASA-CR-166737] p0045 N82-11103
- BEVEN, K. J.**
The effect of spatial variability in precipitation on streamflow [AD-A105955] p0038 N82-14589
- BHATTACHARYYA, B. K.**
Preliminary analysis of gravity and aeromagnetic surveys of the Timber Mountain area, southern Nevada [DE81-029462] p0022 N82-15506
- BIRIUKOV, I. U. L.**
Calculation of the decrease in the contrast of objects of a place due to light scattering in the atmosphere p0042 A82-13633
- BLACK, P. G.**
Some aspects of tropical storm structure revealed by handheld-camera photographs from space p0011 N82-12507
- BLAD, B. L.**
Remote sensing of crop moisture status p0003 A82-17997
- BLAHA, G.**
Seasat altimetry adjustment model including tidal and other sea surface effects [AD-A104188] p0026 N82-10473
- BLANCHARD, B. J.**
A simulation study of the recession coefficient for antecedent precipitation index [NASA-TM-83660] p0038 N82-14549
- BLUMENTHAL, D. L.**
Aircraft data summaries of the SURE intensives, volume 4 [DE82-900311] p0012 N82-13569
- BLYSTRA, A. R.**
Application of Landsat to the inventory of DAMS p0036 A82-12593
- BOGGS, D. H.**
Evaluation of the Seasat wind scatterometer p0025 A82-18716
- BONDELID, T. R.**
Comparison of conventional and remotely sensed estimates of runoff curve numbers in southeastern Pennsylvania p0035 A82-10031
- BOSTROM, R.**
A Swedish proposal for an EISCAT/GEOS-2 experiment [KGI-175] p0052 N82-10484
- BOWKER, D. E.**
Analysis of testbed airborne multispectral scanner data from Superflux II p0027 N82-10682
- BOWLEY, C. J.**
Snow-mapping experiment p0037 N82-12498
- BRACALENTE, E. M.**
Evaluation of the Seasat wind scatterometer p0025 A82-18716
- BRADLEY, G. A.**
Aircraft radar response to soil moisture p0003 A82-17564
- BREED, C. S.**
Desert sand seas p0020 N82-12493
- BRENDEL, P.**
Overall economic impact of an operational Meteosat system [ESA-CR(P)-1457] p0055 N82-13010
- BROCK, R.**
Factorial analysis of terrain feature positioning parameters used in combining radar and digital terrain model data p0015 A82-10029
- BROICHER, H.**
An investigation into the applicability of thermal infrared scanning for exploration [BMFT-FB-T-81-087] p0022 N82-15925
- BROWN, R. A.**
Evaluation of the Seasat wind scatterometer p0025 A82-18716
- BROWN, W. E., JR.**
Radar mapping, archaeology, and ancient land use in the Maya lowlands [NASA-CR-164931] p0010 N82-11514
- BROWNLEE, R. H.**
Remote sensing that motivated community action p0008 A82-12594

- BRYAN, M. L.**
Optically processed Seasat radar mosaic of Florida
p0042 A82-15125
- BUKHARIN, V. D.**
Determination of the length of sea waves by an airborne radar technique
p0024 A82-15213
- BURKE, H. H. K.**
An evaluation of the spatial resolution of soil moisture information
[NASA-CR-166724] p0009 N82-11513
Analysis of soil moisture extraction algorithm using data from aircraft experiments
[NASA-CR-166719] p0046 N82-13470
- BURNASH, R. J. C.**
A systems approach to the real-time runoff analysis with a deterministic rainfall-runoff model
[PB81-224495] p0037 N82-11530
- BUSINGER, J. A.**
Anomalous wind estimates from the Seasat scatterometer
p0026 A82-18724
- BYRNE, G. F.**
Thermal inertia, thermal admittance, and the effect of layers
Use of visible and thermal satellite data to monitor an intermittently flooding marshland
p0008 A82-15027
p0036 A82-15037

C

- CAHILL, L. J., JR.**
Magnetic field observations on DE-A and -B
p0051 A82-16447
- CAMAGNI, P.**
Study of stack emissions by combination of lidar and correlation spectrometer
p0008 A82-12816
- CAMPBELL, J. W.**
Chesapeake Bay Plume Study: Superflux 1980
[NASA-CP-2188] p0026 N82-10661
Superflux I, II, and III experiment design: Remote sensing aspects
p0027 N82-10664
Assessment of Superflux relative to remote sensing
p0028 N82-10694
- CAMPBELL, W. J.**
Visual observations of floating ice from Skylab
p0037 N82-12504
The Norwegian remote sensing experiment (Norsex) in a marginal ice zone
p0031 N82-14566
- CANDIDI, M.**
Use of hydromagnetic waves to map geomagnetic field lines
p0016 A82-16868
- CANTERFORD, R. P.**
Satellite rainfall estimation for hydrologic forecasting
p0035 A82-10032
- CARLSON, C. T.**
Oceanic wind and balanced pressure-height fields derived from satellite measurements
p0023 A82-13214
- CARLSON, T. N.**
Radiative heating rates and some optical properties of the St. Louis aerosol, as inferred from aircraft measurements
p0008 A82-14320
- CARLYLE, S. M.**
The discrimination of winter wheat using a growth-state signature
p0002 A82-15026
- CARMICHAEL, J.**
Shuttle applications in tropospheric air quality observations
[NASA-CR-145374] p0010 N82-11635
- CARNEGIE, D. M.**
Vegetation patterns
p0004 N82-12500
- CARTER, C. R.**
Three bearing method for passive triangulation in systems with unknown deterministic biases
p0050 A82-15920
- CARTER, L. D.**
Visual observations of the ocean
p0028 N82-12502
- CARTER, W. E.**
Report of survey for McDonald Observatory, Harvard Radio Astronomy Station, and vicinity
[PB81-234338] p0016 N82-13606
- CASAS, J. C.**
A new method for inferring carbon monoxide concentrations from gas filter radiometer data
p0009 A82-16837
- CASPER, J. W.**
Remote sensing study of sinkhole occurrence
p0019 A82-12590
- CHAN, F. K.**
Distortion-free mapping of VISSR imagery data from geosynchronous satellites
p0051 N82-10071
- CHELTON, D. B.**
Global satellite measurements of water vapour, wind speed and wave height
p0051 A82-17165
- CHESNOKOV, I. U. M.**
Main results of the Raduga experiment
p0051 A82-16602
Analog methods for processing multispectral photographs
p0044 A82-16623
- CHOUDHURY, B. J.**
A comparison of radiative transfer models for predicting the microwave emission from soils
p0035 A82-10694
A simulation study of the recession coefficient for antecedent precipitation index
[NASA-TM-83860] p0038 N82-14549
- CHUANG, S. L.**
Radiative transfer theory for passive microwave remote sensing of random media
p0049 A82-11533

- CITEAU, J.**
A short review of an oceanographic use of Meteosat data by the ORSTOM remote sensing service
p0031 N82-14570
- CLARK, D. K.**
Clear water radiances for atmospheric correction of coastal zone color scanner imagery
p0025 A82-17292
- COFER, W. R., III**
Automated analyzer for aircraft measurements of atmospheric methane and total hydrocarbons
p0007 A82-11949
- COGAN, J. L.**
Sensitivity analysis of a mesoscale moisture model
[AD-A101528] p0012 N82-14590
- COHEN, S. H.**
An evaluation of the spatial resolution of soil moisture information
[NASA-CR-166724] p0009 N82-11513
- COHENDET, P.**
Overall economic impact of an operational Meteosat system
[ESA-CR(P)-1457] p0055 N82-13010
- COLES, R. L.**
The reduction, verification and interpretation of Magsat magnetic data over Canada
[E82-10006] p0046 N82-15484
- COLLIER, C. G.**
Analysis of bright bands from 3-D radar data
p0035 A82-10208
- COLLINS, J. G.**
Airborne laser acquisition of cross-section data
p0049 A82-12600
- COLWELL, R. N.**
Application of remote sensing to selected problems within the state of California
[E82-10004] p0004 N82-15482
- CONSTANS, J.**
Requirements in pollution monitoring and coastal management
p0030 N82-14558
- CONWAY, C. M.**
Geological features of southwestern North America
p0020 N82-12495
- COTTRELL, D. A.**
Wheat cultivation: Identification and estimation of areas using LANDSAT data
[E82-10007] p0004 N82-15485
- CRACKNELL, A. P.**
Coastal zone research using remote sensing techniques
p0031 N82-14571
- CRAWFORD, J.**
The Norwegian remote sensing experiment (Norsex) in a marginal ice zone
p0031 N82-14566
- CRISMAN, B. W.**
Monitoring the Chesapeake Bay using satellite data for Superflux III
p0027 N82-10668
- CRIST, E. P.**
Development and evaluation of an automatic labeling technique for spring small grains
[E82-10001] p0004 N82-15480
- CROSS, G. H.**
Repetitive aerial photography for assessing marsh vegetation changes
p0001 A82-10048
- CULBERT, T. P.**
Radar mapping, archaeology, and ancient land use in the Maya lowlands
[NASA-CR-164931] p0010 N82-11514
- CURRIE, N. C.**
Reflectivity and emissivity of snow and ground at mm waves
p0042 A82-14860

D

- DABROWSKA-ZIELINSKA, K.**
Use of visible and thermal satellite data to monitor an intermittently flooding marshland
p0036 A82-15037
- DALEY, C.**
An evaluation of Seasat-A data in relation to optimum track ship weather routing and site specific forecasting for the offshore oil industry
p0030 N82-14564
- DAUDRETSCH, F. C.**
Rural development in the humid tropics
p0003 A82-16162
- DAVIES, B. D.**
CTD/O2 measurements during the Equatorial Pacific Ocean Climate Study (EPOCS) in 1979
[PB81-211203] p0026 N82-10461
- DAVIES, M. E.**
Coordinates of features on the Galilean satellites
p0019 A82-12366
- DAVIS, H. W.**
The determination of navigational and meteorological variables measured by NOAA/RFC WP3D aircraft
[PB81-225468] p0028 N82-11743
- DAVIS, J. R.**
Thermal inertia, thermal admittance, and the effect of layers
p0008 A82-15027
- DAWSON, E.**
The reduction, verification and interpretation of Magsat magnetic data over Canada
[E82-10006] p0046 N82-15484
- DE BLUST, E.**
Study of stack emissions by combination of lidar and correlation spectrometer
p0008 A82-12816

- DE GROOT, M.**
Study of stack emissions by combination of lidar and correlation spectrometer
p0008 A82-12816
- DE LOOR, G. P.**
The observation of tidal patterns, currents, and bathymetry with SLAR imagery of the sea
p0023 A82-11201
- DECKER, M. T.**
The influence of gravity waves on radiometric measurements - A case study
p0049 A82-13547
- DEGNER, J. D.**
Remote sensing study of sinkhole occurrence
p0019 A82-12590
- DEJESUSPARADA, N.**
Wheat cultivation: Identification and estimation of areas using LANDSAT data
[E82-10007] p0004 N82-15485
Quantitative analysis of drainage obtained from aerial photographs and RBV/LANDSAT images
[E82-10008] p0039 N82-15486
Remote sensing in forestry: Application to the Amazon region
[E82-10012] p0005 N82-15490
- DELGREGO, F. P.**
Proof of concept study
[AD-A104338] p0010 N82-11639
- DELIMA FERNANDO CELSO SOARES MAIA, A. M.**
Wheat cultivation: Identification and estimation of areas using LANDSAT data
[E82-10007] p0004 N82-15485
- DELKER, C. V.**
Measurements of radar backscatter from Arctic Sea ice in the summer
[AD-A105586] p0032 N82-14592
Measurements of radar backscatter from Arctic Sea ice in the summer. Appendices A and B
[AD-A105736] p0032 N82-14593
- DELOOR, G. P.**
Project Noordwijk. Part 1: Measurements of the radar backscatter coefficient gamma (sigma deg) in 1977 and 1978
[PHL-1979-49-PT-1] p0032 N82-14617
- DEMAN, G.**
Airborne remote sensing of the coastal zone
p0053 N82-14577
- DENCE, M. R.**
The Manicouagan impact structure observed from Skylab
[CONTRIB-544] p0020 N82-12497
- DENNIS, J. M.**
Remote sensing that motivated community action
p0008 A82-12594
- DOERING, J. P.**
Magnetic field-aligned electron distributions in the dayside cusp
p0015 A82-12186
- DOMAIN, F.**
A short review of an oceanographic use of Meteosat data by the ORSTOM remote sensing service
p0031 N82-14570
- DOSSANTOS, A.**
Remote sensing in forestry: Application to the Amazon region
[E82-10012] p0005 N82-15490
- DOZIER, J.**
Effect of grain size and snowpack water equivalence on visible and near-infrared satellite observations of snow
p0035 A82-12553
Use of environmental satellite data for input to energy balance snowmelt models
[PB81-227795] p0039 N82-15673
- DUCHOSSOIS, G.**
ERS-1: Mission objectives and system concept
p0029 N82-14554
- DUGGIN, M. J.**
The effect of angular factors on popularly used indicators of vegetative vigor
p0001 A82-10039
Limitations in the spectral discrimination of the Landsat MSS
p0001 A82-10046
Intercalibration of Landsat 1-3 and NOAA 6 and 7 scanner data
p0049 A82-13293
- DUMAS, R. R.**
Application of Landsat to the inventory of DAMS
p0036 A82-12593
- DUNN, C. W., JR.**
Mapping vegetation association boundaries with Landsat MSS data - An Oklahoma example
p0001 A82-10041

E

- EFREMOVA, O. N.**
Study of the dynamics of the Danube delta using space images
p0036 A82-15961
- EGOROV, V. V.**
Images of sea waves obtained in polarimetric surveys
p0024 A82-16620
The choice of the orientation of the analyzer in polarimetric surveys
p0044 A82-16621
Analysis of the information content of the polarimetric method of remote sensing
p0003 A82-16622
Investigation of the spatial structure of space images of the earth's surface
p0044 A82-16626
- EGOROVA, O. I.**
Concerning the geometric accuracy of infrared scanner photographs
p0042 A82-13634

- EINAUDI, F.**
The influence of gravity waves on radiometric measurements - A case study p0049 A82-13547
- ELLIS, P. J.**
Limitations in the spectral discrimination of the Landsat MSS p0001 A82-10046
- ENDLICH, R. M.**
Oceanic wind and balanced pressure-height fields derived from satellite measurements p0023 A82-13214
- ENSLIN, W. R.**
Introducing remote sensing to county-level agencies in Michigan through the Cooperative Extension Service p0007 A82-10034
- EOM, H. J.**
A theory of wave scattering from an inhomogeneous layer with an irregular interface p0041 A82-12757
- EPIPHANIO, J. C. M.**
Quantitative analysis of drainage obtained from aerial photographs and RBV/LANDSAT images [E82-10008] p0039 N82-15486
- ERB, T. L.**
Remote sensing for vineyard management p0001 A82-10047
- ESAIAS, W. E.**
Superflux I, II, and III experiment design: Remote sensing aspects p0027 A82-10564
- ESTES, J. E.**
Application of remote sensing to selected problems within the state of California [E82-10004] p0004 N82-15482
- ESTOQUE, M. A.**
Analysis of SEASAT wind observations over the Indian Ocean p0023 A82-10671
- EVANS, D. L.**
Identification of lithologic units using multichannel imaging systems p0046 N82-11509
- EVANS, J. B.**
Water temperature mapping by infrared scanner p0036 A82-12598
- F**
- FAELTHAMMAR, C. G.**
A Swedish proposal for an EISCAT/GEOS-2 experiment [KGI-175] p0052 N82-10484
- FAINTICH, M.**
Digital image technology - MC&G impact p0015 A82-10028
- FARNSWORTH, R. K.**
Satellite rainfall estimation for hydrologic forecasting p0035 A82-10032
- FARRELLY, B.**
The Norwegian remote sensing experiment (Norsex) in a marginal ice zone p0031 N82-14566
- FARTHING, W. H.**
Magnetic field observations on DE-A and -B p0051 A82-16447
- FAVIN, S.**
Distant magnetic field effects associated with Birkeland currents /made possible by the evaluation of TRIAD's attitude oscillations/ p0015 A82-12215
- FEIN, J.**
Mesoscale cloud features observed from Skylab p0011 N82-12509
- FELT, R. Y.**
U.S. Navy planning for satellite oceanographic data exploitation [AAS 81-072] p0024 A82-16341
- FERNANDEZ-PARTAGAS, J. J.**
Analysis of SEASAT wind observations over the Indian Ocean p0023 A82-10671
- FERNANDEZ, D.**
Remote sensing for vineyard management p0001 A82-10047
- FERRAL, R. L.**
A systems approach to the real-time runoff analysis with a deterministic rainfall-runoff model [PB81-224495] p0037 N82-11530
- FILHO, M. V.**
Quantitative analysis of drainage obtained from aerial photographs and RBV/LANDSAT images [E82-10008] p0039 N82-15486
- FILHO, P. H.**
Remote sensing in forestry: Application to the Amazon region [E82-10012] p0005 N82-15490
- FINE, B. T.**
Vegetation patterns p0004 N82-12500
- FINNIGAN, J. J.**
The influence of gravity waves on radiometric measurements - A case study p0049 A82-13547
- FISHER, L. T.**
The operational use of Landsat for lake quality assessment p0036 A82-12596
- FITZGERALD, M. P.**
Determination of surface wind speed from remotely measured whitecap coverage, a feasibility assessment p0030 N82-14565
- FIVENSKI, I. I.**
The feasibility of using remotely sensed color as an index of Irish coastal water properties p0032 N82-14581
- FIVENSKI, I. I.**
Methods of instrumental interpretation of multispectral aerial and space photographs p0043 A82-16607
- Characteristics of the photometry of small objects from aerial and space photographs p0044 A82-16616
- FOKIN, A. B.**
Investigation of survey conditions for the ocean surface in the 0.4-1.1 micron spectral range p0024 A82-15960
- FOLVING, S.**
Mapping of surface currents in Greenland fiords by means of LANDSAT images p0038 N82-14579
- FORMAGGIO, A. R.**
Quantitative analysis of drainage obtained from aerial photographs and RBV/LANDSAT images [E82-10008] p0039 N82-15486
- FORSYTH, D. G.**
Mapping of the 1978 Kentucky River Flood from NOAA-5 satellite thermal infrared data p0035 A82-10033
- FOX, L., III**
Identification of conifer species groupings from Landsat digital classifications p0002 A82-12887
- FRAITURE, L.**
Infrared radiance model variation by sensor flight measurements p0052 N82-14171
- FRANSSILA, E.**
Small-scale terrain mapping based on numerical interpretation of LANDSAT imagery [VTT-40] p0045 N82-10485
- FREDERICK, J. E.**
The surface albedo of the earth in the near ultraviolet /330-340 nm/ p0016 A82-15032
- FRENCH, D. W.**
Evaluation of digital photographic enhancement for Dutch elm disease detection p0002 A82-12884
- FRIEDMAN, E.**
Shuttle applications in tropospheric air quality observations [NASA-CR-145374] p0010 N82-11635
- FRIEDMAN, J. D.**
Skylab 4 observations of Volcanoes. Part A: Volcanoes and volcanic landforms. Part B: Summit eruption of Fernandian Caldera, Galapagos Islands, Ecuador p0020 N82-12496
- FRIEDMANN, D. E.**
Two-dimensional resampling of line scan imagery by one-dimensional processing p0041 A82-10860
- FRYBERGER, S. G.**
Desert sand seas p0020 N82-12493
- FUJITA, T. T.**
Mesoscale wake clouds in Skylab photographs p0011 N82-12508
- FUNG, A. K.**
A theory of wave scattering from an inhomogeneous layer with an irregular interface p0041 A82-12757
- Progress in radar snow research [NASA-CR-166709] p0038 N82-12510
- G**
- GAN, M. A.**
Upper tropospheric cyclonic vortices in the tropical South Atlantic p0009 A82-16325
- GANGADHARARAO, L. V.**
Studies of the Indian continental shelf. Application of remote sensing data p0031 N82-14569
- GARCIA, G. J.**
Remote sensing techniques in the study of the agricultural potential of soils under the Cerrado vegetation /Brazil/ p0001 A82-10040
- GARDNER, B. R.**
Remote sensing of crop moisture status p0003 A82-17997
- GARDNER, C. S.**
Remote sensing of sea state by laser altimeters [NASA-CR-165049] p0033 N82-14789
- GARNAKERIAN, A. A.**
Determination of the length of sea waves by an airborne radar technique p0024 A82-15213
- GERTIN, I. U. M.**
Investigation of survey conditions for the ocean surface in the 0.4-1.1 micron spectral range p0024 A82-15960
- GELENS, H. F.**
Rural development in the humid tropics p0003 A82-16162
- GEORGE, T. S.**
Landsat imagery for hydrologic modeling p0036 A82-12592
- GERICKE, W.**
Study of a combined satellite system for remote sensing and earth-oriented research (LOCSS) [BMFT-FB-W-81-002] p0055 N82-14615
- GESING, W. S.**
An inertially-aided aircraft track recovery system for coastal mapping p0037 A82-18166
- GIBSON, J. R.**
An inertially-aided aircraft track recovery system for coastal mapping p0037 A82-18166
- Photo inertial positioning system development at the Canada Centre for Remote Sensing p0045 A82-18167
- GIRD, R. S.**
Interactive techniques for estimating precipitation from GOES imagery p0041 A82-13121
- GLASER, H. C.**
Radar backscattering from ocean waves at low grazing angles p0023 A82-14730
- GOGINENI, S.**
Measurements of radar backscatter from Arctic Sea ice in the summer [AD-A105586] p0032 N82-14592
- Measurements of radar backscatter from Arctic Sea ice in the summer, Appendices A and B [AD-A105736] p0032 N82-14593
- GOLDHIRSH, J.**
Radar correlation with ice depolarization measurements of the 28.56 GHz COMSTAR beacon and associated cross polarization statistics [NASA-CR-166717] p0046 N82-14548
- GOMEZ, R.**
Magnetic Field Satellite (Magsat) data processing system specifications [NASA-CR-166737] p0045 N82-11103
- GONIN, G. B.**
Evaluation of the information content of the channels of spaceborne multispectral photography of the Fergana region by the MKF-6 camera from Soyuz-22 p0043 A82-16605
- Methodology and practice of spectroscopic measurements of landscape elements in the preparation and carrying out of down-looking experiments p0051 A82-16613
- GOODMAN, J. M.**
The radiowave propagation environment - Science and technology objectives for the 80's p0009 A82-18052
- GOODRICK, G. N.**
Use of visible and thermal satellite data to monitor an intermittently flooding marshland p0036 A82-15037
- GORDON, H. R.**
Clear water radiances for atmospheric correction of coastal zone color scanner imagery p0025 A82-17292
- GORMSEN, B. B.**
A new method for inferring carbon monoxide concentrations from gas filter radiometer data p0009 A82-16837
- GRAHAM, D. S.**
Field study for Landsat water quality verification p0036 A82-12597
- GRATZ, R. L.**
Offshore petroleum industry environmental data requirements: Emphasis on remote sensing p0030 N82-14557
- GRAVESTEIJN, H.**
Project Noordwijk. Part 2: Results of North Sea clutter measurements in the I-band performed from the platform Noordwijk in September/October 1977 [PHL-1980-28-PT-2] p0033 N82-14618
- GRAY, C. E.**
Environmental Monitoring Report, Sandia National Labs., Albuquerque, New Mexico, 180 [DE81-027839] p0010 N82-11649
- GREENWALD, R. A.**
Use of hydromagnetic waves to map geomagnetic field lines p0016 A82-16868
- GUCWA, P. R.**
Global Tectonics: Some Geologic analyses of observations and photographs from Skylab p0020 N82-12494
- GUENTHER, H.**
Study of a combined satellite system for remote sensing and earth-oriented research (LOCSS) [BMFT-FB-W-81-002] p0055 N82-14615
- GUPTA, J.**
Shuttle applications in tropospheric air quality observations [NASA-CR-145374] p0010 N82-11635
- GUSTAFSSON, G.**
Distant magnetic field effects associated with Birkeland currents /made possible by the evaluation of TRIAD's attitude oscillations/ p0015 A82-12215
- A Swedish proposal for an EISCAT/GEOS-2 experiment [KGI-175] p0052 N82-10484
- GUSTINCIC, J. J.**
Microwave limb sounder [NASA-CASE-NPO-14544-1] p0011 N82-12685
- GUYMER, T. H.**
Evaluation of the Seasat wind scatterometer p0025 A82-18716
- Anomalous wind estimates from the Seasat scatterometer p0026 A82-18724
- A preliminary evaluation of Seasat performance over the area of JASIN and its relevance to ERS-1 p0031 N82-14567
- H**
- HAGGERTY, S. E.**
The mineralogy of global magnetic anomalies [E82-10009] p0021 N82-15487
- HAINES, G. V.**
The reduction, verification and interpretation of Magsat magnetic data over Canada [E82-10006] p0046 N82-15484
- HALL, D.**
Absolute image registration for geosynchronous satellites p0049 A82-10051
- HAMILTON, D. A., JR.**
Large-scale color aerial photography as a tool in sampling for mortality rates [PB81-214777] p0003 N82-10489

HANDSCHUMACHER, D. W.

A closer examination of the reduction of satellite magnetometer data for geological studies
p0019 A82-11039

HANSEN, R. F.

Winterkill indicator model. Crop Condition Assessment Division (CCAD) data base interface driver, user's manual [E82-10014]
p0005 N82-15492

HARALICK, R. M.

The discrimination of winter wheat using a growth-state signature
p0002 A82-15026

HARDESTY, C. A.

Analysis of testbed airborne multispectral scanner data from Superflux II
p0027 N82-10682

HARDY, K. R.

An evaluation of the spatial resolution of soil moisture information
[NASA-CR-166724]
p0009 N82-11513

HARRINGTON, J. A., JR.

Mapping vegetation association boundaries with Landsat MSS data - An Oklahoma example
p0001 A82-10041

HARRINGTON, R.

The Norwegian remote sensing experiment (Norsex) in a marginal ice zone
p0031 N82-14566

HARRIS, R. P.

Remote sensing techniques in the study of the agricultural potential of soils under the Cerrado vegetation /Brazil/
p0001 A82-10040

HATFIELD, J. L.

Spectral behavior of wheat yield variety trials
p0002 A82-10863

HAVIG, T. F.

Radar backscattering from ocean waves at low grazing angles
p0023 A82-14730

HAYES, R. D.

Reflectivity and emissivity of snow and ground at mm waves
p0042 A82-14860

HAYES, S. P.

CTD/02 measurements during the Equatorial Pacific Ocean Climate Study (EPOCS) in 1979
[PBB1-211203]
p0026 N82-10461

HEDBERG, A.

A Swedish proposal for an EISCAT/GEOS-2 experiment
[KGI-175]
p0052 N82-10484

HEIKEN, G.

Skylab 4 observations of Volcanoes. Part A: Volcanoes and volcanic landforms. Part B: Summit eruption of Fernandian Caldera, Galapagos Islands, Ecuador
p0020 N82-12496

HEIKKILA, J.

Compensation of systematic errors in bundle adjustment
p0042 A82-15764

HENDERSON, F. M.

Preliminary results of mapping urban land cover with Seasat SAR imagery
p0007 A82-10044

HERBERT, G. A.

Geophysical monitoring for climatic change, number 8: Summary Report, 1979
[PBB1-233355]
p0012 N82-13631

HERLAND, E. A.

Seasat SAR processing at the Norwegian Defence Research Establishment
p0046 N82-14584

HIEBER, S.

Space techniques to monitor movements in the earth's crust
p0016 A82-18797

HILL-ROWLEY, R.

Introducing remote sensing to county-level agencies in Michigan through the Cooperative Extension Service
p0007 A82-10034

HILL, J. M.

Field study for Landsat water quality verification
p0036 A82-12597

HILL, R. W.

GPS application to mapping, charting and geodesy
p0015 A82-10645

HLAVKA, C. A.

The discrimination of winter wheat using a growth-state signature
p0002 A82-15026

HO, J. H.

Analysis of soil moisture extraction algorithm using data from aircraft experiments
[NASA-CR-166719]
p0046 N82-13470

HOEJERSLEV, N. K.

The color of the sea and its relation to surface chlorophyll and depth of the euphotic zone
p0030 N82-14562

HOEST, S. E.

Use of Side Looking Airborne Radar (SLAR) for oil pollution monitoring in Norway
p0012 N82-14588

HOFFMAN, R. A.

Magnetic field-aligned electron distributions in the dayside cusp
p0015 A82-12186

HOGE, F. E.

Application of the NASA airborne oceanographic lidar to the mapping of chlorophyll and other organic pigments
p0027 N82-10684

HOLT, B.

Availability of Seasat synthetic aperture radar imagery
p0050 A82-15039

HOLT, H. E.

Reports of Planetary Geology Program, 1981
[NASA-TM-84211]
p0016 N82-14041

HOLZ, R. K.

Cultural features imaged and observed from Skylab 4
p0010 N82-12499

HORJEN, I.

The Norwegian remote sensing experiment (Norsex) in a marginal ice zone
p0031 N82-14566

HORNBERGER, G. M.

The effect of spatial variability in precipitation on streamflow
[AD-A105955]
p0038 N82-14589

HOYLE, F.

Infrared spectroscopy of microorganisms near 3.4 microns in relation to geology and astronomy
[PREPRINT-69]
p0020 N82-12713

HUMMER-MILLER, S.

Geologic applications of thermal-inertia mapping from satellite
[E82-10011]
p0021 N82-15489

HUMMER, R. F.

Scanner
[NASA-CASE-GSC-12032-2]
p0052 N82-13465

HUSSEY, K. J.

Global satellite measurements of water vapour, wind speed and wave height
p0051 A82-17165

HWANG, D.

A method for using aerial photos in delineating historic patterns of beach accretion and retreat
[PBB1-223836]
p0010 N82-11536

HYACINTHE, J. L.

State-of-the-art in using a spaceborne altimeter and scatterometer for the determination of wind, sea state, and marine and ice dynamics
p0052 N82-14560

HYPES, W. D.

Superflux I, II, and III experiment design: Remote sensing aspects
p0027 N82-10664

IANVAREVA, L. F.

Study and mapping of agricultural land use, based on space images
p0003 A82-15963

ILJN, V. B.

Current aerial cameras
p0050 A82-15655

INKILA, K.

Compensation of systematic errors in bundle adjustment
p0042 A82-15764

IRONS, J. R.

Texture transforms of remote sensing data
p0042 A82-15034

IUROV, V. I.

Geometric quality of MKF-6 photographs
p0043 A82-16606

IVASHUTINA, L. I.

Space photographs obtained with the Fragment system as a base for landscape mapping and physical-geographical classification of arid territories
p0009 A82-15967

IYENGAR, V. S.

ISRO satellite mission support facilities - Scope and future plans
p0055 A82-17307

JACKSON, F. C.

An analysis of short pulse and dual frequency radar techniques for measuring ocean wave spectra from satellites
p0024 A82-15318

JACKSON, T. J.

Comparison of conventional and remotely sensed estimates of runoff curve numbers in southeastern Pennsylvania
p0035 A82-10031

JAIN, A.

SAR imaging of ocean waves - Theory
p0023 A82-11202

JAIN, S. C.

Recent work in passive optical imaging of water
p0038 N82-14575

JAMNONGPIPATKUL, P.

Remote sensing studies of some ironstone gravels and plinthite in Thailand
p0019 N82-12491

JOBSON, D. J.

Remote sensing of benthic microalgal biomass with a tower-mounted multispectral scanner
p0024 A82-15031

JOHANNESSEN, J.

Analysis of testbed airborne multispectral scanner data from Superflux II
p0027 N82-10682

JOHANNESSEN, J.

The Norwegian remote sensing experiment (Norsex) in a marginal ice zone
p0031 N82-14566

JOHANNESSEN, O. M.

The Norwegian remote sensing experiment (Norsex) in a marginal ice zone
p0031 N82-14566

JOHNSON, C.

Application of remote sensing to selected problems within the state of California
[E82-10004]
p0004 N82-15482

JOHNSON, R.

Mesoscale cloud features observed from Skylab
p0011 N82-12509

JOHNSON, R. G.

An evaluation of Seasat-A data in relation to optimum track ship weather routing and site specific forecasting for the offshore oil industry
p0030 N82-14564

JOHNSON, R. W.

Synoptic thermal and oceanographic parameter distributions in the New York Bight Apex
p0023 A82-12885

JOHNSON, W. L.

Evaluation of digital photographic enhancement for Dutch elm disease detection
p0002 A82-12884

JONES, L.

The Norwegian remote sensing experiment (Norsex) in a marginal ice zone
p0031 N82-14566

JONES, W. L.

Evaluation of the Seasat wind scatterometer
p0025 A82-18716

Anomalous wind estimates from the Seasat scatterometer
p0026 A82-18724

K**KAIGORODOV, A. I.**

Phototriangulation with map referencing of photographs in linear surveys
p0016 A82-12912

KAMINSKI, H.

Spacelab-research of European regions with strong negative environmental influences, based on AVHRR-data of the satellites Tiros-N and NOAA
p0007 A82-12517

KANE, M. F.

Preliminary analysis of gravity and aeromagnetic surveys of the Timber Mountain area, southern Nevada
[DEB1-029462]
p0022 N82-15506

KARAKUSHIAN, V. L.

Determination of the length of sea waves by an airborne radar technique
p0024 A82-15213

KATAYAMA, F. Y.

Coordinates of features on the Galilean satellites
p0019 A82-12366

KATZBERG, S. J.

Remote sensing of benthic microalgal biomass with a tower-mounted multispectral scanner
p0024 A82-15031

KEAFER, L. S., JR.

Results from the July 1981 Workshop on Passive Remote Sensing of the Troposphere
[AIAA PAPER 82-0207]
p0009 A82-17841

KEIFER, W. S.

Aircraft data summaries of the SURE intensives, volume 4
[DEB2-900311]
p0012 N82-13569

KELNER, I. U. G.

Aerial and space methods in cartography
p0016 A82-12915

KENDALL, B. M.

Remote sensing of the Chesapeake Bay plume salinity via microwave radiometry
p0027 A82-10670

KESSLER, B. L.

Stand density estimation on panoramic transparencies
p0002 A82-10862

KHATUNTSEVA, M. V.

Programs for the statistical analysis of multispectral photographs
p0044 A82-16628

Linear combinations of multispectral images
p0044 A82-16629

KIEFER, R. W.

Civil engineering applications of remote sensing: Proceedings of the Specialty Conference, University of Wisconsin, Madison, WI, August 13, 14, 1980
p0035 A82-12589

KILLPACK, D. P.

An application of Landsat derived data to a regional hydrologic model
p0037 A82-17999

KILPELA, E.

Compensation of systematic errors in bundle adjustment
p0042 A82-15764

Compensation of systematic errors of image and model coordinates
p0043 A82-15765

KIMES, D. S.

Temporal spectral response of a corn canopy
p0002 A82-12886

Temporal relationships between spectral response and agronomic variables of a corn canopy
p0002 A82-15038

KLEMAS, V.

In situ spectral reflectance studies of tidal wetland grasses
p0036 A82-15969

KLOSTER, K.

The Norwegian remote sensing experiment (Norsex) in a marginal ice zone
p0031 N82-14566

KLOTZ, H.

Study of a combined satellite system for remote sensing and earth-oriented research (LOCSS)
[BMFT-FB-W-81-002]
p0055 N82-14615

KOCH, D.

Absolute image registration for geosynchronous satellites
p0049 A82-10051

KOECHLER, C.

Study of stack emissions by combination of lidar and correlation spectrometer
p0008 A82-12816

KOGUT, J.

SMMR data set development for GARP
[NASA-CR-166721]
p0052 N82-11512

KONG, J. A.

Radiative transfer theory for passive microwave remote sensing of random media
p0049 A82-11533

KORNFIELD, J.

Interpolating for the location of remote sensor data
[NASA-TM-82169]
p0052 N82-13469

KOROLEVA, V. P.

Evaluation of the information content of the channels of spaceborne multispectral photography of the Fergana region by the MKF-6 camera from Soyuz-22
p0043 A82-16605

- KOTOVA, T. V.**
Mapping of forest vegetation on the basis of space images p0003 AB2-15984
- KOTSOV, V. A.**
Estimation of the brightness field from results of multispectral photography of the earth from space p0044 AB2-16617
- KOTTISOV, V. A.**
The use of a priori information in the remote sensing of the earth from space p0044 AB2-16618
- KOUSKY, V. E.**
Upper tropospheric cyclonic vortices in the tropical South Atlantic p0009 AB2-16325
- KOWALIK, W. S.**
Estimation of atmospheric path-radiance by the covariance matrix method p0041 AB2-10861
- KRABILL, W. B.**
Airborne laser acquisition of cross-section data p0049 AB2-12600
- KRASIKOV, V. A.**
Geometric quality of MKF-6 photographs p0043 AB2-16606
Processing of multispectral image data on special-purpose computer systems p0044 AB2-16627
Programs for the statistical analysis of multispectral photographs p0044 AB2-16628
Coordinate referencing of MKF-6 photographs and their transformation to the cartographic projection p0045 AB2-16630
- KRAUSH, K. A.**
Structural analysis of aerial and space images p0044 AB2-16625
- KRAVCHUK, N. V.**
Methodology and practice of spectroscopic measurements of landscape elements in the preparation and carrying out of down-looking experiments p0051 AB2-16613
- KRAVTSOVA, V. I.**
Study of the dynamics of the Danube delta using space images p0036 AB2-15961
Development of a coastal relief of the Gulf of Riga, based on results of an analysis of space images p0024 AB2-15962
Mapping of forest vegetation on the basis of space images p0003 AB2-15964
Study of the anthropogenic influence on the environment, based on multispectral scanning images p0008 AB2-15965
- KRIEGER, R.**
Study of a combined satellite system for remote sensing and earth-oriented research (LOCSS) [BMFT-FB-W-81-002] p0055 AB2-14615
- KRUEGER, A. F.**
Skylab 4 observations of Volcanoes. Part A: Volcanoes and volcanic landforms. Part B: Summit eruption of Fernandian Caldera, Galapagos Islands, Ecuador p0020 AB2-12496
- KUZNETSOV, I. U. N.**
Characteristics of the photometry of small objects from aerial and space photographs p0044 AB2-16616
- L**
- LABUTINA, I. A.**
Methods of instrumental interpretation of multispectral aerial and space photographs p0043 AB2-16607
- LAGARDE, J. B.**
Overall economic impact of an operational Meteosat system [ESA-CR(P)-1457] p0055 AB2-13010
- LANNELONGUE, N.**
SPOT data simulations: Littoral applications p0046 AB2-14568
- LAPTEVA, N. I.**
Investigation and mapping of the erosion relief of the Katschkaia upland on the basis of multispectral scanner images p0008 AB2-15966
- LASKER, R.**
The use of satellite infrared imagery for describing ocean processes in relation to spawning of the northern anchovy /Engraulis mordax/ p0025 AB2-17565
- LAURS, R. M.**
The use of satellite infrared imagery for describing ocean processes in relation to spawning of the northern anchovy /Engraulis mordax/ p0025 AB2-17565
- LEDLEY, B. G.**
Magnetic field observations on DE-A and -B p0051 AB2-16447
- LEE, D. C. L.**
Wheat cultivation: Identification and estimation of areas using LANDSAT data [E82-10007] p0004 AB2-15485
- LEE, J. S.**
Magnetic field-aligned electron distributions in the dayside cusp p0015 AB2-12188
- LEE, J. T.**
Mesoscale cloud features observed from Skylab p0011 AB2-12509
- LEFEBVRE, M.**
State-of-the-art in using a spaceborne altimeter and scatterometer for the determination of wind, sea state, and marine and ice dynamics p0052 AB2-14560
- LEGECKIS, R.**
Comparison of polar and geostationary satellite infrared observations of sea surface temperatures in the Gulf of Maine p0024 AB2-15030
- LEGER, G.**
Requirements in pollution monitoring and coastal management p0030 AB2-14558
- LEGG, E.**
Comparison of polar and geostationary satellite infrared observations of sea surface temperatures in the Gulf of Maine p0024 AB2-15030
- LENNERTZ, D.**
ERS-1: Mission objectives and system concept p0029 AB2-14554
- LEUPOLD, R. C.**
An evaluation of the spatial resolution of soil moisture information [NASA-CR-166724] p0009 AB2-11513
- LEVINE, I.**
Computational aspects of geometric correction data generation in the LANDSAT-D imagery processing p0045 AB2-10072
The MSS control point location error filter for LANDSAT-D p0051 AB2-10073
- LEVY, G.**
Application of remote sensing data on the continental shelf: Proceedings of an EARL-ESA Symposium [ESA-SP-167] p0029 AB2-14553
- LILLESAND, T. M.**
Evaluation of digital photographic enhancement for Dutch elm disease detection p0002 AB2-12884
- LIMEBURNER, R.**
Comparison of polar and geostationary satellite infrared observations of sea surface temperatures in the Gulf of Maine p0024 AB2-15030
- LINK, L. E., JR.**
Inclusion of a simple vegetation layer in terrain temperature models for thermal infrared (IR) signature prediction [AD-A104469] p0003 AB2-11910
- LIPA, B. J.**
Ocean surface height-slope probability density function from SEASAT altimeter echo p0024 AB2-15076
- LJOEN, R.**
Fisheries investigations and management benefits from remote sensing p0030 AB2-14559
- LOK, M.**
Use of radar and microwave radiometry for reconnaissance satellites [FOA-C-30204-E1] p0052 AB2-10481
- LONGDON, M.**
Application of remote sensing data on the continental shelf: Proceedings of an EARL-ESA Symposium [ESA-SP-167] p0029 AB2-14553
- LOVEJOY, S.**
Analysis of bright bands from 3-D radar data p0035 AB2-10208
- LOWE, T. W.**
The potential for use of Landsat data in water resources planning for the Missouri River Basin p0037 AB2-18000
- LULLA, K.**
Phytoecozonation of Sevier Lake region of Utah using digitized Landsat MSS data p0001 AB2-10042
- LUSCOMBE, A. P.**
Additional studies of Earth resources synthetic aperture radar payloads [MTR-80/90] p0054 AB2-15500
- LYKASHEVA, E. G.**
The application of holographic gratings in spectrometers for the spatial-spectral analysis of the earth's surface from aerial and space platforms in the visible and near-infrared spectral regions p0044 AB2-16614
- LYON, J. G.**
Data sources for analyses of Great Lakes wetlands p0035 AB2-10054
- LYON, R. J. P.**
Estimation of atmospheric path-radiance by the covariance matrix method p0041 AB2-10861
- M**
- MAAROUF, A. M. S.**
Morphostructural analyses of space imagery in the central Colorado Plateau p0019 AB2-10465
- MACLEOD, N. H.**
Report on Skylab 4 African drought and arid land experiment p0037 AB2-12501
- MAITSON, M. H.**
Report on Active and Planned Spacecraft and experiments [NASA-TM-84025] p0055 AB2-10087
- MAKAREVICH, A. K.**
Mapping of forest vegetation on the basis of space images p0003 AB2-15964
- MALLA, W. A.**
Development and evaluation of an automatic labeling technique for spring small grains [E82-10001] p0004 AB2-15480
- MANGEL, M.**
Three bearing method for passive triangulation in systems with unknown deterministic biases p0050 AB2-15920
- MANGUM, L. J.**
CTD/02 measurements during the Equatorial Pacific Ocean Climate Study (EPOCS) in 1979 [PB81-211203] p0026 AB2-10461
- MANSUR, M. A.**
Geology and linears of Libya p0019 AB2-10618
- MARESCA, J. W., JR.**
Oceanic wind and balanced pressure-height fields derived from satellite measurements p0023 AB2-13214
- MARKARIAN, E. G.**
Calculation of the decrease in the contrast of objects of a plane due to light scattering in the atmosphere p0042 AB2-13633
- MARKHAM, B. L.**
Temporal spectral response of a corn canopy p0002 AB2-12886
Temporal relationships between spectral response and agronomic variables of a corn canopy p0002 AB2-15038
- MARTIN, C. F.**
Boundary detection criteria for satellite altimeters [NASA-CR-156880] p0028 AB2-12734
- MASRY, S. E.**
Digital mapping using entities - A new concept p0041 AB2-12882
- MASSIN, J. M.**
The operational oil pollution surveillance system being used in France: Forecasted future developments in consideration of the NATO/CCMS remote sensing pilot study conclusions p0012 AB2-14573
- MAUL, G. A.**
An assessment of the potential contributions to oceanography from Skylab visual observations and handheld-camera photographs p0028 AB2-12503
- MAUSEL, P.**
Phytoecozonation of Sevier Lake region of Utah using digitized Landsat MSS data p0001 AB2-10042
- MAYER, K. E.**
Identification of conifer species groupings from Landsat digital classifications p0002 AB2-12887
- MCCANDLESS, S. W.**
The Seasat commercial demonstration program p0030 AB2-14561
- MCCASLIN, M.**
An assessment of the potential contributions to oceanography from Skylab visual observations and handheld-camera photographs p0028 AB2-12503
- MCCOY, R. M.**
An application of Landsat derived data to a regional hydrologic model p0037 AB2-17999
- MCCUEN, R. H.**
Comparison of conventional and remotely sensed estimates of runoff curve numbers in southeastern Pennsylvania p0035 AB2-10031
- MCDONALD, J. A.**
Aircraft data summaries of the SURE intensives, volume 4 [DE82-900311] p0012 AB2-13589
- MCGINNIS, D. F., JR.**
Mapping of the 1978 Kentucky River Flood from NOAA-5 satellite thermal infrared data p0035 AB2-10033
Effect of grain size and snowpack water equivalence on visible and near-infrared satellite observations of snow p0035 AB2-12553
- MCKEE, E. D.**
Desert sand seas p0020 AB2-12493
- MCLEESTER, J. N.**
Remote sensing for vineyard management p0001 AB2-10047
- MCMILLAN, J. D.**
A global atlas of GEOS-3 significant waveheight and comparison of the data with national buoy data p0026 AB2-10680
A global atlas of GEOS-3 significant waveheight data and comparison of the data with national buoy data [NASA-CR-156882] p0033 AB2-15498
- MCMURTREY, J. E., III**
Temporal spectral response of a corn canopy p0002 AB2-12886
Temporal relationships between spectral response and agronomic variables of a corn canopy p0002 AB2-15038
- MCNUTT, L.**
Ice conditions in the eastern Bering Sea from NOAA and LANDSAT imagery: Winter conditions 1974, 1976, 1977, 1979 [PB81-220188] p0028 AB2-11537
- MCWILLIAM, B. N.**
An inertially-aided aircraft track recovery system for coastal mapping p0037 AB2-18186
- MEAD, R. A.**
Repetitive aerial photography for assessing marsh vegetation changes p0001 AB2-10048
- MEISNER, D. E.**
Evaluation of digital photographic enhancement for Dutch elm disease detection p0002 AB2-12884
- MENDONCA, F. J.**
Wheat cultivation: Identification and estimation of areas using LANDSAT data [E82-10007] p0004 AB2-15485
- MERCERET, F. J.**
The determination of navigational and meteorological variables measured by NOAA/RFC WP3D aircraft [PB81-225488] p0028 AB2-11743

- METHOD, T. J.**
Radiative heating rates and some optical properties of the St. Louis aerosol, as inferred from aircraft measurements p0008 A82-14320
- METZGAR, B.**
Study of a combined satellite system for remote sensing and earth-oriented research (LOCSS) [BMFT-FB-W-81-002] p0055 N82-14615
- MICHELON, R.**
Study of stack emissions by combination of lidar and correlation spectrometer p0008 A82-12816
- MILLARD, G. C.**
Environmental Monitoring Report, Sandia National Labs., Albuquerque, New Mexico, 180 [DEB1-027839] p0010 N82-11649
- MILLER, A.**
Magnetic Field Satellite (Magsat) data processing system specifications [NASA-CR-166737] p0045 N82-11103
- MILLER, B. P.**
The Seasat commercial demonstration program p0030 N82-14561
- MILLER, C.**
Overall economic impact of an operational Meteosat system [ESA-CRIP]-1457] p0055 N82-13010
- MILLER, D. B.**
User needs and the future of operational meteorological satellites [AIAA PAPER 82-0388] p0051 A82-17918
- MILLER, J. R.**
Variations in upper ocean heat storage determined from satellite data p0025 A82-17567
- MOLENAAR, M.**
Some problem areas in the field of quality control for aerotriangulation p0016 A82-16161
- MOLLO-CHRISTENSEN, E.**
Surface signs of internal ocean dynamics [AD-A101380] p0029 N82-13642
- MONAHAN, E. C.**
Determination of surface wind speed from remotely measured whitecap coverage, a feasibility assessment p0030 N82-14565
The feasibility of using remotely sensed color as an index of Irish coastal water properties p0032 N82-14581
- MONGAIN, E. O.**
Study on calibration methods for Earth observation optical imaging instruments [UCD-207/1/80] p0052 N82-10488
- MONGET, J. M.**
Oil spills: Large scale monitoring by LANDSAT p0012 N82-14572
- MONTGOMERY, D. R.**
The Seasat commercial demonstration program p0030 N82-14561
- MOORE, R. K.**
Measurements of radar backscatter from Arctic Sea ice in the summer [AD-A105586] p0032 N82-14592
Measurements of radar backscatter from Arctic Sea ice in the summer, Appendices A and B [AD-A105736] p0032 N82-14593
- MOREIRA, M. A.**
Wheat cultivation: Identification and estimation of areas using LANDSAT data [EB2-10007] p0004 N82-15485
- MORGAN, K. M.**
Areawide soil loss predictions using CIR airphotos p0007 A82-12591
- MORLEY, L. W.**
The need for integrated off-shore, real-time information and management systems p0055 N82-14555
- MOSES, J. F.**
Interactive techniques for estimating precipitation from GOES imagery p0041 A82-13121
- MOULTON, R. J.**
A look at nonsatellite remote sensing systems for marine use p0032 N82-14586
- MOZGOV, N. N.**
Methodology and practice of spectroscopic measurements of landscape elements in the preparation and carrying out of down-looking experiments p0051 A82-16613
- MUENLBERGER, W. R.**
Global Tectonics: Some Geologic analyses of observations and photographs from Skylab p0020 N82-12494
- MURCHCARTAIGH, I. G.**
Determination of surface wind speed from remotely measured whitecap coverage, a feasibility assessment p0030 N82-14565
- MULDER, N. J.**
Spectral correlation filters and natural colour coding p0043 A82-16160
- MURDIN, J.**
A Swedish proposal for an EISCAT/GEOS-2 experiment [KGI-175] p0052 N82-10484
- MURRAY, J. D.**
Geological features of southwestern North America p0020 N82-12495
- MYERS, V. I.**
Remote sensing applications to resource problems in South Dakota [EB2-10002] p0004 N82-15481

B-6

N

- NALEPA, R.**
Areawide soil loss predictions using CIR airphotos p0007 A82-12591
- NANKERVIS, R.**
Absolute image registration for geosynchronous satellites p0049 A82-10051
- NARAYANAN, M. S.**
Detection of monsoon inversion by TIROS-N satellite p0024 A82-17168
- NAUCK, J.**
Study of a combined satellite system for remote sensing and earth-oriented research (LOCSS) [BMFT-FB-W-81-002] p0055 N82-14615
- NEDWED, C. R.**
Necessity of remote sensing for ocean studies. Part 1: Northwest African missions, Sahara-1 and Ator-1 p0032 N82-14582
- NESTERCZUK, G.**
Ionospheric propagation correction modeling for satellite altimeters [NASA-CR-156881] p0052 N82-12447
- NEVILLE, R. A.**
A recommended sensor package for the detection and tracking of oil spills p0053 N82-14563
- NEWITT, L. R.**
The reduction, verification and interpretation of Magsat magnetic data over Canada [EB2-10006] p0046 N82-15484
- NIBLACK, W.**
The Control Point Library Building System p0043 A82-15971
- NIELSEN, E.**
A Swedish proposal for an EISCAT/GEOS-2 experiment [KGI-175] p0052 N82-10484
- NIKOLAEV, V. A.**
Space photographs obtained with the Fragment system as a base for landscape mapping and physical-geographical classification of arid territories p0009 A82-15967
- NITHACK, J.**
Visual Evaluation of E-SLAR imagery [DFVLR-FB-81-11] p0047 N82-15503
- NIZKAIA, I. S.**
Study of the anthropogenic influence on the environment, based on multispectral scanning images p0008 A82-15965
- NOBLE, V. E.**
U.S. Navy planning for satellite oceanographic data exploitation [AAS 81-072] p0024 A82-16341
- NOLLA, A. B.**
Necessity of remote sensing for ocean studies. Part 1: Northwest African missions, Sahara-1 and Ator-1 p0032 N82-14582
- OFFFIELD, T. W.**
Geologic applications of thermal-inertia mapping from satellite [EB2-10011] p0021 N82-15489
- OHNORST, C. W.**
Preliminary analysis of ocean color scanner data from Superflux III p0027 N82-10672
- OKAMOTO, A.**
Orientation and construction of models. I - The orientation problem in close-range photogrammetry p0049 A82-10858
Orientation and construction of models. III - Mathematical basis of the orientation problem of one-dimensional central perspective photographs p0043 A82-15973
- OLAVENSEN, A. H.**
Infrared spectroscopy of microorganisms near 3.4 microns in relation to geology and astronomy [PREPRINT-69] p0020 N82-12713
- OMUIRCHARTAIGH, I. G.**
The feasibility of using remotely sensed color as an index of Irish coastal water properties p0032 N82-14581
- ONEAL, B. L.**
Environmental Monitoring Report, Sandia National Labs., Albuquerque, New Mexico, 180 [DEB1-027839] p0010 N82-11649
- ONEIL, R. A.**
A recommended sensor package for the detection and tracking of oil spills p0053 N82-14563
- ONSTOTT, R. G.**
Measurements of radar backscatter from Arctic Sea ice in the summer [AD-A105586] p0032 N82-14592
Measurements of radar backscatter from Arctic Sea ice in the summer, Appendices A and B [AD-A105736] p0032 N82-14593
- OPGENOORTH, H.**
A Swedish proposal for an EISCAT/GEOS-2 experiment [KGI-175] p0052 N82-10484

O

- PANFILOV, A. S.**
Investigation of survey conditions for the ocean surface in the 0.4-1.1 micron spectral range p0024 A82-15960
- PARKE, M. E.**
Global satellite measurements of water vapour, wind speed and wave height p0051 A82-17165
- PARR, J. T.**
Snow-mapping experiment p0037 N82-12498
- PEARCE, J. B.**
A marine environmental monitoring and assessment program p0027 N82-10683
- PEDRINI, A.**
Study of stack emissions by combination of lidar and correlation spectrometer p0008 A82-12816
- PELAEZ, J.**
The use of satellite infrared imagery for describing ocean processes in relation to spawning of the northern anchovy /Engraulis mordax/ p0025 A82-17585
- PETERSEN, G. W.**
Texture transforms of remote sensing data p0042 A82-15034
- PETTEY, J. E.**
Report of survey for McDonald Observatory, Harvard Radio Astronomy Station, and vicinity [PBB1-234338] p0016 N82-13606
- PHILIPSON, W. R.**
Remote sensing for vineyard management p0001 A82-10047
- PHOEBUS, R. W.**
Biological patchiness in relation to satellite thermal imagery and associated chemical mesoscale features [AD-A105757] p0047 N82-15504
- PIRKLE, F. J.**
Statistical Techniques Applied to Aerial Radiometric Surveys (STAARS): Series introduction and the principal-components-analysis method [DEB1-029177] p0019 N82-10476
- PITTS, D. E.**
Mesoscale cloud features observed from Skylab p0011 N82-12509
- PITTS, J. N., JR.**
Trace pollutant concentrations in a multiday smog episode in the California South Coast Air Basin by long path length Fourier transform infrared spectroscopy p0007 A82-10700
- PLATE, K.**
Study of a combined satellite system for remote sensing and earth-oriented research (LOCSS) [BMFT-FB-W-81-002] p0055 N82-14615
- POLETAEV, I. U.**
Aspects in the development of aerial-photography tasks p0041 A82-12913
- PONOMARENKO, I. U. V.**
Methodology and practice of spectroscopic measurements of landscape elements in the preparation and carrying out of down-looking experiments p0051 A82-16613
- POOLE, L. R.**
Spectral atmospheric observations at Nantucket Island, May 7-14, 1981 [NASA-TM-83196] p0029 N82-14550
- POTEMRA, T. A.**
Magnetic field-aligned electron distributions in the dayside cusp p0015 A82-12188
Distant magnetic field effects associated with Birkeland currents /made possible by the evaluation of TRIAD's attitude oscillations/ p0015 A82-12215
- POWELL, R. E.**
Geological features of southwestern North America p0020 N82-12495
- PRATT, D. A.**
Two-dimensional model variability in thermal inertia surveys p0042 A82-10529
- PREUSS, H. J.**
Analysis of satellite observations: Theoretical studies on the sampling problem [MITT-31] p0056 N82-15499
- PROKURONOV, I. S.**
The use of a priori information in the remote sensing of the earth from space p0044 A82-16618
- PUCCINELLI, E. F.**
Interpolating for the location of remote sensor data [NASA-TM-82169] p0052 N82-13469
- PURGOLD, G. C.**
Automated analyzer for aircraft measurements of atmospheric methane and total hydrocarbons p0007 A82-11949

R

- RADER, M. L.**
Investigation of the application of remote sensing technology to environmental monitoring [EB2-10010] p0013 N82-15488
- RAMSEIER, R. O.**
Visual observations of floating ice from Skylab p0037 N82-12504
- RANDERSON, D.**
Quantitative analysis of atmospheric pollution phenomena p0010 N82-12505

- RANEY, R. K.**
Wave orbital velocity, fade, and SAR response to azimuth waves p0023 A82-11203
- RAO, B. M.**
Detection of monsoon inversion by TIROS-N satellite p0024 A82-17168
- RAO, V. R.**
Studies of the Indian continental shelf: Application of remote sensing data p0031 N82-14569
Scientific studies using Bhaskara satellite microwave radiometer (SAMIR) data: A short overview p0032 N82-14587
- RASMUSSEN, E.**
An investigation of a polar low with a spiral cloud structure p0007 A82-10616
- REGAN, R. D.**
A closer examination of the reduction of satellite magnetometer data for geological studies p0019 A82-11039
- REICHLER, H. G., JR.**
A new method for inferring carbon monoxide concentrations from gas filter radiometer data p0009 A82-16837
Results from the July 1981 Workshop on Passive Remote Sensing of the Troposphere [AIAA PAPER 82-0207] p0009 A82-17841
- REID, D. B.**
An inertially-aided aircraft track recovery system for coastal mapping p0037 A82-18166
- REYNOLDS, R. M.**
GEM: A simple meteorological buoy with satellite telemetry p0053 N82-14779
- RHODY, B.**
A VHF homing system with VHF radiotelephony for area-representative strip-survey flights conducted, as part of combined forest inventories, with light aircraft carrying 70 mm and 35 mm cameras p0003 A82-15748
- RICE, C. J.**
Satellite observations of the Mt. St. Helens' eruption of 18 May 1980 [AD-A105784] p0012 N82-14591
- RING, W. F.**
Measurement of sea and ice backscatter reflectivity using an OTH radar system p0025 A82-18074
- RITCHIE, A. W.**
Global Tectonics: Some Geologic analyses of observations and photographs from Skylab p0020 N82-12494
- ROBINSON, I. S.**
The use of LANDSAT MSS to observe sediment distribution and movement in the Solent coastal area p0038 N82-14580
- ROGERS, L. K.**
An evaluation of the spatial resolution of soil moisture information [NASA-CR-166724] p0009 N82-11513
- ROHR, R.**
Study of a combined satellite system for remote sensing and earth-oriented research (LOCSS) [BMFT-FB-W-81-002] p0055 N82-14615
- ROSENBERG, N. J.**
Remote sensing of crop moisture status p0003 A82-17997
- ROSENFELD, G. H.**
Analysis of variance of thematic mapping experiment data p0009 A82-15968
- ROSTOKER, G.**
Characteristics of westward travelling surges during magnetospheric substorms p0050 A82-14299
- ROUFOSSE, M. C.**
Study of the time evolution of the lithosphere [NASA-CR-164968] p0016 N82-11696
- RUSCH, D. W.**
Nitric oxide delta band emission in the earth's atmosphere: Comparison of a measurement and a theory p0008 A82-13268
- RUTH, B. E.**
Remote sensing study of sinkhole occurrence p0019 A82-12590
- S**
- SAFIANOV, G. A.**
Development of a coastal relief of the Gulf of Riga, based on results of an analysis of space images p0024 A82-15962
- SAFLEKOS, N. A.**
Distant magnetic field effects associated with Birkeland currents / made possible by the evaluation of TRIAD's attitude oscillations/ p0015 A82-12215
- SAGDEEV, R. Z.**
Airborne and spaceborne multispectral photography of the earth p0043 A82-16601
- SALES, G. S.**
Measurement of sea and ice backscatter reflectivity using an OTH radar system p0025 A82-18074
- SANDRONI, S.**
Study of stack emissions by combination of lidar and correlation spectrometer p0008 A82-12816
- SABAKI, Y.**
Mesoscale cloud features observed from Skylab p0011 N82-12509
- SCARPACE, F. L.**
The operational use of Landsat for lake quality assessment p0036 A82-12596
- SCHAERF, R.**
Investigations concerning the image-controlled segmentation of objects in multispectral imagery data p0042 A82-15003
- SCHNEER, J. A.**
Reflectivity and emissivity of snow and ground at mm waves p0042 A82-14860
- SCHERZ, J. P.**
Remote sensing that motivated community action p0008 A82-12594
- SCHMIDLIN, F. J.**
Repeatability and measurement uncertainty of the United States meteorological rocketsonde p0049 A82-12127
- SCHMIDT, G.**
Study of a combined satellite system for remote sensing and earth-oriented research (LOCSS) [BMFT-FB-W-81-002] p0055 N82-14615
- SCHMUGGE, T. J.**
A comparison of radiative transfer models for predicting the microwave emission from soils p0035 A82-10694
- SCHNAPF, A.**
The 1981 RCA space constellation p0055 A82-12541
The development of the Tiros Global Environmental Satellite System [AIAA PAPER 82-0383] p0025 A82-17915
- SCHNEIDER, G.**
Study of a combined satellite system for remote sensing and earth-oriented research (LOCSS) [BMFT-FB-W-81-002] p0055 N82-14615
- SCHNEIDER, S. R.**
Effect of grain size and snowpack water equivalence on visible and near-infrared satellite observations of snow p0035 A82-12553
- SCHOTT, J. R.**
Role of remote sensing in the study of acid rain impact on aquatic systems [AIAA PAPER 82-0336] p0038 A82-17892
- SCHOWENGERDT, R. A.**
Data compression and reconstruction for mixed resolution multispectral sensors p0049 A82-10045
- SCHROCK, B. L.**
Applications of digital displays in photointerpretation and digital mapping p0041 A82-10038
- SCHROEDER, L. C.**
Evaluation of the Seasat wind scatterometer p0025 A82-18716
- SCHUBERT, J. S.**
Report on Skylab 4 African drought and arid land experiment p0037 N82-12501
- SCIACOVELLI, D.**
Infrared radiance model variation by sensor flight measurements p0052 N82-14717
- SCOFIELD, R. A.**
Analysis of rainfall from flash flood producing thunderstorms, using GOES data p0038 N82-14724
- SCOGGINS, R. K.**
Inclusion of a simple vegetation layer in terrain temperature models for thermal infrared (IR) signature prediction [AD-A104469] p0003 N82-11910
- SELIVANOV, A. S.**
Investigation of survey conditions for the ocean surface in the 0.4-1.1 micron spectral range p0024 A82-15960
- SENU, W. J.**
GPS application to mapping, charting and geodesy p0015 A82-10645
- SHAKHVERDOV, A. SH.**
A new method for computing distortion p0016 A82-12914
- SHAMIS, V. A.**
Processing of multispectral image data on special-purpose computer systems p0044 A82-16627
Programs for the statistical analysis of multispectral photographs p0044 A82-16628
Coordinate referencing of MKF-6 photographs and their transformation to the cartographic projection p0045 A82-16630
- SHARP, W. E.**
Nitric oxide delta band emission in the earth's atmosphere: Comparison of a measurement and a theory p0008 A82-13268
- SHEFFIELD, C.**
Remote sensing contributions to the management of renewable resources p0055 A82-12530
- SHELTON, D.**
Evaluation of the Seasat wind scatterometer p0025 A82-18716
- SHENK, W. E.**
Meteorological lab applications of Skylab handheld-camera photographs p0011 N82-12506
- SHIMABUKURO, Y. E.**
Wheat cultivation: Identification and estimation of areas using LANDSAT data [E82-10007] p0004 N82-15485
Remote sensing in forestry: Application to the Amazon region [E82-10012] p0005 N82-15490
- SHLIAM, E. Z.**
A new method for computing distortion p0016 A82-12914
- SHUBINSKI, R. P.**
Landsat imagery for hydrologic modeling p0036 A82-12592
- SIEBERS, A. L.**
Interactive techniques for estimating precipitation from GOES imagery p0041 A82-13121
- SIELSKI, H.**
Absolute image registration for geosynchronous satellites p0049 A82-10051
- SILVER, L. T.**
Geological features of southwestern North America p0020 N82-12495
- SILVERMAN, J. R.**
User needs and the future of operational meteorological satellites [AIAA PAPER 82-0388] p0051 A82-17918
- SIMKIN, T.**
Skylab 4 observations of Volcanoes. Part A: Volcanoes and volcanic landforms. Part B: Summit eruption of Fernandian Caldera, Galapagos Islands, Ecuador p0020 N82-12496
- SIMMONS, T. M.**
Environmental Monitoring Report, Sandia National Labs., Albuquerque, New Mexico, 180 [DE81-027839] p0010 N82-11649
- SINGH, S. M.**
Coastal zone research using remote sensing techniques p0031 N82-14571
- SITTROP, H.**
Project Noordwijk. Part 2: Results of North Sea clutter measurements in the l-band performed from the platform Noordwijk in September/October 1977 [PHL-1980-28-PT-2] p0033 N82-14618
- SKILLMAN, W. C.**
Meteorological lab applications of Skylab handheld-camera photographs p0011 N82-12506
- SLATOR, T.**
A mathematical model of an over-sea airborne UHF radio link p0049 A82-11406
- SMALLWOOD, M. D.**
An evaluation of the spatial resolution of soil moisture information [NASA-CR-166724] p0009 N82-11513
Snow-mapping experiment p0037 N82-12498
- SMITH, J. T., JR.**
A history of flying and photography: In the Photogrammetry Division of the National Ocean Survey 1919 - 1979 [PB81-246738] p0017 N82-15520
- SMYTH, J. E.**
Photo inertial positioning system development at the Canada Centre for Remote Sensing p0045 A82-18167
- SNETKOVA, N. I.**
Spectrometric studies of the earth's surface p0043 A82-16612
- SOBCHUK, V. G.**
Programs for the statistical analysis of multispectral photographs p0044 A82-16628
Coordinate referencing of MKF-6 photographs and their transformation to the cartographic projection p0045 A82-16630
- SOREIDE, N. N.**
CTD/O2 measurements during the Equatorial Pacific Ocean Climate Study (EPOCS) in 1979 [PB81-211203] p0026 N82-10461
- SPAYD, L. E., JR.**
Interactive techniques for estimating precipitation from GOES imagery p0041 A82-13121
- SPELL, B. D.**
CTD/O2 measurements during the Equatorial Pacific Ocean Climate Study (EPOCS) in 1979 [PB81-211203] p0026 N82-10461
- SRISENGTHONG, D.**
The use of LANDSAT MSS to observe sediment distribution and movement in the Solent coastal area p0038 N82-14580
- STEEN, A.**
A Swedish proposal for an EISCAT/GEOS-2 experiment [KGI-175] p0052 N82-10484
- STEIDLER, F.**
Description and comparison of algorithms for solving large sets of sparse matrix normal equations in geodesy and photogrammetry [SER-C-261] p0017 N82-15812
- STEVENSON, R. E.**
Visual observations of the ocean p0028 N82-12502
- STEWART, R. H.**
Anomalous wind estimates from the Seasat scatterometer p0026 A82-18724
- STILES, W.**
Progress in radar snow research [NASA-CR-166709] p0038 N82-12510
- STONE, R. O.**
Visual observations of the ocean p0028 N82-12502
- STRONG, R. B.**
Aircraft data summaries of the SURE intensives, volume 4 [DE82-900311] p0012 N82-13569
- SUGIURA, M.**
A closer examination of the reduction of satellite magnetometer data for geological studies p0019 A82-11039
Magnetic field observations on DE-A and -B p0051 A82-16447

- SUNDARARAMAN, M. K.**
ISRO satellite mission support facilities - Scope and future plans p0055 A82-17307
- SVENDSON, E.**
The Norwegian remote sensing experiment (Norsax) in a marginal ice zone p0031 N82-14566
- SWANSON, E. R.**
Global Tectonics: Some Geologic analyses of observations and photographs from Skylab p0020 N82-12494
- SWIFT, R. N.**
Application of the NASA airborne oceanographic lidar to the mapping of chlorophyll and other organic pigments p0027 N82-10684
- SWITZER, P.**
Estimation of the atmospheric path-radiance by the covariance matrix method p0041 A82-10861
- SYCHEV, A. G.**
Meteorological support of measurements of earth-surface brightness by the Fragment multispectral scanning system p0050 A82-15958
- T**
- TALAY, T. A.**
Spectral atmospheric observations at Nantucket Island, May 7-14, 1981 [NASA-TM-83196] p0029 N82-14550
- TALSKAIA, N. N.**
Investigation and mapping of the erosion relief of the Kalachkaia upland on the basis of multispectral scanner images p0008 A82-15966
- TARDIN, A. T.**
Wheat cultivation: Identification and estimation of areas using LANDSAT data [E82-10007] p0004 N82-15485
Remote sensing in forestry: Application to the Amazon region [E82-10012] p0005 N82-15490
- TARNOPOLSKII, V. I.**
Meteorological support of measurements of earth-surface brightness by the Fragment multispectral scanning system p0050 A82-15958
- TAYLOR, R. L.**
Boundary detection criteria for satellite altimeters [NASA-CR-156880] p0028 N82-12734
- TAYLOR, R. S.**
Landsat imagery for hydrologic modeling p0036 A82-12592
- TECSON, J. J.**
Mesoscale wake clouds in Skylab photographs p0011 N82-12508
- THIRUVENGADACHARI, S.**
Satellite sensing of irrigation patterns in semiarid areas An Indian study p0002 A82-10864
Cost effective computer processing of airborne scanner data for regional level mapping p0043 A82-15970
- THOMAS, J. P.**
Synoptic thermal and oceanographic parameter distributions in the New York Bight Apex p0023 A82-12885
Chesapeake Bay Plume Study: Superflux 1980 [NASA-CP-2188] p0026 N82-10661
Superflux I, II, and III experiment designs: Water sampling and analyses p0027 N82-10665
- THOMPSON, L. G. S.**
Digitizing and automated output mapping errors p0015 A82-10859
- THOMPSON, T.**
Marine activities in Sweden for which remote sensing data may be of interest p0031 N82-14576
- THOMSON, J. C.**
An evaluation of Seasat-A data in relation to optimum track ship weather routing and site specific forecasting for the offshore oil industry p0030 N82-14564
- TIGHE, W. G.**
Characteristics of westward travelling surges during magnetospheric substorms p0050 A82-14299
- TOLL, D. L.**
Preliminary results of mapping urban land cover with Seasat SAR imagery p0007 A82-10044
- TOMMERDAHL, J. B.**
Aircraft data summaries of the SURE intensives, volume 4 [DE82-900311] p0012 N82-13569
- TRIFONOV, IU. V.**
Satellites of the Meteor series, intended for earth studies from space p0050 A82-15951
Technical equipment of an experiment for remote sensing of the earth from space p0050 A82-15952
- TSAI, B.**
Remote sensing of sea state by laser altimeters [NASA-CR-165049] p0033 N82-14789
- TUAZON, E. C.**
Trace pollutant concentrations in a multiday smog episode in the California South Coast Air Basin by long path length Fourier transform infrared spectroscopy p0007 A82-10700
- TUCKER, C. J.**
Temporal spectral response of a corn canopy p0002 A82-12886
Temporal relationships between spectral response and agronomic variables of a corn canopy p0002 A82-15038

U

- ULABY, F. T.**
Aircraft radar response to soil moisture p0003 A82-17564
Progress in radar snow research [NASA-CR-166709] p0038 N82-12510
- ULBRICHT, K. A.**
Maritime applications of image processing at DFVLR, Oberpfaffenhofen, West Germany p0032 N82-14585
- UPTON, D. T.**
Scanner [NASA-CASE-GSC-12032-2] p0052 N82-13465

V

- VALERIO, C.**
Operational use of remote sensing for coastal zone management and possible contribution of specialized satellites p0031 N82-14574
- VANBEEK, G. J.**
The reduction, verification and interpretation of Magsat magnetic data over Canada [E82-10006] p0046 N82-15484
- VANGENDEREN, J. L.**
Airborne remote sensing of the coastal zone p0053 N82-14577
- VENKATACHARY, K. V.**
ISRO satellite mission support facilities - Scope and future plans p0055 A82-17307
- VONDERHAAR, S. P.**
Visual observations of the ocean p0028 N82-12502
- VOSTREYS, R. W.**
Report on Active and Planned Spacecraft and experiments [NASA-TM-84025] p0055 N82-10087
- VUKOVICH, F. M.**
Monitoring the Chesapeake Bay using satellite data for Superflux III p0027 N82-10668

W

- WAGNER, K.**
Mesoscale cloud features observed from Skylab p0011 N82-12509
- WALD, L.**
Oil spills: Large scale monitoring by LANDSAT p0012 N82-14572
- WALKER, A. D. M.**
Use of hydromagnetic waves to map geomagnetic field lines p0016 A82-16868
- WALKER, J. K.**
The reduction, verification and interpretation of Magsat magnetic data over Canada [E82-10006] p0046 N82-15484
- WALLJO, H. A.**
A new method for inferring carbon monoxide concentrations from gas filter radiometer data p0009 A82-16837
- WANNBERG, G.**
A Swedish proposal for an EISCAT/GEOS-2 experiment [KGI-175] p0052 N82-10484
- WARWICK-SMITH, R. M.**
The use of digitally processed Landsat imagery for vegetation mapping in Sulawesi, Indonesia p0003 A82-17998
- WATSON, K.**
Geologic applications of thermal-inertia mapping from satellite [E82-10011] p0021 N82-15489
- WATTS, D. G.**
Remote sensing of crop moisture status p0003 A82-17997
- WAYENBERG, J. A.**
Visual observations of floating ice from Skylab p0037 N82-12504
- WEAVER, M. G.**
Repetitive aerial photography for assessing marsh vegetation changes p0001 A82-10048
- WEBBING, M. W.**
Preliminary analysis of gravity and aeromagnetic surveys of the Timber Mountain area, southern Nevada [DE81-029462] p0022 N82-15506
- WEEKS, W. F.**
Visual observations of floating ice from Skylab p0037 N82-12504
- WEISE, R. C.**
ERSYS-SPP access method subsystem design [E82-10015] p0053 N82-15493
- WELBY, C. W.**
Satellite imagery and shoreline erosion prediction p0036 A82-12595
- WESTERLUND, S.**
A Swedish proposal for an EISCAT/GEOS-2 experiment [KGI-175] p0052 N82-10484
- WHARTON, S. W.**
Preliminary results of mapping urban land cover with Seasat SAR imagery p0007 A82-10044

- WHITE, F. E., JR.**
Application of satellite Doppler techniques to the national mapping program p0015 A82-10056
- WHITE, J. H.**
Aircraft data summaries of the SURE intensives, volume 4 [DE82-900311] p0012 N82-13569
- WICKRAMASINGHE, N. C.**
Infrared spectroscopy of microorganisms near 3.4 microns in relation to geology and astronomy [PREPRINT-69] p0020 N82-12713
- WILKINSON, M. A.**
Role of remote sensing in the study of acid rain impact on aquatic systems [AIAA PAPER 82-0336] p0036 A82-17892
- WILLIAMS, R. N.**
The potential and requirements for space oceanography p0029 N82-14556
- WINER, A. M.**
Trace pollutant concentrations in a multiday smog episode in the California South Coast Air Basin by long path length Fourier transform infrared spectroscopy p0007 A82-10700
- WINTERBURN, R. F. J.**
The SACLANTCEN oceanographic data base. Volume 1: Design criteria and data structure and content [AD-A103277] p0029 N82-13639
- WOLF, D. E.**
Oceanic wind and balanced pressure-height fields derived from satellite measurements p0023 A82-13214
- WONG, M. C.**
The near-infrared radiation received by satellites from clouds p0025 A82-17492
- WU, C.**
A digital fast correlation approach to produce SEASAT SAR imagery p0042 A82-14870
- WU, S. T.**
An improvement in land cover classification achieved by merging microwave data with Landsat multispectral scanner data p0007 A82-10043

Y

- YOKOYAMA, R.**
The discrimination of winter wheat using a growth-state signature p0002 A82-15026

Z

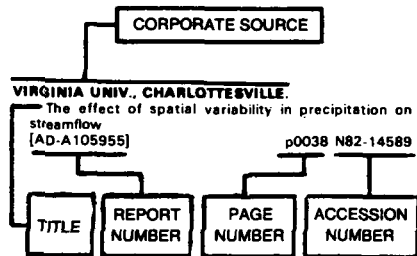
- ZACHOR, A. S.**
Proof of concept study [AD-A104339] p0010 N82-11639
Limit on remote FTIR detection of trace gases [AD-A104842] p0011 N82-12511
- ZANDONELLA, A.**
Multitemporal calibration of LANDSAT images: A method for improving the marine phenomena recognition, with as example the Venice lagoon p0048 N82-14578
- ZANETTI, L. J.**
Magnetic field-aligned electron distributions in the dayside cusp p0015 A82-12186
- ZHUKOV, B. S.**
Polarimetric surveys of oil slicks p0009 A82-16619
Images of sea waves obtained in polarimetric surveys p0024 A82-16620
The choice of the orientation of the analyzer in polarimetric surveys p0044 A82-16621
Analysis of the information content of the polarimetric method of remote sensing p0003 A82-16622
- ZIMAN, IA. L.**
Meteorological support of measurements of earth-surface brightness by the Fragment multispectral scanning system p0050 A82-15958
Main results of the Raduga experiment p0051 A82-16602
Geometric quality of MKF-6 photographs p0043 A82-16606
Coordinate referencing of MKF-6 photographs and their transformation to the cartographic projection p0045 A82-16630
- ZINGMARK, R. G.**
Remote sensing of benthic microalgal biomass with a tower-mounted multispectral scanner p0024 A82-15031
- ZLOBIN, L. I.**
Aerial and space methods in cartography p0016 A82-12915
- ZORN, H. C.**
The application of programmable pocket calculators for computations during survey flights p0050 A82-16164
- ZULCH, D. I.**
Factorial analysis of terrain feature positioning parameters used in combining radar and digital terrain model data p0015 A82-10029
- ZWICK, H. H.**
A recommended sensor package for the detection and tracking of oil spills p0053 N82-14563
Recent work in passive optical imaging of water p0038 N82-14575

CORPORATE SOURCE INDEX

EARTH RESOURCES / A Continuing Bibliography (Issue 33)

APRIL 1982

Typical Corporate Source Index Listing



The title of the document is used to provide a brief description of the subject matter. The page number and the accession number are included in each entry to assist the user in locating the abstract in the abstract section. If applicable, a report number is also included as an aid in identifying the document.

A

- AEROSPACE CORP., EL SEGUNDO, CALIF.**
Satellite observations of the Mt. St. Helens' eruption of 18 May 1980
[AD-A105784] p0012 N82-14591
- AIR FORCE SYSTEMS COMMAND, WRIGHT-PATTERSON AFB, OHIO.**
Meteorological satellites
[AD-A107427] p0053 N82-15110
- AIR RESOURCES LAB., LAS VEGAS, NEV.**
Quantitative analysis of atmospheric pollution phenomena p0010 N82-12505
- AMERICAN UNIV., WASHINGTON, D. C.**
Report on Skylab 4 African drought and arid land experiment p0037 N82-12501
- APPLIED PHYSICS LAB., JOHNS HOPKINS UNIV., LAUREL, MD.**
Radar correlation with ice depolarization measurements of the 28.56 GHz COMSTAR beacon and associated cross polarization statistics
[NASA-CR-166717] p0046 N82-14548
- ARGONNE NATIONAL LAB., ILL.**
Environmental data for sites in the National Solar Data Network
[DE82-000071] p0011 N82-12707
- ARMY ENGINEER WATERWAYS EXPERIMENT STATION, VICKSBURG, MISS.**
Airborne laser acquisition of cross-section data p0049 A82-12600
- Inclusion of a simple vegetation layer in terrain temperature models for thermal infrared (IR) signature prediction
[AD-A104469] p0003 N82-11910
- ATMOSPHERIC RADIATION CONSULTANTS, ACTON, MASS.**
Proof of concept study
[AD-A104338] p0010 N82-11639
- ATMOSPHERIC SCIENCES LAB., WHITE SANDS MISSILE RANGE, N. MEX.**
Sensitivity analysis of a mesoscale moisture model
[AD-A101528] p0012 N82-14590
- ATOMIC ENERGY RESEARCH ESTABLISHMENT, HARWELL (ENGLAND).**
A look at nonsatellite remote sensing systems for marine use p0032 N82-14586
- AUTOMATION INDUSTRIES, INC., SILVER SPRING, MD.**
Environmental data for sites in the National Solar Data Network
[DE82-000071] p0011 N82-12707

B

- BALL AEROSPACE SYSTEMS DIV., BOULDER, COLO.**
Development of the coastal zone color scanner for NIMBUS 7. Volume 1: Mission objectives and instrument description
[NASA-CR-166720-VOL-1] p0028 N82-11511

- BELFOTOP P.V.B.A., WEMMEL (BELGIUM).**
Airborne remote sensing of the coastal zone p0053 N82-14577
- BENDIX FIELD ENGINEERING CORP., GRAND JUNCTION, COLO.**
Statistical Techniques Applied to Aerial Radiometric Surveys (STAARS): Series introduction and the principal-components-analysis method
[OE81-029177] p0019 N82-10476

C

- CALIFORNIA INST. OF TECH., PASADENA.**
Geological features of southwestern North America p0020 N82-12495
- CALIFORNIA UNIV., BERKELEY.**
Vegetation patterns p0004 N82-12500
Application of remote sensing to selected problems within the state of California
[E82-10004] p0004 N82-15482
- CALIFORNIA UNIV., SANTA BARBARA.**
Use of environmental satellite data for input to energy balance snowmelt models
[PB81-227795] p0039 N82-15673
- CALIFORNIA UNIV. AT DAVIS.**
Spectral behavior of wheat yield variety trials p0002 A82-10863
- CANADA CENTRE FOR REMOTE SENSING, OTTAWA (ONTARIO).**
A recommended sensor package for the detection and tracking of oil spills p0053 N82-14563
Recent work in passive optical imaging of water p0038 N82-14575
- CARSON HELICOPTERS, INC., PERKASIE, PA.**
NURE aerial gamma-ray and magnetic reconnaissance survey of Maine and portions of New York. Volume 1: Data acquisition, reduction and interpretation
[DE82-000650] p0053 N82-14599
NURE aerial gamma-ray and magnetic reconnaissance survey of Maine and portions of New York, volume 2
[DE82-000781] p0020 N82-14600
NURE aerial gamma-ray and magnetic reconnaissance survey of Maine and portions of New York, volume 2
[DE82-000401] p0020 N82-14601
NURE aerial gamma-ray and magnetic reconnaissance survey of Maine and portions of New York, volume 2
[DE82-000780] p0021 N82-14602
NURE aerial gamma-ray and magnetic reconnaissance survey of Maine and portions of New York, volume 2
[DE82-000872] p0021 N82-14603
NURE aerial gamma-ray and magnetic reconnaissance survey of Maine and portions of New York, volume 2
[DE82-000772] p0021 N82-14604
NURE aerial gamma-ray and magnetic reconnaissance survey of Maine and portions of New York, volume 2
[DE82-000785] p0021 N82-14605
NURE aerial gamma-ray and magnetic reconnaissance survey of Maine and portions of New York, volume 2
[DE82-000869] p0021 N82-14606
NURE aerial gamma-ray and magnetic reconnaissance survey of Maine and portions of New York, volume 2
[DE82-000794] p0021 N82-14607
NURE aerial gamma-ray and magnetic reconnaissance survey of Maine and portions of New York, volume 2
[DE82-000784] p0021 N82-14608
- CENTRE D'ETUDES DE METEOROLOGIE SPATIALE, LANNION (FRANCE).**
A short review of an oceanographic use of Meteosat data by the ORSTOM remote sensing service p0031 N82-14570
- CENTRE D'ETUDES TECHNIQUES DE L'EQUIPMENT, AIX-EN-PROVENCE (FRANCE).**
Operational use of remote sensing for coastal zone management and possible contribution of specialized satellites p0031 N82-14574
- CENTRE NATIONAL D'ETUDES SPATIALES, PARIS (FRANCE).**
SPOT data simulations: Littoral applications p0046 N82-14568
- CENTRE NATIONAL D'ETUDES SPATIALES, TOULOUSE (FRANCE).**
State-of-the-art in using a spaceborne altimeter and scatterometer for the determination of wind, sea state, and marine and ice dynamics p0052 N82-14560

- CHICAGO UNIV., ILL.**
Mesoscale wake clouds in Skylab photographs p0011 N82-12508
- COLOGNE UNIV. (WEST GERMANY).**
Analysis of satellite observations: Theoretical studies on the sampling problem
[MITT-31] p0056 N82-15499
- COLORADO UNIV., BOULDER.**
Nitric oxide delta band emission in the earth's atmosphere - Comparison of a measurement and a theory p0008 A82-13268
- COMMITTEE ON SCIENCE AND TECHNOLOGY (U. S. HOUSE).**
Civil land remote sensing systems
[GPO-35-265] p0056 N82-15497
- COMPUTER SCIENCES CORP., EL SEGUNDO, CALIF.**
Magnetic Field Satellite (Magsat) data processing system specifications
[NASA-CR-166737] p0045 N82-11103
- COMPUTER SCIENCES CORP., SILVER SPRING, MD.**
Absolute image registration for geosynchronous satellites p0049 A82-10051
A comparison of radiative transfer models for predicting the microwave emission from soils p0035 A82-10694
The surface albedo of the earth in the near ultraviolet /330-340 nm/ p0016 A82-15032
- CONOCO NORWAY, INC., OSLO.**
Offshore petroleum industry environmental data requirements: Emphasis on remote sensing p0030 N82-14557
- CONSIGLIO NAZIONALE DELLE RICERCHE, VENICE (ITALY).**
Multitemporal calibration of LANDSAT images: A method for improving the marine phenomena recognition, with as example the Venice lagoon p0046 N82-14578
- COPENHAGEN UNIV. (DENMARK).**
The color of the sea and its relation to surface chlorophyll and depth of the euphotic zone p0030 N82-14562
- CORNELL UNIV., ITHACA, N. Y.**
Remote sensing for vineyard management p0001 A82-10047
Remote sensing studies of some ironstone gravels and plinthite in Thailand p0019 N82-12491

D

- DANISH METEOROLOGICAL INST., COPENHAGEN.**
The ice-conditions in the Greenland waters, 1965. Coastal maps
[ISBN-87-7478-183-9] p0026 N82-10487
The ice conditions in the Greenland waters
[ISBN-87-7478-183-9] p0028 N82-12533
- DEFENSE MAPPING AGENCY, WASHINGTON, D.C.**
GPS application to mapping, charting and geodesy p0015 A82-10645
- DELAWARE UNIV., NEWARK.**
In situ spectral reflectance studies of tidal wetland grasses p0036 A82-15969
- DEUTSCHE FORSCHUNGS- UND VERSUCHSANSTALT FUER LUFT- UND RAUMFAHRT, OBERPFAFFENHOFEN (WEST GERMANY).**
Maritime applications of image processing at DFVLR, Oberpfaffenhofen, West Germany p0032 N82-14585
Visual Evaluation of E-SLAR imagery
[DFVLR-FB-81-11] p0047 N82-15503
- DEUTSCHES GEODAETISCHES FORSCHUNGSINSTITUT, MUNICH (WEST GERMANY).**
Description and comparison of algorithms for solving large sets of sparse matrix normal equations in geodesy and photogrammetry
[SER-C-261] p0017 N82-15812
- DUNDEE UNIV. (SCOTLAND).**
Coastal zone research using remote sensing techniques p0031 N82-14571

E

- ECOLE NATIONALE SUPERIEURE DES MINES, SOPHIA-ANTIPOLIS (FRANCE).**
Oil spills: Large scale monitoring by LANDSAT p0012 N82-14572

EG AND G WASHINGTON ANALYTICAL SERVICES CENTER, INC., POCOMOKE CITY, MD.

Boundary detection criteria for satellite altimeters
[NASA-CR-156880] p0028 N82-12734
A global atlas of GEOS-3 significant waveheight data and comparison of the data with national buoy data
[NASA-CR-156882] p0033 N82-15498

EG & G WASHINGTON ANALYTICAL SERVICES CENTER, INC., RIVERDALE, MD.

Ionospheric propagation correction modeling for satellite altimeters
[NASA-CR-156881] p0052 N82-12447

ENERGY INFORMATION ADMINISTRATION, WASHINGTON, D.C.

The reduction, verification and interpretation of Magsat magnetic data over Canada
[E82-10006] p0046 N82-15484

ENERGY, MINES AND RESOURCES CANADA, OTTAWA (ONTARIO).

The Manicouagan impact structure observed from Skylab
[CONTRIB-544] p0020 N82-12497

ENVIRONMENTAL RESEARCH AND TECHNOLOGY, INC., CONCORD, MASS.

An evaluation of the spatial resolution of soil moisture information
[NASA-CR-166724] p0009 N82-11513

Snow-mapping experiment p0037 N82-12498
Analysis of soil moisture extraction algorithm using data from aircraft experiments
[NASA-CR-166719] p0046 N82-13470

ENVIRONMENTAL RESEARCH INST. OF MICHIGAN, ANN ARBOR.

Development and evaluation of an automatic labeling technique for spring small grains
[E82-10001] p0004 N82-15480

ERNO RAUMFAHRTTECHNIK G.M.B.H., BREMEN (WEST GERMANY).

Study of a combined satellite system for remote sensing and earth-oriented research (LOCSS)
[BMFT-FB-W-81-002] p0055 N82-14615

EUROPEAN SPACE AGENCY, PARIS (FRANCE).

Application of remote sensing data on the continental shelf. Proceedings of an EAReL-ESA Symposium
[ESA-SP-167] p0029 N82-14553

ERS-1: Mission objectives and system concept
p0029 N82-14554

The need for integrated off-shore, real-time information and management systems
p0055 N82-14555

EUROSAT S.A., GENEVA (SWITZERLAND).

Overall economic impact of an operational Meteosat system
[ESA-CR(P)-1457] p0055 N82-13010

G**GENERAL ELECTRIC CO., LANHAM, MD.**

Computational aspects of geometric correction data generation in the LANDSAT-D imagery processing
p0045 N82-10072

The MSS control point location error filter for LANDSAT-D
p0051 N82-10073

GENERAL ELECTRIC CO., PHILADELPHIA, PA.

LANDSAT-2 and LANDSAT-3 flight evaluation report, 23 April to 23 July 1979
[E82-10005] p0053 N82-15483

LANDSAT-2 and LANDSAT-3 flight evaluation report, 23 October 1978 to 23 January 1979
[E82-10017] p0054 N82-15495

GEOLOGICAL SURVEY, DENVER, COLO.

Desert sand seas p0020 N82-12493
Skylab 4 observations of Volcanoes. Part A: Volcanoes and volcanic landforms. Part B: Summit eruption of Fernandian Caldera, Galapagos Islands, Ecuador
p0020 N82-12496

Geologic applications of thermal-inertia mapping from satellite
[E82-10011] p0021 N82-15489

Preliminary analysis of gravity and aeromagnetic surveys of the Timber Mountain area, southern Nevada
[DE81-029462] p0022 N82-15506

GEOLOGICAL SURVEY, TACOMA, WASH.

Visual observations of floating ice from Skylab
p0037 N82-12504

H**HAWAII UNIV., HONOLULU.**

A method for using aerial photos in delineating historic patterns of beach accretion and retreat
[PB81-229436] p0010 N82-11536

HRB-SINGER, INC., STATE COLLEGE, PA.

Absolute image registration for geosynchronous satellites
p0049 N82-10051

I**IBM FEDERAL SYSTEMS DIV., HOUSTON, TEXAS.**

ERSYS-SPP access method subsystem design specification
[E82-10015] p0053 N82-15493

C-2**IBM FRANCE S. A., PARIS.**

The Control Point Library Building System
p0043 N82-15971

IDAHO UNIV., MOSCOW.

Geology and linears of Libya p0019 N82-10618

ILLINOIS STATE WATER SURVEY, URBANA.

The effect of spatial variability in precipitation on streamflow
[AD-A105955] p0038 N82-14589

ILLINOIS UNIV., URBANA.

Remote sensing of sea state by laser altimeters
[NASA-CR-165049] p0033 N82-14789

INDIAN SPACE RESEARCH ORGANIZATION, BANGALORE.

Scientific studies using Bhaskara satellite microwave radiometer (SAMIR) data: A short overview
p0032 N82-14587

INSTITUTE OF MARINE RESEARCH, BERGEN (NORWAY).

Fisheries investigations and management benefits from remote sensing
p0030 N82-14559

INSTITUTE OF OCEANOGRAPHIC SCIENCES, WORMLEY (ENGLAND).

Evaluation of the Seasat wind scatterometer
p0025 N82-18716

Anomalous wind estimates from the Seasat scatterometer
p0026 N82-18724

A preliminary evaluation of Seasat performance over the area of JASIN and its relevance to ERS-1
p0031 N82-14567

INSTITUTO DE INVESTIGACIONES PESQUERAS, BARCELONA (SPAIN).

Necessity of remote sensing for ocean studies. Part 1: Northwest African missions, Sahara-1 and Atlor-1
p0032 N82-14582

INSTITUTO DE PESQUISAS ESPACIAIS, SAO JOSE DOS CAMPOS (BRAZIL).

Wheat cultivation: Identification and estimation of areas using LANDSAT data
[E82-10007] p0004 N82-15485

Quantitative analysis of drainage obtained from aerial photographs and RBV/LANDSAT images
[E82-10008] p0039 N82-15486

Remote sensing in forestry: Application to the Amazon region
[E82-10012] p0005 N82-15490

INTERMOUNTAIN FOREST AND RANGE EXPERIMENT STATION, OGDEN, UTAH.

Large-scale color aerial photography as a tool in sampling for mortality rates
[PB81-214777] p0003 N82-10489

J**JET PROPULSION LAB., CALIFORNIA INST. OF TECH., PASADENA.**

SAR imaging of ocean waves - Theory
p0023 N82-11202

A digital fast correlation approach to produce SEASAT SAR imagery
p0042 N82-14870

Availability of Seasat synthetic aperture radar imagery
p0050 N82-15039

Optically processed Seasat radar mosaic of Florida
p0042 N82-15125

Global satellite measurements of water vapour, wind speed and wave height
p0051 N82-17165

Evaluation of the Seasat wind scatterometer
p0025 N82-18716

Anomalous wind estimates from the Seasat scatterometer
p0026 N82-18724

Radar mapping, archaeology, and ancient land use in the Maya lowlands
[NASA-CR-164931] p0010 N82-11514

Microwave limb sounder
[NASA-CASE-NPO-14544-1] p0011 N82-12685

The Seasat commercial demonstration program
p0030 N82-14561

JOHNS HOPKINS UNIV., BALTIMORE, MD.

Magnetic field-aligned electron distributions in the dayside cusp
p0015 N82-12186

JOHNS HOPKINS UNIV., LAUREL, MD.

Magnetic field-aligned electron distributions in the dayside cusp
p0015 N82-12186

K**KANSAS UNIV. CENTER FOR RESEARCH, INC., LAWRENCE.**

Aircraft radar response to soil moisture
p0003 N82-17564

Progress in radar snow research
[NASA-CR-166709] p0038 N82-12510

Measurements of radar backscatter from Arctic Sea ice in the summer
[AD-A105586] p0032 N82-14592

Measurements of radar backscatter from Arctic Sea ice in the summer, Appendices A and B
[AD-A105736] p0032 N82-14593

KENTRON INTERNATIONAL INC., HAMPTON, VA.

Synoptic thermal and oceanographic parameter distributions in the New York Bight Apex
p0023 N82-12885

KIRUNA GEOPHYSICAL INST. (SWEDEN).

A Swedish proposal for an EISCAT/GEOS-2 experiment
[KGI-175] p0052 N82-10484

L**LOCKHEED ENGINEERING AND MANAGEMENT SERVICES CO., INC., HOUSTON, TEX.**

Investigation of the application of remote sensing technology to environmental monitoring
[E82-10010] p0013 N82-15488

Fiscal year 1980-81 implementation plan in support of technical development and integration of sampling and aggregation procedures
[E82-10013] p0005 N82-15491

Winterkill indicator model, Crop Condition Assessment Division (CCAD) data base interface driver, user's manual
[E82-10014] p0005 N82-15492

M**MAINE UNIV., ORONO.**

The operational use of Landsat for lake quality assessment
p0038 N82-12598

MARCONI CO. LTD., CHELMSFORD (ENGLAND).

Additional studies of Earth resources synthetic aperture radar payloads
[MTR-80/90] p0054 N82-15500

New baseline system
p0054 N82-15501

Squinted SAR system
p0047 N82-15502

MARTIN MARIETTA CORP., DENVER, COLO.

Onboard utilization of ground control points for image correction. Volume 1: Executive summary
[NASA-CR-166731] p0045 N82-10469

Onboard utilization of ground control points for image correction. Volume 2: Analysis and simulation results
[NASA-CR-166732] p0045 N82-10470

Onboard utilization of ground control points for image correction. Volume 3: Ground control point simulation software design
[NASA-CR-166733] p0045 N82-10471

Onboard utilization of ground control points for image correction. Volume 4: Correlation analysis software design
[NASA-CR-166734] p0045 N82-10472

MASSACHUSETTS INST. OF TECH., CAMBRIDGE.

Radiative transfer theory for passive microwave remote sensing of random media
p0048 N82-11533

Surface signs of internal ocean dynamics
[AD-A101380] p0029 N82-13642

MASSACHUSETTS UNIV., AMHERST.

The mineralogy of global magnetic anomalies
[E82-10009] p0021 N82-15487

METEOROLOGISCHES OBSERVATORIUM, HOHENPEISSENBERG (WEST GERMANY).

Special observations by the Hohenpeissenberg Meteorological Observatory. Number 42: Results of aerological and surface ozone measurements during the first semester of 1980
[SONDERBEOB-42] p0012 N82-12714

METEOROLOGY RESEARCH, INC., SANTA ROSA, CALIF.

Aircraft data summaries of the SURE intensives, volume 4
[DE82-900311] p0012 N82-13569

MIAMI UNIV., CORAL GABLES, FLA.

Clear water radiances for atmospheric correction of coastal zone color scanner imagery
p0025 N82-17292

MICHIGAN STATE UNIV., EAST LANSING.

Introducing remote sensing to county-level agencies in Michigan through the Cooperative Extension Service
p0007 N82-10034

MICHIGAN UNIV., ANN ARBOR.

Nitric oxide delta band emission in the earth's atmosphere
Comparison of a measurement and a theory
p0008 N82-13268

MINISTERE DE L'ENVIRONNEMENT ET DU CADRE DE VIE, NEUILLY (FRANCE).

The operational oil pollution surveillance system being used in France: Forecasted future developments in consideration of the NATO/CCMS remote sensing pilot study conclusions
p0012 N82-14573

MINNESOTA UNIV., MINNEAPOLIS.

Magnetic field observations on DE-A and -B
p0051 N82-16447

MISSISSIPPI STATE UNIV., MISSISSIPPI STATE.

A proposal for continuation of support for the application of remotely sensed data to state and regional problems. Part 1: Technical proposal
[E82-10018] p0056 N82-15496

MITRE CORP., MCLEAN, VA.

Shuttle applications in tropospheric air quality observations
[NASA-CR-145374] p0010 N82-11635

N

NATIONAL AERONAUTICS AND SPACE ADMINISTRATION, WASHINGTON, D. C.

Mission operation report: OSTA-1 [NASA-TM-84053] p0055 N82-10102
 Reports of Planetary Geology Program, 1981 [NASA-TM-84211] p0016 N82-14041

NATIONAL AERONAUTICS AND SPACE ADMINISTRATION, AMES RESEARCH CENTER, MOFFETT FIELD, CALIF.

MATE VAN: Mobile analysis and training extension [NASA-TM-84056] p0045 N82-10466

NATIONAL AERONAUTICS AND SPACE ADMINISTRATION, GODDARD SPACE FLIGHT CENTER, GREENBELT, MD.

Preliminary results of mapping urban land cover with Seasat SAR imagery p0007 A82-10044
 Absolute image registration for geosynchronous satellites p0049 A82-10051

A comparison of radiative transfer models for predicting the microwave emission from soils p0035 A82-10694
 A closer examination of the reduction of satellite magnetometer data for geological studies p0019 A82-11039

Magnetic field-aligned electron distributions in the dayside cusp p0015 A82-12186
 Temporal spectral response of a corn canopy p0002 A82-12886

The surface albedo of the earth in the near ultraviolet /330-340 nm/ p0016 A82-15032
 Texture transforms of remote sensing data p0042 A82-15034

Temporal relationships between spectral response and agronomic variables of a corn canopy p0002 A82-15038
 An analysis of short pulse and dual frequency radar techniques for measuring ocean wave spectra from satellites p0024 A82-15318

Magnetic field observations on DE-A and -B p0051 A82-16447
 Report on Active and Planned Spacecraft and experiments [NASA-TM-84025] p0055 N82-10087

MAGSAT: Vector magnetometer absolute sensor alignment determination [NASA-TM-79648] p0051 N82-10468
 Meteorological lab applications of Skylab handheld-camera photographs p0011 N82-12506

Scanner [NASA-CASE-GSC-12032-2] p0052 N82-13465
 Interpolating for the location of remote sensor data [NASA-TM-82169] p0052 N82-13469

A simulation study of the recession coefficient for antecedent precipitation index [NASA-TM-83860] p0038 N82-14549

NATIONAL AERONAUTICS AND SPACE ADMINISTRATION, LYNDON B. JOHNSON SPACE CENTER, HOUSTON, TEX.

Skylab explores the Earth [NASA-SP-380] p0019 N82-12492
 Mesoscale cloud features observed from Skylab p0011 N82-12509

US/Canada wheat and barley crop calendar exploratory experiment implementation plan [E82-10016] p0005 N82-15494

NATIONAL AERONAUTICS AND SPACE ADMINISTRATION, LANGLEY RESEARCH CENTER, HAMPTON, VA.

Automated analyzer for aircraft measurements of atmospheric methane and total hydrocarbons p0007 A82-11949
 Synoptic thermal and oceanographic parameter distributions in the New York Bight Apex p0023 A82-12885

Remote sensing of benthic microalgal biomass with a tower-mounted multispectral scanner p0024 A82-15031
 In situ spectral reflectance studies of tidal wetland grasses p0036 A82-15969

A new method for inferring carbon monoxide concentrations from gas filter radiometer data p0009 A82-16837
 Results from the July 1981 Workshop on Passive Remote Sensing of the Troposphere [AIAA PAPER 82-0207] p0009 A82-17841

Evaluation of the Seasat wind scatterometer p0025 A82-18716
 Anomalous wind estimates from the Seasat scatterometer p0026 A82-18724

Chesapeake Bay Plume Study: Superflux 1980 [NASA-CP-2188] p0026 N82-10661
 Superflux I, II, and III experiment design: Remote sensing aspects p0027 N82-10664

Remote sensing of the Chesapeake Bay plume salinity via microwave radiometry p0027 N82-10670
 Preliminary analysis of ocean color scanner data from Superflux III p0027 N82-10672

Analysis of testbed airborne multispectral scanner data from Superflux II p0027 N82-10682
 Assessment of Superflux relative to remote sensing p0028 N82-10694

Spectral atmospheric observations at Nantucket Island, May 7-14, 1981 [NASA-TM-83196] p0029 N82-14550
 The Norwegian remote sensing experiment (Norsex) in a marginal ice zone p0031 N82-14566

NATIONAL AERONAUTICS AND SPACE ADMINISTRATION, NATIONAL SPACE TECHNOLOGY LABS., BAY SAINT LOUIS, MISS.

An improvement in land cover classification achieved by merging microwave data with Landsat multispectral scanner data p0007 A82-10043

NATIONAL AERONAUTICS AND SPACE ADMINISTRATION, PASADENA OFFICE, CALIF.

Microwave limb sounder [NASA-CASE-NPD-14544-1] p0011 N82-12685

NATIONAL AERONAUTICS AND SPACE ADMINISTRATION, WALLOPS FLIGHT CENTER, WALLOPS ISLAND, VA.

Repeatability and measurement uncertainty of the United States meteorological rocketsonde p0049 A82-12127
 Airborne laser acquisition of cross-section data p0049 A82-12600

Application of the NASA airborne oceanographic lidar to the mapping of chlorophyll and other organic pigments p0027 N82-10684

NATIONAL GEODETIC SURVEY, ROCKVILLE, MD.

Report of survey for McDonald Observatory, Harvard Radio Astronomy Station, and vicinity [PB81-234338] p0016 N82-13606

NATIONAL HURRICANE AND EXPERIMENTAL METEOROLOGY LAB., CORAL GABLES, FLA.

Some aspects of tropical storm structure revealed by handheld-camera photographs from space p0011 N82-12507

NATIONAL INST. OF OCEANOGRAPHY, GOA (INDIA).

Studies of the Indian continental shelf: Application of remote sensing data p0031 N82-14569

NATIONAL MARINE FISHERIES SERVICE, HIGHLANDS, N. J.

A marine environmental monitoring and assessment program p0027 N82-10663

Superflux I, II, and III experiment designs: Water sampling and analyses p0027 N82-10665

NATIONAL OCEAN SURVEY, ROCKVILLE, MD.

A history of flying and photography: In the Photogrammetry Division of the National Ocean Survey 1919 - 1979 [PB81-246738] p0017 N82-15520

NATIONAL OCEANIC AND ATMOSPHERIC ADMINISTRATION, BOULDER, COLO.

A systems approach to the real-time runoff analysis with a deterministic rainfall-runoff model [PB81-224495] p0037 N82-11530

Geophysical monitoring for climatic change, number 8: Summary Report, 1979 [PB81-233355] p0012 N82-13631

NATIONAL OCEANIC AND ATMOSPHERIC ADMINISTRATION, HIGHLANDS, N. J.

Synoptic thermal and oceanographic parameter distributions in the New York Bight Apex p0023 A82-12885

NATIONAL OCEANIC AND ATMOSPHERIC ADMINISTRATION, MIAMI, FLA.

The determination of navigational and meteorological variables measured by NOAA/RFC WP3D aircraft [PB81-225468] p0028 N82-11743

An assessment of the potential contributions to oceanography from Skylab visual observations and handheld-camera photographs p0028 N82-12503

NATIONAL OCEANIC AND ATMOSPHERIC ADMINISTRATION, ROCKVILLE, MD.

Deep Ocean Mining Environmental Study. Environmental effects of commercial-scale mining [PB81-227753] p0029 N82-13484

NATIONAL OCEANIC AND ATMOSPHERIC ADMINISTRATION, SEATTLE, WASH.

CTD/02 measurements during the Equatorial Pacific Ocean Climate Study (EPOCS) in 1979 [PB81-211203] p0026 N82-10461

Ice conditions in the eastern Bering Sea from NOAA and LANDSAT imagery: Winter conditions 1974, 1976, 1977, 1979 [PB81-220188] p0028 N82-11537

GEM: A simple meteorological buoy with satellite telemetry p0053 N82-14779

NATIONAL OCEANIC AND ATMOSPHERIC ADMINISTRATION, WASHINGTON, D. C.

Analysis of rainfall from flash flood producing thunderstorms, using GOES data p0038 N82-14724

National Hurricane operations plan [PB81-247231] p0013 N82-15697

Environmental satellite imagery, March 1981 [PB81-248049] p0047 N82-15698

NATIONAL OCEANOGRAPHIC INSTRUMENTATION CENTER, WASHINGTON, D. C.

Clear water radiances for atmospheric correction of coastal zone color scanner imagery p0025 A82-17292

NATURAL ENVIRONMENT RESEARCH COUNCIL, GODALMING (ENGLAND).

Study on satellite radar altimetry in climatological and oceanographic research, volume 1 [SP/153/06/01/FR(80)-VOL-1] p0026 N82-10486

Study on satellite radar altimetry in climatological and oceanographic research, volume 2 [SP/153/06/01/FR(80)-VOL-2] p0026 N82-10487

NAVAL OCEAN RESEARCH AND DEVELOPMENT ACTIVITY, BAY ST. LOUIS, MISS.

A closer examination of the reduction of satellite magnetometer data for geological studies p0019 A82-11039

NAVAL OCEANOGRAPHIC OFFICE, BAY ST. LOUIS, MISS.

ICAPS oceanographic data for the Indian Ocean [AD-A103173] p0029 N82-13641

NAVAL OCEANOGRAPHIC OFFICE, WASHINGTON, D. C.

The potential and requirements for space oceanography p0029 N82-14556

NAVAL POSTGRADUATE SCHOOL, MONTEREY, CALIF.

Biological patchiness in relation to satellite thermal imagery and associated chemical mesoscale features [AD-A105757] p0047 N82-15504

NAVAL SURFACE WEAPONS CENTER, DAHLGREN, VA.

GPS application to mapping, charting and geodesy p0015 A82-10645

NEW YORK STATE UNIV., SYRACUSE.

Intercalibration of Landsat 1-3 and NOAA 6 and 7 scanner data p0049 A82-13293

NICE UNIV. (FRANCE).

Requirements in pollution monitoring and coastal management p0030 N82-14558

NORWEGIAN AIR SURVEY CO., OSLO.

Use of Side Looking Airborne Radar (SLAR) for oil pollution monitoring in Norway p0012 N82-14588

NORWEGIAN DEFENCE RESEARCH ESTABLISHMENT, KJELLER.

Seasat SAR processing at the Norwegian Defence Research Establishment p0046 N82-14584

NOVA UNIV., DANIA, FLA.

Seasat altimetry adjustment model including tidal and other sea surface effects [AD-A104188] p0026 N82-10473

O

ODQ CORP., HAMPTON, VA.

Technology transfer of NASA microwave remote sensing system [NASA-CR-165791] p0028 N82-11515

OCEANROUTES, INC., PALO ALTO, CALIF.

An evaluation of Seasat-A data in relation to optimum track ship weather routing and site specific forecasting for the offshore oil industry p0030 N82-14564

OFFICE OF NAVAL RESEARCH, PASADENA, CALIF.

Visual observations of the ocean p0028 N82-12502

OFFICINE GALILEO S.P.A., FLORENCE (ITALY).

Infrared radiance model variation by sensor flight measurements p0052 N82-14171

OLD DOMINION UNIV., NORFOLK, VA.

A new method for inferring carbon monoxide concentrations from gas filter radiometer data p0009 A82-16837

P

PENNSYLVANIA STATE UNIV., UNIVERSITY PARK.

Texture transforms of remote sensing data p0042 A82-15034

PHYSICS LAB. RVO-TNO, THE HAGUE (NETHERLANDS).

Project Noordwijk. Part 1: Measurements of the radar backscatter coefficient gamma (sigma deg) in 1977 and 1978 [PHL-1979-49-PT-1] p0032 N82-14617

Project Noordwijk. Part 2: Results of North Sea clutter measurements in the I-band performed from the platform Noordwijk in September/October 1977 [PHL-1980-28-PT-2] p0033 N82-14618

PREUSSAG A.G. METALL, GOSLAR (WEST GERMANY).

An investigation into the applicability of thermal infrared scanning for exploration [BMFT-FB-T-81-087] p0022 N82-15925

R

RAND CORP., SANTA MONICA, CALIF.

Coordinates of features on the Galilean satellites p0019 A82-12366

RESEARCH AND DATA SYSTEMS, INC., LANHAM, MD.

SMMR data set development for GARP [NASA-CR-166721] p0052 N82-11512

RESEARCH INST. OF NATIONAL DEFENCE, LINKOEPING (SWEDEN).

Use of radar and microwave radiometry for reconnaissance satellites [FOA-C-30204-F1] p0052 N82-10481

RESEARCH TRIANGLE INST., RESEARCH TRIANGLE PARK, N. C.

Monitoring the Chesapeake Bay using satellite data for Superflux III p0027 N82-10688

Aircraft data summaries of the SURE intensives, volume 4 [D82-900311] p0012 N82-13569

ROSKILDE UNIV. (DENMARK).

Mapping of surface currents in Greenland fiords by means of LANDSAT images p0038 N82-14579

**ROYAL AIRCRAFT ESTABLISHMENT,
FARNBOROUGH (ENGLAND).**

Remote Sensing Information Bulletin: Issue number 6
p0053 N82-14616

**ROYAL NETHERLANDS METEOROLOGICAL INST., DE
BILT.**

Meteorological and oceanographic observations on board
Netherlands lightvessels and the lightplatform 'Goeree' in
the North Sea
[KNMI-141-28] p0033 N82-15684

**ROYAL NORWEGIAN COUNCIL FOR SCIENTIFIC AND
INDUSTRIAL RESEARCH, KJELLER.**

Application of remote sensing data on the continental
shelf: Proceedings of an EARL-ESA Symposium
[ESA-SP-167] p0029 N82-14553

S**SACLANT ASW RESEARCH CENTER, LA SPEZIA
(ITALY).**

The SACLANTCEN oceanographic data base. Volume
1: Design criteria and data structure and content
[AD-A103277] p0029 N82-13639

SANDIA LABS., ALBUQUERQUE, N. MEX.

Environmental Monitoring Report, Sandia National Labs.,
Albuquerque, New Mexico, 180
[DE81-027839] p0010 N82-11649

**SANTA BARBARA RESEARCH CENTER, GOLETA,
CALIF.**

Scanner
[NASA-CASE-GSC-12032-2] p0052 N82-13465

**SCIENCE AND EDUCATION ADMINISTRATION,
BELTSVILLE, MD.**

Temporal spectral response of a corn canopy
p0002 A82-12886

Temporal relationships between spectral response and
agronomic variables of a corn canopy p0002 A82-15038

SCIENCE APPLICATIONS, INC., BELLEVUE, WASH.

Ice conditions in the eastern Bering Sea from NOAA
and LANDSAT imagery: Winter conditions 1974, 1976,
1977, 1979
[PB81-220188] p0028 N82-11537

**SCIENCE RESEARCH COUNCIL, SLOUGH
(ENGLAND).**

Study on satellite radar altimetry in climatological and
oceanographic research, volume 1
[SP/153/06/01/FRI80)-VOL-1] p0026 N82-10486

Study on satellite radar altimetry in climatological and
oceanographic research, volume 2
[SP/153/06/01/FRI80)-VOL-2] p0026 N82-10487

**SCIENTIFIC ANALYSTS AND CONSULTANTS, INC.,
ROCKVILLE, MD.**

Distortion-free mapping of VISSR imagery data from
geosynchronous satellites p0051 N82-10071

**SMITHSONIAN ASTROPHYSICAL OBSERVATORY,
CAMBRIDGE, MASS.**

Study of the time evolution of the lithosphere
[NASA-CR-164968] p0016 N82-11696

SOUTH CAROLINA UNIV., COLUMBIA.

Remote sensing of benthic microalgal biomass with a
tower-mounted multispectral scanner p0024 A82-15031

SOUTH DAKOTA STATE UNIV., BROOKINGS.

Remote sensing applications to resource problems in
South Dakota
[E82-10002] p0004 N82-15481

SOUTHAMPTON UNIV. (ENGLAND).

The use of LANDSAT MSS to observe sediment
distribution and movement in the Solent coastal area
p0038 N82-14580

STATE UNIV. OF NEW YORK, ALBANY.

Preliminary results of mapping urban land cover with
Seasat SAR imagery p0007 A82-10044

**SWEDISH METEOROLOGICAL AND HYDROLOGICAL
INST., NORKOEPING.**

Marine activities in Sweden for which remote sensing
data may be of interest p0031 N82-14576

**SYSTEMS AND APPLIED SCIENCES CORP.,
HAMPTON, VA.**

A new method for inferring carbon monoxide
concentrations from gas filter radiometer data
p0009 A82-16837

T**TECHNICAL RESEARCH CENTRE OF FINLAND,
ESPOO.**

Small-scale terrain mapping based on numerical
interpretation of LANDSAT imagery
[VTI-40] p0045 N82-10485

TEXAS UNIV. AT ARLINGTON.

A global atlas of GEOS-3 significant waveheight and
comparison of the data with national buoy data
p0026 N82-10660

TEXAS UNIV. AT AUSTIN.

Global Tectonics: Some Geologic analyses of
observations and photographs from Skylab
p0020 N82-12494

Cultural features imaged and observed from Skylab 4
p0010 N82-12499

U**UNIVERSITY COLL., CARDIFF (WALES).**

Infrared spectroscopy of microorganisms near 3.4
microns in relation to geology and astronomy
[PREPRINT-69] p0020 N82-12713

UNIVERSITY COLL., DUBLIN (IRELAND).

Study on calibration methods for Earth observation optical
imaging instruments
[UCD-207/1/80] p0052 N82-10488

UNIVERSITY COLL., GALWAY (IRELAND).

Determination of surface wind speed from remotely
measured whitecap coverage, a feasibility assessment
p0030 N82-14565

UTAH STATE UNIV., LOGAN.

The feasibility of using remotely sensed color as an index
of Irish coastal water properties p0032 N82-14581

UTAH STATE UNIV., LOGAN.

Proof of concept study
[AD-A104338] p0010 N82-11639

Limit on remote FTIR detection of trace gases
[AD-A104842] p0011 N82-12511

UTAH UNIV., SALT LAKE CITY.

Morphostructural analyses of space imagery in the central
Colorado Plateau p0019 N82-10465

V**VIRGINIA UNIV., CHARLOTTESVILLE.**

The effect of spatial variability in precipitation on
streamflow
[AD-A105955] p0038 N82-14589

W**WASHINGTON UNIV., SEATTLE.**

Evaluation of the Seasat wind scatterometer
p0025 A82-18716

- Anomalous wind estimates from the Seasat
scatterometer p0026 A82-18724

Identification of lithologic units using multichannel
imaging systems p0046 N82-11509

Adaptation of land use to surficial geology in metropolitan
Washington, D.C. p0010 N82-11718

WISCONSIN UNIV. - MADISON.

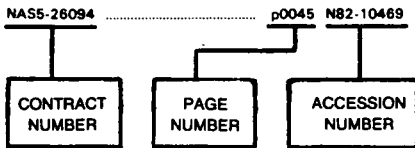
The operational use of Landsat for lake quality
assessment p0036 A82-12596

CONTRACT NUMBER INDEX

EARTH RESOURCES / A Continuing Bibliography (Issue 33)

APRIL 1982

Typical Contract Number Index Listing



Listings in this index are arranged alphanumerically by contract number. Under each contract number, the accession numbers denoting documents that have been produced as a result of research done under that contract are arranged in ascending order with the AIAA accession numbers appearing first. The accession number denotes the number by which the citation is identified in the abstract section. Preceding the accession number is the page number on which the citation may be found.

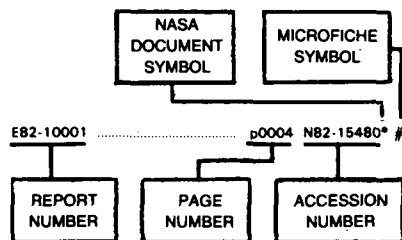
NAS5-26094	p0045	N82-10469	NAS5-26094	p0045	N82-10469
				p0045	N82-10470
				p0045	N82-10471
				p0045	N82-10472
			NAS5-26361	p0046	N82-13470
			NAS5-26414	p0021	N82-15487
			NAS6-2639	p0033	N82-15498
			NAS6-3075	p0052	N82-12447
				p0028	N82-12734
			NAS7-100	p0023	A82-11202
				p0042	A82-14870
				p0010	N82-11514
			NAS9-14052	p0003	A82-17564
			NAS9-14350	p0053	N82-15493
			NAS9-15476	p0004	N82-15480
			NAS9-15800	p0013	N82-15488
				p0005	N82-15491
				p0005	N82-15492
			NATO-9-4-02-SRG.19	p0031	N82-14566
			NA79AA-D-00085	p0010	N82-11536
			NAB1FA-C-00002	p0027	N82-10668
			NCA2-OR-180-607	p0002	A82-10863
			NGL-23-004-083	p0007	A82-10034
			NGL-25-001-054	p0056	N82-15496
			NGL-33-010-171	p0001	A82-10047
			NGL-42-003-007	p0004	N82-15481
			NGR-23-005-360	p0008	A82-13268
			NOAA-MO-A01-78-00-4319	p0024	A82-15076
			NOAA-NA-79SAC00737	p0023	A82-10671
			NOAA-NA-79SA00741	p0025	A82-17292
			NOAA-NA-80RAC00003	p0025	A82-17494
			NOAA-NA-79SAC0073	p0023	A82-13214
			NOAA-NA79-KA-C-00026	p0051	N82-10071
			NOAA-01-8-M01-1864	p0051	N82-10071
			NOAA-04-7-158-44104	p0024	A82-15030
			NOAA-04-8-MO	p0039	N82-15673
			NOAA-04-8-M01-134	p0035	A82-10054
			NOAA-04-8-M01-149	p0024	A82-15030
			NSF ATM-78-08865	p0038	N82-14589
			NSF ATM-78-20419	p0025	A82-17494
			NSF ATM-80-03300	p0016	A82-16868
			NSF ENG-78-23145	p0049	A82-11533
			NSF ENG-79-09374	p0041	A82-12757
			NSF OCE-80-24116	p0025	A82-17494
			NSG-1334	p0024	A82-15031
			NSG-5049	p0033	N82-14789
			NSG-5335	p0038	N82-12510
			NSG-5372	p0008	A82-13268
			NSG-7220	p0004	N82-15482
			N00014-76-C-1105	p0032	N82-14592
				p0032	N82-14593
			N00014-78-G-0052	p0030	N82-14565
			N00014-79-C-0853	p0019	A82-11039
			N00014-80-C-0273	p0029	N82-13642
			N00014-80-G-0003	p0031	N82-14566
			N00014-81-K-0030	p0050	A82-15920
			PROJ. AGRISTARS	p0004	N82-15480
				p0005	N82-15491
				p0005	N82-15492
				p0053	N82-15493
				p0005	N82-15494
				p0029	N82-14550
			146-40-15-07	p0028	N82-10661
			146-40-15-50		
AF PROJ. 2309	p0026	N82-10473			
AF PROJ. 2310	p0010	N82-11639			
AF PROJ. 7670	p0011	N82-12511			
CNPQ-37/78	p0009	A82-16325			
DA PROJ. 1L1-61102-B-53A	p0012	N82-14590			
DA PROJ. 4A7-62719-AT-40	p0003	N82-11910			
DA PROJ. 4A7-62730-AT-42	p0003	N82-11910			
DAAG29-80-K-0018	p0041	A82-12757			
DAAG29-80-K-0053	p0038	N82-14589			
DE-AC01-79CS-30027	p0011	N82-12707			
DE-AC04-76DP-00789	p0010	N82-11649			
DE-AC13-76GJ-01664	p0019	N82-10476			
	p0053	N82-14599			
	p0020	N82-14600			
	p0020	N82-14601			
	p0021	N82-14602			
	p0021	N82-14603			
	p0021	N82-14604			
	p0021	N82-14605			
	p0021	N82-14607			
	p0021	N82-14608			
DE-AC13-76GT-01664	p0021	N82-14606			
DE-AI08-78ET-44802	p0022	N82-15506			
EPA-R-804546	p0007	A82-10700			
EPA-R-805500-01	p0008	A82-14320			
EPA-R-806048-01-2	p0008	A82-14320			
EPRI PROJ. RP-862	p0012	N82-13569			
ESA-4237/80/NL-PP(SC)	p0052	N82-10488			
ESA-4355/80/F-FC(SC)	p0026	N82-10486			
	p0026	N82-10487			
ESA-4421/80/F-FC(SC)	p0055	N82-13010			
ESA-6225/80-F-CG(SC)	p0054	N82-15500			
FINEP-B/28-79-002-00-00	p0009	A82-16325			
F04701-80-C-0081	p0012	N82-14591			
F19628-77-C-0203	p0010	N82-11639			
	p0011	N82-12511			
F19628-78-C-001	p0010	N82-11635			
F19628-78-C-0013	p0026	N82-10473			
F19628-80-C-0052	p0049	A82-11533			
JPL-916331	p0049	A82-13293			
JPL-953613	p0019	A82-12366			
NAG5-16	p0049	A82-11533			
NAG5-30	p0003	A82-17564			
NAG5-150	p0016	N82-11696			
NASA ORDER S-40258-B	p0021	N82-15489			
NASW-3321	p0019	A82-12366			
NAS1-16380	p0028	N82-11515			
NAS5-11415	p0015	A82-12186			
NAS5-20900	p0028	N82-11511			
NAS5-20983	p0036	A82-15969			
NAS5-21808	p0053	N82-15483			
	p0054	N82-15495			
NAS5-22963	p0025	A82-17292			
NAS5-22999	p0043	A82-15971			
NAS5-23790	p0043	A82-15971			
NAS5-24391	p0045	N82-11103			
NAS5-25300	p0045	N82-10072			
	p0051	N82-10073			
NAS5-25527	p0009	N82-11513			
NAS5-25781	p0052	N82-11512			
NAS5-25882	p0019	A82-11039			

REPORT/ACCESSION NUMBER INDEX

EARTH RESOURCES / A Continuing Bibliography (Issue 33)

APRIL 1982

Typical Report/Accession Number Index Listing



Listings in this index are arranged alphanumerically by report number. The page number indicates the page on which the citation is located. The accession number denotes the number by which the citation is identified. An asterisk (*) indicates that the item is a NASA report. A pound sign (#) indicates that the item is available on microfiche.

E82-10001	p0004	N82-15480*	DOE/ET-44802/T2	p0022	N82-15506	#	JHU/APL-SIR-80U-026	p0046	N82-14548*	#
AD-A101380	p0029	N82-13642	EPRI-EA-1019-VOL-4	p0012	N82-13569	#	JSC-16759	p0013	N82-15488*	#
AD-A101528	p0012	N82-14590	ERADCOM/ASL-TR-0079	p0012	N82-14590	#	JSC-16812	p0005	N82-15494*	#
AD-A103173	p0029	N82-13641	ERIM-152400-3-T	p0004	N82-15480*	#	JSC-16819	p0005	N82-15491*	#
AD-A103277	p0029	N82-13639	ERT-P-7505-F	p0009	N82-11513*	#	JSC-16918	p0053	N82-15493*	#
AD-A104188	p0026	N82-10473	ESA-CR(P)-1437-VOL-1	p0026	N82-10486	#	JSC-17117	p0005	N82-15492*	#
AD-A104338	p0010	N82-11639	ESA-CR(P)-1437-VOL-2	p0026	N82-10487	#	KGI-175	p0052	N82-10484	#
AD-A104469	p0003	N82-11910	ESA-CR(P)-1443	p0052	N82-10488	#	KMRD-5.4-8103	p0047	N82-15698	#
AD-A104842	p0011	N82-12511	ESA-CR(P)-1457	p0055	N82-13010	#	KNMI-141-28	p0033	N82-15684	#
AD-A105586	p0032	N82-14592	ESA-CR(P)-1469	p0054	N82-15500	#	L-14680	p0026	N82-10661*	#
AD-A105736	p0032	N82-14593	ESA-SP-167	p0029	N82-14553	#	LC-77-829	p0019	N82-12492*	#
AD-A105757	p0047	N82-15504	EW-L1-00713	p0005	N82-15492*	#	LEMSCO-15168	p0005	N82-15491*	#
AD-A105784	p0012	N82-14591	E82-10001	p0004	N82-15480*	#	LEMSCO-15175	p0013	N82-15488*	#
AD-A105955	p0038	N82-14589	E82-10002	p0004	N82-15481*	#	LEMSCO-16033	p0005	N82-15492*	#
AD-A107427	p0053	N82-15110	E82-10004	p0004	N82-15482*	#	MCR-81-576-VOL-1	p0045	N82-10469*	#
AFGL-TR-81-0134	p0010	N82-11639	E82-10005	p0053	N82-15483*	#	MCR-81-576-VOL-2	p0045	N82-10470*	#
AFGL-TR-81-0152	p0026	N82-10473	E82-10006	p0046	N82-15484*	#	MCR-81-576-VOL-3	p0045	N82-10471*	#
AFGL-TR-81-0272	p0011	N82-12511	E82-10007	p0004	N82-15485*	#	MCR-81-576-VOL-4	p0045	N82-10472*	#
AIAA PAPER 82-0207	p0009	A82-17841*	E82-10008	p0039	N82-15486*	#	MITT-31	p0056	N82-15499	#
AIAA PAPER 82-0336	p0036	A82-17892	E82-10009	p0021	N82-15487*	#	MTR-80/90	p0054	N82-15500	#
AIAA PAPER 82-0383	p0025	A82-17915	E82-10010	p0013	N82-15488*	#	MU-11-00300	p0053	N82-15493*	#
AIAA PAPER 82-0388	p0051	A82-17918	E82-10011	p0021	N82-15489*	#	NASA-CASE-GSC-12032-2	p0052	N82-13465*	#
ARO-16816.3-GS	p0038	N82-14589	E82-10012	p0005	N82-15490*	#	NASA-CASE-NPO-14544-1	p0011	N82-12685*	#
BMFT-FB-T-81-087	p0022	N82-15925	E82-10013	p0005	N82-15491*	#	NASA-CP-2188	p0026	N82-10661*	#
BMFT-FB-W-81-002	p0055	N82-14615	E82-10014	p0005	N82-15492*	#	NASA-CR-145374	p0010	N82-11635*	#
CONTRIB-500	p0028	N82-11537	E82-10015	p0053	N82-15493*	#	NASA-CR-156880	p0028	N82-12734*	#
CONTRIB-544	p0020	N82-12497*	E82-10016	p0005	N82-15494*	#	NASA-CR-156881	p0052	N82-12447*	#
CRINC/RSL-TR-331-20	p0032	N82-14592	E82-10017	p0054	N82-15495*	#	NASA-CR-156882	p0033	N82-15498*	#
CRINC/RSL-TR-331-22	p0032	N82-14593	E82-10018	p0056	N82-15496*	#	NASA-CR-161030	p0005	N82-15491*	#
CSC/TM-80/6214	p0045	N82-11103*	FC-JO-00611	p0005	N82-15494*	#	NASA-CR-161031	p0005	N82-15492*	#
DE81-027839	p0010	N82-11649	FC-LO-00612	p0005	N82-15491*	#	NASA-CR-161039	p0053	N82-15493*	#
DE81-029177	p0019	N82-10476	FOA-C-30204-E1	p0052	N82-10481	#	NASA-CR-161071	p0013	N82-15488*	#
DE81-029462	p0022	N82-15506	FSRP/INT-269	p0003	N82-10489	#	NASA-CR-161080	p0004	N82-15480*	#
DE82-000071	p0011	N82-12707	FTD-ID(R)SIT-1059-81	p0053	N82-15110	#	NASA-CR-163348	p0053	N82-15483*	#
DE82-000401	p0020	N82-14601	F78-11-REV-A	p0028	N82-11511*	#	NASA-CR-164755	p0005	N82-15490*	#
DE82-000650	p0053	N82-14599	GJBX-114(81)	p0019	N82-10476	#	NASA-CR-164817	p0056	N82-15496*	#
DE82-000772	p0021	N82-14604	GJBX-327-81-VOL-1	p0053	N82-14599	#	NASA-CR-164818	p0021	N82-15489	#
DE82-000780	p0021	N82-14602	GJBX-327-81-VOL-2-BANGOR	p0021	N82-14607	#	NASA-CR-164819	p0004	N82-15481*	#
DE82-000781	p0020	N82-14600	GJBX-327-81-VOL-2-BINGHAMT ON	p0021	N82-14606	#	NASA-CR-164822	p0004	N82-15482*	#
DE82-000784	p0021	N82-14608	GJBX-327-81-VOL-2-EDMUNDST ON	p0021	N82-14605	#	NASA-CR-164904	p0046	N82-15484*	#
DE82-000785	p0021	N82-14605	GJBX-327-81-VOL-2-FREDERICT ON	p0021	N82-14605	#	NASA-CR-164905	p0004	N82-15485*	#
DE82-000794	p0021	N82-14607	GJBX-327-81-VOL-2-FREDERICT ON	p0021	N82-14604	#	NASA-CR-164906	p0039	N82-15486*	#
DE82-000869	p0021	N82-14606	GJBX-327-81-VOL-2-FREDERICT ON	p0021	N82-14603	#	NASA-CR-164907	p0021	N82-15487*	#
DE82-000872	p0021	N82-14603	GJBX-327-81-VOL-2-FREDERICT ON	p0021	N82-14603	#	NASA-CR-164931	p0010	N82-11514*	#
DE82-900311	p0012	N82-13569	GJBX-327-81-VOL-2-MILLINOCK ET	p0021	N82-14602	#	NASA-CR-164968	p0016	N82-11696*	#
DFVLR-FB-81-11	p0047	N82-15503	GJBX-327-81-VOL-2-OGDENSBU RG	p0021	N82-14602	#	NASA-CR-165049	p0033	N82-14789*	#
DOC-79SDS4201	p0054	N82-15495*	GJBX-327-81-VOL-2-OGDENSBU RG	p0020	N82-14601	#	NASA-CR-165791	p0028	N82-11515*	#
DOC-79SDS4242	p0053	N82-15483*	GJBX-327-81-VOL-2-SHERBROO KE	p0020	N82-14600	#	NASA-CR-166640	p0054	N82-15495*	#
			GJBX-327-81-VOL-2-UTICA	p0021	N82-14608	#	NASA-CR-166709	p0038	N82-12510*	#
			GPO-35-265	p0056	N82-15497	#	NASA-CR-166717	p0046	N82-14548*	#
			INPE-2035-RPE/292	p0005	N82-15490*	#	NASA-CR-166719	p0046	N82-13470*	#
			INPE-2054-RPE/300	p0004	N82-15485*	#	NASA-CR-166720-VOL-1	p0028	N82-11511*	#
			ISBN-3-7696-9313-2	p0017	N82-15812	#	NASA-CR-166721	p0052	N82-11512*	#
			ISBN-87-7478-183-9	p0026	N82-10467	#	NASA-CR-166724	p0009	N82-11513*	#
			ISBN-87-7478-183-9	p0028	N82-12533	#	NASA-CR-166731	p0045	N82-10469*	#
			ISBN-951-38-1180-8	p0045	N82-10485	#	NASA-CR-166732	p0045	N82-10470*	#
			ISSN-0065-5325	p0017	N82-15812	#	NASA-CR-166733	p0045	N82-10471*	#
			ISSN-0069-5882	p0056	N82-15499	#	NASA-CR-166734	p0045	N82-10472*	#
			ISSN-0170-1339	p0055	N82-14615	#	NASA-CR-166737	p0045	N82-11103*	#
			ISSN-0340-7608	p0022	N82-15925	#	NASA-SP-380	p0019	N82-12492*	#
			ISSN-0347-6405	p0052	N82-10484	#	NASA-TM-79648	p0051	N82-10468*	#
			ISSN-0355-3477	p0045	N82-10485	#	NASA-TM-82169	p0052	N82-13469*	#
			ISSN-0379-6566	p0029	N82-14553	#	NASA-TM-83198	p0029	N82-14550*	#
			ISSN-0581-1287	p0012	N82-12714	#	NASA-TM-83860	p0038	N82-14549*	#
							NASA-TM-84025	p0055	N82-10087*	#
							NASA-TM-84034	p0005	N82-15494*	#
							NASA-TM-84053	p0055	N82-10102*	#
							NASA-TM-84056	p0045	N82-10466*	#
							NASA-TM-84211	p0016	N82-14041*	#

REPORT/ACCESSION NUMBER INDEX

NOAA-DR-ERL-PMEL-1	p0026 N82-10461 #	US-PATENT-CLASS-343-100PE ..	p0011 N82-12685*
NOAA-FCM-P12-1981	p0013 N82-15697 #	US-PATENT-CLASS-343-781P ...	p0011 N82-12685*
NOAA-TM-ERL-PMEL-24	p0028 N82-11537 #	US-PATENT-CLASS-358-109	p0052 N82-13465*
NOAA-TM-ERL-RFC-7	p0028 N82-11743 #	US-PATENT-4,282,525	p0011 N82-12685*
NOAA-TM-NOS-NGS-32	p0016 N82-13606 #	US-PATENT-4,300,159	p0052 N82-13465*
NOAA-TM-NWS-WR-162	p0037 N82-11530 #	USGS-OPEN-FILE-81-189	p0022 N82-15506 #
		VTT-40	p0045 N82-10485 #
		WES/MP/EL-81-4	p0003 N82-11910 #
NOAA-81041501	p0026 N82-10461 #		
NOAA-81042706	p0010 N82-11536 #		
NOAA-81043005	p0028 N82-11537 #		
NOAA-81050501	p0039 N82-15673 #		
NOAA-81050703	p0037 N82-11530 #		
NOAA-81051503	p0028 N82-11743 #		
NOAA-81052103	p0029 N82-13484 #		
NOAA-81062603	p0016 N82-13606 #		
NOAA-81062615	p0012 N82-13631 #		
NOAA-81071405	p0017 N82-15520 #		
NOAA-81071411	p0013 N82-15697 #		
NOAA/NEMP-111-81-ABCD-0	p0026 N82-10661* #		
042			
NOO-RP-32C	p0029 N82-13641 #		
NSSDC/WDC-A-R&S-81-10	p0055 N82-10087* #		
P-AB26	p0046 N82-13470* #		
PB81-211203	p0026 N82-10461 #		
PB81-214777	p0003 N82-10489 #		
PB81-220188	p0028 N82-11537 #		
PB81-223836	p0010 N82-11536 #		
PB81-224495	p0037 N82-11530 #		
PB81-225468	p0028 N82-11743 #		
PB81-227753	p0029 N82-13484 #		
PB81-227795	p0039 N82-15673 #		
PB81-233355	p0012 N82-13631 #		
PB81-234338	p0016 N82-13606 #		
PB81-246738	p0017 N82-15520 #		
PB81-247231	p0013 N82-15697 #		
PB81-248049	p0047 N82-15698 #		
PHL-1979-49-PT-1	p0032 N82-14617 #		
PHL-1980-28-PT-2	p0033 N82-14618 #		
PR-3	p0046 N82-15484* #		
PREPRINT-69	p0020 N82-12713 #		
RRL-PUBL-514	p0033 N82-14789* #		
RSL-TR-410-1	p0038 N82-12510* #		
S-420-81-01	p0055 N82-10102* #		
SACLANTCEN-SM-150-VOL-1 ...	p0029 N82-13639 #		
SAND-81-0566	p0010 N82-11649 #		
SAPR-1	p0016 N82-11696* #		
SD-TR-81-70	p0012 N82-14591 #		
SDSU-RSI-81-11	p0004 N82-15481* #		
SER-C-261	p0017 N82-15812 #		
SOLAR/0010-81/08	p0011 N82-12707 #		
SONDERBEOB-42	p0012 N82-12714 #		
SP/153/06/01/FR(80)-VOL-1 ...	p0026 N82-10486 #		
SP/153/06/01/FR(80)-VOL-2 ...	p0026 N82-10487 #		
SR-EL-04065	p0004 N82-15480* #		
SR-3	p0026 N82-10473 #		
SR-6	p0010 N82-11639 #		
SSL-SER-22-ISSUE-18	p0004 N82-15482* #		
TDCK-73426	p0032 N82-14617 #		
TDCK-74302	p0033 N82-14618 #		
TR-CSL-8001	p0039 N82-15673 #		
TR-6	p0038 N82-14589 #		
TR-0081(6640)-3	p0012 N82-14591 #		
UCD-207/1/80	p0052 N82-10488 #		
UNIHI-SG-CR-81-04	p0010 N82-11536 #		
US-PATENT-APPL-SN-078612 ...	p0011 N82-12685*		
US-PATENT-APPL-SN-578700 ...	p0052 N82-13465*		
US-PATENT-APPL-SN-583219 ...	p0052 N82-13465*		
US-PATENT-CLASS-250-235	p0052 N82-13465*		
US-PATENT-CLASS-250-236	p0052 N82-13465*		
US-PATENT-CLASS-343-100ME	p0011 N82-12685*		

1. Report No. NASA SP-7041 (33)	2. Government Accession No.	3. Recipient's Catalog No.	
4. Title and Subtitle EARTH RESOURCES A Continuing Bibliography (Issue 33)		5. Report Date April 1982	
		6. Performing Organization Code	
7. Author(s)		8. Performing Organization Report No.	
		10. Work Unit No.	
9. Performing Organization Name and Address National Aeronautics and Space Administration Washington, DC 20546		11. Contract or Grant No.	
		13. Type of Report and Period Covered	
12. Sponsoring Agency Name and Address		14. Sponsoring Agency Code	
15. Supplementary Notes			
16. Abstract This bibliography list 436 reports, articles, and other documents introduced into the NASA Scientific and Technical Information System between January 1 and March 31, 1982. Emphasis is placed on the use of remote sensing and geophysical instrumentation in spacecraft and aircraft to survey and inventory natural resources and urban areas. Subject matter is grouped according to agriculture and forestry, environmental changes and cultural resources, geodesy and cartography, geology and mineral resources, hydrology and water management, data processing and distribution systems, instrumentation and sensors, and economic analysis.			
17. Key Words (Suggested by Author(s)) Bibliographies Earth Resources Remote Sensors		18. Distribution Statement Unclassified - Unlimited	
19. Security Classif. (of this report) Unclassified	20. Security Classif. (of this page) Unclassified	21. No. of Pages 104	22. Price* \$10.50 HC

* For sale by the National Technical Information Service, Springfield, Virginia 22161

PUBLIC COLLECTIONS OF NASA DOCUMENTS

DOMESTIC

NASA distributes its technical documents and bibliographic tools to eleven special libraries located in the organizations listed below. Each library is prepared to furnish the public such services as reference assistance, interlibrary loans, photocopy service, and assistance in obtaining copies of NASA documents for retention.

CALIFORNIA

University of California, Berkeley

COLORADO

University of Colorado, Boulder

DISTRICT OF COLUMBIA

Library of Congress

GEORGIA

Georgia Institute of Technology, Atlanta

ILLINOIS

The John Crerar Library, Chicago

MASSACHUSETTS

Massachusetts Institute of Technology, Cambridge

MISSOURI

Linda Hall Library, Kansas City

NEW YORK

Columbia University, New York

OKLAHOMA

University of Oklahoma, Bizzell Library

PENNSYLVANIA

Carnegie Library of Pittsburgh

WASHINGTON

University of Washington, Seattle

NASA publications (those indicated by an "*" following the accession number) are also received by the following public and free libraries:

CALIFORNIA

Los Angeles Public Library

San Diego Public Library

COLORADO

Denver Public Library

CONNECTICUT

Hartford Public Library

MARYLAND

Enoch Pratt Free Library, Baltimore

MASSACHUSETTS

Boston Public Library

MICHIGAN

Detroit Public Library

MINNESOTA

Minneapolis Public Library and Information Center

NEW JERSEY

Trenton Public Library

NEW YORK

Brooklyn Public Library

Buffalo and Erie County Public Library

Rochester Public Library

New York Public Library

OHIO

Akron Public Library

Cincinnati and Hamilton County Public Library

Cleveland Public Library

Dayton Public Library

Toledo and Lucas County Public Library

TEXAS

Dallas Public Library

Fort Worth Public Library

WASHINGTON

Seattle Public Library

WISCONSIN

Milwaukee Public Library

An extensive collection of NASA and NASA-sponsored documents and aerospace publications available to the public for reference purposes is maintained by the American Institute of Aeronautics and Astronautics, Technical Information Service, 555 West 57th Street, 12th Floor, New York, New York 10019.

EUROPEAN

An extensive collection of NASA and NASA-sponsored publications is maintained by the British Library Lending Division, Boston Spa, Wetherby, Yorkshire, England. By virtue of arrangements other than with NASA, the British Library Lending Division also has available many of the non-NASA publications cited in *STAR*. European requesters may purchase facsimile copy of microfiche of NASA and NASA-sponsored documents, those identified by both the symbols "*" and "#", from: ESA - Information Retrieval Service, European Space Agency, 8-10 rue Mario-Nikis, 75738 Paris CEDEX 15, France.

National Aeronautics and
Space Administration

Washington, D.C.
20546

Official Business

Penalty for Private Use, \$300

THIRD-CLASS BULK RATE

Postage and Fees Paid
National Aeronautics and
Space Administration
NASA-451



9 1 SP-7041, 820527 503487BSR
NASA
SCIEN & TECH INFO FACILITY
ATTN: REFERENCE & RETRIEVAL DEPT
P O BOX 8757 BWI ARPT
BALTIMORE MD 21240

NASA

POSTMASTER: If Undeliverable (Section 158
Postal Manual) Do Not Return
